DOCTOR OF PHILOSOPHY

Mitochondrial division inhibitor (Mdivi-1) and CaMKII inhibitor (KN-93) attenuate Ipratropium Bromide mediated myocardial injury in in vitro models of myocardial Ischaemia/Reperfusion

Khalefah, Fatmah Abubaker Ahmed

Award date:
2022

Awarding institution:
Coventry University

Mitochondrial division inhibitor (Mdivi-1) and CaMKII inhibitor (KN-93) attenuate Ipratropium Bromide mediated myocardial injury in *in vitro* models of myocardial Ischaemia/Reperfusion

By

Fatmah Abubaker Ahmed Khalefah

Award (PhD)

June 2021

Supervisory team: Dr. Katherine Harvey, Dr. Afthab Hussain & Dr. Bernard Burke

Mitochondrial division inhibitor (Mdivi-1) and CaMKII inhibitor (KN-93) attenuate Ipratropium Bromide mediated myocardial injury in *in vitro* models of myocardial Ischaemia/Reperfusion

Fatmah Abubaker Ahmed Khalefah

A thesis submitted in partial fulfilment of the University's requirements for the Degree of Doctor of Philosophy of Research

June 2021

Supervisory team: Dr. Katherine Harvey, Dr. Afthab Hussain & Dr. Bernard Burke

Certificate of Ethical Approval

Applicant:

Fatmah Khalefah

Project Title:

Investigating the cellular, molecular and intracellular cardiotoxic effects of the anti-muscarinic Ipratropium in order to identify the signalling pathways involved in cardiomyocyte death.

This is to certify that the above named applicant has completed the Coventry University Ethical Approval process and their project has been confirmed and approved as Medium Risk

Date of approval:

14 March 2017

Project Reference Number:

P50702

Content removed on data protection grounds

Acknowledgements

My main thank goes to my director of studies Dr. Kate Harvey and the team that supervised me Dr. Afthab Hussain and Dr. Bernard Burke, who helped, guided and supported me during my studies. They advised me throughout my PhD and answer all my questions.

I really appreciate the help I had from the technician team especially for Bethan Grist, Mark Bodycote, Alex Pragnell and Dr. Hugh Kikuchi for their technical support and for always being there for me.

I would like to mention my lab mates/friends who managed to fulfil the requirement for the degree for Doctor of Philosophy Shabana, Jasmin, Sehar, Sophie and many more who supported during the long days in the lab during my MSc and PhD.

Special thanks to my Husband Ali who puts up with me every single day and gives me unconditional love, support and generous gifts including my cute cat Kikyo.

Thank you to my lovely family especially mother and father who support me remotely all the way from Libya and they are keeping me in their prayers.

And I would like to thank my Libyan embassy and Coventry University that enabled me to achieve my goal.

Abstract

Introduction:

A common background links ischaemic heart disease (IHD) with chronic obstructive pulmonary disease (COPD) with regards to systemic inflammation and underlying morbidity and mortality due to myocardial infarction (MI). The symptoms and clinical manifestations of both COPD and IHD are similar, however, compounds that are designed to target both diseases are yet to be fully evaluated. For patients with COPD and IHD who are treated, there is much evidence that muscarinic antagonists, such as ipratropium, whilst acting as effective bronchodilators also pose the risk of adverse cardiovascular events, such as myocardial infarction and stroke, due to underlying cardiotoxic effects of these bronchodilatory drugs. According to the World Health Organization (WHO) 2019 statistics, COPD is considered to be a disease which highly contributes to mortality as well as morbidity across a wide-range of socioeconomic economies with a considerable increase in the burden and impact on global health.

Previous work in our laboratory has shown that Ipratropium Bromide (Ip), a non-selective muscarinic receptor antagonist prescribed for the treatment of COPD, exacerbates myocardial injury. After administration during reperfusion in clinically relevant *in vitro* models of ischaemia/reperfusion (I/R) for the heart muscular (left ventricular) and hypoxia/reoxygenation (H/R) for isolated cardiac myocytes. The injury was via triggering both apoptosis, necrosis and increase the infarction of the heart tissue significantly, in a dose dependent mechanism. Ip's mechanism of action in I/R and H/R was measured by determining the effect of the drug treatment during these conditions and to further gain an insight of its action.

Despite evidence to suggest that the cytotoxic effect of administrating Ip during reperfusion might involve mitochondrial fission and the opening of mitochondrial permeability transition pore (mPTP) as well as altered calcium signalling, the mechanism of this drug-induced toxicity is yet to be fully elucidated.

Aims:

The aim of this work was to try to further elucidate the mechanisms which lead to Ip induced myocardial injury, with a specific focus on the role of Ca^{2+} signalling and mitochondrial involvement. By investigating the cytotoxic effects of Ip in *in vitro* models, such as Langendorff perfused hearts as well as the cytotoxic effects in adult cardiac myocytes in stressed conditions which were clinically relevant to myocardial I/R.

Methods:

Multiple methods were employed in order to identify of the mechanisms of toxicity for Ip and associated signalling pathways. Langendorff, Western Blotting, flow cytometry and PCR were all carried out under simulated conditions of I/R and H/R for the isolated rat hearts and cardiac myocytes in order to identify if there was a mitochondrial role in Ip induced cardiotoxicity. This was primarily by using mitochondrial division inhibitor (Mdivi-1), which has inhibition properties for cell death as well as providing protection against heart failure progression, the protective effects of mdivi-1 is thought to be by preventing mitochondrial fragmentation and blocking pro-apoptotic BAX-dependent cytochrome c release. And using KN-93 which can be defined as an inhibitor with a selectivity and a high potency against CaM kinase II, KN-93 works in the cardiomyocytes via maintaining the homeostasis of calcium, to confirm the involvement of calcium

overload as a calcium signalling indicator. As well as trying to identify whether Ip increases the expression of Dnm1l, which is Dynamin-1-like protein the gene encoded GTPase for Drp1. Drp1 is a member of the conserved dynamin large GTPase superfamily which regulates mitochondrial fission functions. As Ip significantly increases infarction, apoptosis, caspase-3 activity, the expression of Akt these have been preciously shown to be correlated with a reduction in the cell viability following I/R injury.

Results:

One of the main findings in this study is that the administration of Mdivi-1 provides cardio-protection when co-administered with Ip at both 15 and 30 minutes after reperfusion by the reduction in Dynamin related protein 1 (Drp-1), Akt and Erk1/2 when compared with the untreated control. Moreover, this study also showed it can reduce myocardial injury exacerbated by Ip via reduction in the infarct size significantly by (82.7 ± 2.9% vs. 158.5 ± 6.2%) ($p < 0.001$) and total apoptosis as shown through the flow cytometry caspase-3 activity and it also significantly increased cardiac myocyte viability. The effect that occurred on Akt and Erk1/2 might be a result due to the action of Mdivi-1 on the mitochondria, indicating protection, although by a mechanism which has not previously been described and remains to be fully characterised.

Similar results were found in the KN-93 studies with protective properties to cardiac myocytes in all cellular models used. KN-93 mainly reduced the infarction size by (74 ± 4.4% vs. 100 ± 0) ($p < 0.001$). as well as caspase-3 activity, significantly. This is assumed to be mainly by inhibiting CaMKII which also inhibits calcium overload. Since calcium overload resulted in the cell death as found by

the study, confirming the involvement of calcium signaling and, again, indicating involvement of the mitochondria which is linked to calcium overload.

Combining the obtained results, the injury exacerbated by Ip was attenuated by both Mdivi-1 and KN-93 when co-administered with Ip, both agents have shown significant reduction in the injury when co-administered with Ip in infarction via the measurement of AAR% using Langendorff, TTC staining technique data were normalized to I/R control. caspase-3 activity usig flow cytometry for isolated cardiac myocyrtes stimulated H/R and addition of treatment stain to measure caspase-3 activity, data were normalized to H/R control. Mdivi-1 provided a higher level of protection since it decreased apoptosis and increased cell viability which, while there was attenuation, was not seen in KN-93 results.

In conclusion:

The injury caused by Ip is potentially due to both calcium overload and phosphorylation of Drp1, although further studies are required to fully understand the mechanism of action and the full pathway. This work provides further elucidation into the mechanism by which ipratropium elicits its cardio-toxic effects and this holds promise for the development for future treatments for both COPD and IHD.

Publications from this thesis

Khalefah, F. A. A., Hussain, A., Burke, B. and Harvey, K. L. (2017) 'Evidence for Mitochondrial Involvement in Ipratropium Bromide Mediated Myocardial Injury' **Poster and Abstract** British Pharmacology Society conference Centre, London, December 2018

Khalefah, F. A. A., Hussain, A., Burke, B. and Harvey, K. L. (2018) 'Attenuation of Ipratropium Bromide Mediated myocardial injury by the mitochondrial division inhibitor Mdivi-1' Injury' **Poster and Abstract** British Pharmacology Society conference Centre, London, December 2019

Khalefah, F. A. A., Hussain, A., Burke, B. and Harvey, K. L. (2020 - postponed) 'Attenuation of Ipratropium Bromide Mediated myocardial injury by the CaMKII inhibitor KN-93' Injury'' **Abstract and Accepted for Oral Presentation** Winter British Toxicology Society Congress, Cardiff, April 2021.

Khalefah, F. A. A., Hussain, A., Burke, B. and Harvey, K. L. (2021) 'Evidence for Mitochondrial Involvement in Ipratropium Bromide Mediated Myocardial Injury via Ca^{2+} dependent signalling mechanisms' **Pending submission to *"Toxicological Sciences"***

Table of Contents

List of Figures

Chapter 1 Literature Review

Chapter 2 Materials and Methods

Chapter 3 Assessment of the Exacerbation of Myocardial Reperfusion Injury due to Ipratropium Administration

Chapter 4 Ipratropium Bromide Mediated Myocardial Injury is Attenuated by the Mitochondrial Division Inhibitor Mdivi-1

Chapter 5 KN-93 (CaMKII inhibitor) protects against Ipratropium Exacerbation of Injury in *in vitro* models of Ischaemia/Reperfusion

Chapter 6 General discussion

List of Tables

List of Abbreviations

AAR%	Area at risk
Ach	Acetylcholine
Akt	Cellular AKT/protein kinase B
AL	Airflow limitation
AMI	Acute myocardial infarction
ANOVA	Analysis of variance
APAF-1	Apoptotic protease activating factor-1
ATP	Adenosine Tri-phosphate
BAD	Bcl-2 family, BH-3 only domain, pro-apoptotic protein
BAK	Bcl-2 family, BH-1, BH-2 & BH-3 domain, pro-apoptotic protein
BAX	Bcl-2 family, BH-1, BH-2 & BH-3 domain, pro-apoptotic protein
Bcl-2	B-cell lymphoma 2
Bcl-X	B-cell lymphoma-extra large
BID	Bax-like BH3 protein
Bp	base pair
BSA	Bovine serum albumin
CAD	Coronary artery disease
CaMK II	Ca^{2+}/calmodulin-dependent protein
Caspase	Cysteine aspartate specific protease
CF	Coronary flow
CHD	Coronary heart disease
COPD	Chronic Obstructive Pulmonary Disease
CsA	Cyclosporin A
CVEs	Cardiovascular events
CVD	Cardiovascular disease
DEPC	Diethyl pyrocarbonate
DEVD	Z-DEVE-FMK, Benzyloxycarbonyl-Asp(OMe)-Glu(OMe)-ValAsp(OMe)-fluromethylketone

DNA	Deoxyribonucleic acid
Dnm1l	Dynamin-1-like protein
Drp1	Dynamin-1-like protein is a GTPase
ER	Endoplasmic reticulum
Erk	Extracellular signal regulated kinase
ETC	Electron transport chain
FACS	Flow Activated Cells Sorting
FAS	Fas receptor
GAPDH	Glyceraldehyde 3-phosphate dehydrogenase
HF	Heart failure
H/R	Hypoxia/Re-oxygenation
HR	Heart rate
IHD	Ischaemic heart disease
I/R	Ischaemia/Reperfusion
I/R%	Infarct size to Risk ratio
Ip	Ipratropium bromide
JNK	c-Jun N-terminal kinase
KHB	Krebs-Heinsleit buffer
KN-93	CaM kinase II inhibitor
KRB	Krebs-Ringer Modified Buffer
LVDP	Left ventricular developed pressure
MAChR	Muscarinic acetylcholine receptor
MAPKs	Mitogen-activated protein kinases
MCU	Mitochondrial calcium uniporter
MEK	Mitogen-activated protein kinase
Mdivi-1	Mitochondrial division inhibitor 1
MI	Myocardial infarction
Mins	Minutes
mmHg	Milemiter of mercury
MMP	Matrix-metalloprotease

MOMP	Mitochondria outer membrane permeability
mPTP	Mitochondrial permeability transition pore
MTT	3-(4,5-dimethylthiazol-2,5-diphenyl tetrazolium bromide
NAC	N-acetylcysteine
NCLX	Na^{+}/Ca^{2+} exchanger
PARP1	Poly [ADP-ribose] polymerase 1
PBS	Phosphate-buffered saline
PCR	Polymerase chain reaction
pH	Potential of hydrogen
PI3K	Phosphoinositide 3-kinases
PS	Phosphatidylserine
RI	Reperfusion injury
RISK	Reperfusion injury salvage kinase
RNA	Ribonucleic acid
ROS	Reactive oxygen species
RPM	Revolutions per minute
SEM	Standard error of the mean
SMAC	Second mitochondria-derived activator of caspase
SR	Sarcoplasmic reticulum
TRAILR	Tumour necrosis factor-related apoptosis-inducing ligand
TTC	(2,3,5-Triphenyltetrazolium chloride)
VDAC	Voltage-dependent anion channel
XIAP	X-linked inhibitor of apoptosis protein

Chapter 1: Literature Review

1.1 Introduction

Chronic obstructive pulmonary disease (COPD) is the third most prevalent cause of mortality globally and is frequently considered to be an umbrella term for individuals suffering from chronic bronchitis, emphysema, or both (Whittaker 2004). Ischaemic heart disease (IHD) is a cardiovascular condition which occurs due to limitation of blood flow to the myocardium. Both conditions frequently occur concomitantly due to their systemic influences on both the respiratory and pulmonary systems which can lead to systemic organ damage and, ultimately, death (Deshmukh and Khanna 2021).

A common background that links IHD with COPD is underlying systemic inflammation, primarily located in the respiratory and pulmonary systems (Rabe, Hurst and Suissa 2018). Smoking a cigarette is likely to be a noxious environmental stimulant triggering inflammatory activity such as C-reactive protein and white blood cell count, by activating white blood cells which release inflammatory molecules which alert immune response (Griffo et al. 2017). That occurs due to following prolonged exposure is likely to damage the lungs epithelium and vascular endothelium induce pulmonary inflammation by damaging the respiratory epithelial barrier (Han et al. 2010). Tobacco smoking is the factor most correlated with COPD according to Olloquequ et al. (2018) study, however there are other shared risk factors as well, such as advanced age, pathophysiological mechanism, individuals with lower levels of physical activity as well as genetic factors such as α-1 anti-trypsin deficiency (Griffo et al. 2017).

All smokers experience a decline in lung function in a dose and duration-dependent manner, which occurs in dose-duration dependent manner and lung inflammation also occurs during COPD leading to adverse effects that depend on the age and other risk factors (Onishi 2017). The management of COPD is important because of the production of systematic inflammation and oxidative stress, these significant factors have impacts COPD patients (Griffo et al. 2017). The symptoms and clinical manifestation of both COPD and IHD are similar which gives a strong evidence linking COPD and IHD, no compounds are designed or evaluated to target both diseases, with few pre-clinical studies, although for COPD and IHD patients, there has not yet been a clinical trial conducted (Roversi et al. 2014). COPD patients are suffering from atherosclerosis with abnormal decreased in the expiratory force volume at a period of one second vital capacity force (the ratio of FEV1/FVC) (Deshmukh and Khanna 2021). Since 2020 COPD has been considered the third largest killer in developing countries and uncontrolled COPD increases the morbidity and mortality in IHD patients and the diagnostic delay leading premature death (Deshmukh and Khanna 2021).

Despite our current understanding of the association of COPD with IHD, there is much evidence to suggest that pharmacological agents, such as muscarinic receptor antagonists, for example ipratropium, may cause adverse cardiovascular outcomes. This was first recognised through a metanalysis by Sing el at in 2008 which indicated that the potential for premature death in patients suffering from both COPD and IHD was increased by up to 47% (Singh, Loke and Furberg 2008). Published literature had demonstrated that Ipratropium had the capacity to initiate both apoptosis and necrosis in myocardial cells

providing an indication inhaled anticholinergics could potentially provide a risk of adverse cardiovascular events in patients with COPD and underlying IHD (Harvey, Hussain and Maddock 2014). This work, for the first time, supported clinical observations of a study by Singh et al. in 2008 (meta-analysis) which indicated that premature death from adverse cardiovascular events could be increased COPD patients receiving ipratropium (Singh, Loke and Furberg 2008). Ipratropium causes the smooth muscle to relax which occurs due to intercellular cyclic guanosine monophosphate (cyclic GMP) degradation (Irvin-Sellers and White 2015). Acytalcoline release at the cholinergic nerve endings is inhibited due to its antagonist effect on mAChRS thus the feedback to the receptor is inhibited (Irvin-Sellers and White 2015).

1.2 Chronic Obstructive Pulmonary Disease (COPD)

According to the World Health Organization (WHO) statistics, chronic obstructive pulmonary disease is considered to be a disease which highly contributes to mortality as well as morbidity of a wide number of individuals with a considerable increase on the impact of global health (Siouta et al. 2016). COPD is most common in developed countries and in 2010 it was estimated that 384 million cases of COPD were reported with the equivalent prevalence of 11.7% in the United Kingdom (UK) it was estimated to be approximately 3% within the total adult population of the UK (Morgan, Zakeri and Quint 2018). In 2016 due to the 251 million reported cases, the WHO ranked the global prevalence of COPD as the third leading cause of deaths especially in developed countries and it is expected to further increase due to poor awareness, aging population, tobacco

exposure and poor access to diagnosis (Alqahtani et al. 2020). It is characterised by inflammation in the pulmonary system and is mainly found in patients with a cigarette smoking history by 50% due to higher levels of inflammatory biomarkers, it is considered to be the basic cause of mortality related to chronic lower-respiratory diseases (Garcia-Lucio et al. 2016). COPD patients usually experience a reduction and limitation in the air flow (airflow limitation (AL)) that happens gradually due to inflammation, which can irritate cells lining airways, over time, they may become scarred, this airway scarring makes airways abnormally thick with no treatment for this in respiratory system which leads for the patients with either chronic bronchitis or Emphysema or both, as shown in Figure 1.1 (Forey, Thornton and Lee 2011, Harvey, Hussain and Maddock 2014). It is common, persistent and complex disease caused by dysfunction of the lungs with many triggering factors such as viral infection including coronavirus, not to mention the symptoms worsening, the end result is hospitalization, and given the irreversible nature of the condition ultimately death (Alqahtani et al. 2020). The triggers can be smoking, or air pollution and its symptoms are shortness of breath which gradually gets worse, coughing, wheezing and frequent infections of the lungs, the inflammatory cells and mediators and the effect and response to therapy vary however in COPD the predominant type of inflammatory cells is neutrophilic inflammation in the airway (Forey, Thornton and Lee 2011). COPD is twice as common in patients with IHD and it is estimated approximately 33% of IHD patients also suffer from underlying COPD (Harvey, Hussain and Maddock 2014, Deshmukh and Khanna 2021). The comprehensive mechanisms of the inflammatory response in COPD is beyond the scope of this thesis, but

can found in the following two excellent reviews Saha and Brightling (2006) and He et al. (2010). The inflammatory response is complex and it involves many defense mechanisms against pathogens, in the lung pathogen or exposure to toxin or pollutants is one the main cause of inflammation during which many types of inflammatory cell are activated and they released cytokines and mediators to enhance the inflammatory cells in the presence of active chronic inflammation is present can such as asthma and COPD (Saha and Brightling 2006). The involvement of immunity system to evoke rapid response especially since lung is a vital organ and excessive inflammation can be life threatening (He et al. 2010). Inflammation due to COPD is heterogeneous, but they key inflammatory cell types involve are macrophages, neutrophils and T cells inflammatory mediators are tumor necrosis factor alpha interleukin 1 and protases (Griffo et al. 2017). It linked to systemic inflammation which increase of cardiovascular disease. Inflammation associated with manifestation as well as airflow obstruction. Accumulation of inflammatory mucous exudated in the lumen and ireverase in tissue volume of bronchial wall (Saha and Brightling 2006).

Figure 1.1 COPD conditions of chronic bronchitis and Emphysema.

Figure 1. 1: COPD with the two conditions chronic bronchitis which is a long-term inflammation of the bronchi and Emphysema when the air sack is damaged, which are what COPD patients are suffering from (Garcia-Lucio et al. 2016).

Many studies have linked COPD with other diseases such as cardiovascular disease (CVD), coronary artery disease (CAD) and lung cancer (Bhatt and Dransfield 2013, Roversi et al. 2014, Xia et al. 2020). Multiple therapeutic compounds have been prescribed for COPD such as β2-agonists and anticholinergics (also known as muscarinic receptor antagonists) (Roversi et al. 2014). Some therapies, such as chemokine antagonists, are directed against the influx of inflammatory cells into the airways and lung parenchyma that occurs in COPD, whereas others target inflammatory cytokines such as tumour necrosis

factor-α (Barnes and Stockley 2005). However, adverse effects on the heart causing damage to cardiomyocytes was observed in COPD patients as a consequence of these treatments inducing toxicity associated with cardiovascular disease pathology (Finegold Asaria and Francis 2013). This correlates to the metaanlysis conducted by Singh et al. (2008) who specidically demonstrated that antimuscarinics may contribute to adverse cardiovascular outcomes (Singh, Loke and Furberg 2008).

1.3 Cardiovascular Events (CVEs)

Cardiovascular events occur due to the damage to the myocardium and symptoms of such events primarily included myocardial infarction or stroke, they are considered as pulmonary vascular disorders and include coronary heart disease (CHD) as a risk factor (Akyea et al. 2020). In the past decade, CVD treatment has significantly improved, however, an increased risk for age group of 65 years patients with COPD to develop CVD, which is associated with a rise in risk of mortality, despite the fact that smoking is the main shared link between the two diseases, it is not the only reason (Morgan, Zakeri and Quint 2018). Due to potential higher levels of systemic pathologies in COPD patients, such as short of breath, weight loss, skeletal dysfunction, cardiovascular diseases, and depression (Morgan, Zakeri and Quint 2018). This is to develop cardiovascular diseases "cardiovascular events (CVEs)" IHD, heart failure (HF) and cardiac arrhythmias are the most common observed CVDs to occur in patients with COPD (Ogale et al. 2009, Finegold Asaria and Francis 2013). IHD prevalence with COPD patients in the study by Morgan, Zakeri and Quint (2018) it was

estimated that between 20% and 60% depends on the study population whereas the other disease found to be 10-30% in HF and 10-15% in cardiac arrhythmias (Morgan, Zakeri and Quint 2018). COPD patients have 28-70% chance to develop CVEs and if they have, they are susceptible to have exacerbation within 3 months' period (Acute exacerbation), therefore they need close attention and observation (Hu et al. 2020). With complexity of the mechanism CVDs is the leading cause for COPD patients to be hospitalized, COPD deaths are estimated to be between 12% and 60% depending on the population of the study and approximately a third of the deaths is a result of CVDs, not to mention people with hypertension and diabetes have high risk of mortality (Morgan, Zakeri and Quint 2018) (Figure.1.2).

Figure.1.2 ischaemic heart disease.

Figure 1. 2: ischaemic heart disease in which the coronary artery is blocked, and the blood does not flow to the left ventricle muscle (Ogale et al. 2009).

1.3.1 Ischaemic Heart Disease (IHD)

The remaining leading cause for mortality worldwide is ischaemic heart disease (IHD) with acute myocardial infarction (AMI) being the most serious fatal consequence of IHD (Finegold, Asaria and Francis 2013). AMI is the leading cause of death in the developed world as it is irreversible damage to the heart muscle and can lead to serious complications (Roversi et al. 2014). Although death from IHD is declining due to the decrease in incidence and increase in treatment effectiveness, IHD conditions are chronic, relapsing and the effect are not known (Koch et al. 2015). Strong association has been indicated by many studies linking AL and CAD, leading to the assumption that patients who suffer from COPD are highly at risk to develop IHD, and patients who have IHD have the same amount of risk of developing COPD (Roversi et al. 2014, Akyea et al. 2020). Approximately a third of patients who developed IHD, are likely to have COPD, it is now established that the increased risk of COPD is mainly due to MI and stroke with COPD patients having double the risk due to MI (Morgan, Zakeri and Quint 2018).

1.3.2 Cardiac Ischaemia (Myocardial Infarction, MI)

Cardiac ischaemia (myocardial infarction, MI) which occurs in the myocardium after receiving insufficient supply of blood, the tissue will become dysfunction due to the shortages of elements required for cellular metabolism such as glucose and O_2 (Zhao et al. 2003, Hausenloy and Yellon, 2013). This has a determinate effect on the cardiac tissue for the heart muscle prevented from receiving enough oxygen reducing its ability to pump the blood leading to heart attack and

developed complications and the damage is irreversible and the heart can not regenerated like other organs such as the liver (Zhao et al. 2003, Hausenloy and Yellon, 2013). Biochemical and metabolic changes after injury such as limited glucose uptake within the myocardium are likely to occur due to the deprivation of oxygen and nutrient supply, the cell will switch metabolism to anaerobic respiration since oxygen is absent, as a result of the lactate produced, intracellular pH is also drastically decreased (Hausenloy and Yellon, 2013). In cardiac tissue is necessary to maintenance of myocardial preservation during ishaemia or hypoxia via creation of energy through the combustion of carbohydrates in the absence of oxygen complication, glycolysis occurred, however, limited as by produce lactate protons inhibit glycolysis (Zhao et al. 2003, Hausenloy and Yellon, 2013). This leads to the activation of the Na^+/Ca^{2+} exchanger function which occurs due to intracellular Na^+ overload as a result of extrude H^+ by the Na^+/H^+ exchanger. Since the Na^+/Ca^{2+} exchanger acts to reverse intracellular Na^+ overload by the extruding of Na^+ and replaces it with intercellular Ca^{2+}, this eventually leads to calcium overload (Ottolia et al. 2013). During ischaemia, intracellular Na^+ overload is exacerbated due to the function of the Na^+/K^+ ATPase, however, also during ischaemia the acidic pH prohibits the opening of mitochondrial permeability transition pore (mPTP) in cardiomyocytes and causes contractile dysfunction due to paralysis of cardiac myofibrils, simultaneously (Seidlmayer et al. 2015). Ultimately, there is a build-up of metabolic residues due to the cessation in ATP production and oxidative phosphorylation due to this reduction in pH; a mechanism which was first proposed in 2000 by Dhallla et al. (2000) and still remains as the primary

proposed series of events despite continued research in the past two decades (Dhalla et al. 2000, Halestrap and Richarsdon 2015) (Figure 1.3).

Figure 1.3 myocardial injury caused by Ischaemia/ reperfusion injury.

Figure 1. 3: Schematic to show myocardial injury caused by Ischaemia/ reperfusion pathway leading to calcium overload and oxidative stress which emerge from imbalance exists between free radical formation and the cells to bae able to clear them, via the use of antioxidants which are substances that neutralize or remove free radical by donating electron (Dhalla et al. 2000).

1.4 Reperfusion Injury (RI)

Additional, irreversible, damage then occurs due to the restoration of the blood supply to the ischaemic tissue, this process is termed “reperfusion injury” and is due to the production of further free radicals, such as hydrogen peroxide, in the cell and the generation of reactive oxygen species (ROS) due to the sudden increase in O_2 (Harvey, Hussain and Maddock 2014). The damage occurred via microvascular impairment, inducing contractile dysfunction and further myocytes death (Hausenloy and Yellon 2013). Since the cellular proteins are damaged by the restored O_2 and there are still high levels of intracellular Ca^{2+} (due to the previously mentioned calcium overload), plasma membrane changes and DNA damage initiates and accelerates cellular self-destruction via both necrosis and apoptosis mediated pathways such as tumor necrosis factor-related, inducing ligand or caspase-3 dependent cell death (Kalogeris et al. 2012). However, the restored O_2 also reinstates activation of the electron transport chain (ETC), generating further ROS such as peroxides, superoxide, and leading to further dysfunction of oxidative metabolism (Hausenloy and Yellon 2013).

The culmination of these mechanisms, ultimately leading to cellular death during RI in cardio myocytes, due to the opening of the mPTP mediated by ROS and the contribution of the increased levels of intracellular Ca^{2+}, as well as providing further damage by lipid peroxidation of the plasma membrane which lead to enzymes denaturing and provide direct oxidative damage to DNA (Hausenloy and Yellon 2013, Shah, Yellon and Davidson 2020). Lipid peroxidation alters the physiological function of cell membrane, the damage occurs via the increase in membrane permeability due to oxidized lipids believed to be involved in cardiac

ischaemia/reperfusion injury and inflammatory diseases, it can be disrupt ion gradients hence alerting metabolic process their cytotoxic role inhibiting gene expression and promoting cell death the lipids work as signalling molecules (Kalogeris et al. 2012).The main enzyme which generate lipids mediator such as lipoxygenase might activate receptors such as G-protein coupled receptors and nuclear receptors some involved in signal transduction leading to Ca^{2+} homeostasis (Yellon and Davidson 2020). At reperfusion the lactic acid (produced due to anaerobic metabolism during ischaemia) is discareded via the activation of the Na^{+}/H^{+} exchanger, as a result the physiological level of the pH is readily restored, often accelerating to more than pH7, together with calcium overload, this potentially will lead to mPTP opening (Hausenloy and Yellon, 2013). The induction in mPTP opening is based on Ca^{2+} driven into the mitochondrial membrane causing it to rupture, after which apoptosis is initiated upon the release of ROS and cytochrome c to the cytoplasm initiating an apoptotic dependent caspase cascade via activation of caspase-9 through the formation of the heptodimeric-apoptosome (Hausenloy et al. 2002, Singh, Loke and Furberg 2008). Irreversible damage to mitochondria is associated with the opening of mPTP by opening which lead to matrix swelling release of apoptotic molecules such as cytochrome c from intermembrane space (Chinnaswamy, Zameer and Muthuchelian 2020). During ishaemia factors such as intracellular Ca^{2+} accumulation and ROS progressively increase, during reperfusion the factors occurred during ischaemia cause the opening mPTP leading to apoptosis as mentiomned because the recovery of cardiac function depends on mitochondria recovery (Kalogeris et al. 2012). After reperfusion onset, as an

immunological response to ROS and the release of pro-inflammatory cytokines such as TNF-α, lL-1, IL-6, IL-8, accumulation of neutrophils by 80% occurs after several hours in the infarcted myocardial tissue (Chatelian et al. 1987, Kalogeris et al. 2012). Apoptotic bodies start to appear due to apoptosis (programmed cell death) in which no risk of inflammation occurs since these bodies maintain their integrity until phagocytes digest them (Chinnaswamy, Zameer and Muthuchelian 2020).

Figure 1.4 illustrate Anaerobic respiration during ischaemia as well as the restoration of oxygen at the onset of reperfusion in cardiac myocytes.

Figure 1. 4: The metabolic changes due to ischaemia into anaerobic metabolism in which the exchanger channel appears to cause calcium to overload in the low level of pH in which the mPTP is closed but once reperfusion take a please calcium overload and ROS causes the mPTP to be open leading to reperfusion injury explained above in detail (Hausenloy and Yellon, 2013).

1.4.1 Ischaemia /Reperfusion Cardiac Cell Death

Cell death is considered to be a selective process of physiological cell deletion in normal tissue which plays an important role in shaping morphological and functional maturity in a number of systems and can occur in different forms such as apoptosis or necrosis (Tanaka et al. 1994). These processes are very important in normal condition for the body to develop, however it can be damaging if the cell death process was correlated with pathological conditions casing further damage to the tisse such as in ischaemia reperfusion injury (Wu et al. 2018). Ischaemia of the heart, causes the induction of fibrosis, replaced by cardiomyocyte death; despite the classic belief that the death of cardiomyocytes results from mechanisms of accidental cell death known as necrosis during ischaemia, its precise mechanism remains unclear (Kalogeris et al. 2012). After the restoration of the blood (reperfusion), local inflammation and potential increases in ROS production appear to result in secondary injury leading to cell death via processes which are from the traditionally defined apoptosis and necrosis mechanisms (Wu et al. 2018). It has been recently reported that ischaemia induces apoptotic death in the liver and in the brain (*in vivo*) (Luo et al 2019). Thus, in addition to necrotic death, the mechanism of cardiomyocyte death during ischaemia may be involved in the apoptotic process (Chinnaswamy, Zameer and Muthuchelian 2020). There are currently treatments aimed to reduce cardiomyocyte death due to RI such as Melatonin, but this recent work implies more potential treatment and therapy significantly targeting both ischaemia and RI in myocardium should be developed especially since MI is a leading cause of premature death in the western world with the major factor contributing to

morbidity being the infarct size (Xu et al. 2018). Therefore, self-DNA targeted to inhibit inflammation during I/R as a complete process may help limit cardiomyocyte loss during both ischaemia and RI, since it is mentioned by Shah, Yellon and Davidson (2020). that self-DNA misplaced initiates the inner immune response resulting in chronic activation of inflammation which can occur due to necrotic cell death doting RI (Shah, Yellon and Davidson 2020). However, this poses a challenge for physicians since the end result is often organ dysfunction and no novel treatments to limit these adverse consequences (Wu et al. 2018). In apoptosis and necrosis death by ischaemia ending in releasing histones, which happened upon apoptotic execution weather the stimulus was extrinsic or intrinsic the core nucleosomal histones and their release from DNA correlated with the progression of apoptosis, the latter was shown to be able to trigger inflammation and subsequently cell death which occurred by activation of cell death pathway (Shah, Yellon and Davidson 2020). The injury can be caused by cascade of deleterious inflammatory response and cell death; however, these exact processes have not been fully elucidated (Xu et al. 2018).

1.4.1.1 Apoptosis (Programmed Cell Death)

Apoptosis (programmed cell death) usually occurs following stressful conditions to the cell such as ischaemia during which the cytoplasm condense, nucleus is segmented, loss of plasma membrane microvilli, and the chromosomes are extensively degraded into oligomers of about 180 bp caused by activation of endogenous endonuclease, however it is also an essential process in normal cellular turnover (Tanaka et al 1994). It can be defined as an organised process that is regulated by transduction cascades and cellular proteins (primarily

caspases), many diseases occur due to imbalanced apoptosis such as cancer and AIDS, thus a profound understanding in apoptosis and its mechanistic pathway is essential in order to understand disease and how to treat them (Abotaleb, et al. 2019). Apoptosis is a very critical process in development and homeostasis by eliminating unwanted cells (Pfeffer and Singh 2018). It was suggested by many studies that various pathological conditions and chemical agents, cardiac ischaemia/reperfusion injury can cause the induction of apoptosis such as exposure to irradiation, ultraviolet and anticancer treatments (Tanaka et al 1994, Brentnall et al. 2013). During the stress conditions of ischaemia apoptosis cell damage is mediated by DNA cleavage or mitochondria dysfunction which activate caspases as a result, the loss of DNA lead to cell death consequently causing the cell to shrink, the chromatin will condense and fragment which occurs during reperfusion when the mitochondria release apoptotic proteins to initiate apoptosis, apoptotic bodies are produced as a result of budding from the plasma membrane, the apoptotic bodies will be phagocytosed, but, in contrast to phagocytosis following infection, this does not elicit an inflammatory response (Hausenloy and Yellon, 2013). Caspases and Bcl-2 family proteins are the main regulators for intrinsic apoptosis as pro-apoptotic proteins, after cytochrome c release from the intermembrane mitochondrial space, cell death is executed by a caspase cascade which is initiated by the formation of the apoptosome leading to activation of the initiator caspase, caspase-9 (Brentnall et al. 2013). There are two main routes for apoptosis shown in figure 1.5, the first one occurs due to extracellular signalling factors and is named extrinsic pathway apoptosis which can be initiated by extrinsic death receptor, such as FASL

binding to FAS, whereas the other pathway is intracellular signaling (intrinsic pathway) which occurs mainly by the release of cytochrome c from the stressed mitochondria, as is observed in cardiomyocytes following I/R (Abotaleb, et al. 2019). Which is the first link to the area of study since Ipratropium bromide was found to exacerbate reperfusion injury by causing apoptosis in cardiac myocytes. For efficient execution of apoptosis, cell death programme, caspase-3 is required, caspase-9, which is activated post cytochrome c, activates effective caspases and Bid leading to cell death, however, the process is more efficient in the presence of casdpase-3 (Brentnall et al. 2013). Other important factors that play a crucial role in apoptosis induction are ROS and mitochondrial involvement in both physiologic and pathologic conditions (Zorov, Juhaszova and Sollott 2014). Interestingly, mitochondria is considered to be a target and source of ROS, since mitochondria releases cytochrome c to trigger caspase activation, which appears to be mediated by direct or indirect ROS action (Brentnall et al. 2013). Although, ROS have also anti-apoptotic effects (Simon, Haj-Yehia, and Levi-Schaffer 2000). The rodox signalling is tightly regulated which is ensured via metabolism and ROS interplay with other messenger molecules, hence providing cellular function control form cell proliferation to apoptosis a balance in ROS level is essential and target of specific to proximity can be achived for the activation of cancer- growth-promoting pathways such as MAPK (Erk1/2, p38, and JNK PI3K/AKT) which is anti-apoptotic property (Simon, Haj-Yehia, and Levi-Schaffer 2000).

Figure 1.5 illustrate the two main pathways of apoptosis: Extrinsic caused by extrinsic death receptor and Intrinsic occurs mainly by the release of cytochrome c from the mitochondria.

Figure 1. 5: Presentation for apoptotic pathways. Extrinsic pathway characterised by the activation of the death receptors which cleave the initiator caspases such as caspase-8 which cleave both Bid and the executioner caspases as caspase-3 leading to apoptosis. Intrinsic pathway involves BAX/BAK activation via tBid, Bcl-2 and other factors in mitochondria surface releasing cytochrome c which bind to APAF-1 making Apoptosome which cleave the initiator caspase-9 the later cleaved the executioner caspases such as caspase-3 leading to apoptosis (Ichim and Tait 2016). All abbreviations within the list of abbreviations.

1.4.1.2 Necrosis (Unprogrammed Cell Death)

Necrosis (unprogrammed cell death) is considered as a passive form of cell death, the incompatible depletion of ATP level for the cell to survive leading the cell to enter the bioenergetic catastrophe known as necrosis cell death (Wu et al. 2018). Cellular 'accidents' such as toxic insults or physical damage are mainly considered to be the initiator to ATP of bioenergetic deselection which lead to necrotic cell death this usually occurs during ischaemia due to the anaerobic metabolism when the cells produce lactic acids rather than ATP as well as the lack of oxygen, in contrast to apoptosis, it is irregular irreversible cell death often initiated by damage to the plasma membrane (Edinger and Thompson 2004, Wu et al. 2018). The morphological characteristics of necrosis are cytoplasm vacuolation and the resultant attributable inflammation induced around the necrotic cell causes the cellular contents and proinflammatory molecules to accumulate due to the breakdown of the plasma membrane (Edinger and Thompson 2004). Changes in nuclear morphology, which are frequently exhibited in cells that die by necrosis, are not organised chromatin condensation and fragmentation of DNA into 200 bp fragments that are shown in apoptotic cell death but appear to be almost random and sporadic abnormal cellular events (Edinger and Thompson 2004). Furthermore, cell death by necrosis as a consequence of cell swelling due to loss of plasma membrane integrity may be mediated via increased levels of Ca^{2+}, and severe oxidative stress providing a further damage after the onset of reperfusion the link to the study is necrosis due to ATP depletion occur during ischaemia and during reperfusion calcium overload cause mitochondria damage leading to necrosis (Miller and Zachary 2017).

During necrosis, the cell rupture and release of enzymes, such as proteases, which can break down membrane protein pumps, indicate the activation of cell death for neighboring cells, this form of cell death was found during ischaemia due to the lack of oxygen which is one of the main causes of necrotic cell death in myocardium (Mao and Zhuang 2014). In addition, one of the events attributed to necrosis is the induction of the inflammatory response leading to additional damage in the tissue which during reperfusion injury will be more exaggerated in the heart tissue even after the restoration of oxygen (Mao and Zhuang 2014). Cells that become necrotic upon death, which is caused by irreversible changes occurring in the nucleus (karyolysis, pyknosis and karyorrhexis) (Miller and Zachary 2017), include signalling in necrosis as well as condensation intense eosinophilia, loss of structure, and fragmentation in the cytoplasm (Majno, and Joris, 1995). During ischaemia, when the cells become necrotic, they are called ischemic necrosis or massive necrosis, in which the mechanism is unknown (Wang et al. 2016). (Figure 1.6).

Figure 1.6 Necrotic cell death pathway in the cell due to external stress.

Figure 1. 6: Present necrotic pathway caused by stress leading to the hyper activation of Poly (ADP-ribose) polymerase-1 (PARP1) by Ca^{2+} /Calpain, causing caspase-independent necrosis via the translocation of BAX to mPTP, which cause the release of ROS and apoptotic-inducing factor which translocate to the nucleus (Hou et al. 2013, Douglas and Baines 2014).

1.4.1.3 Eryptosis

Another type of cell death is known as eryptosis (also known as suicidal erythrocyte death) (Shaik et al. 2012). It is characterised by shrinkage of erythrocyte protease activation, membrane blebbing, asymmetrical

phosphatidylserine (PS) breakage accompanied by features that are found in apoptotic cell death in nucleated cells although the nucleus is absent in erythrocytes (Mahmud et al. 2013). The eryptotic cell death is thought to be utilised in preventing haemolysis of aged and defective erythrocytes that occur spontaneously (Mahmud et al. 2013). On the other hand, it has been suggested that anaemia might occur due to excessive eryptosis, moreover, many pathophysiological pathways are shared by eryptosis and heart failure (HF) (Bissinger et al. 2018). It has been demonstrated that these pathophysiological pathways presented in HF, which include oxidative stress, energy depletion, and a dysregulated osmotic balance, are the main reasons that trigger eryptosis (Mahmud et al. 2013). Furthermore, eryptotic events appear to affect organs for example eryptotic erythrocytes adhere to the endothelial cells which possibly contribute to impaired microcirculation and ultimately contribute to organ failure area where this have been observed in heart failure (HF)-associated anaemia (Mahmud et al. 2013). The link between eryptosis cell death and the study is ipratropium bromide stimulate eryptosis which is similar to apoptosis, via calcium overload the same manner Ip induced injury in cardiac cells via apoptosis. Calcium permeable cation channels are found to be triggered by eryptotic associated Ca^{2+} entry, which leads to cell shrinkage as a result to activate Ca^{2+} sensitive K^{+} channels (Ullrich and Apell 2021). In addition, Ca^{2+} entry causes phospholipid scrambling of the cell membrane subsequently phosphatidylserine (PS) will be exposed at the cell surface which can be measured as a mark of eryptosis (Rysavy et al. 2014). These are also important pathological consequences altered by intracellular Ca^{2+} handling in failing cardio myocytes

(Mahmud et al. 2013). Shaik et al. (2012) has also found erythrocyte death was triggered during Ipratropium bromide administration as shown in the flow cytometry data presented as caspase-3 increasing activity, indicating that cardiac toxicity due to muscarinic antagonist administration is not limited to cardiomyocytes (Shaik et al. 2012). The two main shared features are the erythrocyte death which is similar to apoptosis and the fact it was caused by Ip, suggest that Ip method of action require increase in calcium ions in the cell to produce the cell death (Figure 1.7).

Figure 1.7 Eryptosis cell death due to Ca^{2+} overload and the similarity shared with apoptosis.

Figure 1. 7: Presents Eryptosis cell death with the deferent stages starting by Ca^{2+} overload, Eryptosis inducer is increased intracellular calcium which results in PS exposure into the other membrane leading in cell shrinkage as a result to activate calcium sensitive potassium channels then membrane blebbing as explained above (Boulet, Doerig and Carvalho 2018).

1.5 Signalling Mechanisms Involved In I/R

Signalling mechanisms require many molecular components to be involved for the establishment of myocardial inflammation in the setting of diseases and I/R which promotes the upregulation of cytokines, chemokines and adhesion molecules, and are highly active in contributing to cardiovascular damage (Frati et al 2017).

1.5.1 Reperfusion Injury Signalling Kinase (RISK) Signalling Pathway

The RISK pathway was first proposed in 2003 (Hausenloy et al 2004) and refers to signal transduction pathways which confer cardio-protection and appears to be specifically activated during reperfusion (Rossello and Yellon 2018).

Phosphoinositide 3-Kinase /Protein Kinase B (PI3K/Akt) phosphorylation, part of the pro-survival RISK signalling cascade, contributes to cell survival mechanisms by the inhibition of apoptosis (Li et al. 2013). The basic mechanism is through sending a signal from the cell membrane to activate AKT and Erk for cell surivival via the G-protein- coupled receptors ligands, that is protective to the cell from the cell surface to the mitochondria, this can occur via various mechanisms including agonism of G-protein coupled receptors, or, in the context of cardiovascular I/R, the signal can occur due to ischaemic preconditioning in which a non-lethal ischaemia and reperfusion confer cycle, which has been demonstrated to protect against I/R injury (Hausenloy and Yellon 2013). As a result, oxidative stress and I/R activate the RISK pathway PI3K/Akt /eNOS branch which indicate a higher

possibility for the cell to survive (Li et al. 2013) (Figure 1.8). Specific aspects of RISK signalling include PI3K-AKT, MAPKs, Erk1/2 and JNK.

Figure 1.8 Ischeamic pre-conditions and the follow up activation of RISK pathway which promote cell survival via activating Akt and Erk.

Figure 1. 8: Present the RISK pathway activation due to Ischaemia the MEK activate Erk and PI3K activate Akt both are the survival kinases which allow the cell to survive (Luna-Ortiz et al. 2011).

1.5.1.1 Phosphoinositide 3-Kinase (PI3K)/Protein Kinase B (Akt) Signalling Pathway

Phosphoinositide 3-kinase (PI3K)/protein kinase B (Akt) pathway occurs through phosphorylation of Akt to P-Akt which then activates protein kinase C, a protein that is capable of providing protection to the heart against ischaemia via initiation of transcription of pro-survival proteins, resulting in reductions in apoptosis and necrosis (Winnay et al. 2013). Cardio-protection obtained from Akt is also thought to involve the inhibition of mitochondrial K_{ATP} channels, although these exact mechanisms are yet to be fully known (Li et al. 2013, Huang, Qin and Lu 2014). Moreover, the phosphorylation of the apoptotic proteins such BAD and BAX is highly affected by Akt, since apoptosis is due to the release of cytochrome-c which may otherwise occur because of the opening of mPTP, is a result of BAX, activation, this activation is prevented via Akt action which also suppresses BAK and activate anti-apoptotic proteins (Liang et al. 2014). From an evolutionary perspective and according to previous studies the mechanism of Akt action is that it provides an upstream regulator for apoptosis, since its phosphorylation appears to have a great role in caspase-independent apoptosis (Li et al. 2013, Winnay et al. 2013). In general, increases in the activity of Akt and Erk1/2 is considered to be protective to insults to the cell, such as ischaemia/reperfusion injury (Cai et al. 2017). However, detrimental effects have been demonstrated in different animal models including rat, upon the over activation of Akt results in opposite action to survival pathway during ischaemia during which an acute activation of Akt is what the cell need to survive for RI, however chronic activation of Akt lead to complications and it was found in heart falling patients (Harvey, Hussain and

Maddock 2014, Mockridge 2002). According to previous studies, possibility of myocardial injury because of Akt over expression happening due to mutation in mammalian hearts or that constitutive activation interferes with the protective mechanisms (Harvey, Hussain and Maddock 2014, Cai et al. 2017). The pathological effects of this appeared to be worsened when Ip was administered under conditions of I/R as it occurred in (Harvey, Hussain and Maddock 2014).

1.5.2 Mitogen-Activated Protein Kinases (MAPKs)

Mitogen-activated protein kinase (MAPK) signalling pathways are also involved in the apoptotic processes and inflammatory response of ischaemia and reperfusion I/R injury (Lan et al. 2017). Suchal et al. (2016) found that Erk1/Erk2 activation, a pro-survival kinase, inhibits JNK and p38 protein activities and decreases apoptosis by weakening the expression of pro-apoptotic proteins such as BAX and caspase-3 as was ascertained using terminal deoxynucleotidyl transferase dUTP nick end labeling (TUNEL assay) positive cells, and increased level of anti-apoptotic proteins (Bcl-2) (Suchal et al. 2016).

1.5.2.1 Extracellular Regulated Signalling Kinase (Erk1/2) Signalling Pathway

Extracellular signal-regulated kinase 1/2 (Erk1/2) is a prototypic mitogen-activated protein kinase (MAPK) signalling cascade protein (Tanimura and Takeda 2017). Erk1/2 regulates cell motility which is thought to be via the phosphorylation of many components that are involved in cell motility machinery as well as regulating many cellular functions including cell proliferation, survival and differentiation in response to extracellular cues. It was found that the

inhibition of Erk1/2 signalling is a promising strategy for cancer therapy as well as I/R injury due to its known involvement in RISK signalling, the latter provide cardio protection by the use of growth factor by reducing the infarct size (Tanimura and Takeda 2017). Erk1/2 is one of the majorly important signalling kinases in the RISK pathway. After I/R injury, the occurrence of Erk1/2's phosphorylation appears to be at a various periods of time throughout I/R during which Erk1/2's activation may lead to protection or damage in cardiac ischaemia, although its association remains to be determined unequivocally (Jiang et al. 2014). The proposed theory are that Ip exacerbate injury due to calcium overload and mitochondria fission as well as chronic activation of Erk1/2 causes more damage however, if just acute activation at the onset of reperfusion it will have a positive effect. Similar to Akt, Erk1/2's action is as an upstream regulator of apoptosis during reperfusion and Erk1/2's activation involves caspase-dependent apoptosis with properties that inhibit apoptosis, which is the main action of the PI3K/Akt signalling pathway of cellular defense. This means that Erk1/2's mechanism also results in a reduction in myocardial injury by inhibiting apoptosis and triggering cell proliferation (Yin et al. 2013). Erk1/2 was found to provide protective factors to I/R with an important key element in injury initiated after reperfusion through RISK signalling (Yin et al. 2013). By inhibiting Bcl-2 dephosphorylation, which is a known associated death promoter (BAD), BAD causes the development of the apoptosome to be inhibited thus restricting executioner caspase activation (Yin et al. 2013). As Akt overexpression may damage the cell in a similar manner to the chronic activation of Erk1/2, similar pattern appeared in Harvey, Hussain and Maddock study (2014). Given that

Erk1/2 activation is up-stream of Akt and both signalling pathways converge, this is not an unsurprising observation, although the exact mechanism still needs to be elucidated (Harvey, Hussain and Maddock 2014).

1.5.2.2 JNK Signalling Pathway

One of the MAP kinases group members identified in mammals and insects is c-Jun amino-terminal kinase, c-Jun N-terminal kinase (JNK) (Qu et al. 2020). It is activated by environmental stress and cell exposure to pro-inflammatory cytokines which implies a contribution to inflammatory responses by this pathway (Ip and Davis 1998). Studies based on genetic and biochemical aspects have demonstrated the potential of regulating cellular proliferation, apoptosis, and tissue morphogenesis by this pathway (Jiang et al. 2014, La Marca and Richardson 2020). Stress responses by the cell and physiological processes are both established by the functional role for JNK (Ip and Davis 1998). After ischaemia c-Jun NH_2-terminal kinases (JNKs) are activated this has been demonstrated with enormous evidence from studies in which JNK inhibitors are used in gene knockout mice, and other transgenic animals, in which JNK was not produced, thus shows the crucial role of JNK in I/R induced apoptosis (Jiang et al. 2014).

1.5.3 Drp1 Signalling Pathway

Drp1 is a member of the conserved dynamin large GTPase superfamily encompassing diverse membrane tubulation and fission functions, dynamic large GTPase Drp1/Dnm1Dynamin related proteins (Ko et al. 2016). The mitochondria

balance fission and fusion, and the gene encoded GTPase. Fusion when two adjacent mitochondria join, whereas fission, which relates to DNA replication, is when one mitochondrion separates into two during mitosis; both processes require Drp1 activation, via phosphorylation, which plays an important role in mitosis, apoptosis and programmed necrosis (Roe and Qi 2018).

Dephosphorylation of Drp1 at Serine ($_{637}$) stimulates apoptosis and inhibits fission, however, Drp1 Serine ($_{616}$) phosphorylation by B/cycl dependent kinase 1 inhibits apoptotic cell death (Ko et al. 2016). The mitochondria have two main functions in metabolic and survival pathways via various signalling cascades thus it is a therapeutic target for cancer (Roe and Qi 2018). Production and phosphorylation of Drp1 at Serine ($_{616}$) against the dephosphorylation of Drp1 at Serine ($_{637}$) results in Drp1 increasing mitochondria fission via Drp1 recruitment onto the surface of mitochondria followed by fission of two lipids in the membranes of mammalian cells where the process of fission is mediated by Drp1 with other proteins (Ko et al. 2016). However, the fission machinery is not fully known, despite knowing the balance between fission and fusion is crucial for a healthy cell. In cases of imbalance this will lead to pathological conditions (Liu et al. 2020). In the case of programmed cell death, Drp1 phosphorylation leads to its translocation onto the mitochondrial surface and activates voltage dependent anion channels (VDAC) (Helle et al. 2013). The latter is an important Ca^{2+} regulator in and out of mitochondrial membrane in pathological conditions it is modifying mPTP releasing apoptotic factors leading to the induction of free radicals from incomplete transfer of electron through the ETC resulting in swelling of mitochondria matrix and rupture 1.5 KDa from free radical (Managò, 2016,

Elnatan and Agard 2018). Drp1 also activate pro-apoptotic protein BAX leading to the release of cytochrome c leading apoptosis (Managò, 2016, Elnatan and Agard 2018). (Figure 1.9).

Figure 1.9 Drp1 pathway of inducing cardiac myocytes death via activation of mitochondrial fission

Figure 1. 9: The phosphorylation of Drp1 can lead to present the risk which produce mitochondria fission in pathological condition this leads to oxidative stress and the end result is apoptosis (Luna-Ortiz et al. 2011).

1.6 Calcium Signalling

Many essential cellular functions and processes required for intracellular signalling are performed by Ca^{2+}, including cardiovascular muscle contraction (Santulli et al. 2015).

With regards to cell cycle progression, the induction of resting cells (G_0) to re-enter the cell cycle is due to calcium signalling which helps activate the immediate early genes, it also plays an important role in promoting DNA synthesis initiation

(to move to S phase) and, also it stimulates events at mitosis contributing to the completion of the cell cycle (Berridhe 1995). An increasing number of anticancer therapies such as Fluorouracil (5FU), and immunosuppressant drugs are directed to the Ca^{2+} signalling pathway's role in cell proliferation (Humeau et al. 2018). The intracellular concentration of calcium (calcium homeostasis) stimulates various processes, these processes such as mechanism of Ca^{2+} and both 'on' and 'off' switches, which for intracellular Ca^{2+} act to either increase or decrease the concentration (Yang et al. 2015). The plasma membrane has a channel which is included in the Ca^{2+} 'on' mechanisms, which is responsible for regulating Ca^{2+} supply in the extracellular space (Bootman et al. 2001). The switch 'off' mechanisms is based on the removal process of calcium ions from the cytoplasm (Yang et al. 2015). Ca^{2+} ATPases are also involved, as well as exchangers which require other ions (e.g. Na^{+}/Ca^{2+} exchange) in order for Ca^{2+} to transporter out of the cell (Kohajda et al. 2020). Another important factor for cytosolic Ca^{2+} level regulation is mitochondria which despite its low affinity, it has high-capacity for the rapid Ca^{2+} uniporter that can significantly reduce cytosolic Ca^{2+} transients and diminish adverse cellular responses (Bootman et al. 2001). In addition, as for Ca^{2+} sequestration, the mitochondria are capable of activating and responding to cytosolic calcium signals if the mPTP is activated and small increases of intracellular Ca^{2+} levels are capable of initiating apoptosis via the mitochondria (Bootman et al. 2001). However, intercellular The Increase concentration of Ca^{2+} in myocardium following reperfusion injury increase the damage occurred to the heart muscles due to reperfusion injury, during ischaemia the calcium level increase intracellular and ATP is significantly reduced and the oxidative

phosphorylation is decreased as well and due to the increase in calcium level within the mitochondria following ischaemia which resulted in acidosis, as a consequence of reperfusion and the change in the pH, mPTP openned and oxidative stress occur causing the mitochondria to swelling and apoptosis or necrosis due to the depletion level of ATP, via the mPTP and initiation of apoptosis (Santulli et al. 2015). An important element for mitochondrial function is Ca^{2+} providing action to help the stimulation to ATP synthesis which is absent during I/R injury, as previously mentioned (Santulli et al. 2015). Therefore, there is a fine balance between there being sufficient Ca^{2+} levels to support oxidative phosphorylation and Ca^{2+} overload causing cardiomyocyte death.

Many pathologies occur when mitochondrial Ca^{2+} homeostasis is dysregulated, this is in part due to the generation of ROS due to calcium overload in the mitochondrial matrix, which may trigger the mPTP resulting in cytochrome c release, leading to apoptosis and it is considered that mPTP opening is a pivotal event initiating irreversible cell-death pathways following I/R (Brookes et al. 2004) (Figure.1.10).

Figure.1.10 illustrate the calcium signalling in normal condition against the case of calcium overload within the mitochondria.

Figure 1. 10: Calcium signaling in steady state and Calcium overload in the later the end result is apoptosis as prescribed in apoptosis cell death via the release of cytochrome c (Sterea and El Hiani 2020).

1.7 Oxidative Stress

Oxidative stress defention is imbalancelevel of ROS and antioxidants, it is the most common denominator of toxicity and many agents can lead to oxidative stress, such as chemical or physical factors such as exposure to UV, ionizing

radiations, pollutants, and heavy metals) and xenobiotics (i.e., antiblastic drugs) radiation, many fundamental aspects in cells are mediated by oxidative reactions such as cellular respiration and lipid synthesis (Srinivas et al. 2019). Patients who died from CHD and according to recent work carried out by Li et al. (2021) the reason for their death was AMI, I/R injury has also a detrimental effect on CHD patients. Given the restriction of blood as a result of the blockage is due to plaque accumulated in the coronary arteries, supply the left ventricular, the restricted blood flow results in a lack of oxygen to the heart muscle. This condition is known as coronary artery disease. Insufficient blood flow to the heart muscle can lead to symptoms of chest pain (Srinivas et al. 2019). Inadequate blood flow to the heart muscle is not being supplied, therefore there is a limitation of oxygen and nutrients leading to reduction in ATP and rising in Ca^{2+} which contributes to myocyte atrophy and necrosis. As previously described, the return of the blood, during reperfusion, results in exacerbation of the injury to the tissue, harm to cardiomyocytes, an inflammatory response and, depending on severity, irreversible myocardial damage and death (Srinivas et al. 2019). Ischaemic diseases are correlated with oxidative stress hence it is now, therapeutically, targeted to help improve ischaemic disease outcomes (Li et al. 2021). Oxidative stress usually can occur as a result of metabolism demand leading to free radical formation, during reperfusion, mitochondria dysfunction as a result of ROS production and calcium elevation as a well and changes in membrane potential leading to mitochondria swelling (Yu et al. 2018). A healthy amount of ROS is essential for cell survival whereas excess ROS could cause pathological conditions such as ROS can therefore be both essential and lethal, and the

various responses to ROS are important to normal physiology and in the development of many diseases, including cancer; it was also found that reactive nitrogen species (RNS) such as nitrogen dioxide (NO_2) and Peroxynitrite ($ONOO^-$), are also associated with oxidative stress (Li et al. 2021). A recent study, Yu et al. (2018), suggested strong evidence that mPTP opening is enhanced due to oxidative stress and ROS targeted mitochondria during reperfusion causing lipid peroxidation and oxidative change in protein function and structure resulting in mitochondria dysfunction and loss in matrix metalloproteases (MMP) during I/R (Yu et al. 2018) (Figure 1.11).

Figure 1.11 Oxidative stress and its sources and its effects.

Figure 1. 11: Sources of ROS and the general mechanisms by which oxidative stress can alter cellular function. Ataxia telangiectasia-mutated (ATM) is a member of the phosphoinositide 3-kinase-related protein kinase family that plays key role in DNA damage response (Wells et al. 2009).

1.8 Reactive Oxygen Species (ROS)

Reactive oxygen species (ROS) can be defined as highly reactive chemical from O_2 (Yang, Chen and Shi 2019). they act with a double function; they act as a second messenger for signalling in the cell this regulate many physiological functions (Li et al. 2021). However, ROS can be toxic products resulted from aerobic metabolism the latter can kill cells by oxidation (oxidative stress) (Yang, Chen and Shi 2019). ROS production can occurs as a consequence of a disequilibrium between detoxification, ROS and mitochondrial dysfunction (Li et al. 2021). High demand for metabolism features in many pathologies, such as heart diseases, diabetes, and liver cancer, as ROS often triggers adverse physiological events or a programmed pathway for cell death (Yang, Chen and Shi 2019, Oddone et al. 2020). During oxidative stress ROS targets DNA, RNA, proteins and lipids, they must be maintained at basal non-toxic levels in order to avoid initiation of death-signalling pathways (Yang, Chen and Shi 2019). Inflammatory diseases are characterised by ROS overload; thus, many compounds, such as Twenty-seven benzylidenecyclohexenone-based PL analogues (2a-v and 15a-e), are synthesised to target ROS (Oddone et al. 2020, Qian et al. 2020). ROS can induce DNA damage as short-lived molecules they are the hazardous byproducts from mitochondrial respiration and this leads to downstream cell death signalling cascades (Yang, Chen and Shi 2019). Hydroxyl radical ·OH produced from the decomposition of hydroperoxides (ROOH) and/or superoxide anion (it breaks down to water) they are formed when molecules or atoms gain or lose electrons, is one of the main reasons for DNA damage as well

as ionizing radiation inducing double strand breaks (DSBs) via direct high energy damage to the sugar backbone of DNA preventing cell division and inhibiting DNA repair mechanisms (Srinivas et al. 2019). Both ROS and the mitochondria have crucial roles in mediating apoptosis in physiological and pathological conditions. The mitochondria is both the source and the target of ROS as increases in ROS production leads to the release of cytochrome c triggering caspase-cascade activation this action appears to be mediated by ROS, either directly or indirectly (Oddone et al. 2020). However, it is thought that ROS can be used as cancer prevention mechanism or to enhance the therapeutic response since they have anti-apoptotic properties (Srinivas et al. 2019). ROS level may result in different outcomes depending on their abundance and this property may be exploited for cardiovascular conditions, including salvage of cells following an ischaemic event in patients with IHD (Srinivas et al. 2019).

1.9 Mitochondrial Permeability Transition Pore

The mitochondria, sometimes termed “the powerhouse of the cell” have a crucial role in determining the fate of a cell (Brand, Perevoshchikova and Quinlan 2013). In healthy cardiac myocytes, the basic function performed by mitochondria is the ATP synthesis via oxidative phosphorylation in order to cater for the continuous demands of the beating heart (Doenst, Nguyen and Abel 2013). All of the demands for the cell cannot be met by only glycolysis especially in the case of ischaemia as the oxidative phosphorylation changes from aerobic to anaerobic, leading to failure or causing heart function to stop (Halestrap, Clarke and Javadov 2004). However, the mitochondria have some mechanisms that means increases

in activation could change this organelle from a life supporter to a cause of cell death by inducing apoptosis or necrosis (Halestrap, Clarke and Javadov 2004). Since reperfusion injury correlate with nonspecific pore in the inner mitochondrial membrane (mPTP) opening, once opened, mPTP release apoptotic protein cytochrome c initiating apoptosis, which makes it essentially to become a target for the by preventing it to open (Halestrap, Clarke and Javadov 2004). In normal conditions of the cell mPTP remains closed, however, under stress cellular stress condition of calcium overload and oxidative stress which increases ROS production leading to mPTP opening as a consequence apoptotic cell death programme (Halestrap, Clarke and Javadov 2004, Mannella 2020). The opening of the mPTP can lead to the disruption with two major consequences; first any molecule less than 1.5 KDa can pass through to the mitochondrial membrane, despite the fact that in normal conditions small molecules are already moving across the membrane freely, but not proteins, therefore, in the case of mPTP opening intracellular fluid quickly enters the mitochondria leading to swelling, and eventual rupture, of the mitochondria (Halestrap, Clarke and Javadov 2004). The inner membrane of the mitochondria can be expanded because of the unfolding matrix without rupture (Mannella 2020). However, the outer membrane does not have this plasticity and will rupture which means the intermembrane space will be filled with proteins such as cytochrome c and APAF-1 in addition to other factors that indicate potential apoptotic cell death (Feldmann et al. 2000). The second outcome is that there becomes free accessibility to protons which are present in the inner membrane space (Zhao et al. 2019). This results in the uncoupling of oxidative phosphorylation leading to the activation of ATP

hydrolysation instead of synthesis due to the reverse action performed by proton-translocating ATPase (Lippe et al. 2019). Under these conditions, the concentration of intracellular level of ATP decreases readily causing degradative enzymes such as nucleases, and proteases to be activated and thus metabolic and ionic homeostasis is disturbed (Halestrap, Clarke and Javadov 2004). Once the above-mentioned changes to the cell occur, the damage is irreversible leading to necrosis if the pore cannot close (Halestrap, Clarke and Javadov 2004). Since the rupture of the outer membrane of the mitochondria results in ATP depletion due to the oxidative stress this leads to mitochondrial function collapsing (Halestrap, Clarke and Javadov 2004). High intercellular Ca^{2+} levels are a predominant key for the opening of mPTP when the pH is 7 or above, which explains why mPTP opening is not permitted during the acidic conditions of ischaemia (Feldmann et al. 2000) (Figure.1.12).

Figure.1.12 Mitochondrial Permeability Transition Pore in normal and diseased cells.

Figure 1. 12: Mitochondrial Permeability Transition Pore in normal heathy cell when the pore is closed with no calcium overload nor depletion of ATP maintaining the mitochondrial integrity, and diseased cells due to ATP decreased level and increase concentration of calcium with in the mitochondria mPTP open and cytochrome c is to be released to initiate apoptosis, hypothetical model of mPTP (Feldmann et al. 2000).

1.10 Muscarinic Receptors

Muscarinic Acetylcholine receptors (mAChRs) are G-protein coupled receptors (GPCRs) called seven-transmembrane receoptors which share high sequence homology with other GPCRs whose endogenous agonists are hormones and neurotransmitters and, as such, have an important role in cellular survival, ATP

production and smooth muscle contraction, many processes are stimulated and regulated by acetylcholine binding and activating muscarinic receptors (mAChRs) (Irvin-Sellers and White, 2015). Their structer is distinct and is haas a sngal polypeptide within the plasma membrane the external propotien provide the clefts for the ligand to bind towhich resulted in conformational change the latter start a signalling pathway via the subunit dissociation (Yue et al. 2006, Patanè 2015). mAChRs can be broadly classified into five subtypes distributed throughout the body with neuronal and non-neuronal action responsibility named M1, M2, M3, M4 and M5 based (Irvin-Sellers and White, 2015). Primarily Ipratropium bromide (Ip), which is a non-specific muscarinic antagonist, which bind to mAChRs instead of Ach with antagonism effect, Ip works on the M2 and M3 subtype of mAChRS group found to be situated on the surface of the cells in the smooth muscles including the bronchi in the lungs (Irvin-Sellers and White, 2015). mAChRS can mediate calcium influx, by which they can increase intracellular calcium (Irvin-Sellers and White, 2015). This action leads to smooth muscle contraction, which was confirmed via the observation during bronchoconstriction (Yue et al. 2006, Patanè 2015). A study, conducted by Yue et al. (2006) demonstrated that there are high levels of the expression of the M3-mAChR subtype located in ventricular myocytes, they also found that the expression of mAChRs was increased upon initiating ischaemia in myocytes especially the expression of M3-mAChR. Yue et al. (2006) showed that ischaemia, surprisingly, did not lead to that increase of M1, M2, M4 and M5- mAChR expression despite all five subtypes being present in the myocardium (Yue et al. 2006). The understanding that antagonist agents for mAChR receptors can cause smooth

muscle relaxation makes them a popular target for different pathophysiological conditions, especially respiratory conditions, such as COPD, in particular after being patented in 1966 (Yue et al. 2006). However, since 2008, morbidity and mortality has increased in (COPD) and asthma patients with underlying cardiovascular disease has been attributed to mAChR antagonists, due to the positive ionotropic and chronotropic effects they have on the mAChRs in the cardiovascular system, this has raised concern regarding the cardiovascular safety of these agents (Irvin-Sellers and White, 2015). Activation of mAChR provide both negative and positive inotropic and chronotropic effects in the heart, positive inotropic effects of cholinergic agonists are present only at high concentration of the agonist the dual effects of mAChR activation in heart may be a result of the presence of multiple subtypes of mAChRs (Yue et al. 2006). mAChR subtypes (M1–M5) have been identified, and each subtype is encoded by a different gene. Although M2 receptors have been considered to be the only functional mAChRs in the myocardium, new observations reveal that M3 receptors are also present in the hearts of various species (Irvin-Sellers and White, 2015). In the setting of *in vitro* myocardial ischaemia I/R injury and oxidative stress models, Khan (2015) investigated the effects of individual mAChR antagonists such as atropine. As well as the potential for the inhibition of the mitochondrial permeability transition pore (mPTP), Khan's study assessed individual mAChR antagonists using cyclosporine-A (CsA) which appeared to be protective and limited I/R injury (Khan 2015). Ca^{2+} ions create interactions between proteins myosin and actin by binding to c component of actin filament, the latter expose the binding site for myosin head to bind for stimulation of muscle

contraction binds to M3 muscarinic receptors on airway smooth muscle, a series of events is initiated which results in an increase in intracellular calcium (Ca^{2+}) and smooth muscle contraction (Yue et al. 2006). Furthermore, Khan (2015) linked the association between intracellular signalling pathways and the mAChRs antagonists that were investigated; the results indicated that there was a link to cause myocardial injury mediation which occurred in stressful conditions (Khan 2015). Langendorff results presenting that -M3 mAChR antagonist, where the ratio size of infraction was increased significantly of the heart ischaemia and reperfusion conditions, was caused by ipratropium (Khan 2015). Indicating that the muscarinic signalling involvements was because of the competing blocking effect at the cardiac mAChRs by ipratropium which causes the injury (Khan 2015). Acetylcholine (ACh) provided a mechanism of protection in which caspase-3 and Bcl-2 proteins were regulated preventing apoptosis (Khan 2015). In addition, the muscarinic activation induced by ACh also activate the Akt and Erk1/2 to protect the heart during reperfusion by inhibiting the opening of mPTP (Harvey, Hussain and Maddock 2014) (Figure.1.13).

Figure.1.13 Muscarinic Acetylcholine receptors mechanism of action upon the activation by ACh agonist.

Figure 1. 13: Acetylcholine muscarinic receptors signalling pathway mechanism of action upon the activation by ACh agonist binding leading to dissociation of subunit leading to generating signal to provide either inhibition effect when potassium is out of the cell or excitation in the cell once sodium/ calcium enters the cell causing smooth muscles to contract as discussed above (Khan 2015).

1.11 Ipratropium Bromide

Ipratropium bromide (8-isopropyl-noratropine-methobromide) (Ip) was the first anticholinergic agent approved for use as a bronchodilator (Figure 1.14) and has

been widely prescribed for the treatment of COPD since 1987, with a duration of action that lasts for six to eight hours Ipratropium bromide's mechanism of action is by blocking muscarinic acetylcholine receptors mAChRS that are located in the lung and in airway via its antagonist properties, specifically those present on the bronchial smooth muscle (Irvin-Sellers and White 2015). Ipratropium causes the smooth muscle to relax which occurs due to intercellular cyclic guanosine monophosphate (cyclic GMP) degradation (Irvin-Sellers and White 2015). ACh release at the cholinergic nerve endings is inhibited due to its antagonist effect on mAChRS thus the feedback to the receptor is inhibited (Irvin-Sellers and White 2015). Published literature had demonstrated that Ipratropium had the capacity to initiate both apoptosis and necrosis in myocardial cells providing an indication inhaled anticholinergics could potentially provide an adverse cardiovascular events risk in patients with COPD and underlying IHD (Harvey, Hussain and Maddock 2014). This work, for the first time, supported clinical observations from a met-anaylsis in 2008 preforemed by Singh et al. (2008) which indicated that premature death from adverse cardiovascular events could be increased by up to as much as 47% in COPD patients receiving ipratropium (Singh, Loke and Furberg 2008) (Figure 1.14).

Figure.1.14 the chemical structure of Ipratropium bromide.

Figure 1. 14: Ipratropium bromide chemical structure (Irvin-Sellers and White 2015).

1.12 Acetylcholine And Ipratropium Bromide Signalling

Acetylcholine (ACh) is the natural transmitter and endogenous stimulator of muscarinic receptors providing protection against apoptosis by which Bcl-2 proteins and caspase-3 are regulated through the RISK signalling pathway. It is well documented that acetylcholine is responsible for cytoprotective activities, including tissue salvage following I/R, the plasma level of Ach was not measured in the study however, in other study Acetylcholine assay for myocytes lysate under normoxia and Hypoxic conditions endogenous level of acetylcholine in normoxic control was 1.7 $x10^{-9}$ M and in the hypoxic control was 1.3 x 10^{-9} M (Harvey, Hussain and Maddock 2014). The Kinases signalling pathways indicate that ipratropium bromide antagonist action could be the reason for RISK degradation via salvage kinase signalling involving Akt, (Erk1/2) and PI(3)K

(Hausenloy and Yellon 2007, XY et al. 2016). In the execution of apoptosis, the main element is mainly by increasing activity of caspase-3 which probably occurs because of phosphorylation of serine/threonine residues due to the activation of pro-survival kinase such as Akt which regulates caspase-3 activity thus apoptosis (Wu et al. 2013). Harvey, Hussain and Maddock (2014) result presents acetylcholine effect upon the administration at the start and trough out reperfusion was able to reduce the damage induced by ipratropium, however, the exact mechanisms have not been elucidated (Harvey, Hussain and Maddock 2014) (Figure.1.15).

Figure.1.15 Acetylcholine chemical structure.

Some materials have been removed from this thesis due to Third Party Copyright. Pages where material has been removed are clearly marked in the electronic version. The unabridged version of the thesis can be viewed at the Lanchester Library, Coventry University

Figure 1. 15: The chemical structure of Acetylcholine (Wu et al. 2013).

1.13 KN-93 And CaM Kinase II

Ca^{2+}/calmodulin-dependent protein kinase II (CaMKII), is a protein kinase that is a potent transducer of Ca^{2+}signalling (Zhang and Brown 2004, Hegyi et al. 2015). This protein kinase modulates cellular functions in response to high levels of intracellular Ca^{2+} which mediates a range of phosphorylation to substrates in order maintain survival of the cell and reduce the possibility of cell death (Zhang

and Brown 2004, Hegyi et al. 2015). Ca^{2+}/calmodulin complex CaMKII regulates CaM kinase II providing a function in order to prevent myocyte apoptosis and regulates cardiac performance (Wang et al. 2004).

KN-93 (2-[N-(2-hydroxyethyl)-N-(4-methoxybenzenesulfonyl)] Amino-N-(4-chlorocinnamyl)-N-methylbenzylamine) can be defined as an inhibitor of CaM kinase II with a selectivity and a high potency (Zhang and Brown 2004). Many signalling pathways are related to CaMKII, KN-93 works in the cardiomyocytes via maintaining the homeostasis of calcium (Hegyi et al. 2015). CaMKII mis-regulation was demonstrated to cause heart arrhythmia related and contribute to cardiomyocyte loss during I/R (Erickson 2013, Hegyi et al. 2015).

The basic mechanism for KN-93, as shown (*in vitro*) in rat myocardium, is by providing a significant inhibition to the activities of CaM kinase activity by blocking Ca^{2+} channels and, as a result, the calcium overload is prevented (Hegyi et al. 2015). Previous studies have suggested that MI resulting from the antagonist action provided by Ipratropium bromide on myocardial mAChRS, is calcium signalling related due to calcium overload through a mechanism pathway that is unknown (Erickson 2013, Yang et al. 2021). However, Ca^{2+} homeostasis is known to play a crucial role in myocyte survival, therefore, investigations in nonclinical models (*in vitro*) were carried out for the determination of the relationship between the effects of Ipratropium bromide (CVEs) on myocytes in clinically relevant model of I/R, although the exact involvement of Ca^{2+} signalling was not fully determined (Figure.1.16).

Figure.1.16 KN-93 chemical structure.

Figure 1. 16: The chemical structure CaMKII inhibitor of KN-93 (Cassambai et al. 2019).

1.14 Mdivi-1 (Mitochondrial Division Inhibitor)

Mdivi-1 (mitochondrial division inhibitor) is also known as 3-(2,4-Dichloro-5-methoxyphenyl)-2,3-dihydro-2-thioxo-4(1H)-quinazolinone (Deng et al. 2021). Mdivi-1 has inhibition properties for cell death through myocardial ischaemia and reperfusion injury as well as providing protection against heart failure progression, it also prevents increase of apoptosis and abnormal mitophagy occurring following Ca^{2+} overload (Gharanei et al. 2013). Moreover, specific and non-specific actions of mdivi-1 is in reducing ischaemia reperfusion injury (Gharanei et al. 2013). The protective effects of mdivi-1 is thought to influence the mitochondrial fragmentation directly, which is found to occur simultaneously with the release of cytochrome c (Deng et al. 2021). The Gharanei et al. (2013)

study also showed that mdivi-1 is involved in delaying depolarisation and hypercontraction, parameters measured to identify mPTP opening, providing extra protection against ROS induced mPTP opening (Gharanei et al. 2013). Mitochondrial division inhibitor 1 (mdivi-1) inhibits Drp1-dependent mitochondrial fission, Mdivi-1 also blocks pro-apoptotic BAX-dependent cytochrome c release from isolated mitochondria (Cassidy-Stone et al. 2008) and attenuates neural cell death (*in vitro*) and (*in vivo*) (Figure.1.17).

Figure.1.17 the chemical structure of Mdivi-1.

Some materials have been removed from this thesis due to Third Party Copyright. Pages where material has been removed are clearly marked in the electronic version. The unabridged version of the thesis can be viewed at the Lanchester Library, Coventry University

Figure 1. 17: Mdivi-1 chemical structure (Gharanei et al. 2013).

1.15 Aims, Objectives And Hypothesis

1.15.1 Aims

The ultimate aim of this work was to try to further elucidate the mechanisms which lead to Ip induced myocardial injury, with a specific focus on the role of Ca^{2+} signalling and mitochondrial involvement. The aim of this project was to investigate the cytotoxic effects of Ipratropium bromide in *in vitro* models, such as Langendorff perfused hearts as well as the cytotoxic effects in adult cardiac myocytes in stressed conditions which were clinically relevant to myocardial I/R. The role of apoptosis and necrosis in Ip induced myocardial injury, cell signalling pathways associated with Ipratropium induced cardiotoxicity via assessing the phosphorylation status of extracellular signal-regulated kinase (Erk), phosphoinositide 3-kinase (PI3K)/protein kinase B (Akt) and caspases was investigated to try to further identify the signalling pathways. The role of the mitochondrial permeability transition pore in Ipratropium induced cardiac injury was investigated with the use of adjunctive agents (e.g KN-93 CaMKII inhibitor and Mdivi-1 mitochondrial division inhibitor) to identify whether these influence Ipratropium induced cardiotoxicity. Investigating the role of dynamin related protein1 (Drp1)-triggered mitochondrial fission which contributed to apoptosis under pathological conditions which it has emerged as a promising therapeutic target.

1.15.2 Objectives

Using clinically relevant, *in vitro* models of I/R, Adult Male Sprague Dawley rats were used to identify:

1. Whether ipratropium exacerbates myocardial injury following I/R, this was carried out using Langendorff and flow cytometry techniques using isolated myocytes.
2. Whether there was involvement of RISK signalling proteins in ipratropium mediated myocardial injury.
3. The role of Ca^{2+} and mitochondrial involvement in ipratropium mediated myocardial injury with use of KN-93 and Mdivi-1 as well as looking at the Drp-1 associated protein. This was carried out by co-administration of KN-93 and Mdivi-1 with ipratropium bromide and assessed via flow cytometry and Western Blotting.
4. Whether these changes occur at a protein or molecular level by also using PCR, if possible, to look at the template of the proteins involved in the pathways identified.

1.15.3 Hypothesis

Ipratropium bromide has previously been shown to exacerbate myocardial injury in *in vitro* models of I/R, however, despite evidence that this mechanism has mitochondrial involvement, the pathways have not been elucidated. For this work, it was hypothesised that, given the available evidence, the co-administration of KN-93 and Mdivi-1 with Ipratropium will demonstrate protection against the

observed Ipratropium induced injury and help to clarify the signalling pathways involved in ipratropium induced injury, specifically by confirming mitochondrial involvement.

Chapter 2: Material, Methods And Validation Studies

2.1 Materials And Reagents

Mdivi-1 Mitochondria division inhibitor, Ipratropium bromide were bought from Tocris Cookson (Bristol, UK). KN-93 CaMKII inhibitor was bought from Sigma Aldrich (Poole, UK). Salts in normal and modified Krebs-Heinsleit (Krebs-Ringer's) buffer, restoration buffer and Esumi ischaemic buffer: Sodium chloride, Sodium bicarbonate, Potassium chloride, Magnesium sulphate, Potassium dihydrogen phosphate, Glucose, Calcium chloride dehydrate and Dimethyl sulphoxide (DMSO) were obtained from Fisher Scientific (Loughborough, UK). Apart from Deoxyglucose, taurine, bovine serum albumin (BSA), HEPES, sodium pyruvate, Lactate and Penicillin Streptomycin, Formaldehyde which were purchased from Sigma Aldrich (Poole, UK). The Type II collagenase was bought from Lorne Laboratories (Berkshire, UK).

Red Active caspase-3 staining Kit, DRP1 Dynamin-related protein Antibody Bio Techne (Minneapolis, USA). Annexin V-FITC Apoptosis Staning / Detection Kit were purchased from Abcam (Cambridge, UK). CellROX ™ Green Flow Cytometry Assay was bought from Fisher Scientific (Loughborough, UK). Samples were analysed using a FACS Calibur™ flow cytometer from BD systems (St. Edmunds, Suffolk, UK).

For transfer of proteins onto PVDF membranes, Trans-Blot® Turbo™ transfer packs were used in conjunction with a Trans-Blot® Turbo™ transfer system as well as Mini-PROTEAN® TGX™ Precast Gels (4 - 20%) and a Mini PROTEAN® II system were used for electrophoretic protein separation and Precision Plus

Protein™ WesternC™ Standards were purchased from Bio-Rad (Hemel Hempstead, Hertfordshire, UK). Reagents required for the preparation of solutions used for Western Blotting Running Buffer, Restore ™ PLUS Western Blot Stripping Buffer were purchased from Fisher Scientific (Loughborough, UK), Bio Rad (Hemel Hempstead, Hertfordshire, UK) and Sigma Aldrich (Poole, UK). For the Western blotting studies, antibodies used (phospho-Erk1/2 (Thr_{202}/Thr_{204}) were purchased from New England BioLabs (Ipswich, MA, USA). Cleaved Caspase-3 (Asp_{175}) Rabbit anti-Human, Mouse, Clone: 269518, R&D Systems™, Phospho-AKT1 (Ser_{473}), clone: 99H9L9, Invitrogen™ were purchased from Fisher Scientific (Loughborough, UK). Phospho-DRP1 (Ser_{616}) (D9A1) Rabbit mAb brought from Cell Signailling Technology® (Massachusetts, USA). Western blotting buffers TBS, Tris Buffered Saline, 10X Solution, pH 7.4, Priece™ BCA Protein Assay Kit and for detection of proteins on the PVDF membranes, SuperSignal® West Femto Chemiluminescent Substrate™ were bought from purchased from Fisher Scientific (Loughborough, UK) which was used in order to detect target proteins in ranges as small as femtograms, to ensure maximum visualisation of proteins. Tris base from Fisher Bio- Reagent (Loughborough, UK). 5X First strand buffer was brought from Invitrogen (Loughborough, UK). Gen5 2.07 all microplates' reader software attached to Epoch™ 2 Microplate Spectrophotometer was bought from BioTek Instruments (Winooski, Vermont, USA). Tween 20 Fisher-bio reagent (Loughborough, UK). SDS, RNase Zap were bought from Ambion® (Loughborough, UK). PBS (10X), Trypan blue from Fisher Scientific (Loughborough, UK). Ethidium Bromide was purchased from Fisher Bio-Reagent (Loughborough, UK). Glycerol was bought from Fisher Scientific

(Loughborough, UK). EDTA, glycine, Methanol, NaOH, 20% SDS were brought from Fisher Chemical (Loughborough, UK). Bromophenol Blue, Isopropyl alcohol from Acros Organic (Loughborough, UK). $NaHCO_3$, MOPS were bought from Sigma Aldrich (Poole, UK). Milk powder from (Marvel, UK), Ethanol, Sodium acetate were purchases from Fisher Bio-Reagent (Loughborough, UK). IKA T 25 Digital ULTRA-TURRAX® Homogenizer Total pharmacy supply (Arlington, USA).

DNA Ladder GeneRuler 100 bp Plus, BACT Fwd and Rvs Primers, HPRT1 Fwd and Rvs Primers and Nanodrop spectrophotometer were bought from Thermo Fisher Scientific (Loughborough, UK) PrimePCR™ SYBR® Green Assay: GAPDH Rat, PrimePCR™ SYBR® Green Assay Dnm1l, Rat, SsoAdvanced Universal SYBR Green Supermix and dNTP solution at 10 mM and Bio-Rad CFX Connect™ PCR machine were brought from Bio-Rad (Hemel Hempstead, Hertfordshire, UK). Tetro cDNA Synthesis Kit and TRIsure™ Bioline (London, UK). GAPDH primer (QuantiTect, Qiagen, Manchester, UK). (In DEPC-treated water), DEPC-treated water (Diethyl pyrocarbonate) was purchased from Ambion® (Loughborough, UK). RNALater® were purchased from Sigma Aldrich (Poole, UK). Oligo dT $_{(20)}$ primer kit from Invitrogen (Loughborough, UK), (MTT [3-(4, 5-dimethylthiazol-2, 5-diphenyl tetrazolium bromide)] was bought from Melford (Chelsworth, Suffolk, UK). GelRed® Nucleic Acid Gel Stain bought from Biotium (Cambridge, UK).

2.1.1 Drugs Concentration Preparation And Solubility

Ipratropium bromide (diluted in RO water) Mdivi-1 and KN-93 (diluted in DMSO) to make (1 x 10^{-3} M) stock of each drug treatment, aliquoted into 1.5 ml microfuge tubes and kept at -20 ˚C, which were then added to Krebs-Heinsleit buffer (KHB) to give final experimental concentrations of Ipratropium bromide (1 x 10^{-9} M - 1 x 10^{-7} M), Mdivi-1 (1 x 10^{-7} M) and KN-93 (4 x 10^{-7} M) the concentrations were chosen due to clinical relevance. And they were added into restoration buffer to give the final concentration of (1 x 10^{-7} M) to all drug treatments. DMSO concentration in the working solution is <0.02%.

2.1.2 Animals

The animals used for all experiments were male Sprague-Dawley rats, which were adults 12-18 weeks old (340 g ± 30 g body weight) n=6 purchased from Charles River (Margate, Kent, UK). Animals were resided with the same conditions with free access to water and consistent, standard diet. Procedures were carried out following Home Office regulations and Animals (Scientific Procedure) Act 1986 complying with the Home Office / UK regulation, (which is accordance with a Schedule 1 Home Office Procedure).

2.2 Methods And Validation Studies

2.2.1 Langendorff Model Of Isolated Perfused Rat Heart

The technique used was established by Oscar Langendorff in 1897 for the isolation and perfusion of mammalian heart, this *ex vivo* method helped understand the heart physiology and the effect of important elements such as temperature, oxygenation as well as the importance of Ca^{2+} in myocardial contraction (Bell, Mocanu and Yellon 2011). The general principle is to maintain the heart for a couple of hours while it is receiving nutrition and oxygen to measure cardiac mechanical function, it is a cost-effective method and useful for pharmacological and cardiovascular research and has given crucial advances in ischaemia/reperfusion injury (Skrzypiec-Spring et al. 2007). ischaemia/reperfusion injury (Skrzypiec-Spring et al. 2007). The perfusion process occurs in reverse function in Langendorff apparatus via the cannulation of the aorta which is perfused with KHB (containing nutrition and oxygen 95%) (Skrzypiec-Spring et al. 2007). KHB, which is still used to mimic plasma, it contains the ions required for heart function. the buffer is widely used as perfusion buffer for isolated hearts mounted on Langendorff apparatus in which the drug treatments are usually added in the perfusate this enables the observation of their effect on the isolated heart also the method enables the digestion process into individual cells to harvest the cells for further measurements (Powell and Wapnir 1994).The Langendorff protocol was followed to measure haemodynamic function of the left developed ventricular pressure, heart rate and coronary flow, infarct size (I/R%) and area at risk ratio (AAR%) were also measured. For the hearts that were treated with Ipratropium bromide

(1 x 10^{-9} M-1 x 10^{-7} M), Mdivi-1 (1 x 10^{-7} M) ± Ipratropium bromide (1 x 10^{-7} M), or KN-93 CaMKII inhibitor (4 x 10^{-7} M) ± Ipratropium bromide (1 x 10^{-7} M) which was compared with I/R controls. All pharmacological agents were added at the onset, and throughout, reperfusion. At the onset of reperfusion, KHB was exchanged for KHB containing the appropriate drug concentration. The heart was perfused with KHB + drug(s) throughout reperfusion.

2.2.1.1 Rat Hearts Isolation And Perfusion

Cervical dislocation was the method used to sacrifice the adult male Sprague-Dawley rats (which was accordance with a Schedule 1 Home Office Procedure). The obtained heart was immediately put into ice cold Krebs-Heinsleit buffer (KHB) and transferred to Langendorff apparatus. Krebs-Heinsleit buffer (NaCl 1.18 x 10^{-1} M, $NaHCO_3$ 2.5 x 10^{-2} M , KCl 4.8 x 10^{-3} M, $MgSO_4$ 1.2 x 10^{-3} M, KH_2PO_4 1.2 x 10^{-3} M, $C_6H_{12}O_6$ 1.2 x 10^{-2} M) all of the salts mentioned were added in MilliQ water and dissolved before adding $CaCl_2 2H_2O$ at (1.7 x 10^{-3} M). The buffer was oxygenated 95% for 30 minutes prior to reverse loading into Langendorff apparatus to prevent bubbles from forming in the setup, the heart was mounted via aortic cannulation the apparatus was maintained at a temperature of 37 ˚C, KHB was oxygenated prior and during perfusion with 95% O_2 and 5% CO_2 for 175 minutes (Maddock, Mocanu and Yellon 2003) (as shown in Figure 2.1).

Figure 2. 1: Schematic diagram of Langendorff apparatus that have been utilized for hearts isolation experiments in which KHB buffer was running through water bath of 37 ˚C for 30 minutes prior and throughout the buffer is oxygenated which is reverse perfusion from the aorta (Watanabe and Okada 2018).

2.2.1.2 Inducing Ischaemia

The obtained heart was mounted on the Langendorff apparatus and left to stabilise for 20 minutes, which is determined by measuring the haemodynamic every 5 minutes and make sure they are within the inclusion criteria, (perfusion with KHB with regular assessment of haemodynamic function as described in section 2.2.1.6.1 - 2.2.1.6.3). Ischaemia was performed by insertion of a surgical suture under the descending branch of the left coronary arteries in which the thread was tightened using a snare structure initiating regional ischaemia which lasted for 35 minutes (Maddock, Mocanu and Yellon 2002). In order for the

regional ischaemia protocol to be effective left ventricular develop pressure and coronary flow decreased by 30 % and this was same for each heart.

2.2.1.3 Reperfusion

The snare was loosened in order to induce reperfusion by allowing restoration of KHB flow (as shown in Figure 2.2), which lasted for 120 minutes. In the drug treatment groups, the drugs were added at the initiation of reperfusion via perfusion with KHB solution containing the drugs. The treatment groups administered are (described in section 2.2.1.5). During the 175 minutes protocol the haemodynamic readings were taken even 15 minutes.

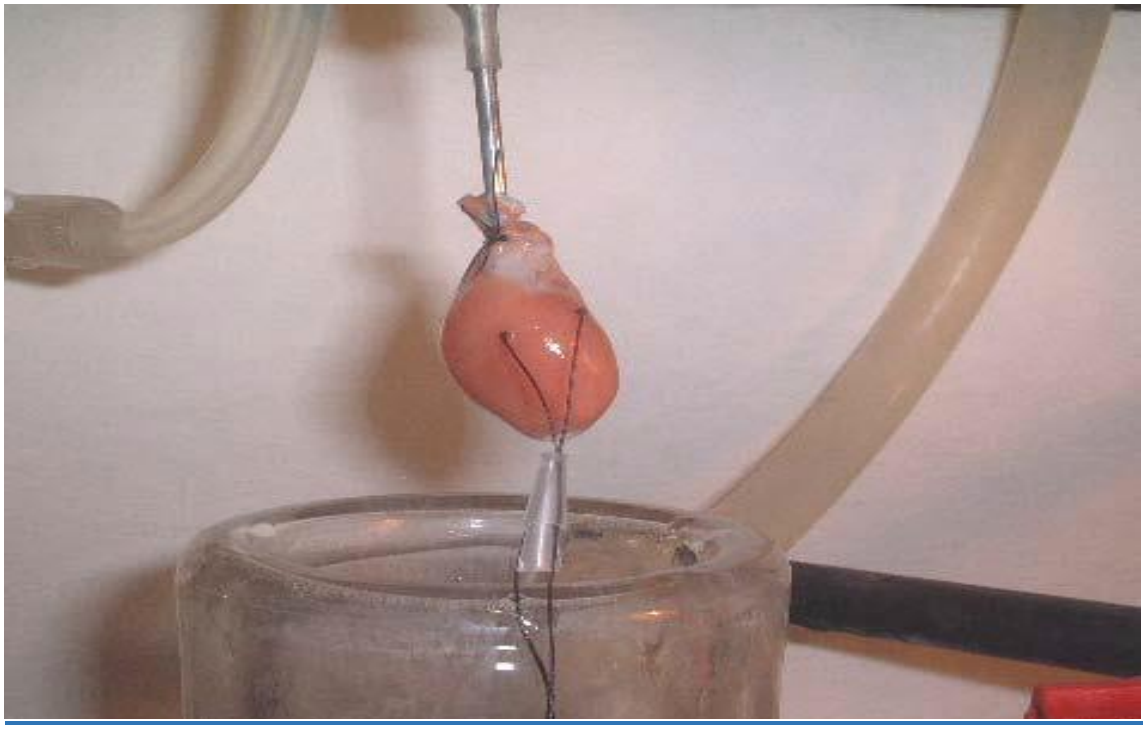

Figure 2. 2: Representative image showing a surgical suture inserted around the left descending coronary arties. The thread passed through tow plastic tubes to form snare and tightened to initiate regional ischaemia, reperfusion initiation by releasing the snare and loosening the thread.

2.2.1.4 Drug Treatment Administration

The period in which the drug reached the heart was calculated in relation to the overall volume with in the Langendorff apparatus (250 ml) and the average of the first and second coronary flow (CF) taken after inducing ischaemia by dividing the length of the system over the average CF obtained. This ensured that the administration of the drugs occurred at the onset of reperfusion. The complete protocol is shown in Figure 2.3.

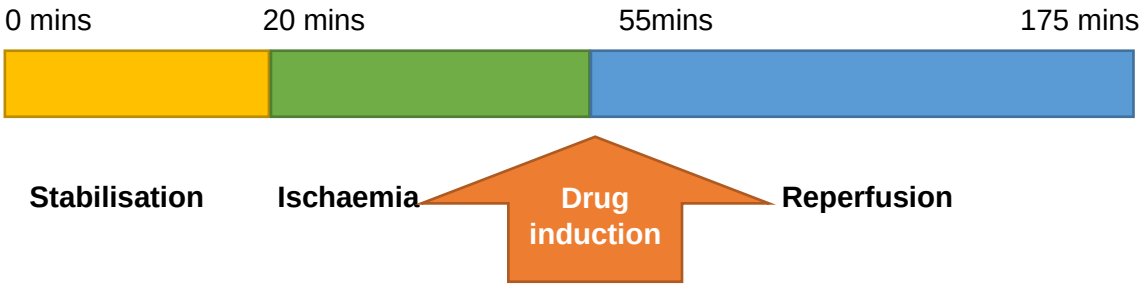

Figure 2. 3: Protocol to show where ischaemia, reperfusion and drug induction occurred. 20 minutes stabilisation, 35 minutes regional ischaemia followed by 120 minutes of reperfusion after which the heart was collected for AAR% assessments, the perfused buffer during reperfusion contains the appropriate drug concentration mentioned in table 2.1.

2.2.1.5 Experimental Design For Langendorff Study.

For the normoxic controls, hearts were perfused for 175 minutes with KHB with no I/R protocol, nor drugs were added to these hearts.

For the Ischaemia/reperfusion controls (I/R), regional ischaemia was initiated after 20 minutes stabilisation and lasted for 35 minutes. This was followed by reperfusion (for 120 minutes) without any drug treatment, therefore, KHB was

perfused to the heart for the total of 175 minutes protocol. For the drug treated groups, the Ischaemia/reperfusion protocol was carried out, and at reperfusion onset drugs were added. All drugs were dissolved in KHB and the treatment groups are shown in (table 2.1).

All the drug treatments used for Langendorff study.	Time
Ipratropium bromide (1 x 10^{-7} M) + KHB.	120 mins
Ipratropium bromide (1 x 10^{-8} M) + KHB	120 mins
Ipratropium bromide (1 x 10^{-9} M) + KHB	120 mins
Mdivi-1(1 x 10^{-7} M) + KHB	120 mins
Mdivi-1(1 x 10^{-7} M) + Ipratropium bromide (1 x 10^{-7} M) + KHB	120 mins
KN-93 (4 x 10^{-7} M) + KHB	120 mins
KN-93 (4 x 10^{-7} M) + Ipratropium bromide (1 x 10^{-7} M) + KHB	120 mins

Table 2. 1: Representation of the experimental design, which explain the addition of the drug treatments, n=6 per treatment, as well as the different concentrations used, the experiments lasted for 120 minutes reperfusion for Langendorff study.

After the last reading all the hearts were stained with Evans Blue and incubated at -20 ˚C overnight prior to infarct measurement (as described in section 2.2.1.7).

2.2.1.6 Assessment Of Haemodynamic Parameters (Normoxia, I/R Control)

During all the Langendorff experiments, the parameters (left ventricular developed pressure (LVDP), heart rate (HR) and coronary flow (CF)) readings were taken during the 55 minutes period, every 5 minutes and for the rest of 120 minutes every 15 minutes were recorded of the 175 minutes protocol, due to its relevancy, then the heart was taken out and frozen in the -20 ˚C freezer to calculate the infarct risk ratio (AAR%) (as described in section 2.2.1.7).

2.2.1.6.1 The Left Ventricular Developed Pressure (LVDP)

Left ventricular developed pressure (LVDP) was ascertained via use of a balloon made of latex filled with water that connected to pressure transducer, the balloon was placed in the left ventricular chamber. In order to validate the I/R method, it was necessary for there to be a significant reduction in haemodynamic function following initiation of ischaemia. Hearts where there was less than 50% decrease in LVDP were excluded as it indicates that the I/R protocol was not successful. Results are displayed as a percentage of the mean LVDP during the 175 minutes normoxic control, and stabilisation (first 20 minutes), ischaemia (for 35 minutes) and reperfusion (for 120 minutes) for I/R control. Figure 2.4 shows representative LVDP measurements comparing normoxia groups with I/R control groups with significant difference from the start of ischaemia until the last reading of the hearts used, thus validating the experimental technique.

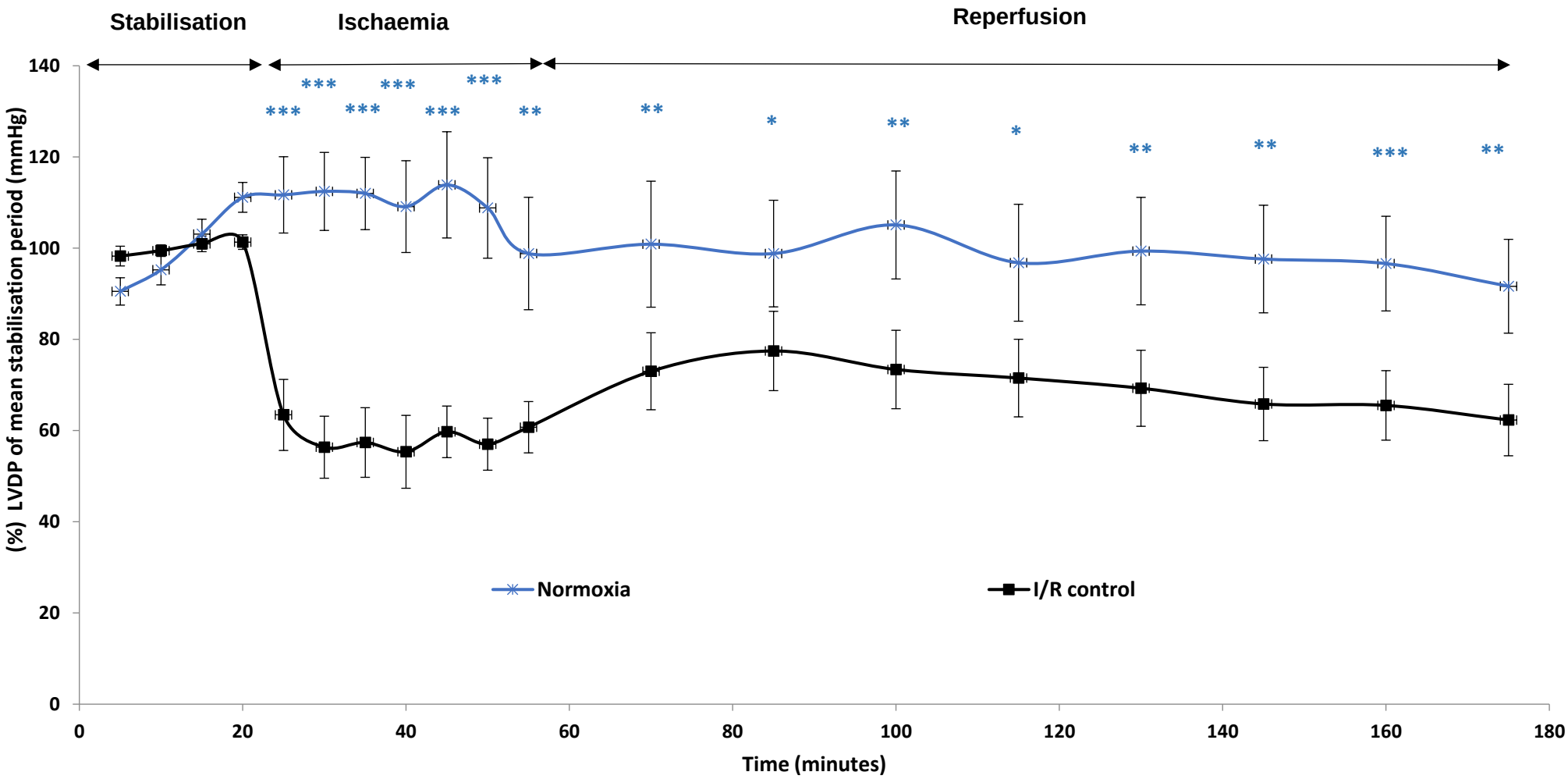

Figure 2. 4: Changes in left ventricular developed pressure % of (mmHg) in isolated perfused rat hearts group's for nomoxia and I/R control, to validate the technique, n=6. * p<0.05 vs. I/R control, ** p<0.01 vs. I/R control, *** p<0.001 vs. I/R control.

2.2.1.6.2 Heart Rate (HR)

Heart rate (HR) was also measured via a latex balloon filled with water that connected to pressure transducer, the balloon was placed in the left ventricle. There should not have been a statistical difference in heart rate observed following the onset of ischaemia. As demonstrated in Figure 2.5. Hearts where there was a haemodynamically significant difference in HR following the initiation of ischaemia were excluded. Results are displayed as a percentage of the means HR during the 175 minutes normoxic control, and stabilisation period (first 20 minutes), ischaemia period (for 35 minutes) and reperfusion (for 120 minutes) for I/R control.

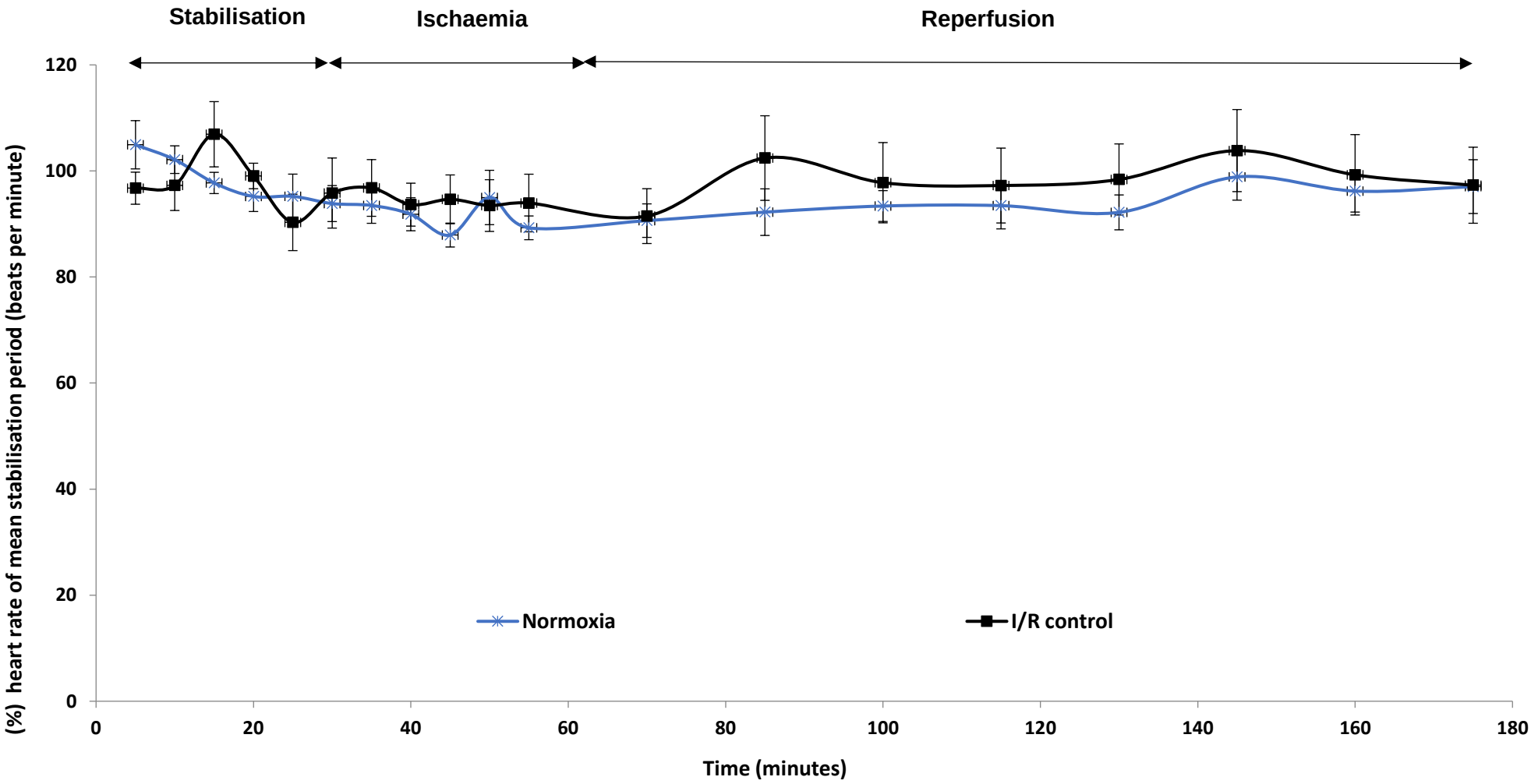

Figure 2. 5: Changes in heart rate (bpm) in isolated perfused rat hearts to validate the technique. For normoxia and I/R control, n=6. Overall, all there was no significant difference in terms of heart rate measurements.

2.2.1.6.3 Coronary Flow (CF)

Coronary flow (CF) readings and recordings were obtained via the collection of the volume of fluid dripping from the perfused hearts at a duration of one minute. In order to validate the I/R method, it was necessary for there to be a significant reduction in haemodynamic function following initiation of ischaemia. Hearts where there was less than 50% decrease in CF were excluded as it indicates that the I/R protocol was not successful. The obtained data were represented as percentage of the average of CF recordings throughout the period of the 175 minutes normoxic control, and stabilisation period (first 20 minutes), ischaemia period (for 35 minutes) and reperfusion (for 120 minutes) for I/R control (Figure 2.6). Shows representative CF measurements comparing normoxia groups with I/R control groups. During ischaemia there was a significant difference ($p<0.01$).

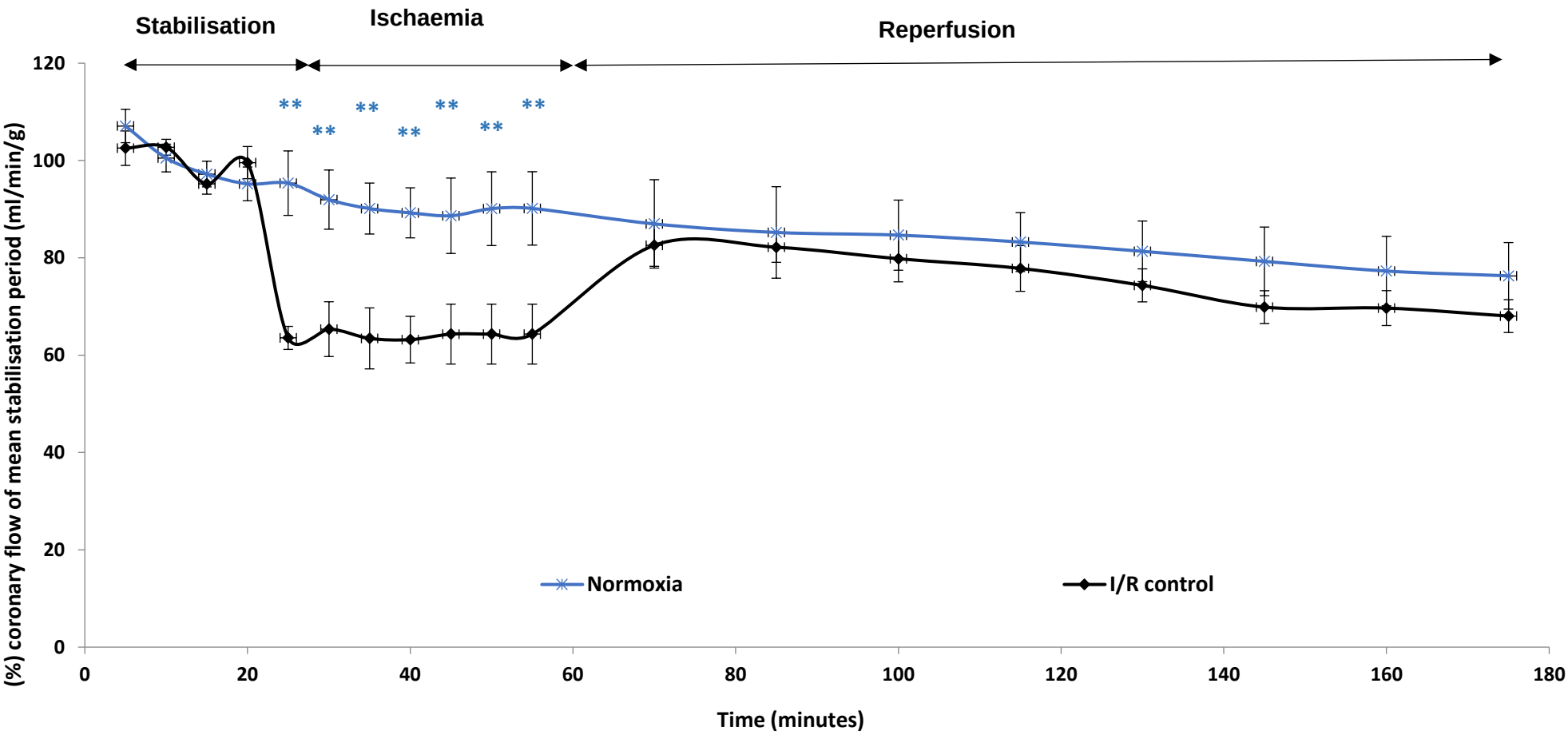

Figure 2. 6: Changes in coronary flow (ml.min-1) in isolated perfused rat hearts. For nomoxia and I/R control, n= 6. ** p<0.01 compared to I/R control.

2.2.1.7 Assessment Of The Infarct To Risk Ratio (AAR%)

During 175 minutes the isolated rat hearts were perfused with Krebs Heinsleit Buffer (KHB) for (normoxia and I/R controls), However, the other experiments perfusion with KHB lasted for 55 minutes 20 minutes stabilisation and 35 minutes regional ischaemia followed by KHB + drug treatments group for 120 minutes (described in table 2.1) (administered at the onset and throughout reperfusion). The determination of the infarct development was via the comparison between the percentage of tissue that is tetrazolium negative to tetrazolium positive (Infarct/Risk (%)). 0.25% Evans blue solution was injected after the last reading for reperfusion (at the last 175-minute time point) the thread used to cause regional ischaemia was tightened before perfusing the heart with Evans blue (1 ml) when the heart colour changed to blue, then the heart was quickly weighed and placed at -20 ˚C until frozen. Phosphate buffer Solution (NaH_2PO_4 1.06 x 10^{-1} M, $NaHPO_4$ 2 x 10^{-2} M) in 10 ml volume was made then it was put into 37 ˚C water bath. TTC (2,3,5-Triphenyltetrazolium chloride) was added into the phosphate buffer, to produce a 1% TTC solution. The TTC solution was warmed to 37 ˚C in a 50 ml centrifuge tube. Frozen hearts were taken out of the freezer, and sliced carefully, using forceps to hold the heart and using a scalpel cut approximately five ~2 - 3 mm sections then the heart sections were added to the TTC solution ensuring all sections were fully immersed, before being left to incubate at 37 ˚C for 15 minutes. Following the 15 minutes of incubation, the buffer was drained, 15 ml of 10% formaldehyde was added, and the heart sections were left to fix in formaldehyde for a minimum of 4 hours before analysis. Following four hours, slices were drained, blotted dry, and heart sections were

transferred to a glass board. To determine the development of the infarct, the heart pieces were aligned onto one glass board then compressed by adding other glass board on top, the boards were held in place with clips. A clear acetate sheet was used to outline and trace the heart sections and highlight areas of infarct compared with viable tissue in the areas subjected to the regional I/R protocol (infarcted areas appeared pale due to cell death, meaning no reaction with the TTC, whereas tissue 'at risk' appeared red due to the presence of mitochondrial dehydrogenase reacting with the TTC). The glass board was used to trace the heart slice against light lamp which will help differentiate between pale areas of thin tissue (yellow) and areas 'at risk' (pink) the infarct areas (white), viable (blue). Using a Planimetry software tool (ImageJ) the traces can be quantified, by tracing the heart slice, excluding the left ventricular cavity, measuring full area then tracing the infraction area within the heart slice. Image J then generate a value which can be used to calculated in infraction within the heat slice. The infarct ratio and an infarct-risk ratio was determined preforming the TTC for infarct and area at risk ratio (AAR%) (Figure 2.7). This Figure identifies that the protocol was successful as there is a significant increase in the I/R group compared with normoxia. (16.91 ± 1.89 % vs. 100 ± 0%) with ($p<0.001$).

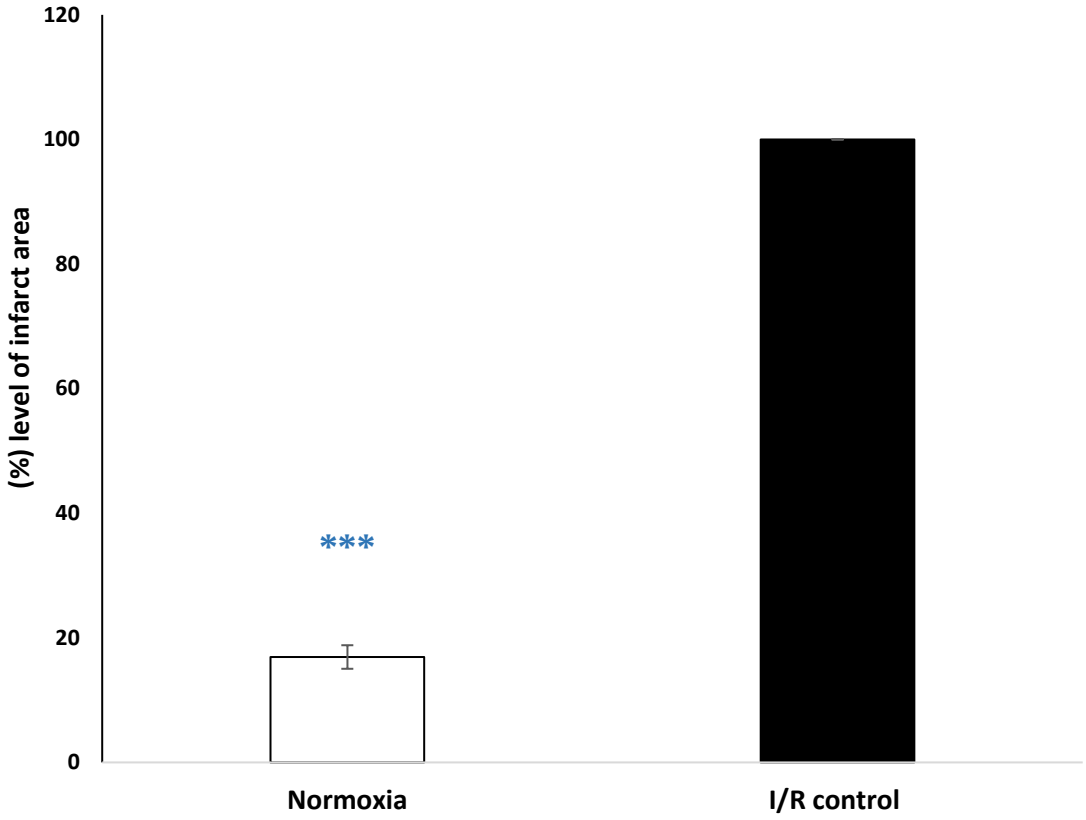

Figure 2. 7: Infarct development in normoxia and I/R control perfused isolated rat hearts. Results displayed as means + SEM, n=6. *** p<0.001 against I/R control.

2.2.1.8 Exclusion Criteria

The hearts that were not stabilised after 20 minutes for extraction and mounting into Langendorff apparatus were discarded based on the haemodynamic parameters displayed reading as well as the hearts that did not decreased after ischaemia and the ones that did not recover after inducing regional ischaemia these heart were not according to the criteria for the experiment used.

2.2.2 Flow Cytometry

Flow cytometry is to identify information based on physical characteristics and/or markers called antigens on the cell surface or within cells that are unique to that cell type (Hegde et al. 2005). For example, this technique is useful to evaluate certain type of cells such as blood cells from bone marrow or tumours (McKinnon 2018). An additional function of flow cytometry is the ability to sort cell types based on their characteristics (Rieseberg et al. 2001). Once a sample has passed through the laser light the detectors generate a photo based on the cell property (Rieseberg et al. 2001) (Figure 2.8).

Figure 2. 8: A diagram of flow cytometry technique works, , the technique utilised laser as a light source to produce scattered and fluorescent detectors to read the light signal (labtestsonline, 2021).

Throughout this work, flow cytometry protocols were followed to measure apoptosis, necrosis, live cells and caspase-3 for the cardiomyocytes that were treated as described in table 2.2 in comparison with nomoxia and Hypoxia and Reoxygenation (H/R) controls.

2.2.2.1 Cardiomyocyte Isolation Protocol

Following the same cervical dislocation method to sacrifice the rats, (as described in section 2.2.1.1) the obtained isolated heart was attached to a modified Langendorff apparatus in which Krebs-Ringer's buffer (KRB) (modified) was perfused (NaCl 1.16 x 10^{-1} M, $NaHCO_3$ 2 x 10^{-2} M, KCl 5.4 x 10^{-3} M, $MgSO_4$ 4 x 10^{-4} M, KH_2PO_4 1.2 x 10^{-3} M, $C_6H_{12}O_6$ 1.2 x 10^{-3} M , $C_2H_7NO_3S$ 2 x 10^{-2} M, $C_3H_3NaO_3$ 5 x 10^{-3} M, the buffer was warmed to 37 ˚C for 30 minutes and oxygenated during that time with 5% CO_2 and 95% O_2, pH 7.4) The heart was perfused with this buffer for 2 - 3 minutes until the heart stopped beating then the buffer was changed to KRB containing collagenase (0.05% collagenase type II and $CaCl_2$ (4.4 × 10^{-6} M)) and perfused for 5 - 6 minutes, then the heart was cut into smaller pieces and added into a 50 ml centrifuge tube containing the KRB + collagenase using a Pasteur pipette enzymatic dissociation was carried out by agitating the heart pieces with the pipette. After ~ 2 - 3 minutes, 15 ml of the digestion buffer was collected in a 15 ml centrifuge tube and centrifuged at 500 RPM for 2 minutes. Mechanical dissociation continued with the remaining heart pieces continued for a further 2 minutes before using nylon mesh to filter the cells into another 15 ml centrifuge tube and centrifuged for 2 minutes at 500 RPM. The supernatant was removed, and the two pellets combined and resuspended in restoration buffer (NaCl 1.16 x 10^{-1} M, $NaHCO_3$ 2.5 x 10^{-2} M, KCl 5.4 x 10^{-3} M, $MgSO_4$ 4 x 10^{-4} M, $C_6H_{12}O_6$ 1 x 10^{-2} M, $C_2H_7NO_3S$ 2 x 10^{-2} M, $C_3H_3NaO_3$ 5 x 10^{-3} M, KH_2PO_4 9 x 10^{-4} M, 1% Bovine Serum Albumin in the fridge Pen-strep 1%, $CaCl_2$ 1.13 x 10^{-3} M at pH 7.4 and 37 ˚C). Cell viability of the myocytes was ascertained via microscope inspection, myocytes with a viability of less than 75%

were discarded. Myocytes which were to be used in experiments then had 3.4 µl of 1M of $CaCl_2$ was added every 5 minutes for 20 minutes (Maddock, Mocanu and Yellon 2002). Cell viability measurements was again conducted via microscope and haemocytometer using Trypan blue exclusion and viability must exceed 65% or myocytes were excluded from further experiments.

2.2.2.2 Hypoxia And Reoxygenation Protocol

The cells obtained were divided, half were placed in the incubator with 5% CO_2, 20% O_2 and 37 ˚C for 1 hour in one of labelled 24 well plates for the normoxic controls, whereas the rest of the cardiac myocytes were centrifuged at 1,200 RPM for 2 minutes, discarding the supernatant and hypoxic buffer was added (KCl 12 x 10^{-3} M, MgCl 2 0.49 x 10^{-3} M, $CaCl_2$ 0.9 x 10^{-3} M, HEPES 4 x 10^{-3} M) to make the ischemic buffer (10 x 10^{-3} M, $C_6H_{12}O_5$ and 20 x 10^{-3} M $C_3H_6O_3$) were added to the ischaemic buffer (50 ml) in order to make hypoxic buffer at 37 ˚C. Hypoxic chamber in which the cells were incubated for a period of 2 hours at 37 ˚C in an air-tight with 0.2% O_2 and 5% CO_2 in 95% N_2 atmosphere. After putting the cells into hypoxic condition, they were centrifuged for 2 minutes at 1,200 RPM, and the hypoxic buffer was discarded. The myocytes were re-suspended in restoration buffer to initiate reoxygenation. Once drug treatments had been added at and during reoxygenation with final concentration of (1 x 10^{-7} M) as described in table 2.2, cells were incubated at 37 ˚C for two hours prior to experimental use (Figure 2.9).

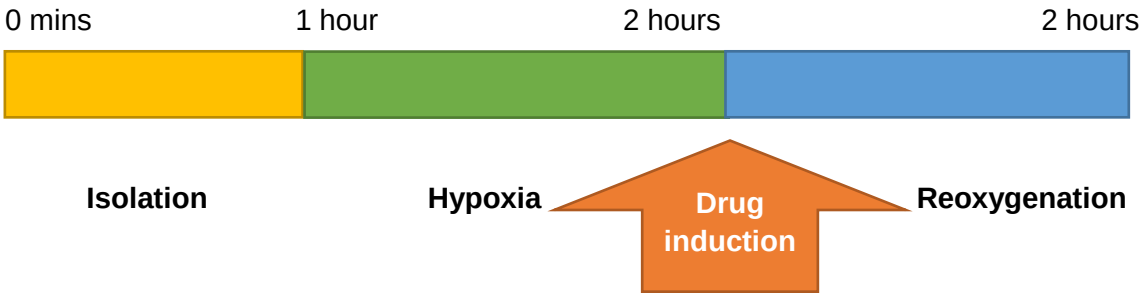

Figure 2. 9: Protocol to show where Hypoxia, Reoxygenation and drug induction occurred. Isolation of cardiac myocytes for 1 hour, 2 hours Hypoxia followed by 2 hours Reoxygenation with restoration buffer of KHB containing the appropriate drug concentration mentioned in table 2.2.

All the drug treatment used for flow cytometry study.	Time point
Ipratropium bromide (1 x 10^{-7} M) + restoration buffer.	2 hours
Mdivi-1(1 x 10^{-7} M) + restoration buffer.	2 hours
Mdivi-1(1 x 10^{-7} M) + Ipratropium bromide (1 x 10^{-7} M) + restoration buffer.	2 hours
KN-93 (1 x 10^{-7} M) + restoration buffer.	2 hours
KN-93 (1 x 10^{-7} M) + Ipratropium bromide (1 x 10^{-7} M) + restoration buffer.	2 hours

Table 2. 2: Representation of the drug treatments used, which explain the addition of the drug treatments, n=6 per treatment, as well as the different concentrations used, the experiments lasted for 2 hours reoxygenation for flow cytometry study.

2.2.2.3 Fixing Cardiomyocytes For Flow Cytometric Analysis

After reoxygenation, cells went through centrifugation at 1,200 RPM for 2 minutes discarding the supernatant then adding 6% formaldehyde 250 µl and 250 µl PBS on ice (1 tablet of PBS in 200 ml RO water) for 10 minutes at 37 ˚C following centrifugation, the supernatant was replaced with 250 µl of 90% methanol to fix and the samples were kept in the -80 ˚C freezer until ready for experimental use for caspase-3 assay.

2.2.2.4 Using The FACS (Flow Activated Cell Sorting) To Visualise The Cells

FACS Calibur™ flow cytometer was used to analyse samples, the fixed cells for the measurement of caspase-3 activity were used with the caspase-3 template provided, whereas for live cells the template has a different setting for the samples in which the cells were alive. Due to different templates provided by the software to measure live cells Annexin V templated to Annexin V-FITC A and Propidium iodide specific channel. It is divided quadrants to measure specific emission wavelength with 3 distinct populations live, necrosis and apoptosis which were plotted with different population, used in the template, was gated to count 10,000 cells per sample.

2.2.2.4.1 Cell Death Assay

Annexin V-FITC Apoptosis Staining / Detection Kit Stain. The same protocol for cell isolation and Hypoxia/Reoxygentaion induction was carried out (described in section 2.2.2.2), the cells were needed alive therefore, the cells were pipetted into 1.5 ml microfuge tubes after two-hour reoxygenation period had elapsed, centrifuged for 2 minutes at 1,200 RPM, discarding the supernatant. 200 µl Binding buffer was added and the myocytes were centrifuged again before adding 500 µl Binding buffer with 5 µl of Annexin V-FITC A and 5 µl Propidium iodide. The cells were incubated for apoptosis and necrosis detection for a period of for 5 minutes at 25 ˚C covered in foil prior to analysis by the flow cytometry. Figures 2.10 - 2.12 show comparisons between normoxic and H/R controls which verify the experimental technique and confirm that the H/R protocol had been successful via the observed increase in apoptosis.

The apoptosis was significantly less in the normoxic control compared with H/R. the stressed conditions led to cardiac myocytes to trigger programed cell death according to the results, this means that the technique been used is valid. (56.71 ± 11% vs. 100 ± 0%) with ($p<0.01$).

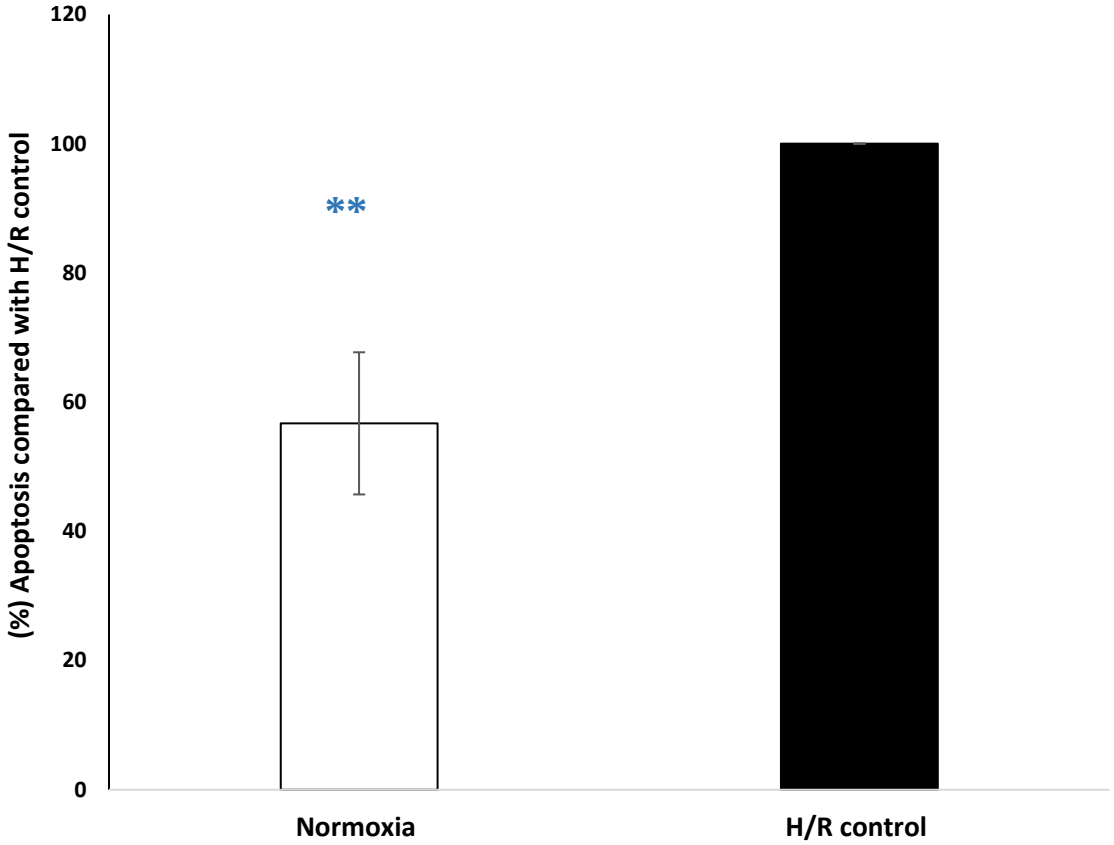

Figure 2. 10: Total apoptosis percentage results stained by Annexin V shown in flow cytometry for normoxia and H/R controls, the data was analysed after changing it into arithmetic means by normalised to H/R control, ± SEM, the recorded number myocytes is 10,000, n = 6. ** p<0.01 against HR control.

The results for necrotic cell death however, presented no significant difference with values (104.36 ± 6% vs. 100 ± 0%). Against H/R control.

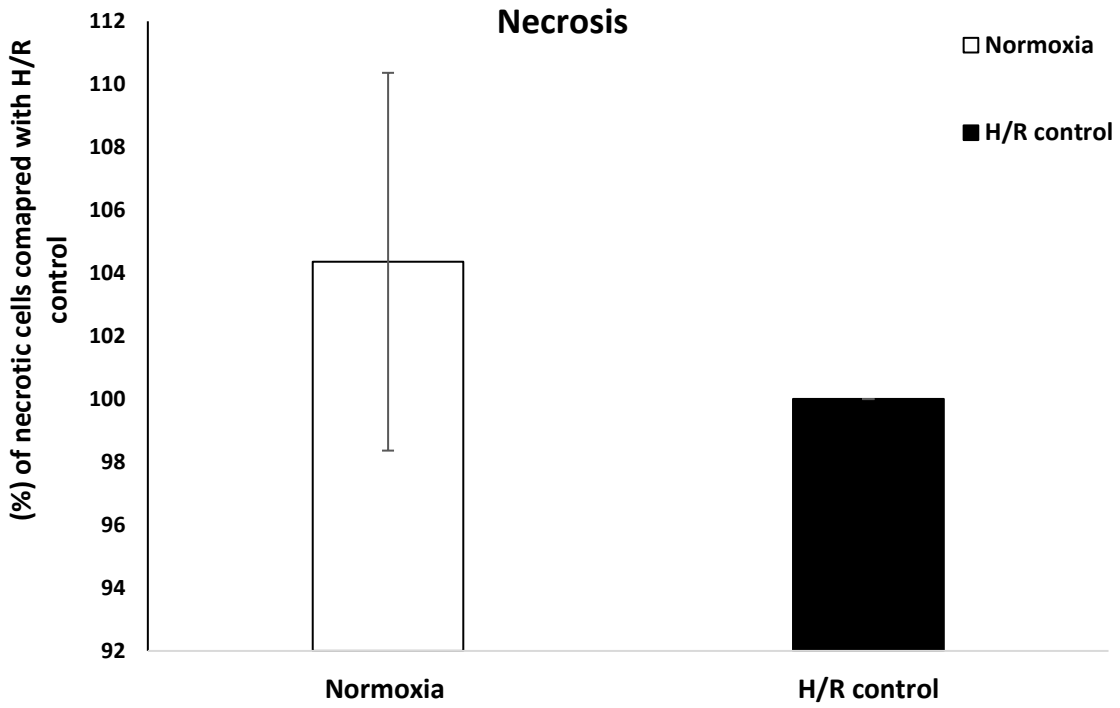

Figure 2. 11: Necrotic cells percentage results stained by Annexin V shown in flow cytometry for normoxia and H/R controls, the data was analysed after changing it into arithmetic means by normalised to H/R control, ± SEM, the recorded number myocytes is 10,000, n = 6. The results for necrotic cell death however, presented no significant difference with values (104.36 ± 6% vs. 100 ± 0%). Against H/R control. The reason for the high variation is due to the data obtained in the flow cytometry software which generated the data, and the statistical analysis presented no significant difference. Other reason is the data was generated with cell viability and apoptosis that might affect the variation of necrotic death.

The percentage of live cells detected in normoxic control is significant compared with the H/R control. More live cells are to be in normoxic control since the stimulated H/R will eventually stress the cells and lead to cardiac myocytes death (168.74 ± 7.99% vs. 100 ± 0%) with ($p<0.001$).

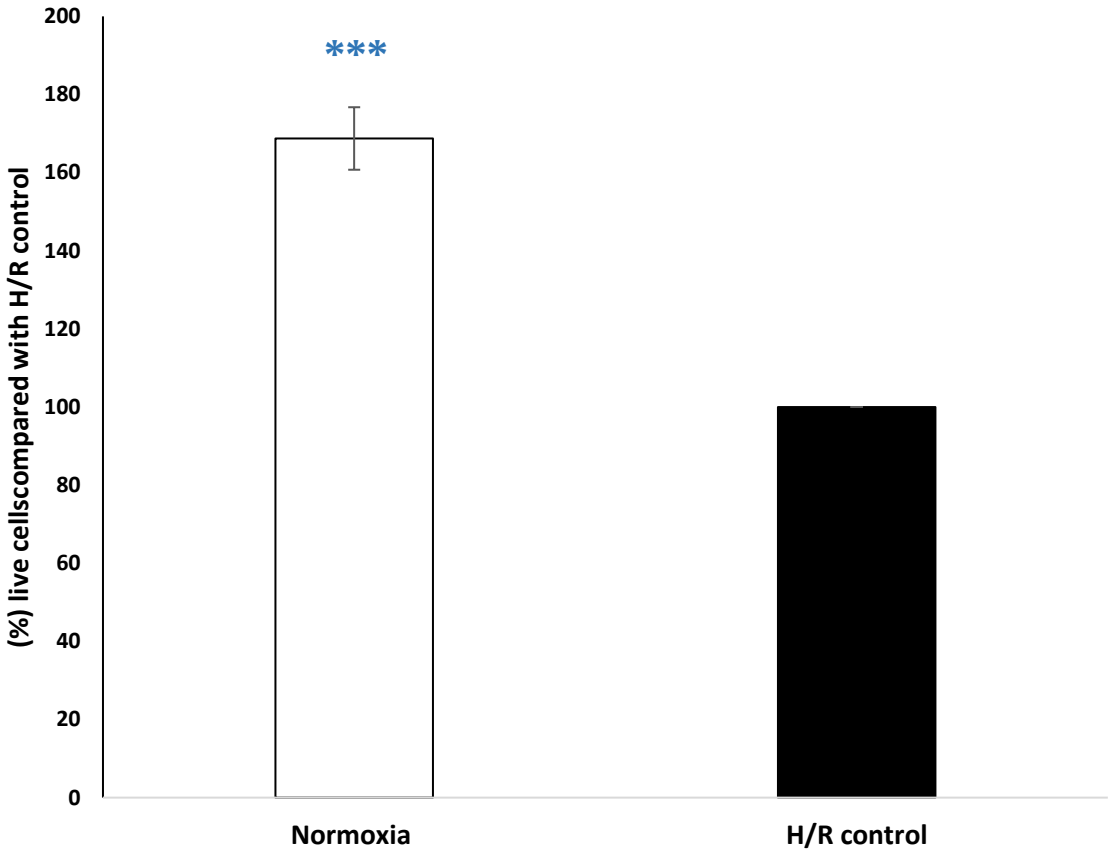

Figure 2. 12: Cell viability level in normoxic and H/R control the data was analysed after changing it into arithmetic means by normalised to H/R control, ± SEM, the recorded number myocytes is 10,000, n = 6. *** p<0.001 vs.HR control.

For all of the figures above, this forms part of methods flow cytometry validation.

2.2.2.4.2 Caspase-3 Assay

The fixed cells were taken out of the freezer, centrifuged for 3 minutes at 1,200 RPM the supernatant removed and 300 µl incubation buffer (0.25 g BSA in 50 ml PBS) was added to the pellet. 1 µl of Red-DEVD-FMK was added to each group after that it was incubated for 1 hour at 37 ˚C and 5% CO_2. Centrifuged for 5

minutes at 3,000 RPM, then washed with 500 µl wash buffer twice centrifuged after every wash at 12,000 RPM for 2 minutes and discarded the supernatant replacing it with 300 µl wash buffer. The cells were analysed by FACS Calibur™ flow cytometer (Al-Rajaibi, 2008) the channels used were FITC-A and PerCP-A which was according to the manufacture instructions for caspase-3 template. (Figure 2.13) demonstrates the difference between the normoxic and H/R control groups in change of caspase-3 activity, with a significant increase in the H/R control group compare to the normoxic control. The protocol used was to verify and validate the H/R protocol which was successful. (57.49 ± 14.27% vs. 100 ± 0%) with ($p<0.01$).

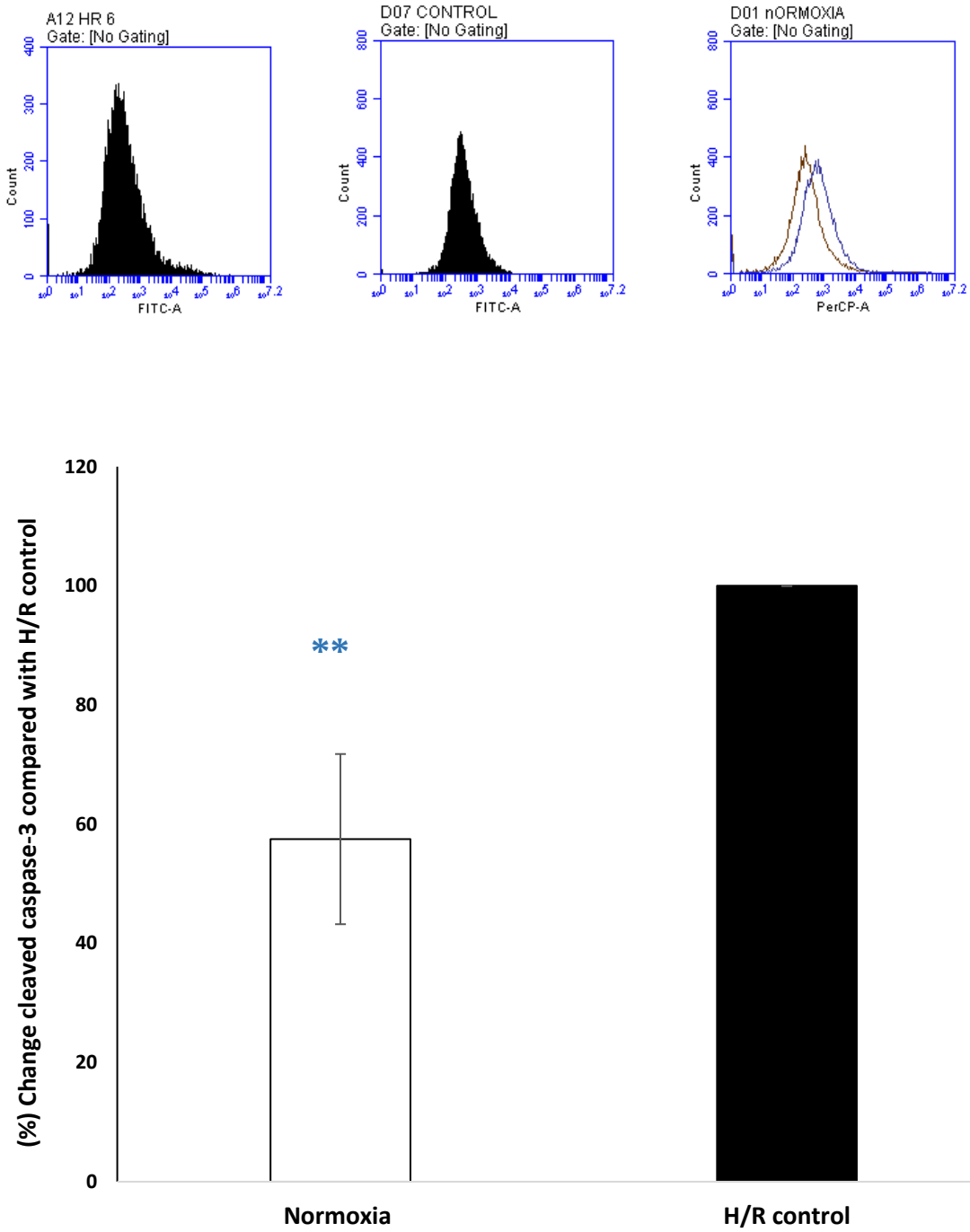

Figure 2. 13: The level of caspase-3 activity for normoxia in comparison to H/R control the data was analysed after changing it into arithmetic means by normalised to H/R control, ± SEM, the recorded number myocytes is 10,000, n = 6. ** $p<0.01$ against HR control.

2.2.2.4.3 Drp1 Dynamin-Related Protein Flow Cytometry Protocol

Cardiac myocytes were isolated, and hypoxia was carried out (as previously described in section 2.2.2.2), then the cells were incubated with the additions of drugs treatment during re-oxygenation. The cells were not fixed though instead the protocol was carried out while the cells are still alive, after the incubation period had passed the cells were put into the corresponding labelled microfuge tubes centrifuged for 2 minutes at 1,200 RPM discarding the supernatant before adding and 100 µl of staining buffer, incubation buffer (0.5% BSA in PBS) containing the Dynamin-related protein Antibody was added to the pellet. The dilution for the Drp1 Dynamin-related protein Antibody was 1:200 in incubation buffer for the flow cytometry protocol. The cells were incubated in the dark for 1 hour on ice 2 – 8 ˚C. Once finished incubating the cells were washed twice with incubation buffer 200 µl per wash centrifuged at 1,200 RPM for 2 minutes then 500 µl of staining buffer was added to the cells to be analysed by the flow cytometry.

2.2.2.4.4 CellROX

The negative and the positive controls for the CellROX assay were prepared according to the manufacturer's instruction. The negative control N-acetylcysteine (NAC) was prepared by resuspend 10 mg of NAC with 245 µl PBS to obtain (25 x 10^{-3} M). The positive control Tert-Butyl Hydro Peroxide Solution (TBHP) was prepared by adding 3.22 µl of TBHP with 496.8 µl of PBS to obtain

(5 x 10^{-2} M). The cells were incubated for a total of 4 hours in normoxic condition at 37 ˚C, 5% CO_2. The negative control was added before the incubation period started 4 µl in 1 ml cells to obtain (1 x 10^{-3} M). After one hour of incubation the cells were treated with the positive control 4 µl in 1 ml of cells to obtain 200 µM. CellRox (2.5 x 10^{-3} M). Component A was diluted 1:10 in DMSO. 11 µl CellROX in 9 µl DMSO to make (25 x 10^{-5} M). Then 2 µl of the diluted CellROX was added to the cells incubated for the last hour cells the final concentration was (5 x 10^{-7} M). During the last 15 minutes 1 µl of SYTOX green was added to the cells, to make the final concentration of (5 x 10^{-9} M).

2.2.2.4.5 MTT Assay

Colorimetric MTT [3-(4, 5-dimethylthiazol-2,5-diphenyl tetrazolium bromide)] is an assay that is utilised to the evaluate the viability of the cells. The MTT colour is yellow that was added to PBS buffer (5 mg/ml) placed in dark protector container; PBS was sterile; autoclaved the amount required before adding MTT. Ventricular myocytes were isolated (as described in section 2.2.2.1) and they were counted via haemocytometer. Using trypan blue exclusion which helps distinguish between cells that are alive (viable) and dead cells. If the viability exceeded 65% the experiment was continued otherwise the cells were discarded. The isolated cardiac myocytes were resuspended in hypoxic buffer and exposed to 2 hours hypoxia and 1 ml were kept and incubated in the normal incubator as a normoxic control (as described in section 2.2.2.2). To initiate reoxygenation, myocytes were placed into groups with the treatment drugs randomly assigned and

counting 1 x 10^6 cells.ml^{-1} to be resuspended in restoration buffer containing the drug treatments (described in table 2.2) treatment group. The number of cells were calculated via the use of haemocytometer and trypan blue exclusion so the number of cells per well it is equivalent to 1000,000 cells per ml (1000 µl) with restoration buffer.

The cells were placed into 96 well plate at 1x10^3 cells /100 µl cell suspension of concentration (100 µl of the produced suspension per well) the calculation required is based on the cells number that were counted using the haemocytometer. 100 µl of restoration buffer were used as a control in replicates in the presence and absence of the drug treatments were used and aliquot into the 96 well plates. Re oxygenation lasted 2 hours at 37 ˚C in the cell culture incubator with the drug treatment, in well + replicates then take the restoration buffer and treatments out then place it with 50 µl MTT to each well and then incubate for overnight, in the next day spin the 96 well plate for 2 minutes at 1,000 RPM using the centrifuge specific for the plates the supernatant was discarded of every well carefully without disturbing the cells. Add 50 µl per well DMSO place the plate platform that mix for a duration of 10 minutes place the plates on the plate reader before the analysis of colorimetric at OD 450 nm wavelength, using the microplate reader.

In cardiac myocytes isolation if cell viability was less than 65% the cells were discarded for it will affect the number of cells in the wells thus effecting the results.

2.2.3 Western Blotting Protocol

The Langendorff protocol was followed to isolate left ventricular tissue with haemodynamic measurements to make sure the tissue is within the inclusion criteria and that ischaemic protocol was successful (described in sections 2.2.1.1 to 2.2.1.4). Figure 2.14 shows the overall principle of Western Blotting.

Figure 2. 14: A western blot diagram of the technique used for isolated proteins from left ventricle tissue isolated from rat heart experiments. To measure the effect of the treatments on the proteins of interest (Western blot protocol - Creative BioMart 2002).

Apart from the hearts were not stained with Evans blue at the end of the protocol. The tissues (left ventricle) were collected for normoxia, I/R and the treatments (mentioned in table 2.3) which was compared with normoxia and I/R controls, at different time points, either 15 minutes after reperfusion or 30 minutes (Figure 2.15).

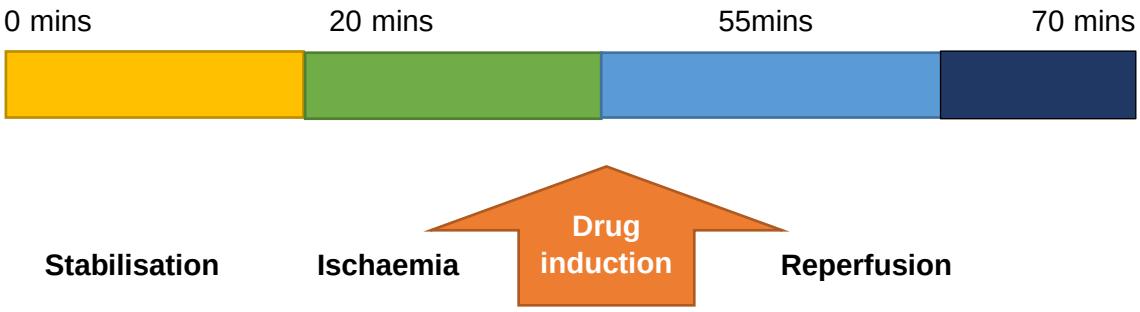

Figure 2. 15: Protocol to show where ischaemia, reperfusion and drug induction occurred. 20 minutes stabilisation, 35 minutes regional ischaemia followed by eighter 15 or 30 minutes of reperfusion when tissue was collected of KHB containing the appropriate drug concentration mentioned in table 2.3.

2.2.3.1 Experimental Design For Western Blot Protocol

Each group was n=6: normoxic controls, the heart was perfused with normal KHB buffer for 70 or 85 minutes. Ischaemia/reperfusion controls (I/R) regional ischaemia was initiated followed by reperfusion without any drug treatment for 15 or 30 minutes. Ischaemia/reperfusion protocol for regional ischaemia was performed then at reperfusion onset; the drug treatment groups were added + KHB 15 or 30 minutes was perfused as described in table 2.2 (table 2.3).

Experimental design of drug treatments used for western blot protocol	Time point 1	Time point 1
Ipratropium bromide (1 x 10^{-7} M) + KHB.	15 mins	30 mins
Ipratropium bromide (1 x 10^{-8} M) + KHB	15 mins	30 mins
Ipratropium bromide (1 x 10^{-9} M) + KHB	15 mins	30 mins
Mdivi-1(1 x 10^{-7} M) + KHB	15 mins	30 mins
Mdivi-1(1 x 10^{-7} M) + Ipratropium bromide (1 x 10^{-7} M) + KHB	15 mins	30 mins
KN-93 (4 x 10^{-7} M) + KHB	15 mins	30 mins
KN-93 (4 x 10^{-7} M) + Ipratropium bromide (1 x 10^{-7} M) + KHB	15 mins	30 mins

Table 2. 3 : Representation of the drug treatments, explain the addition of the drug treatments at the onset and throughout reperfusion, n=6 per treatment, as well as the different concentrations used, the experiments lasted for 15 minutes or 30 minutes reperfusion for western blot study.

The left ventricular tissue (area exposed to the I/R protocol) was then cut and snap frozen in liquid nitrogen then placed in -80 ˚C.

2.2.3.2 Tissue Homogenising

Approximately 75 mg was sliced from the frozen left ventricular tissue (area subjected to the I/R protocol) and put into 2 ml microfuge tubes that has rounded bottoms and 400 µl lysis buffer was added (NaCl at 1 x 10^{-1} M, $C_4H_{11}NO_3$ (pH 7.6) 1 x 10^{-2} M, $C_{10}H_{16}N_2O_8$ (pH 8.0) 1 x 10^{-3} M, $Na_4P_2O_7$ 2 x 10^{-3} M, NaF 2 x10^{-}

^{3} M, β-glycerophosphate 2 x 10^{-3} M, $C_7H_7FO_2S$ 5.7 x 10^{-8} M, Aprotinin 1.5 x 10^{-10} M, Leupeptin 23.4 x 10^{-10} M, cocktail tablets protease inhibitor 1/1.5 2 x 10^{-3} M, $C_8H_{11}ClFNO_2S$ 4.1 x 10^{-8} M) the homogeniser IKA Labortechnik T25 was used at the power of 5 to homogenise the tissue into solution the tube then was placed on ice. The tubes were put into the centrifuge at the power of 11,000 RPM which lasted for 10 minutes at 4 ˚C. The supernatant, which contains the proteins needed, was decanted into new labelled microfuge tubes that were placed on ice. The pellets were discarded (Maddock, Mocanu and Yellon 2002, Yue et al. 2006).

2.2.3.3 Protein Concentration Measurements

The measurement for protein concentration was carried out utilising the Pierce™ BCA Protein Assay Kit, the standard in which the concentration of the protein was measured, were made by adding BSA standards into lysis buffer as the diluent, 9 standards labelled A-I in which A was the most concentrated without dilution and I was lysis buffer with no BSA (Bovine Serum Albumin) reagent in it, the assay range of concentration was 2000- 0 µg/ml. The standards were replicated and 10 µl of each standard was added into 96 well plates, whereas 2 µl of each sample was added into the same 96 well plates which means they were 5 times less concentrated than the known standards and the samples were triplicated 18 samples were used 9 were normoxia, I/R and 7 treatment group (mentioned in table 2.3) at the time point 30 minutes after reperfusion and the other 9 samples were in the same order at the 15 minutes after the start of reperfusion in total 54 unknown samples . After preparing the BCA assay, the well plate was covered

with foil put into the well plate shaker then for 30 minutes it was incubated at 37 ˚C. The well plate was left at room temperature before it was inserted into plate reader which was a Gen5 2.07 all microplates' reader software attached to Epoch™ 2 Microplate Spectrophotometer, BCA assay in which the plate was read at a wavelength of 562 nm which provide numbers of the protein concentrations. The data was exported to an Excel sheet. The calculations for unknown protein concentration were based absorbance to concentration ratio for the standards to generate a standard curve (Figure 2.16).

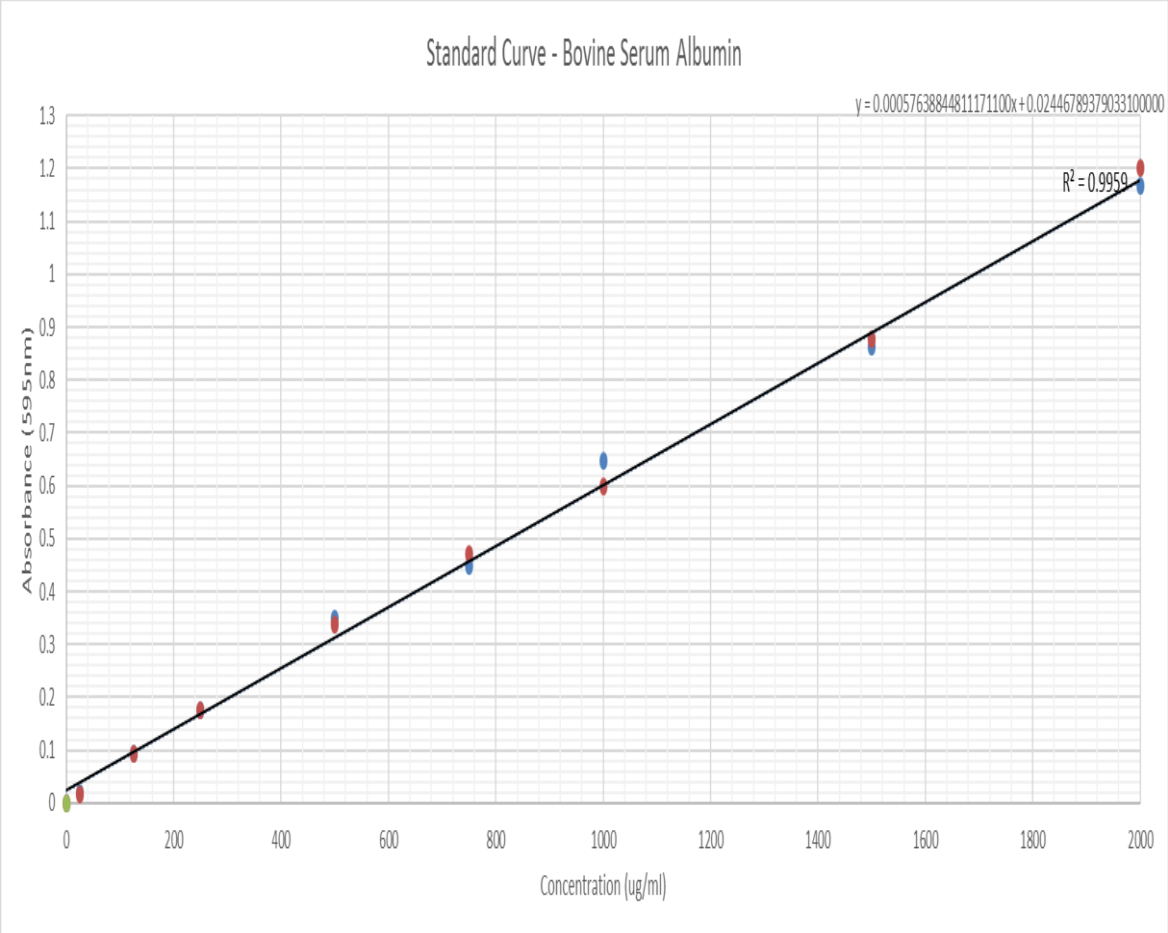

Figure 2. 16: The generated standard curve from BCA assay generated using Gen.5 software.

The obtained values were used to calculate 60µg of protein per sample for the gel run, this concentration was chosen in order to depict a clear image of the proteins used as it was advised by the supervisory team for protein abundance quality and dilution of the antibody for the detection system for common protein kinases. With the right concentration, which was optimised and calculated using the BCA assay, the samples were diluted in sample buffer 1:1, sample buffer (2.5 x 10^{-1} M $C_4H_{11}NO_3$-HCl (pH 6.8), 10% $C_3H_8O_3$, 0.006% Bromophenol blue, 4% $C_{12}H_{25}NaSO_4$, β- C_2H_6OS (pH 6.8)). After measuring their concentration, the samples were placed at 90 ˚C in a heating block in order to boil for 5 minutes followed by placing immediately on ice for electrophoresis measurement (Yue et al. 2006).

2.2.3.4 Electrophoresis

Bio-Rad PowerPac Basic Mini Electrophoresis System was used separate the samples utilising Mini PROTEAN® Tetra system and precast gels. The acrylamide gel was placed in the electrode assembly unit after removing the green strip at the bottom of the gel. The gel was put in the cast and the comb was removed gently. The inner chamber was filled with 125 ml running buffer, ($C_2H_5NO_2$ 1.9 x 10^{-8} M, $C_{12}H_{25}NaSO_4$ 3.4 x 10^{-6} M, $C_4H_{11}NO_3$ 2.4 x 10^{-7} M) and poured to be filled up and the outer chamber above the wire. 5 µl of visible ladder Precision Plus Protein ™ Western C™ Standards was pipetted into number 1 well of the gel well number 2 was left blank then a labelled microfuge tube containing 15 µl sample + sample buffer was loaded after it was centrifuged at the power of 11,000 RPM,

and 4 ˚C for 2 minutes starting from well number 3 the samples loaded at 11 well the last well was loaded with sample buffer. At least 2 gels were run at a time one for n=1 at 15 minutes after the onset of reperfusion and the other gel for n=1 at 30 minutes after reperfusion. Power-Pac 3000 for 60 minutes the electrophoresis was run at 130V (Yue et al. 2006).

2.2.3.5 Transferring Protein Samples From The Gels To The Membrane

Transferring the loaded samples from the gel onto the membrane was carried out using the Trans-Blot® Turbo™ Transfer system from Bio-Rad one membrane was used to transfer loaded samples from two gels where the end the gel was placed into the centre of the membrane using the Trans-Blot® Turbo™ Transfer Pack Midi Format 0.2 um PVDF, the power was set for 2 mini gels for 7 minutes at 25 V and 2.5 A after placing the cassette that has the transferred gels and membrane into the tank. After running the system for 7 minutes (transferring) the gels were discarded and the membrane was cut in half where the gels meet and placed into blocking buffer (15 ml (10X) TBST (0.1 x 10 M NaCl, 1.9 x 10^{-8} M $C_4H_{11}NO_3$, 10% Tween 20) + 5% milk powder for signal membrane for one hour on orbital shaker at 25 ˚C to help remove any non-specific binding proteins following by washing the membrane using 15 ml TBST 3 x 5 minutes then the membrane was incubated with primary antibodies for phospho-Akt, phospho-Drp1, phospho-Erk1/2, cleaved caspase-3 and GAPDH (TBST 5 ml + primary antibody 5 µl + milk powder 5%) for each signal blot the primary anti body dilution was in the ratio 1:10, as advised by the manufacturer. Membranes were placed in 50 ml

centrifuge tubes with 5 ml of the antibody solution and put on a roller at 4 ˚C overnight. The next day the membrane was once again placed on an orbital shaker plate washed with 15 ml TBST per membrane for 3 times that lasted 5 minutes followed by 60 minutes period of incubation with anti-rabbit IgG, HRP-linked the secondary antibody (TBST 15 ml, milk powder 5%, secondary antibody1.5 µl) the membrane was incubated at 25 ˚C washed with TBST 3 x 5 minutes (Yue et al. 2006). The milk was substituted with BSA with the same amount in the making of primary antibody, blocking buffer or secondary antibody for caspase-3 and Drp1 experiments.

2.2.3.6 Blot Visualising Using The ChemiDoc

The blot analysis was carried out by using the SuperSignal West Femto® sensitive substrate and the Bio Rad software ChemiDoc™ Touch Imaging System. Once the blot was ready to be visualised SuperSignal West Femto® buffer was made by adding 500 µl of each component into 15 ml centrifuge tube that was wrapped with foil to form 1ml that was added into the blot, 500 µl peroxide buffer and 500 µl of luminol/enhancer solution sensitive toward the light the blot was put into clear acetate sheet placed then visualised using the ChemiDoc system the UV enable the proteins to be visible during which time the phospho form of the antibody was visible in the shape of bands as the machine was turned on signal channel was selected then application selection for blot then chemiluminesence then run (Yue et al. 2006). The western blot ladder is visible

in the colorimetric image whereas the protein band can be seen via chemiluminescence, all in the transilluminator.

2.2.3.7 Stripping The Membranes To Re-probe For Total Level Of Proteins

In order to measure of the total of phosphorylated antibodies, the membranes that were incubated with the primary antibodies were stripped for 5 minutes using Restore™ PLUS Western Blot Stripping Buffer on an orbital shaker to remove unwanted and strip the pervious used phosphorylated antibodies following by blocking the membranes for 60 minutes at 25 ˚C ((1X) TBST 15 ml + milk powder 5%) then they were washed with TBST buffer 3 x 5 minutes then the membrane were incubated overnight at 4 ˚C on a roller with primary total form of the antibodies Akt , Drp 1, Erk1/2 and caspase-3 or GAPDH. The next day 3 x 5 minutes TBST buffer washing then 60 minutes incubation in 15 ml secondary antibody buffer anti-rabbit IgG HRP-linked (TBST 15 ml, milk powder 5% secondary antibody 1.5 µl) washing again with 3 x 5 minutes TBST buffer before utilising the West Femto® kit buffers were mixed 1 ml of each added 1 ml per blot and the ChemiDoc (BioRad) was used to visualise the membrane (Yue et al. 2006).

2.2.3.8 Confirmation Of Successful Protocol: 15 Minute Post-reperfusion Studies

Adult male Sprague-Dawley rats (300 ± 50 g) were sacrificed via cervical dislocation (as previously described in sections 2.2.1.1 - 2.2.1.5) prior to extraction of the heart which was mounted on a modified Langendorff perfusion apparatus. Apart from the normoxia control groups, regional ischaemia was induced via ligation of the descending left coronary arteries for 35 minutes followed by 15 minutes' reperfusion. Apart from normoxia, and I/R control, the drug treatments were added at the onset of, and throughout, reperfusion (as previously described). The tissues were collected after reperfusion when the hearts were removed and the left ventricle was cut from the heart, snap frozen in liquid nitrogen before being wrapped in foil and incubated at -80 ˚C for the preparation for execration proteins. Tissue was homogenised and prepared for Western blot analysis, as previously described. (Figures 2.17 - 2.20). These Figures demonstrate the difference between the normoxic and I/R control groups to verify the I/R protocol had been successful with a pattern of reduction in normoxic control.

2.2.3.9 Confirmation Of Successful Protocol: 30 Minute Post-reperfusion Studies

Protocol was carried out as for the 15 minutes of reperfusion experiments. However, reperfusion lasted for 30 minutes for this protocol I/R control significantly increase the phosphorylation of Akt. (28.16 ± 5.76% vs. 100 ± 0%) with ($p<0.05$) for Akt at 30 minutes reperfusion. The validation of the technique which showed that the protocol was successful (48.73 ± 10.64% vs. 100 ± 0%)

with ($p<0.05$) for Erk1/2 at 15 minutes. (36.58 ± 9.72% vs. 100 ± 0%) with ($p<0.05$) at 30 minutes.

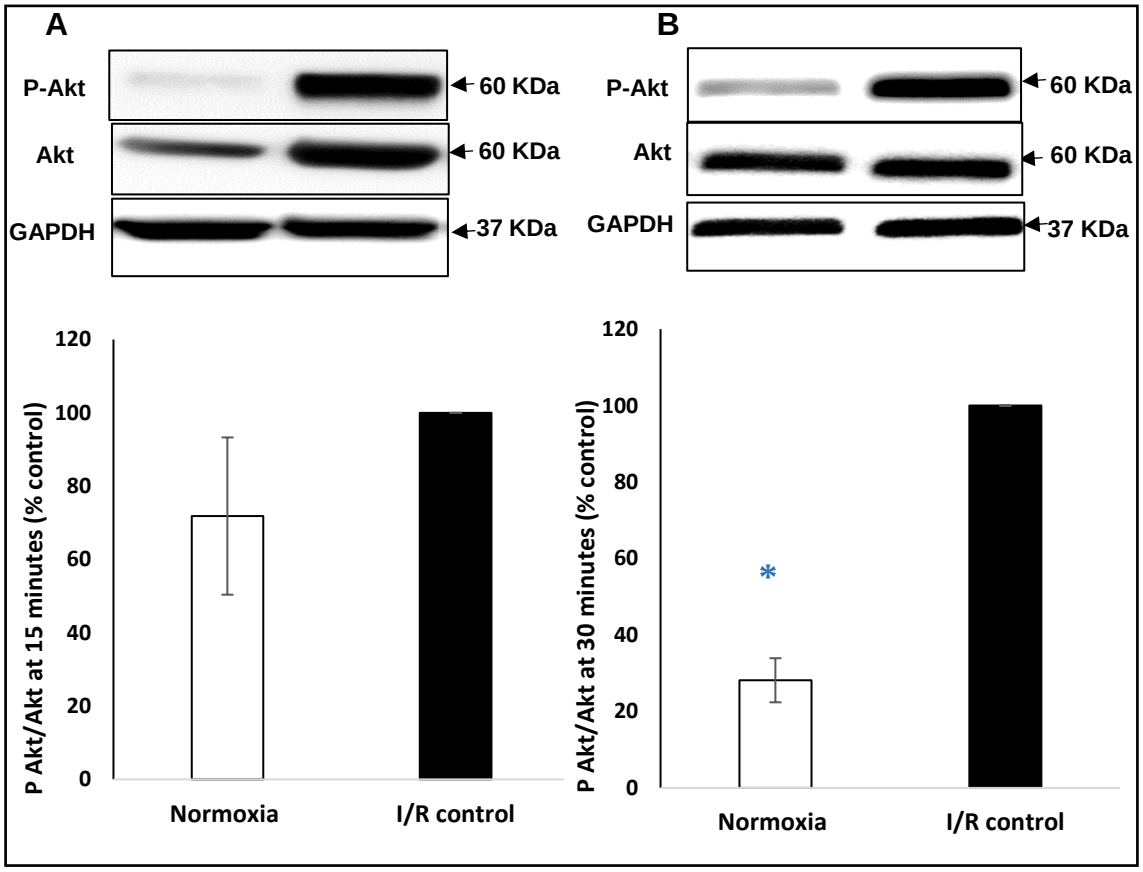

Figure 2. 17: The levels of phospho and Total Akt Normoxia in I/R control. A is the control groups perfused for 15 minutes isolated rat hearts. B is the control groups perfused for 30 minutes isolated rat hearts. Results displayed as means + SEM, n=6. I/R control significantly increase the phosphorylation of Akt. * $p<0.05$ vs. I/R control. I/R control significantly increase the phosphorylation of Akt

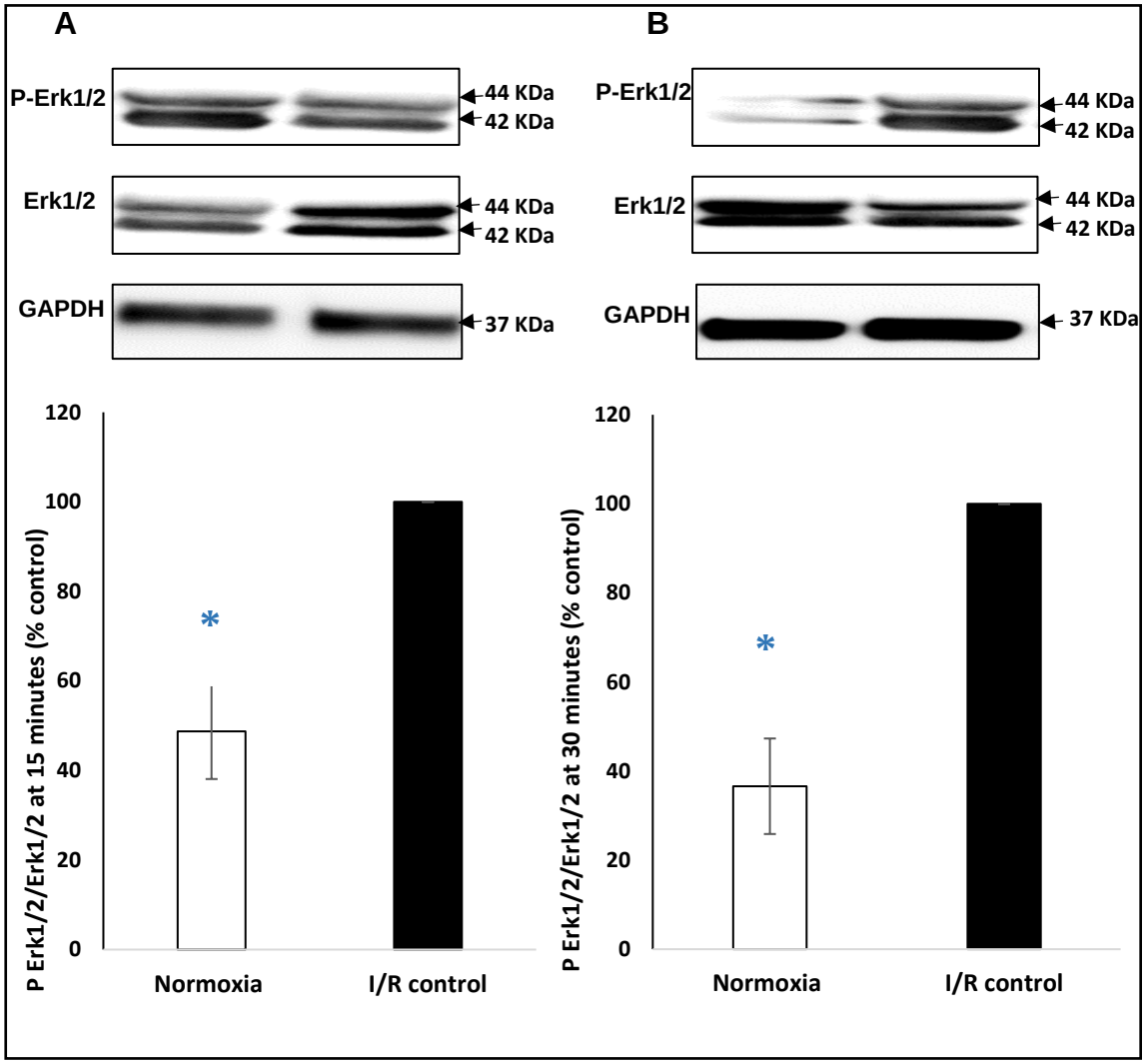

Figure 2. 18: The levels of phospho and Total Erk1/2 Normoxia in I/R control. A is the control groups perfused for 15 minutes isolated rat hearts. B is the control groups perfused for 30 minutes isolated rat hearts. Results displayed as means + SEM, n=6. * p<0.05 vs. I/R control.

In the blots normalized data to measure the expression of Drp1 (figure 2.23) the values were (40.01 ± 11.88% vs. 100 ± 0%) at 15 minutes with a significant different of (p<0.01), for 30 minutes (37.31 ± 9.35% vs. 100 ± 0%) (p<0.05). This validation of the technique which showed that the protocol was successful.

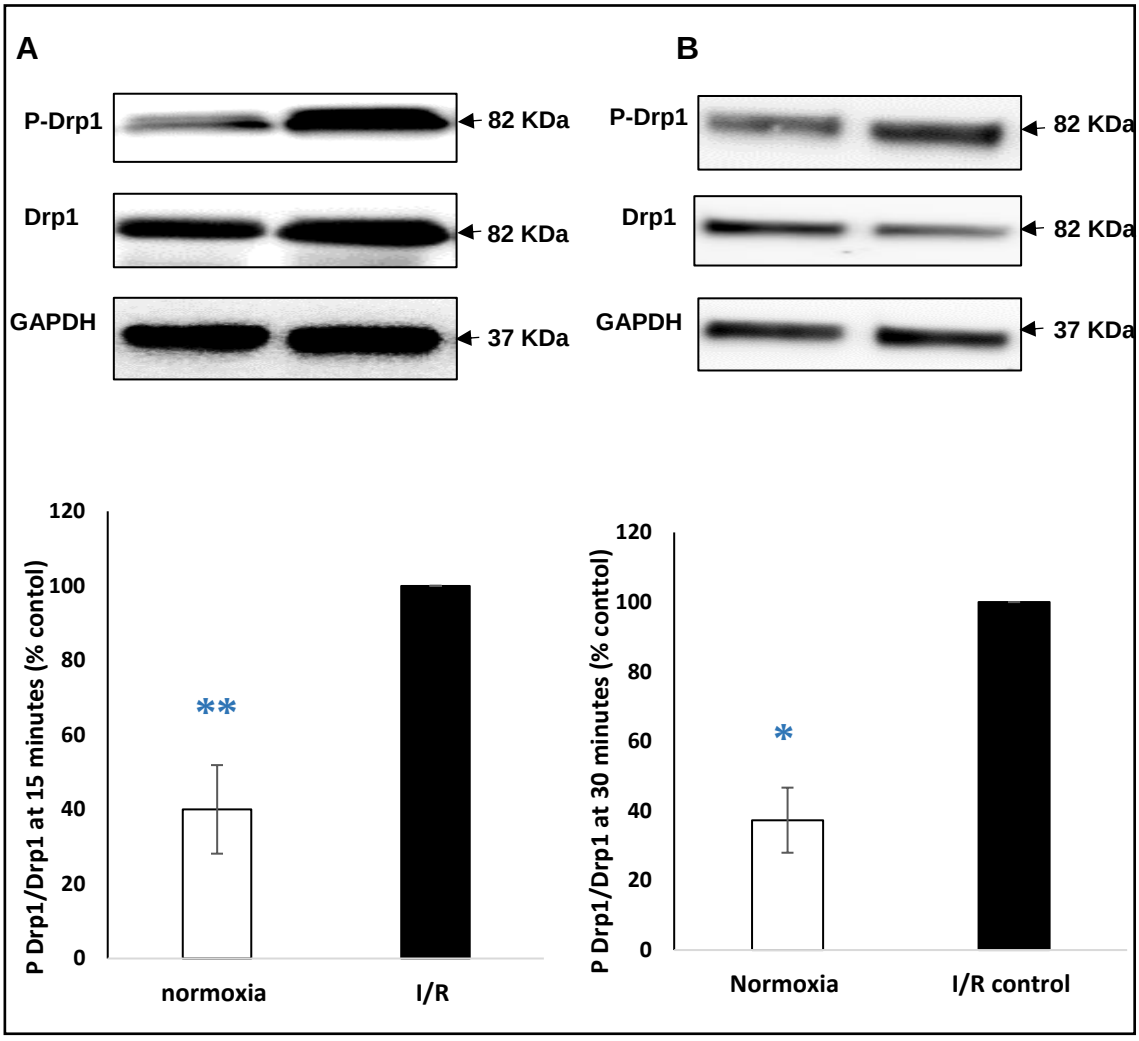

Figure 2. 19: The levels of phospho and Total Drp1 normoxia in I/R control. A is the control groups perfused for 15 minutes isolated rat hearts. B is the control groups perfused for 30 minutes isolated rat hearts. Results displayed as means + SEM, n=6. * p<0.05 vs. I/R control. **p<0.01 vs. I/R control.

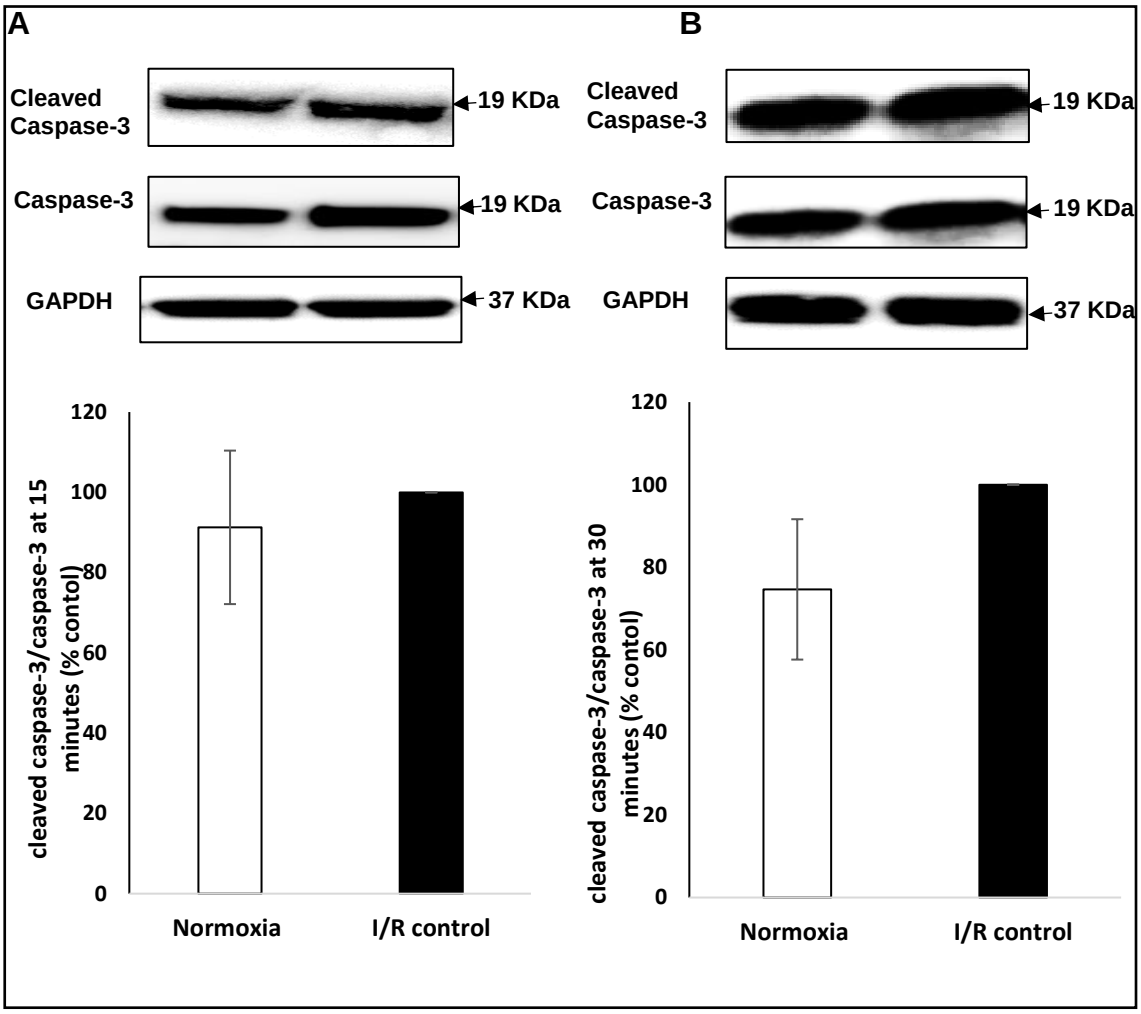

Figure 2. 20: The levels of cleaved caspase-3 normoxia in I/R control, A is the control groups perfused for 15 minutes isolated rat hearts. B is the control groups perfused for 30 minutes isolated rat hearts. Results displayed as means + SEM, n=6.

This validates the technique utilised. Since in the I/R control Akt, Erk1/2 and Drp1 were significantly increased in comparison with normoxia, that indicated that the tissue is undergoing stressed conditions, as it was found that the overexpression of Akt has a detrimental effect on the tissue been used (O'Neill and Abel 2005, Nagoshi et al. 2005). And although caspase-3 results did not show significant

difference it clearly represents a pattern where I/R was expressing higher levels of cleaved-caspase 3 than in normoxia and according to the pattern the gap increases by adding extra 15 minutes of time, the reason for no significant difference as suggested by Harvey, Hussain and Maddock (2014) may be due to the concept that 30 minutes of reperfusion might not be enough. Not to mention the expression of Drp1 in I/R group indicates as well that the tissue was undergoing apoptosis cell death (Roe, and Qi, 2018). Which was significantly reduce in normoxic control. These validations indicate that the tissue was under stress conditions and that the experimental protocol used was appropriate.

2.2.4 Real Time PCR Protocol (RNA Isolation And cDNA Synthesis)

The tissues were collected for PCR from the left ventricle after reperfusion, (as previously prescribed in sections 2.2.1.1 to 2.2.1.4) at the same time points as western blot tissue collection. However, tissue was submerged in 1.5 ml microfuge tubes that contained 300 µl RNALater® where the tissue was fully immersed and little cuts were made then it was stored at -80 ˚C until ready for RNA extraction (Figure 2.21).

Figure 2. 21: Polymerase Chain Reaction principle which is a technique for DNA replication that allows a “target” DNA sequence to be selectively amplified. PCR can use the smallest sample of the DNA to be cloned and amplify it to millions of copies in just a few hours. (Pray, 2008).

2.2.4.1 RNA Isolation

The frozen adult male Sprague-Dawley rat’s heart tissue (left ventricle) in RNAlater® was defrosted while placed on ice before it was put into round bottom microfuge tube 2 ml, the tissue sample was homogenised in TRIsure™, 1 ml reagent per 50 - 100 mg of tissue sample, the homogeniser IKA Labortechnik T25 was used at the power of 5 to homogenise the tissue into solution and process was carried out in the hood (fume hood or cell culture cabinet). The homogenised samples (mentioned in table 2.3) were then incubated at room temperature for 5 minutes for phase separation by adding 0.2 ml chloroform per sample of 1 ml

TRIsure™ and mixed vigorously for 15 seconds by hand, then the tubes containing the tissue, TRIsure™ and chloroform were incubated at room temperature for 3 minutes. The homogenised tissue samples were then centrifuged at 12,000 RPM for 15 minutes at 4 ˚C to separate into the different phases which are pale green, organic phase, an interphase, and a colourless upper aqueous phase, the RNA is found in the aqueous layer. The aqueous layer was pipetted very carefully without disturbing the interphase to 1.5 ml microfuge tube which is further processed to RNA precipitation. In order to precipitate the RNA, cold isopropyl alcohol was mixed with the RNA. 0.5 ml of isopropyl alcohol per 1 ml of TRIsure™ was used per sample. The contents of the tube were then mixed at room temperature then incubated for 10 minutes followed by 10 minutes centrifugation at 12,000 RPM, 4 ˚C. For the RNA washing step, the supernatant was removed. The pellet was washed once by adding ethanol at 75% at a quantity of 1 ml per 1 ml of TRIsure™ used. The samples were vortexed subsequently centrifuged for 5 minutes at 7,500 RPM at a temperature of 4 ˚C. The re-dissolving of the RNA the obtained pellet from the previous step was to air-dry after discarding the supernatant and in diethyl pyrocarbonate (DEPC)-treated water the pellet was dissolved using up and down pipetting technique, before analysis of RNA, the RNA was stored in the freezer at -80 ˚C. The experimental design is the same mentioned in (table 2.3 in section 2.2.3.1).

2.2.4.1.1 RNA Concentration

The collected RNA using the TRIsure^{TM} method was measured and calculated utilizing Nanodrop spectrophotometer set for RNA at a wavelength 260/280 and 260/230 ratios. RNA will absorb and peak at 260 nm collected from normoxia, I/R and the treated group (mentioned in table 2.3) treatment group, 260/280 ratios of around 2.0 that gives the assumption that the measured RNA is pure (Kiefer, Heller and Ernst 2000). Lower ratio was considered less pure, and it indicates impurity samples with low ratio were discarded.

2.2.4.1.2 Preparing Formaldehyde Agarose Gels (For RNA Analysis)

The measurement of the intact RNA, if in an environment where RNase is present, the collected RNA could have degraded rapidly. Water treated with DEPC was used for optimal results. 1.2 g agarose ($C_{24}H_{38}O_{19}$) was melted in treated water DEPC 87 ml, by heating the mix using a microwave until the suspension is clear and no agarose particles are present. The gel then was brought to the melting temperature of 60 ˚C. 10 ml 10X MOPS Buffer (0.2 x 10 M $C_7H_{15}NO_4S$ pH 7 with NaOH, $5x10^{-7}$ M, $C_2H_3NaO_2$, 1 x 10^{-7} M $C_{10}H_{16}N_2O_8$) following by adding 37% CH_2O of 3 ml then 3 µl Ethidium bromide was added. The DEPC treated water as well as reagents that are RNase free were used in the gel preparation. In the hood the gel was poured. The gel was allowed to set for 1 hour, the rubber stop, and the comb were removed, the gel was placed in the assembly unit and run in 1X MOPS Buffer.

2.2.4.1.3 The Preparation Of The Samples

For this gel sample preparation sample buffer was used at 40 µl and it was mixed by adding 10 µl of the sample was vortexed then placed in heat blot the samples were heated to 55 ˚C for a duration of 15 minutes. The components of the sample buffer are 65% CH_3NO 22% CH_2O (37% CH_2O) and 13% 10X MOPS buffer. 10 µl was also added from the following (50% $C_3H_8O_3$, 1 $x10^{-3}$ M $C_{10}H_{16}N_2O_8$, 0.3% each $C_{19}H_{10}Br_4O_5S$ and 0.3% Xylene Cyanol FF). The sample was loaded into the well with a marker ladder GeneRuler 100 bp Plus DNA marker in the outer wells, the system was run for 75 minutes with the 120 voltage then it was carefully removed to be visualised in the ChemiDoc (Bio-Rad) for ethidium bromide where the band of the intact RNA should be visualised.

2.2.4.1.4 Preparing TAE Agarose Gels (For DNA Analysis)

The measurement of the presence of DNA in the isolated RNA is also necessary. 2 g agarose ($C_{24}H_{38}O_{19}$) was melted in 50 ml of 1X TAE buffer, TAE 10X ($C_4H_{11}NO_3$ 3.9 $x10^{-8}$ M, $C_{10}H_{18}N_2Na_2O_{10}$ 1.9 $x10^{-7}$, CH_3COOH 11 $x10^{-6}$ M), the gel preparation was similar to the one (described in section 2.2.4.1.2) apart from the addition of the GelRed (2 µl) instead of ethidium bromide for each 50 ml gel and the gel was left to reach 55 ˚C before it was poured into the tray. 1X TAE buffer was poured into the unit containing the gel.

2.2.4.1.5 Sample Preparation

The marker ladder GeneRuler 100 bp Plus DNA was loaded into the first well followed by the RNA samples. The RNA samples were measured for the concentration and 1000 ng was the concentration used, by adding the RNA samples at 1000 ng and 6 µl loading dye and up to 20 µl water. The samples were than vortexed and centrifuged prior to loading 10 µl into the wells corresponding with the correct samples. The gel was run on ice and the run lasted for 75 minutes, the power supply 120 voltage. DNA and RNA are negatively charged molecules; therefore, they migrate from the negative side to the positive side of the gel as a result the comb should be put at the black side of the unit. To be visualized in the ChemiDoc (Bio-Rad) for GelRed gel where the band of the DNA and RNA should be visualised (Figure 2.22).

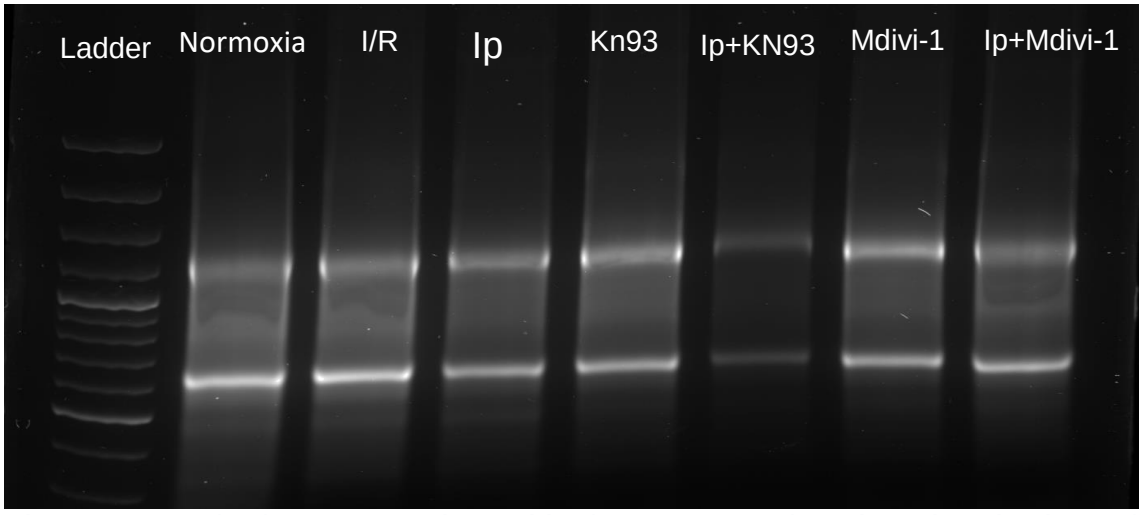

Figure 2. 22: The intact RNA showed in the TAE1% gel as the 2 bands showed the 18S band and the 28S band if the RNA sample did not show these bands, the sample was discarded.

2.2.4.2 cDNA Synthesis

To synthesis cDNA from RNA obtained from the samples, Tetro cDNA Synthesis Kit was used, this is a one-step synthesis in microfuge tubes free from DNase and RNase, the solutions in the kit and the RNAs were vortexed and centrifuged gently before use after thawing. The premix, was placed on ice, was prepared in RNase and DNase free tubes, master mix consisting of Tetro Reverse transcriptase (200 u/µl) (1 µl per reaction), 4 µl per reaction of 5x RT strand buffer 1µl of the Oligo $dT_{(18)}$ primer kit 1 µl of premixed dNTP solution at (10×10^{-3} M), and 1 µl of RiboSafe RNase inhibitor (10 u/µl) (Tetro cDNA Synthesis Kit ~ 5000 ng of RNA based on the amount as well as purity of the isolated RNA, the final volume was made up to 20 µl for the reaction by adding DEPC treated water. This was following manufacture instructions. Synthesising cDNA for 9 samples which are normoxia, I/R, Ipratropium bromide, Mdivi-1 ± Ipratropium bromide or KN-93 ± Ipratropium bromide, negative and positive controls. master mix was made for up to 10 samples just in case for pipetting error. 8 µl of the master mix from the kit reagents into 9 different 0.5 ml RNA, DNA free microfuge tubes labelled according to the RNA sample used. Then RNA samples at ~ 5000 ng then adding DEPC treated water. The final volume is 20 µl for a signal reaction that was mixed by pipetting up and down. Negative control (-cDNA) was prepared by replacing the RNA template with DEPC treated water (Tetro cDNA Synthesis Kit). Samples were vortexed, mixed gently (by pipetting) then centrifuged, the tubes containing cDNA reaction were placed in the thermal cycler, according to the protocol in Tetro cDNA synthesis kit, the reaction was run for cDNA Oligo primer cdnaoligodt the programme sets 45 °C at a duration of 30

minutes, the second step was to terminate the reaction by an increase in the temperature to 85 ˚C for 5 minutes, once the run was finished the products were placed directly on ice, the quantity of the produced cDNA was measured utilising spectrophotometry on dsDNA (double standards) in which the measurement allowed for quantification of the amount of the cDNA needed for the PCR, or Gene expression, reaction. The cDNA products were kept in the -20 ˚C freezer before use in PCR. Intact, high-quality RNA is crucial for the reaction reverse-transcription occurrence.

2.2.4.3 PCR in Qiagen Roto-Gene Absolute Quantification (Standard Curve Method)

The cDNA was synthesised from 5 µg RNA, that was neat cDNA and standards were made from that cDNA samples. Standards were made for the dilution values of 1, 0.2, 0.04, 0.008 by pooling 5 µl of each cDNA samples to make standard 1 then 1:5 dilution was performed by taken 4 µl of standard 1 into new tube then 16 µl water, that is DNase and RNase free, added to make up 0.2 and 4 µl of standard 2 into new tube then adding 16 µl DNase / RNase free water to make for 0.04 and 4 µl of standard 3 into new tube then 16 µl DNase and RNase free water was added to make up 0.008 standard 4. This method is made from stock of cDNA and accurate pipetting is important, units to express this dilution are irrelevant. PCR reaction in small PCR tubes was prepared for the samples in the hood/cell culture cabinet. 2 µl of the GAPDH (Glyceraldehyde-3-phosphate dehydrogenase) prime assay, 10 µl of Ssoadvanced SYBR Green supermix were also added as well as the cDNA 3 µl the final volume was made to 20 µl by adding

5 µl DNase and RNase free water as well as no template control (NTC) in which instead of 3 µl cDNA was replaced with 3 µl DNase and RNase free water. In that case, 18 samples that were normoxia, I/R, and treatment groups (mentioned in table 2.3) negative control, positive control, NTC and 4 standards in duplicates. 17 µl of the mix was pipette into small PCR tubes of 19 samples were also added cDNA 3 µl and the volume made up to 20 µl the tubes. The reaction was made first in one 1.5 ml microfuge tube by adding GAPDH prime assay, DNase and RNase free water and Ssoadvanced SYBR Green super mix. Then 17 µl was aliquotted by pipetting into the PCR tubes before adding the standard in duplicates, cDNA of the samples, -cDNA, positive control or DNase and RNase free water (NTC) negative PCR control and the PCR tubes were closed with the lids and labelled. All samples were briefly vortexed and centrifuged before loading into the PCR Qiagen Roto-Gene machine. A protocol which used the following settings was used, activation step at 95 ˚C for a 5 minutes cycle, denaturation at 95 ˚C for 10 seconds for 40 cycles, annealing/extension at 60 ˚C for 15 seconds for 40 cycles, extension (acquiring) at 72 ˚C for 20 seconds for 40 cycles followed by a melt curve at 72-95 ˚C for a 5 second cycle in Qiagen Rotor-Gene Q Real time PCR System. cDNA for the PCR reaction was used at a concentration of 100 ng. The GAPDH primers, for rats, were used as the prime assay from QuantiTect, Qiagen. The same protocol was followed for Dnm1l (Dynamin-1-like protein) prime assay, only the amount of the prime assay was less because the Dnm1l prime assay was 20x concentrated, therefor 10 µl Ssoadvanced SYBR Green, 1 µl Dnm1l prime assay and 6 µl DNA/RNA free water to make up 17 µl followed by 3 µl cDNA or DNA/RNA free water.

CCAGCTTTATTTGTGCCTGAAGTTTCATTTGAGTTACTGGTCAAACGTCAGA
TTAAGCGTCTAGAGGAGCCCAGCCTCCGCTGTGTGGAGCTGGTCCACGA
GGA

The Dnm1l amplicon size is 74 bp.

Whereas the primers that were bought from for HLRT1 (Housekeeping gene), were made into stock by pipetting 198 µl DNA/RNA free water and adding 1µl forward primers then add 1µl reverse primer to make 200 µl stock from there only 2 µl was needed for a signal PCR reaction thus for 20 samples 40 µl was needed.

These figures represent the amplification process of the amplicon resulted from using GAPDH and Dnm1l genes. The GAPDH product started amplification at the 18^{th} cycle whereas the Dnm1l gene is amplified at 22^{nd} cycle, as mentioned in the manufacture protocol, which helped determine the Ct value for the amplicons as well as the difference appeared in the melt curve between the two products. The melt curve is an indicator for the correct process of PCR reaction. It shows the resulted product and can indicate for the accuracy of the product as well as the presence of primer dimer. The melt curve of the resulted amplicon must be identical to the one depicted in the product manufacture protocol. The amplification for the melt curve of the product must peak then start decline as presented in (Figures: 2.23 - 2.28), thus validating the technique.

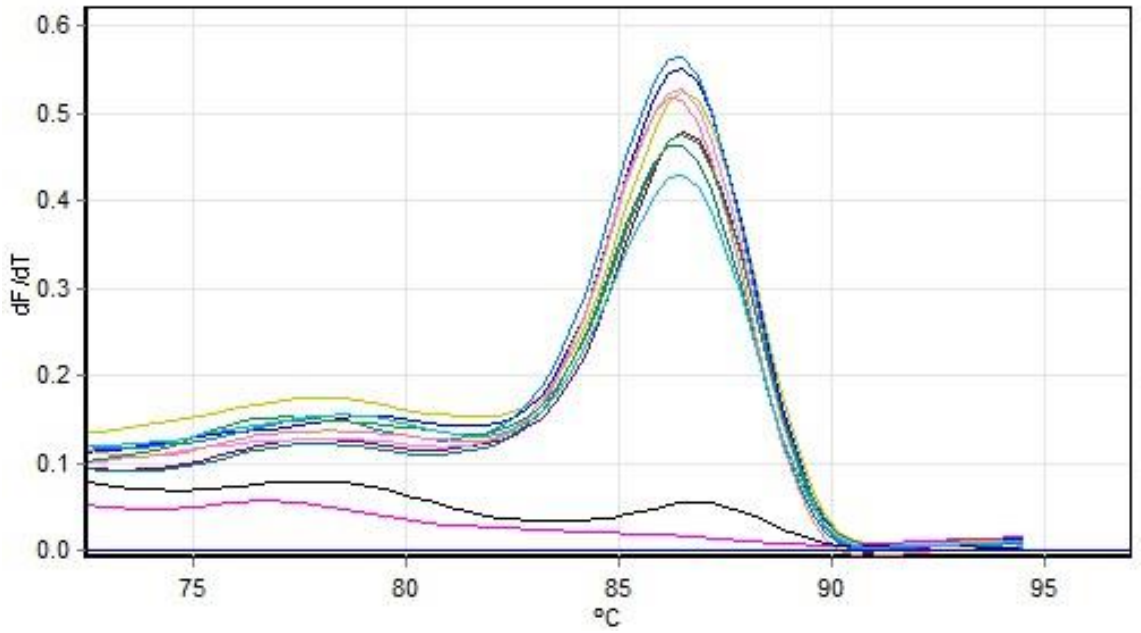

Figure 2. 23: GAPDH amplicons melt curve. The melt curve generated is as mentioned in the protocols given in section 2.2.4.3 with the product from Biorad the same height of peak with the same position.

Other PrimePCR™ Template for SYBR® Green Assay: GAPDH, Rat was used from Bio-Rad

TGATGGCAACAATGTCCACTTTGTCACAAGAGAAGGCAGCCCTGGTAACC AGGCGTCCGATACGGCCAAATCCGTTCACACCGACCTTCACCATCTTGTCT ATGAGAC GAGGCTGGCACTGCACAAGAAGATGCGGCTGTCTCTA

Amplicon size 115bp.

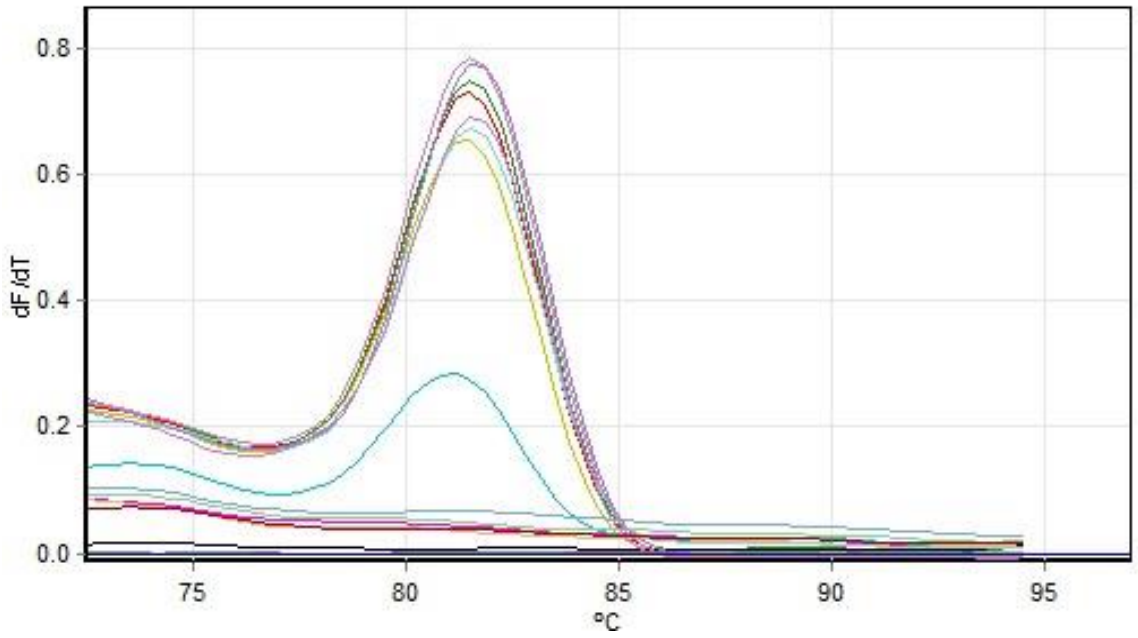

Figure 2. 24: Dnm1l amplicons melt curve. The melt curve generated is as mentioned in the protocols given in section 2.2.4.3 with the product from Biorad the same height of peak with the same position

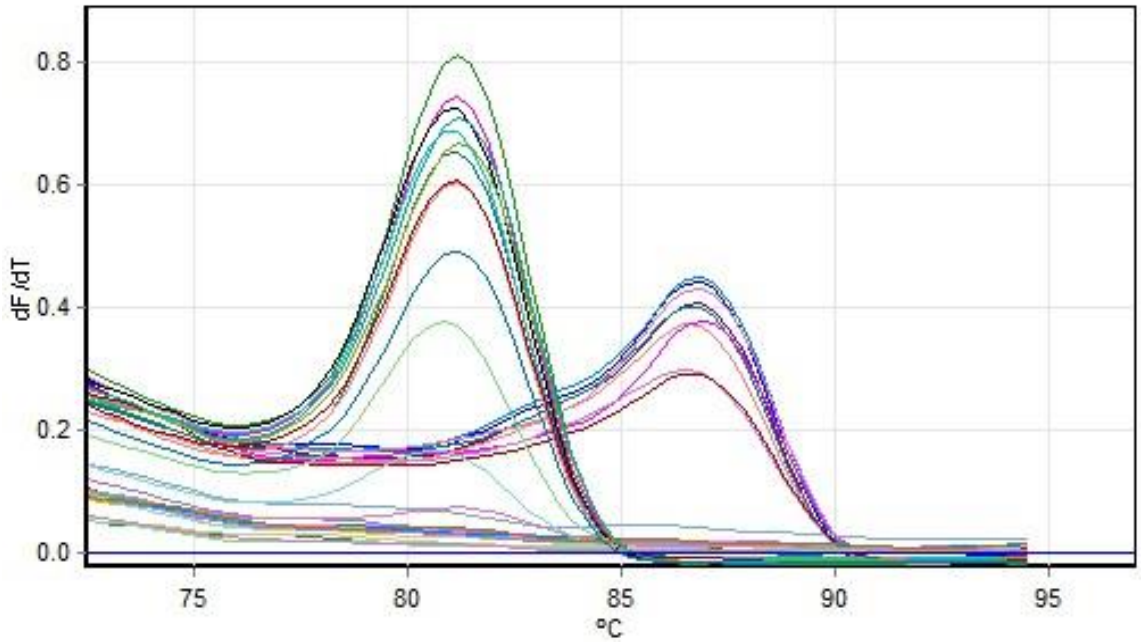

Figure 2. 25: GAPDH amplicons and Dnm1l amplicons melt curves generated from Qiagen Roto-Gene.

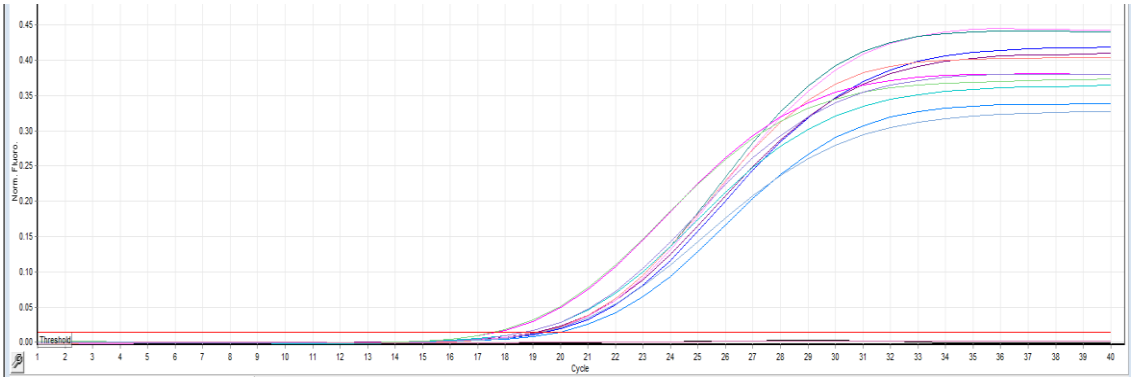

Figure 2. 26: SYBR-Green real time PCR detection for GAPDH amplicons Auto-Scale. generated by Qiagen Roto-Gene. Which showed the amplification which started at 18 cycles as mentioned in the product description. This showed the presence of the gene of interested in the isolated samples.

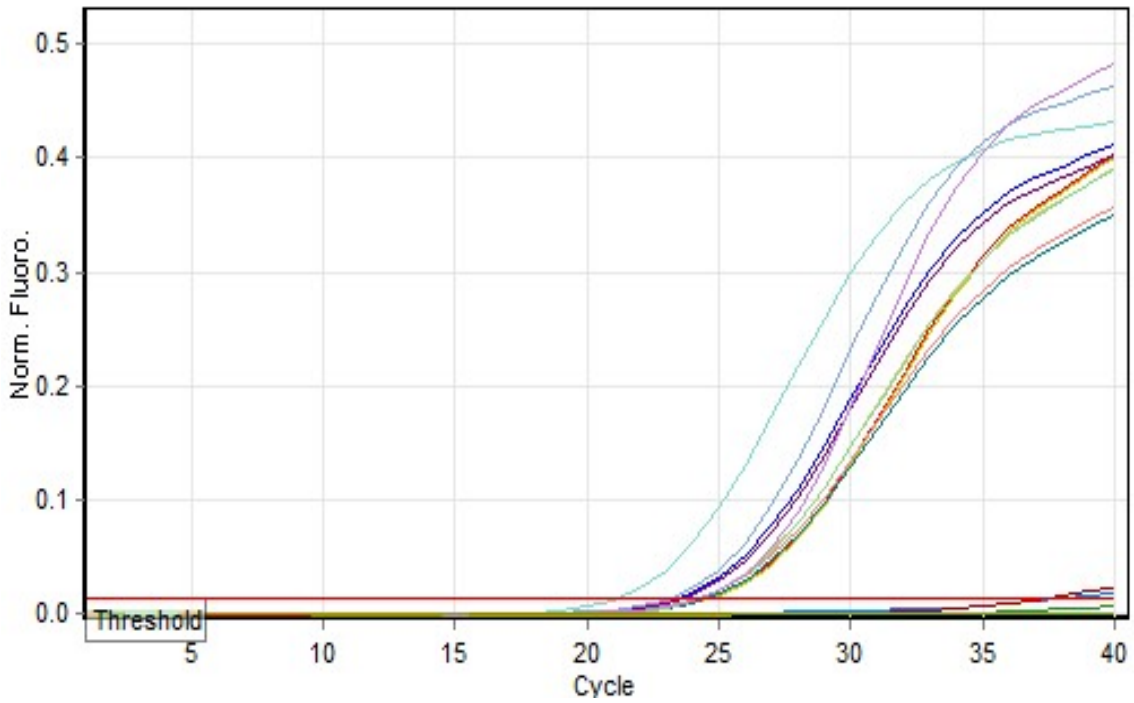

Figure 2. 27: SYBR-Green real time PCR detection for Dnm1l amplicons Auto-Scale generated by Qiagen Roto-Gene. Which showed the amplification which started at 22 cycles as mentioned in the product description. This showed the presence of the gene of interested in the isolated samples.

The normoxic control and I/R control fold induction after measuring the ΔΔ CT Value Dnm1l against GAPDH was (178.92 ± 90% vs. 100 ± 0%) respectively.

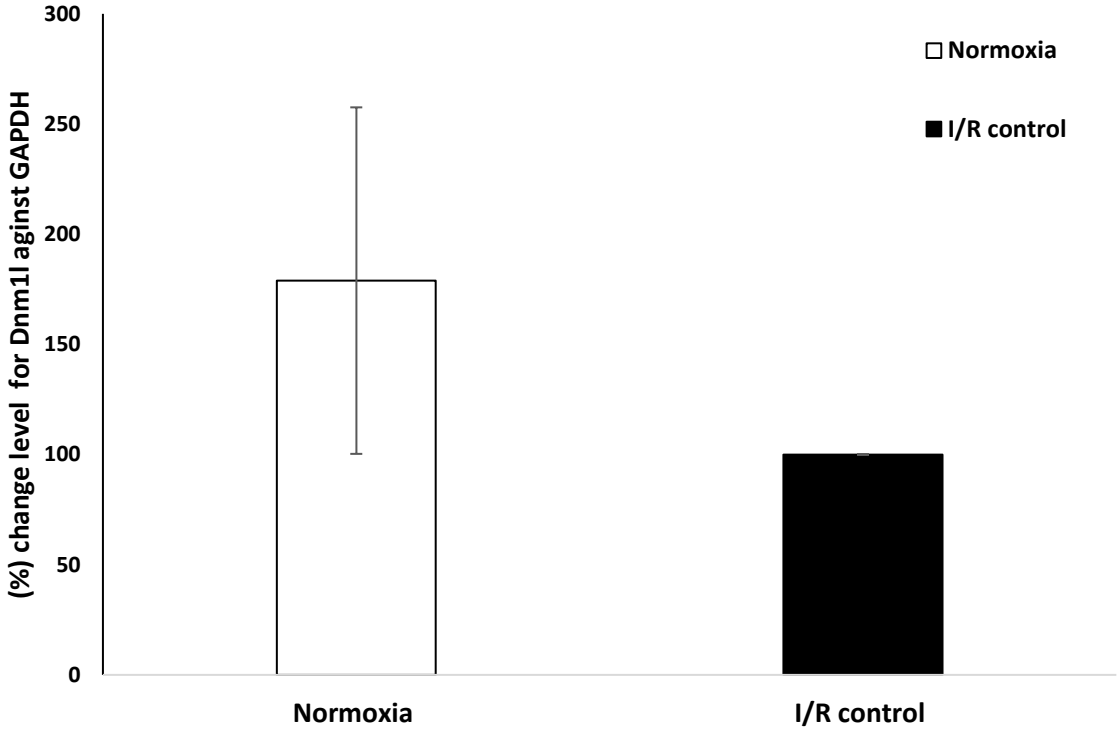

Figure 2. 28: The level of Dnm1l expression/induction normalised to GAPDH housekeeping gene using Relative quantification method for normoxia in comparison to I/R control the data was analysed after changing it into arithmetic means by normalised to I/R control, ± SEM, n = 6. The error bar for the I/R is 0 since the data were normalised to the I/R control.

2.2.4.4 Gene Expression Relative Quantification

The cDNA samples with no template controls (NTC), were prepared in individual microfuge tubes that were DNase and RNase free prior to being pipetted, in duplicates, into a microplate for PCR and standards which were from a diluted stock solution of the original cDNA. 2 µl of the GAPDH primer, 10 µl of SYBR

Green supermix also 3 µl cDNA or water total volume was made to 20 µl by DNA/RNA free water. All reactions were mixed well then briefly centrifuged to get the reaction at the bottom prior to plating, a seal was placed on the plate and the plate was then briefly centrifuged and set up in the Bio-Rad CFX Connect™ PCR machine. A protocol which used the following settings was used, activation at a temperature of 95 ˚C lasted for 2 minutes followed by 40 cycles of step lasted for 5 seconds at 95 ˚C (denaturation) 40 cycles of (annealing/extension) that lasted for 30 seconds decreasing the temperature to 60 ˚C followed by a melt curve at 65-95 ˚C for a 5 second cycle. The same protocol was made for Dnm1l prime assay, only the amount was less because the prime assay was 20x concentrated there for 10 µl Ssoadvanced SYBR Green, 1 µl Dnm1l prime assay and 6 µl DNA/RNA free water to make up 17 µl followed by 3 µl cDNA or DNA/RNA free water.

2.2.4.4.1 Running TAE Gel For The Amplicon

PCR product (amplicon) was run in TAE 1% gel, in which the ladder was loaded into the first well the second kept empty the third-sixth were standards from 1 to 0.008 followed by the samples normoxia, I/R, and the treated group (mentioned in table 2.3), –cDNA negative control and lastly no template control (NTC). The ladder solution was made from 1 µl marker ladder, 1 µl loading dye and 3 µl DNA/RNA free water to make 5 µl that was loaded into the first well, the sample were made by adding 3 µl DNA/RNA free water, 2 µl loading dye and 5 µl of the amplicon. However, in one microfuge tube for the15 amplicons a stock of loading

dye and DNA/RNA free based on the number of the amplicons used and the mix was vortexed and centrifuged briefly prior to placing 5 µl into each new microfuge tubes followed by adding the correspondent amplicon to each microfuge tube vortexed then loaded into the gel (Figure.2.29).

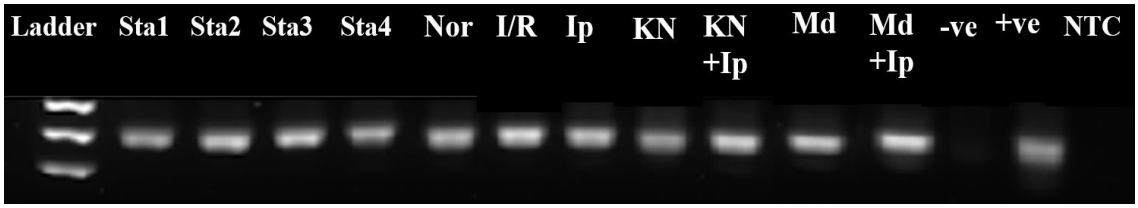

Figure 2. 29: Representative electrophoresis gel showing the PCR amplicon of GAPDH samples which were diluted with DNA/RNA free water, loading dye. Starting by the marker and standards 1 to 4 followed by the samples loaded as well as positive, negative and no template controls. Run for the measurements of the amplicon which helped confirm the protocol.

2.2.6 Data Analysis

IBM® SPSS® Statistics Version 24 statistical software was utilised to analyse raw data obtained from Langendorff (Haemodynamic parameters (LVDP, HR and CF)), (AAR%), apoptosis, cell viability, necrosis, Akt, Erk1/2, Drp1 and caspase-3 data and Ct value from the PCR and the means value from the flow cytometry data the activity of caspase-3. For all data, SPSS was utilised for analysis via One-way ANOVA analysis and Fisher's least significant difference test (LSD) post hoc test. All data presented as mean ± standard error of the mean (SEM) (n=6 for all experiments) and statistical analysis conducted a p value <0.05 was considered statistically significant. The software utilized in regard to determine western blot bands was ImageJ. This chapter is validation of the techniques used.

Chapter 3: Assessment Of The Exacerbation Of Myocardial Reperfusion Injury Due To Ipratropium Bromide Administration

Previous work in our laboratory has implied that in *in vitro* models of I/R, the non-selective muscarinic receptor antagonist Ipratropium Bromide (Ip) was able to exacerbate mediated myocardial injury (Harvey, Hussain and Maddock 2014). However, the mechanism of induced injury has not been fully elucidated. The aim of this chapter was to identify whether, in the experimental models employed in this project, ipratropium bromide exacerbated myocardial injury in clinically relevant *in vitro* models of myocardial ischaemia and reperfusion to support previously reported experimental findings.

3.1 Langendorff Model Of Perfused Rat Heart Results

For the Langendorff model studies, (explained in detail in section 2.2.1.1 - 2.2.1.5 in chapter 2). Adult male Sprague-Dawley rats were sacrificed, the heart was mounted onto Langendorff perfusion apparatus (constant perfusion rate of 9.8 ± 0.5 ml.min^{-1} with Krebs-Heinsleit buffer), regional ischaemia was induced via ligation of the descending left coronary arteries followed by 120 minutes reperfusion. Ipratropium bromide (1 x 10^{-7} M - 1 x 10^{-9} M) were added at the start and during reperfusion, these concentrations were due to clinical relevancy. The Langendorff model was performed to measure haemodynamic parameters which were measured during and after reperfusion. Infarct sizes were assessed via Evans Blue staining and 2,3,5-triphenyl tetrazolium chloride exclusion treatment to delineate between live and infarcted tissue within the ischaemic area studies.

3.1.1 Haemodynamic Parameters (I/R And Ipratropium Bromide (1 x 10^{-9} M - 1 x 10^{-7} M).

The haemodynamic parameters measured were LVDP, HR and CF. Every 5 minutes the measurements were recorded during the period of stabilisation and ischaemia and every 15 minutes after initiating reperfusion for 120 minutes. The perfusion protocol due to its clinical relevancy for dose response curve then the heart was taken out and frozen in the -20 ˚C freezer to take the infarct risk ratio (I/R%).

3.1.1.1 The Left Ventricular Developed Pressure (LVDP)

The method in which LVDP was determined was by using the left ventricular pressure changes effect on a latex balloon that was filled with water, inserted into the left ventricular chamber, (explained in detail in section 2.2.1.6.1 in chapter 2). I/R control, and Ipratropium bromide (1 x 10^{-9} M - 1 x 10^{-7} M) were used and the results show that Ip (1 x 10^{-7} M) significantly decreased compared to the I/R control at 160 minutes (65.5 ± 7.6% vs. 47.5 ± 6.2%) against Ip (1 x 10^{-7} M) and 175 minutes (62.3 ± 7.8% vs. 45.4 ± 6.7%) and Ip (1 x 10^{-9} M) against Ip (1 x 10^{-7} M) at 160 minutes of reperfusion (46.7 ± 5.2% vs. 47.5 ± 6.2%) ($p<0.05$). Left ventricular developed pressure measurements for I/R control, Ipratropium bromide (1 x 10^{-9} M - 1 x 10^{-7} M) (Figure 3.1).

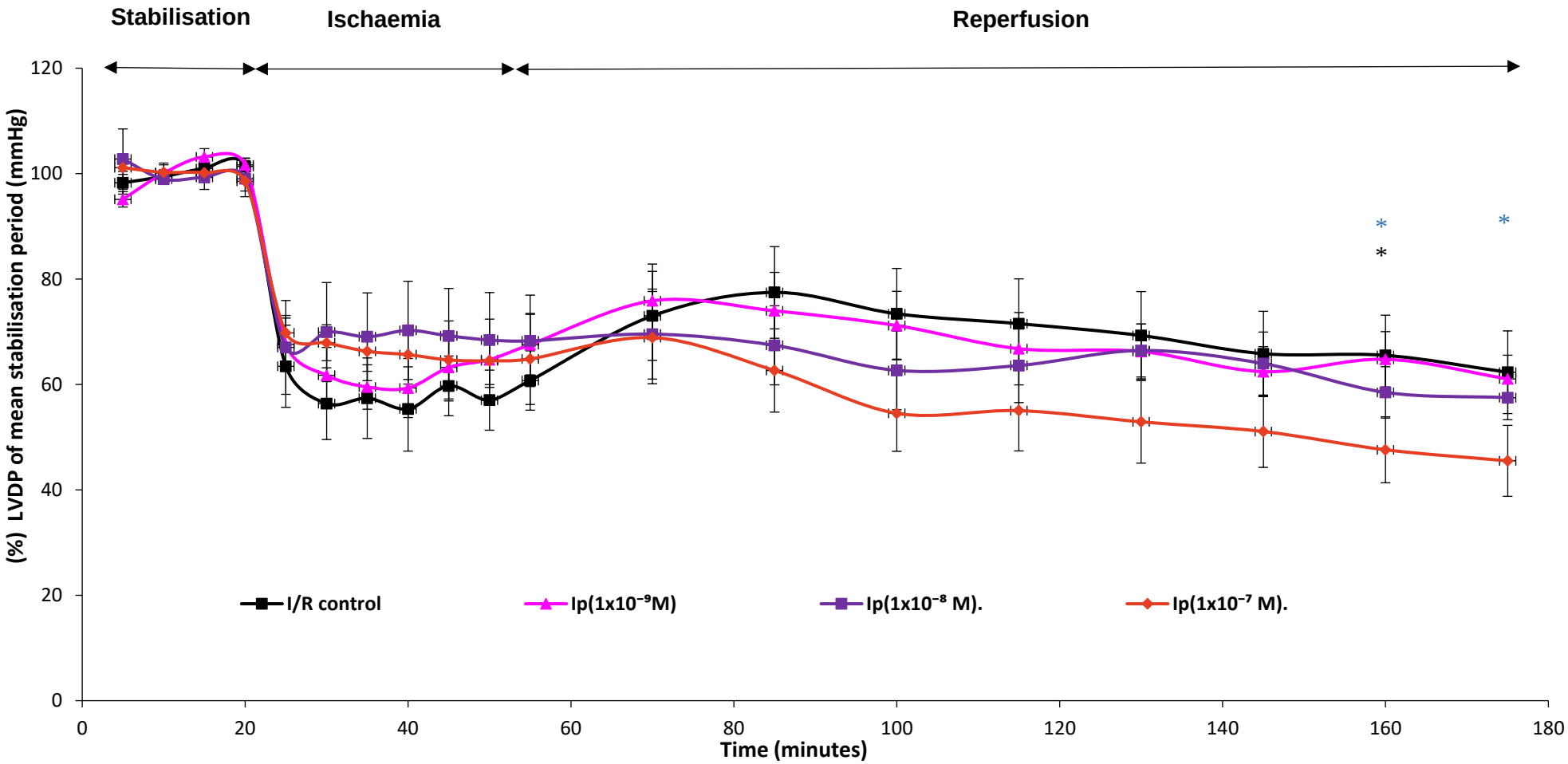

Figure 3. 1: Changes in left ventricular developed pressure % of (mmHg) in isolated perfused rat hearts group's I/R control, n=6. Ipratropium bromide (1 x 10^{-9} M -1 x 10^{-7} M). * p<0.05 vs. I/R control against Ipratropium bromide (1 x 10^{-7} M). * p<0.05 vs. Ipratropium bromide (1 x 10^{-7} M) against Ipratropium bromide (1 x 10^{-9} M).

3.1.1.2 Heart Rate (HR)

The method in which HR was determined in similar principle to LVDP (explained in detail in section 2.2.1.6.2 in chapter 2). for I/R control, Ipratropium bromide (1 x 10^{-9} M – 1 x 10^{-7} M) results show that Ip (1 x 10^{-7} M) significantly increased HR compare to I/R control at 70 minutes (109.2 ± 5.3% vs. 91.4 ± 4.7%), 100 minutes (113.8 ± 6.2% vs. 97.7 ± 6.9%) and 175 minutes of reperfusion (114.1 ± 5.2% vs. 97.3 ± 6.5%) ($p<0.05$) and 115 minutes (116 ± 6.9% vs. 97.2 ± 6.4%) and 130 minutes (118 ± 6.4% vs. 98.3 ± 6.1%) ($p<0.01$) and Ip (1 x 10^{-9} M) at 70 minutes (107.9 ± 6.5% vs. 91.4 ± 4.7%) all against I/R control, Ip (1 x 10^{-8} M) at 115 minutes of reperfusion (100.5 ± 2.3% vs.116 ± 6.9%) ($p<0.05$) against Ip (1 x 10^{-7} M). Heart rate for I/R control, Ipratropium bromide (1 x 10^{-9} M- 1 x 10^{-7} M) (Figure 3.2).

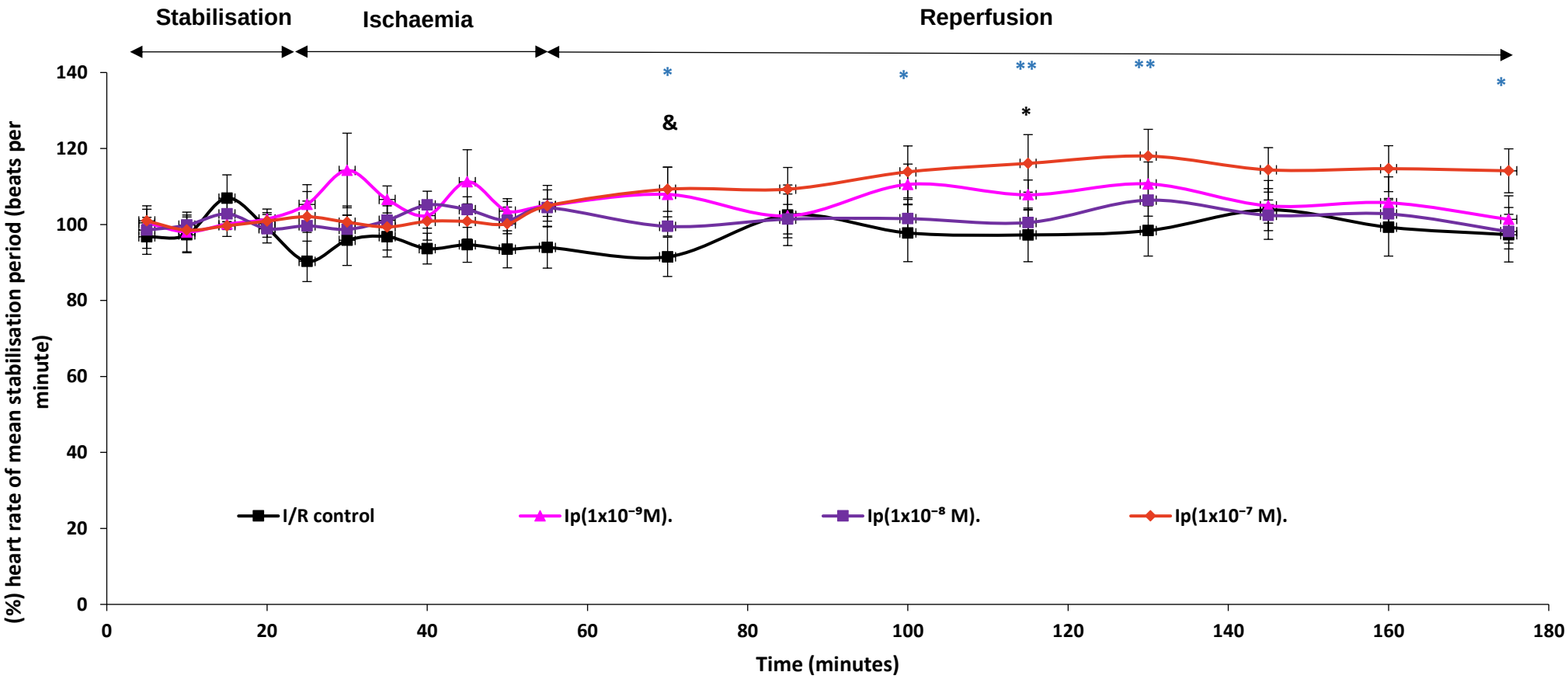

Figure 3. 2: Changes in heart rate (bpm) in isolated perfused rat hearts. All groups I/R control, Ipratropium bromide (1 x 10^{-9} M –1 x 10^{-7} M), n=6. ** p<0.01 compared to I/R control. * p<0.05 compared to I/R control all against Ipratropium bromide (1 x 10^{-7} M). * p<0.05 compared to Ipratropium (1 x 10^{-7} M) against Ipratropium bromide (1 x 10^{-8} M). & p<0.05 compared to Ipratropium (1 x 10^{-9} M) against I/R control.

3.1.1.3 Coronary Flow (CF)

Coronary flow (CF) was measured via the collection and recording the obtained amount of the coronary effluent (explained in detail in section 2.2.1.6.3 in chapter 2) for I/R control, Ipratropium bromide (1×10^{-9} M – 1×10^{-7} M). The results for coronary flow shows no significant difference. With a significant difference once compared to the control. Coronary flow results for I/R control, Ipratropium bromide (1×10^{-9} M – 1×10^{-7} M) (Figure 3.3).

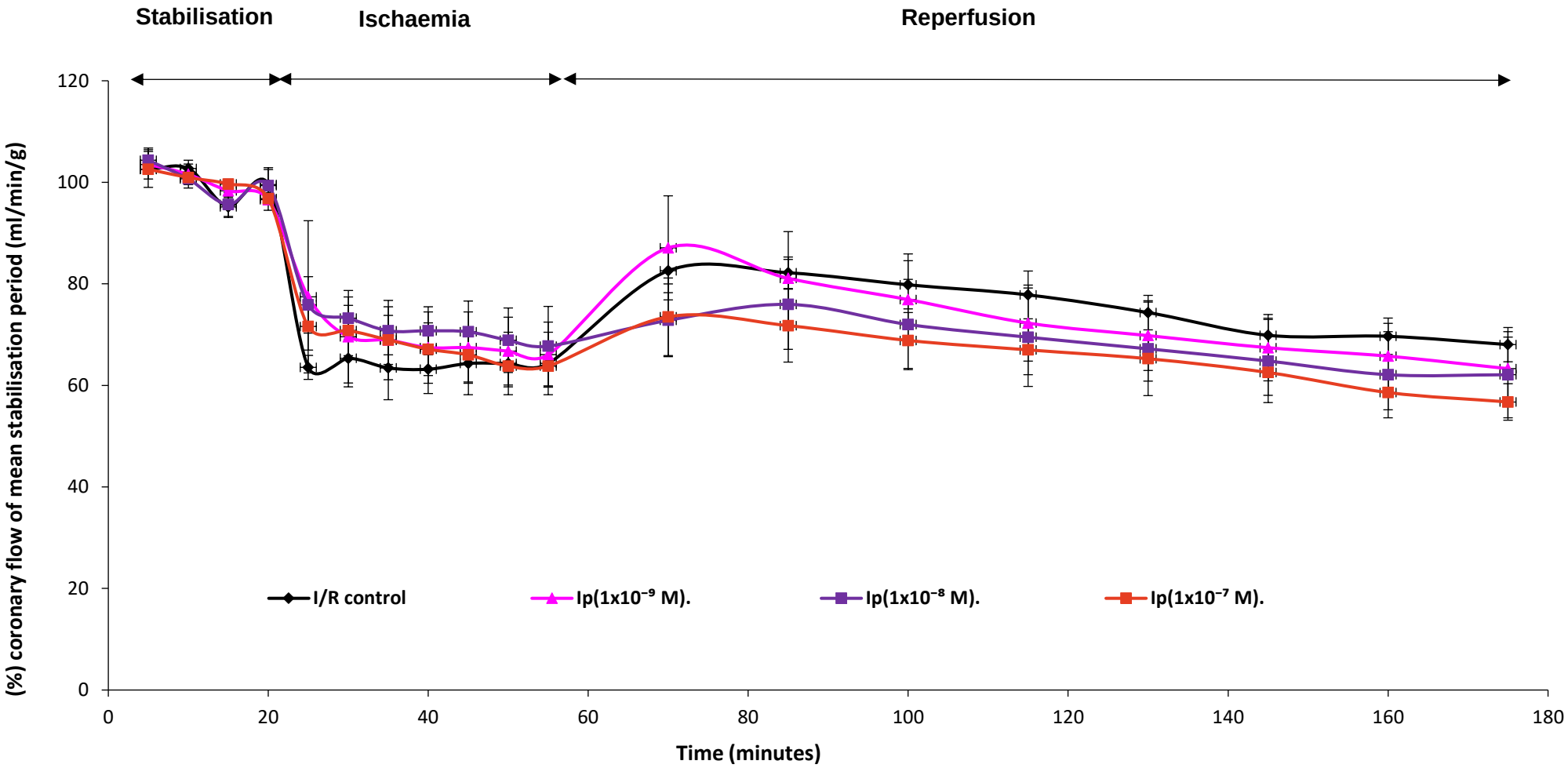

Figure 3. 3: Changes in coronary flow (ml.min^{-1}) in isolated perfused rat hearts, n= 6. I/R control, Ipratropium bromide (1 x 10^{-9} M – 1 x 10^{-7} M).

3.1.2 The Infarct Risk Ratio (AAR %)

Krebs Heinsleit Buffer (KHB) was perfused to the isolated rat hearts for stabilisation and regional ischeamia followed by perfusion with Ipratropium bromide (1 x 10^{-9} M – 1 x 10^{-7} M) + KHB for 120 minutes, the thread, used to cause regional ischaemia, was tightened before perfusing the heart with Evans blue prior to 1%TTC protocol staining to determine the AAR% (explained in detailed in section 2.2.1.7). Similar to the Haemodynamic parameters Ip was cardiotoxic since the infract size was increase at the highest concentration of Ip with a significant difference to the control Ipratropium bromide (1 x 10^{-7} M – 1 x 10^{-9} M) (158.5 ± 6.2, 135.9 ± 5, 124.4 ± 14.5% vs. 100 ± 0%) against I/R control, with ($p<0.001$, 0.01, 0.05) respectively. Ip (1 x 10^{-8} M) against Ip (1 x1 0^{-7} M) (135.9 ± 5%, vs. 158.5 ± 6.2%) and Ip (1 x 10^{-9} M) against Ip (1 x 10^{-7} M) (124.4 ± 14.5% vs.158.5 ± 6.2%). Ip (1 x 10^{-7} M) $p<0.05$. These results showed the comparison between untreated I/R control, Ipratropium bromide (1 x 10^{-9} M – 1 x 10^{-7} M) treatment groups (Figure3.4).

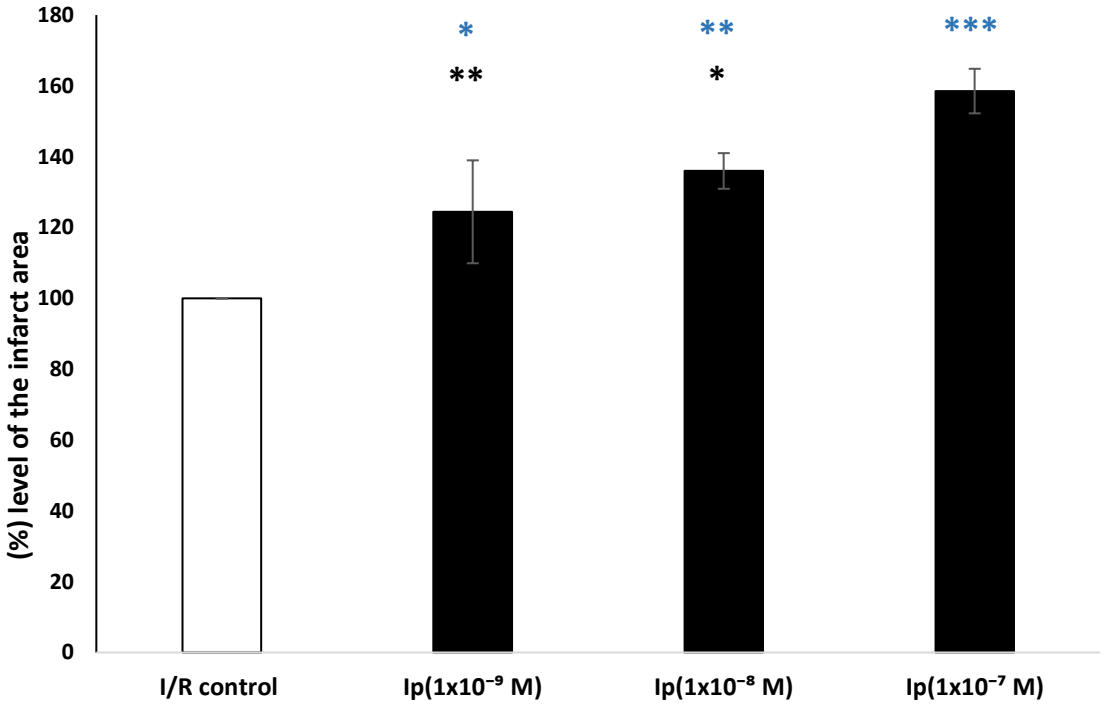

Figure 3. 4: Infarct development in I/R control, Ipratropium bromide (1 x 10^{-9} M – 1 x 10^{-7} M) treatment groups perfused isolated rat hearts. Results displayed as means + SEM, n=6. *** p<0.001 against I/R control. ** p<0.01 against I/R control. * p<0.05 against I/R control. ***p*<0.05 against Ipratropium (1 x 10^{-7} M), ** p<0.01 against Ipratropium (1 x 10^{-7} M).

3.2 Flow Cytometry Results

Flow cytometry protocol was followed to measure Apoptosis Necrosis, live cells and caspase-3 for the cardio myocytes. The template was gated for 10,000 cells count that were treated with Ipratropium bromide (1 x 10^{-7} M), in comparison with H/R control (explained in detailed in section 2.2.2.1 and 2.2.2.2).

3.2.1 Cell Death Assay Results

Annexin V-FITC Apoptosis Staning / Detection Kit Stain. Same protocol for cell isolation and Hypoxia/Reoxygentaion induction was carried out, the cells were needed alive therefore, the cells were centrifuge discarding the supernatant followed by adding binding buffer twice adding Annexine V-FITC A and Propidium iodide and the cells incubated with the for apoptosis and necrosis detection for a period of 5 minutes at 25 ˚C in foil prior to analysis by the flow cytometry.

3.2.2 Effects Of Ipratropium Bromide On Apoptosis

For apoptosis Ip was able to increase the level of apoptotic cell (total apoptosis) measured by the flow cytometry. There was an increase in total apoptosis induced by Ipratropium during H/R. The percentages of apoptosis are presented in (Figure 3.5). H/R control against ipratropium (1×10^{-7} M) (100 ± 0 vs. 116.22 ± 6.4%) with ($p<0.05$).

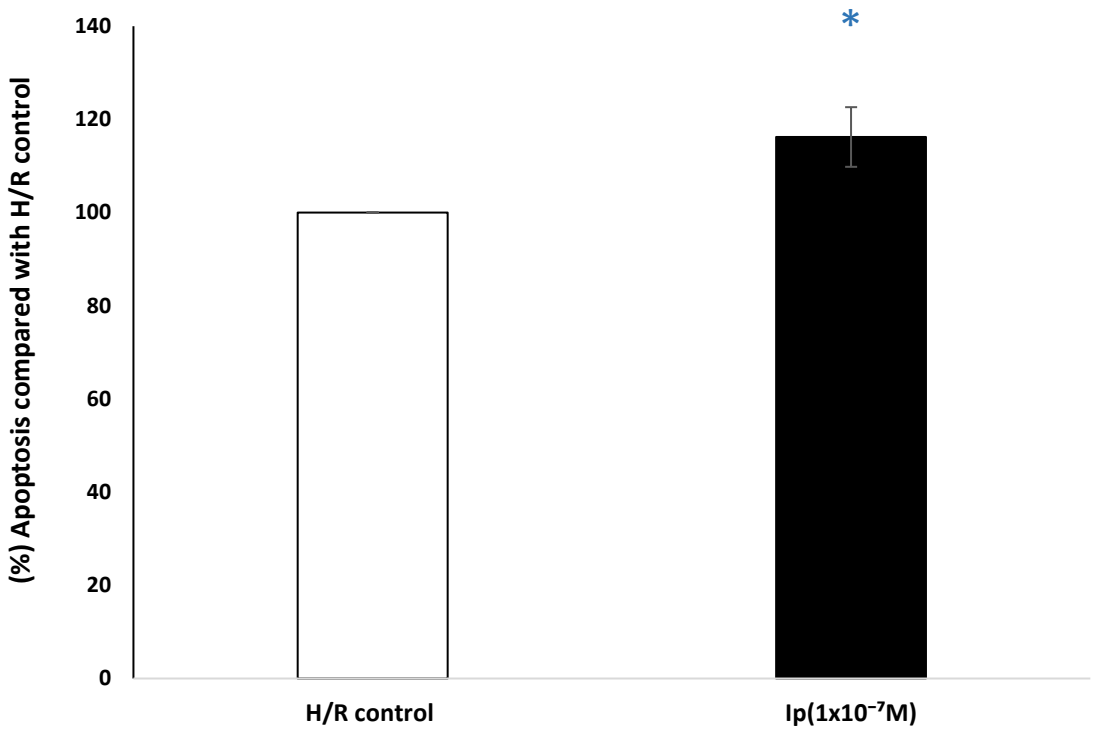

Figure 3. 5: Total apoptosis percentage results stained by Annexin V shown in flow cytometry for H/R controls and Ip (1×10^{-7} M). the data was analysed after changing it into arithmetic means by normalised to H/R control, ± SEM, the recorded number myocytes is 10,000, n = 6, * = $p<0.05$ vs H/R control.

3.2.3 Effects Of Ipratropium Bromide On Necrosis

The percentages of necrosis are presented in (Figure 3.6). Despite the obtained pattern that suggest that Ip caused more necrotic cell death than H/R control, there was no significant difference overall, H/R control vs Ip (100 ± 0 vs. 119.3 ± 14.22%).

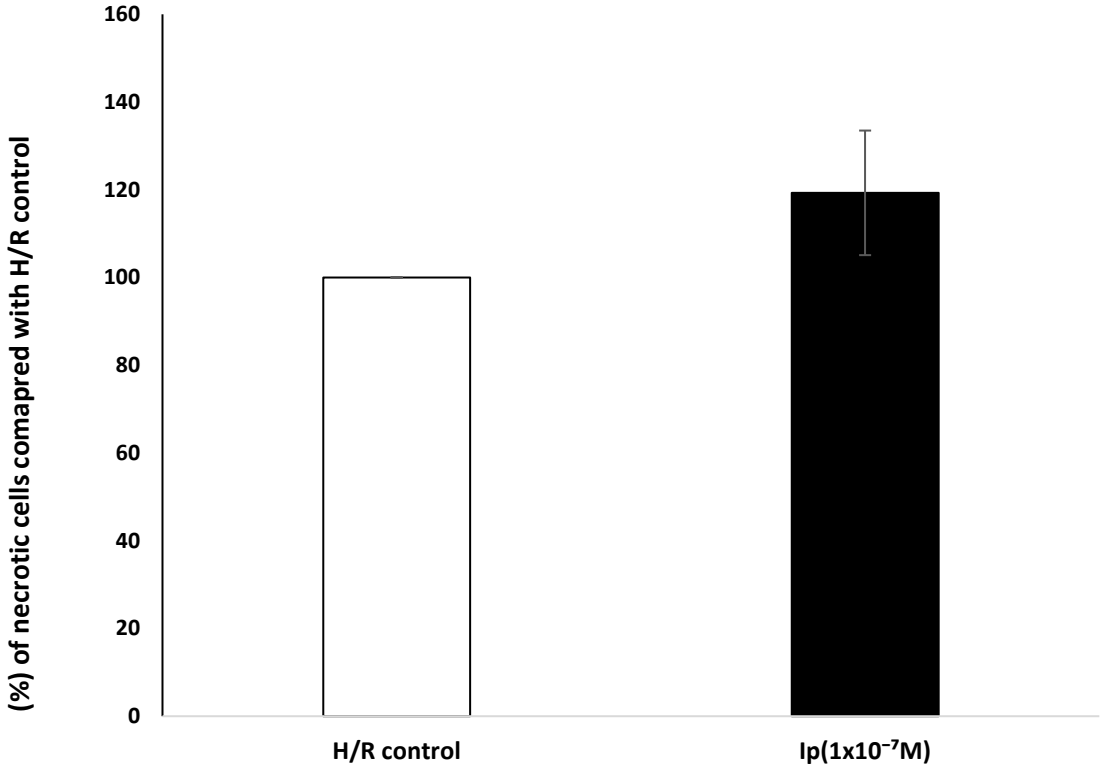

Figure 3. 6: Necrotic cells percentage results stained by Annexin V shown in flow cytometry for H/R controls and ipratropium (1 × 10^{-7} M). the data was analysed after changing it into arithmetic means by normalised to H/R control, ± SEM, the recorded number myocytes is 10,000, n = 6.

3.2.3 Effects Of Ipratropium Bromide On Cell Viability

The isolated myocytes were stain with cell death assay to determine cell viability to measure the effect of Ip (1 x 10^{-7} M), in comparison with H/R control (explained in detailed in section 2.2.2.1 - 2.2.2.2 and 2.2.2.4.1).

3.2.4 Annexin V-FITC Apoptosis Kit

The percentages of live cells are presented in (Figure 3.7). The cell viability results showed that Ip deceased the percentage of live cells indicating its toxicity

compared to the control. H/R control against ipratropium (1×10^{-7} M) (100 ± 0 vs. 80.44 ± 9.4%) with ($p<0.05$).

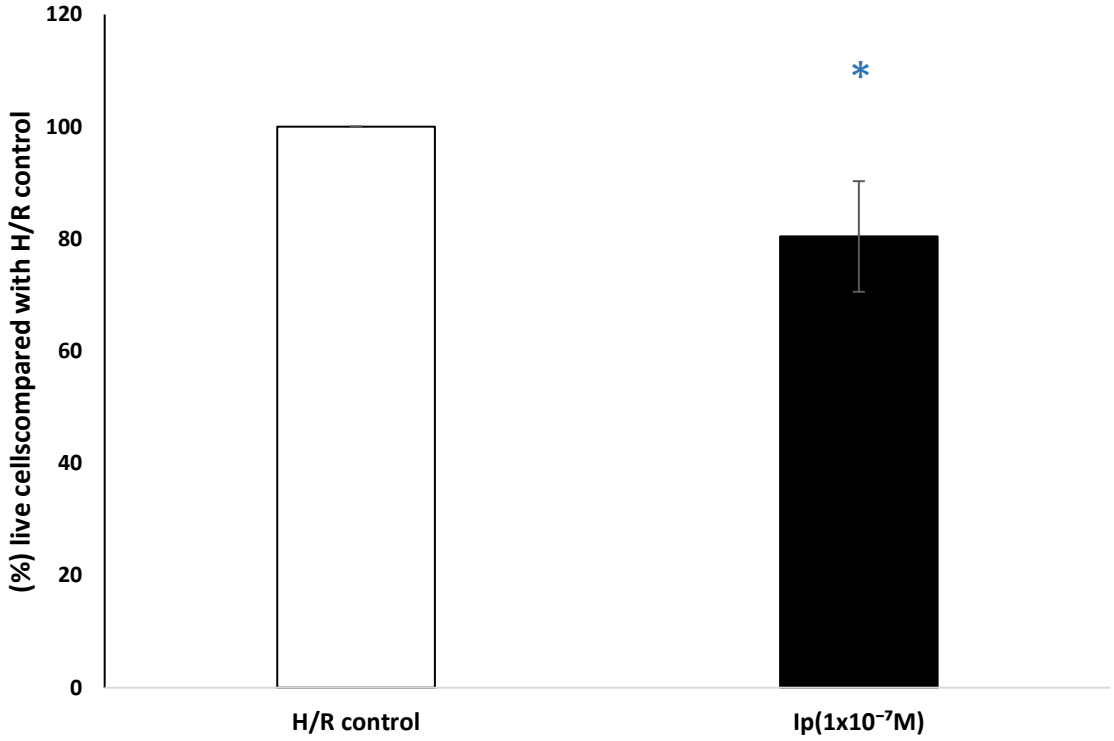

Figure 3. 7: Effect of ipratropium (1×10^{-7} M), Cell viability level in comparison to H/R control the data was analysed after changing it into arithmetic means by normalised to H/R control, ± SEM, the recorded number myocytes is 10,000, n = 6. * = $p<0.05$ vs. H/R control.

3.2.5 The Level Of Caspase-3 Activity

The percentages of caspase-3 level is presented in (Figure 3.8). The activity of caspase-3 was significantly more than the control as the results obtained from apoptosis. H/R control against ipratropium (1×10^{-7} M) (100 ± 0 vs. 116.83 ± 4%) with ($p<0.01$).

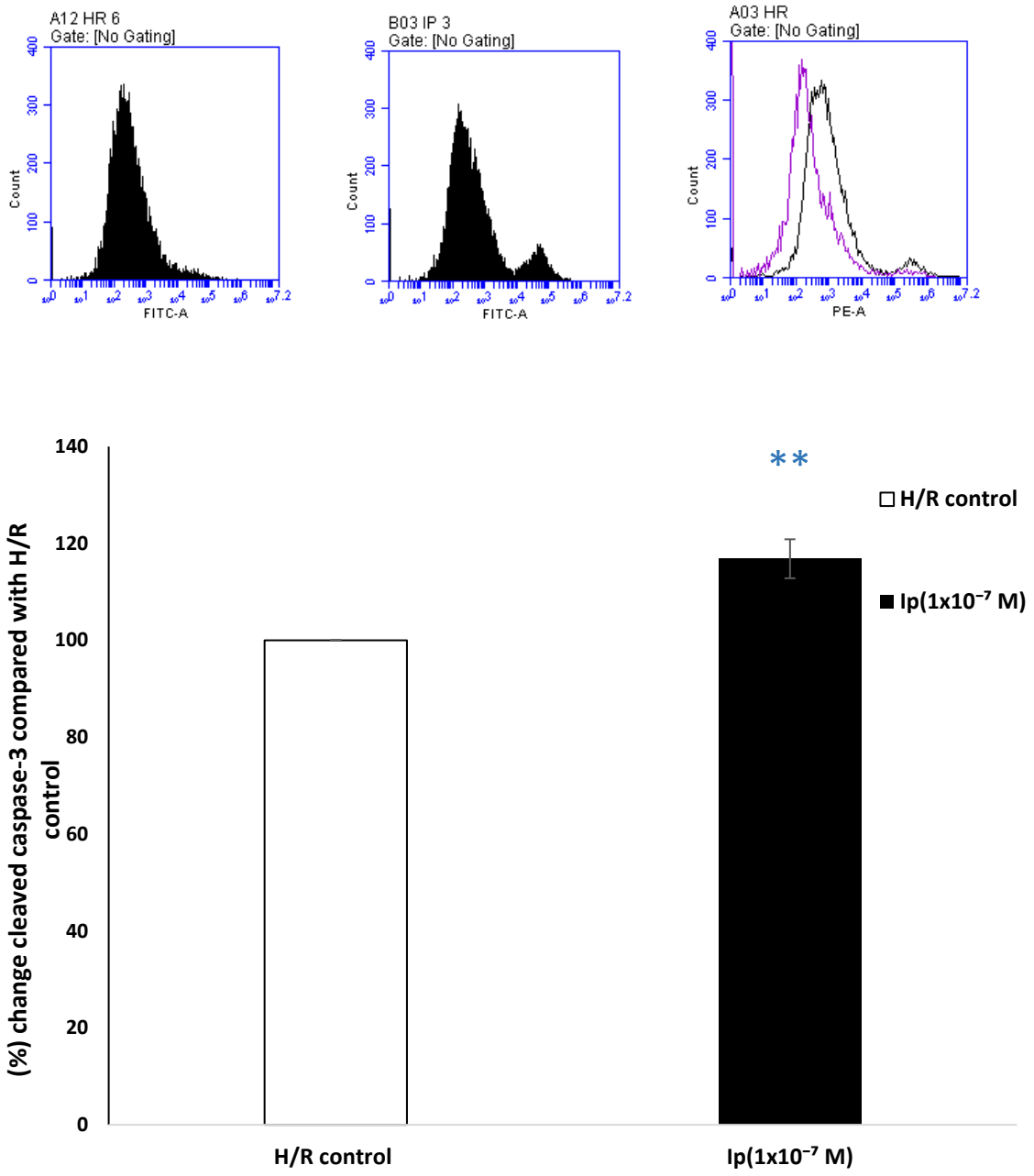

Figure 3. 8: Effect of ipratropium (1 × 10^{-7} M), caspase-3 activity in comparison to H/R control the data was analysed after changing it into arithmetic means by normalised to H/R control, ± SEM, the recorded number myocytes is 10,000, n = 6. * *= p<0.01 vs. H/R control which showed Ip was able to significantly increase the % of activity of caspase-3.

3.3 Western Blot Results

In Western blotting studies the rats were sacrificed prior to extraction of the heart which was mounted on a modified Langendorff perfusion apparatus. Regional ischeamia was induced in which the descending left coronary arteries was ligated for 35 minutes after that a period of 15 or 30 minutes' reperfusion. I/R, Ipratropium bromide (1×10^{-7} M – 1×10^{-9} M), were administered at the onset, and throughout, reperfusion. Tissue was homogenised and prepared for Western blot analysis for Drp1, Akt, Erk1/2 and caspase-3 (Explained in detailed in section 2.2.3.1-2.2.3.7).

3.3.1 Western Blot Results For The 15 And 30 Minutes Post Reperfusion

These results were presented in the Figures 3.9 - 3.12 (explained in detailed in section 2.2.3.8 and 2.2.3.9). To determine the effect of time points in the expression of the proteins of interest, which were Akt, Erk1/2, Drp 1, Active caspase-3 and, after the addition of Ip (1×10^{-7} M – 1×10^{-9} M).

3.3.1.1 The Measurements Of (I/R And Ipratropium Bromide (1×10^{-9} M – 1×10^{-7} M)).

The level (phosphorylation to total) of Akt, Erk 1/2, Drp1 and cleaved caspase-3 show an increased in the isolated perfused hearts treated with Ip (1×10^{-7} M – 1 x1 0^{-9} M) compared with I/R control with the highest concentration having the most phosphorylation of Akt, Erk 1/2, Drp1 and cleaved caspase-3 (Figures 3.9 -

3.12). However, there was no significant difference against the untreated control apart from Akt at 15 minutes (1 x 10^{-7} M) against the untreated control (167.08 ± 29.93% vs.100 ± 0 control). No significant difference for other treatment group against the control at 15 minutes reperfusions nor against the treated group. Ip (1x10^{-7}) significantly increase the phosphorylation of Akt after 30 minutes reperfusion vs. I/R control (208.49 ± 24.42% vs.100 ± 0 control).

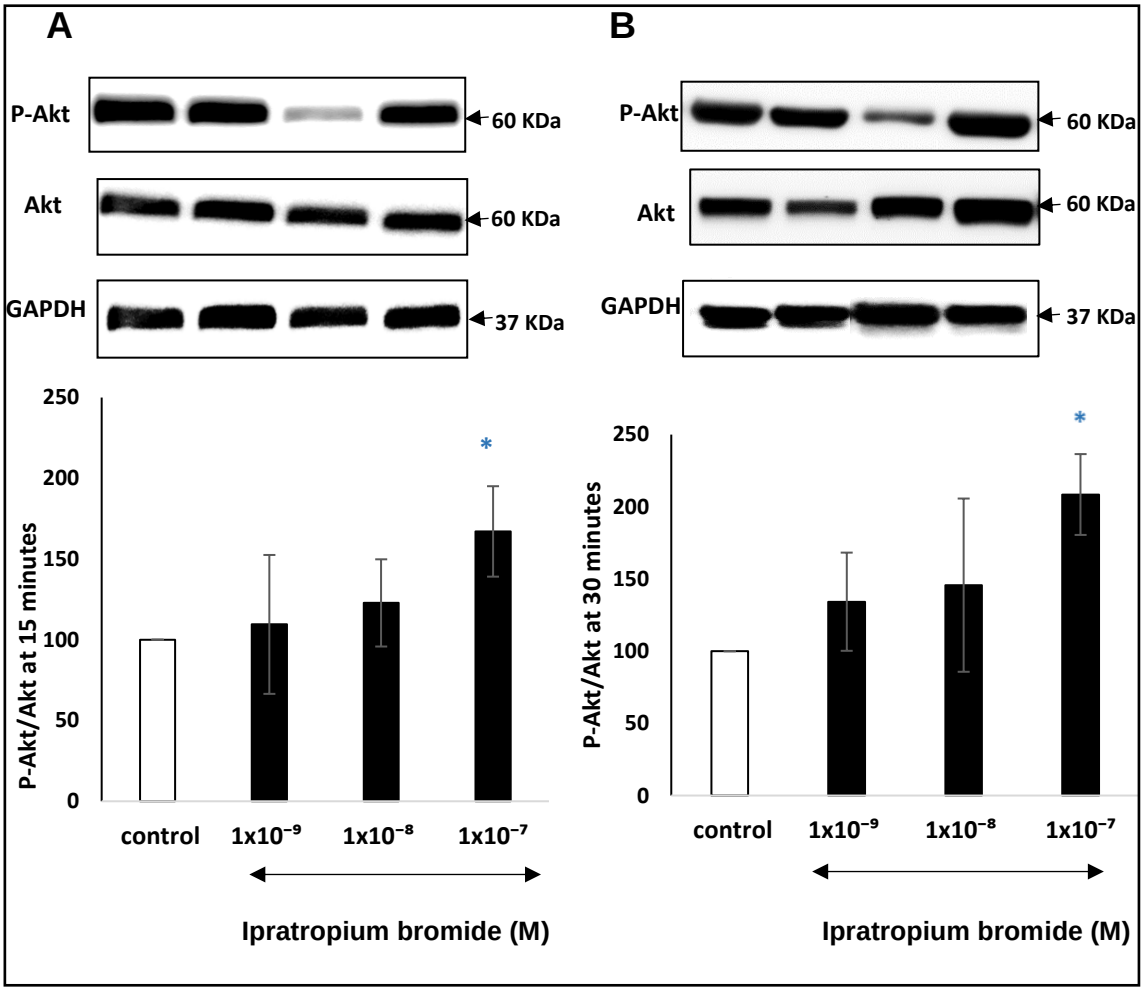

Figure 3. 9: The levels of phospho and Total Akt in I/R control, Ipratropium bromide (1 x 10 -^{9} M – 1 x 10^{-7} M). A is treatment groups perfused for 15 minutes isolated rat hearts. B is treatment groups perfused for 30 minutes isolated rat hearts. Results displayed as means + SEM, n=6. * p<0.05 vs. I/R control.

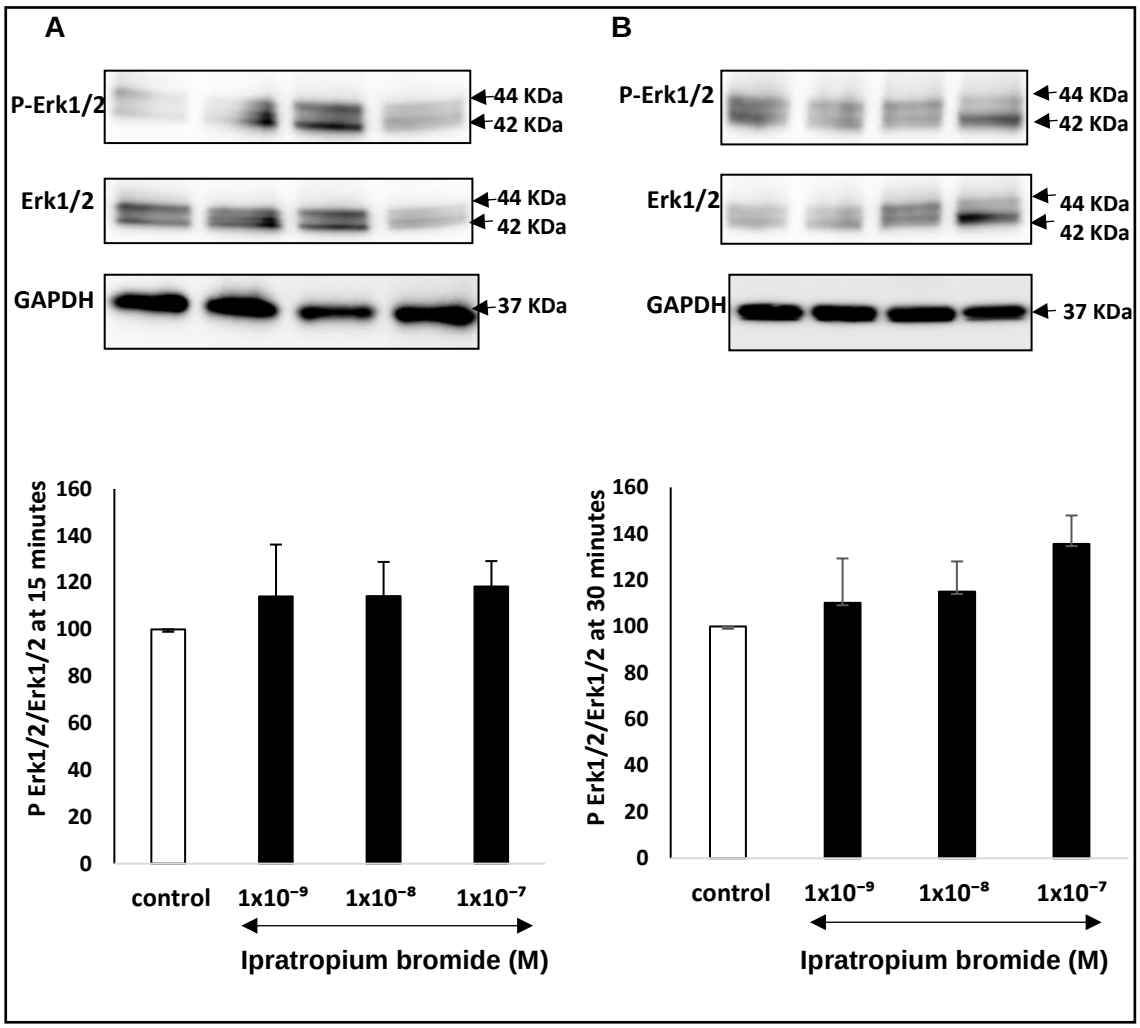

Figure 3. 10: The levels of phospho and Total Erk 1/2 in I/R control, Ipratropium bromide (1×10^{-9} M – 1×10^{-7} M). A is treatment groups perfused for 15 minutes isolated rat hearts. B is treatment groups perfused for 30 minutes isolated rat hearts. Results displayed as means + SEM, n=6.

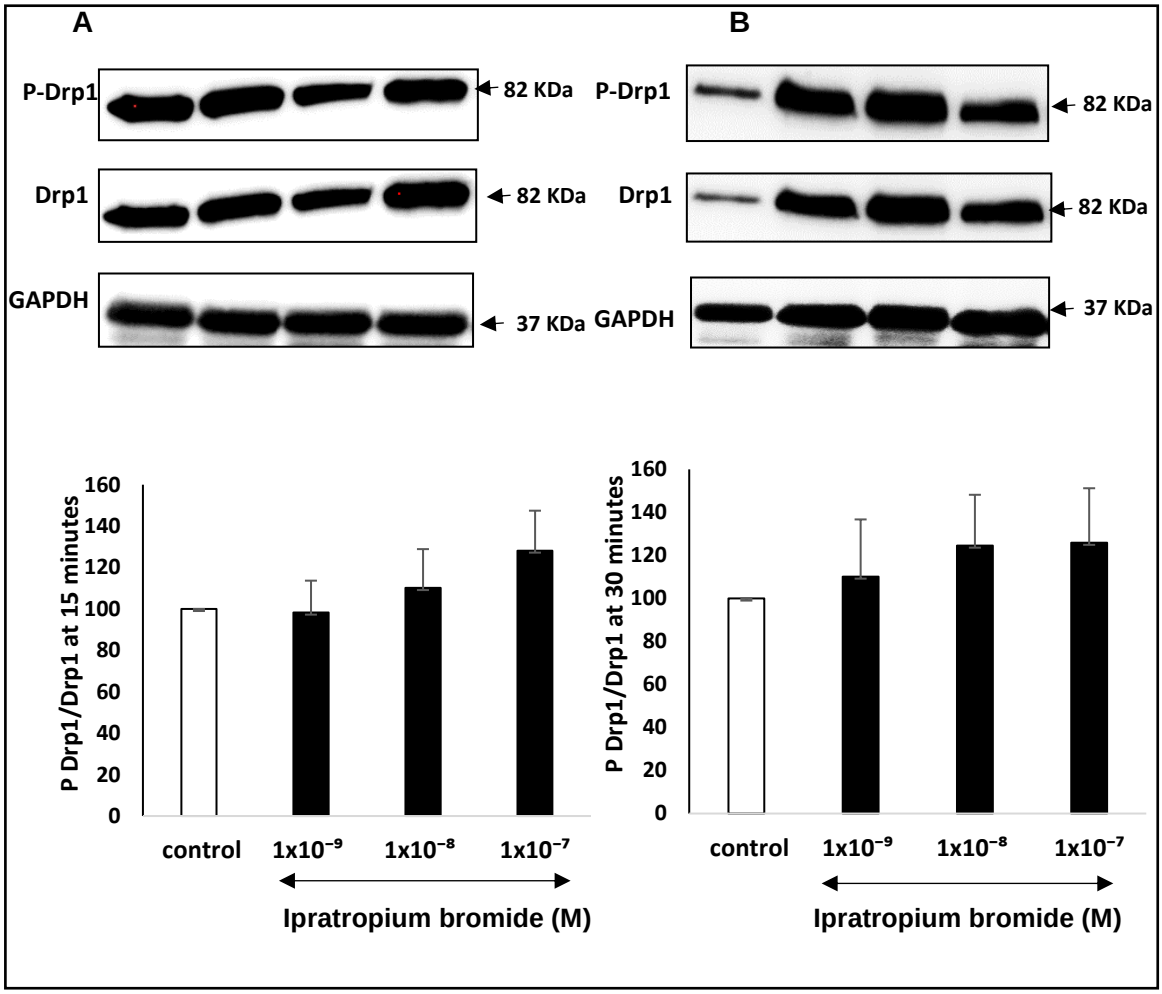

Figure 3. 11: The levels of phospho and Total Drp1 in I/R control, Ipratropium bromide (1×10^{-9} M – 1×10^{-7} M). A is treatment groups perfused for 15 minutes isolated rat hearts. B is treatment groups perfused for 30 minutes isolated rat hearts. Results displayed as means + SEM, n=6.

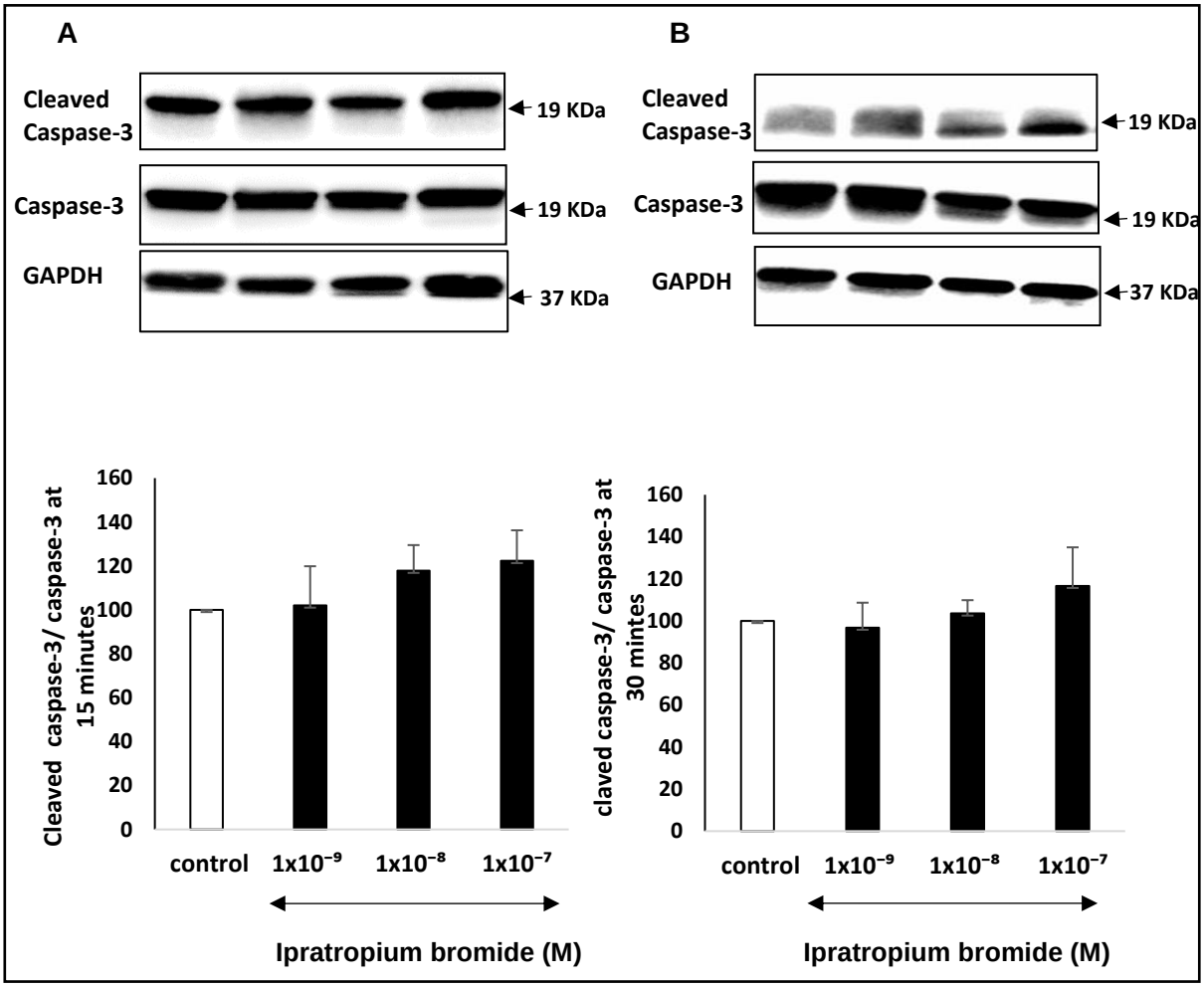

Figure 3. 12: The levels of cleaved and active capsae-3 in I/R control, Ipratropium bromide (1 x 10^{-9} M – 1 x 10^{-7} M) A is treatment groups perfused for 15 minutes isolated rat hearts. B is treatment groups perfused for 30 minutes isolated rat hearts. Results displayed as means + SEM, n=6.

3.4 PCR Results

The obtained tissue was submerged in RNAlater® and kept in the -80 ˚C freezer for PCR analysis the tissue was homogenised in Trisure™ to extract RNA in order to synthesise cDNA to make PCR reaction in order to measure the percentage change induced by the drug treatment against the control using the house

keeping gene as the baseline. The gene of interest used was Dnm1l against GAPDH primers for I/R control and Ipratropium bromide (1 x 10^{-7} M) (Explained in detailed in section 2.2.4.1- 2.2.4.3). No significant difference appeared between the control and Ip treated groups (1419 ± 900.45% vs. 100 ± 0) (Figure 3.13). Despite the pattern shown which suggest that Ip was able to increase the expression of Dnm1l, the high variation seen in the figure is due to the data being inconclusive. As preforming the statistical analysis test provided that there was no significant difference (explain in detail in the limitations section.

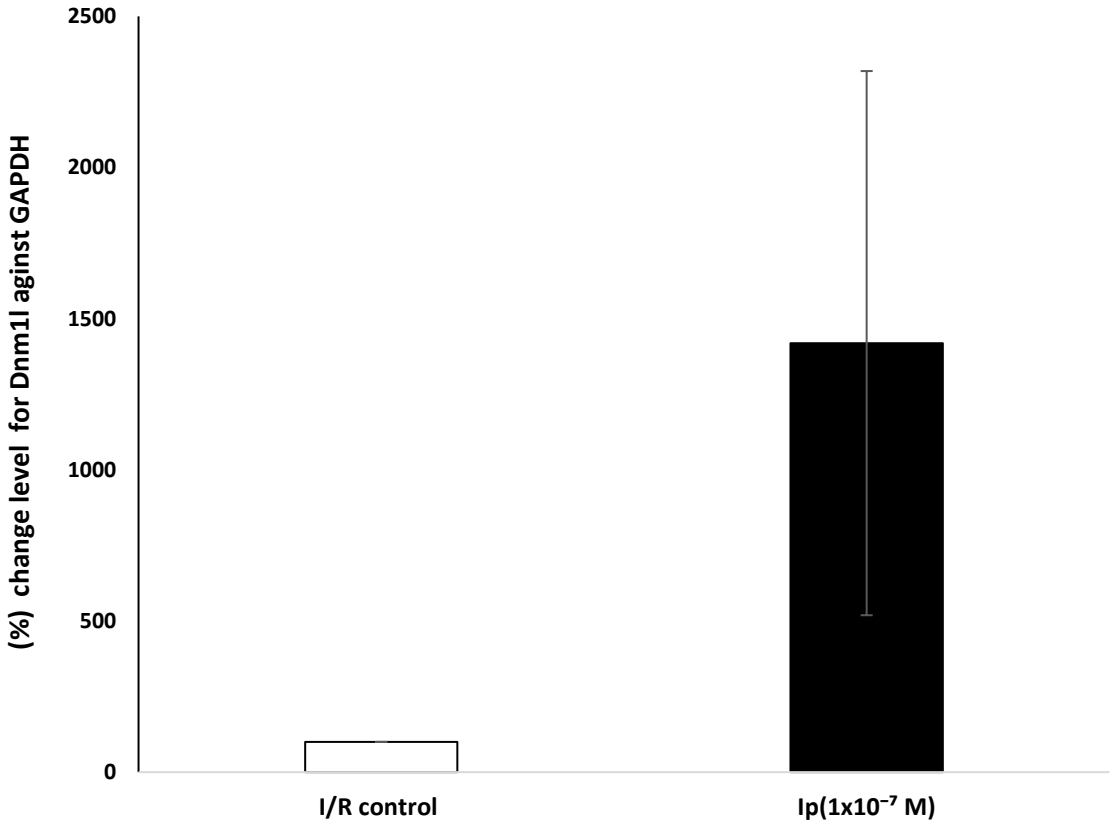

Figure 3. 13: The levels of fold change in Dnm1l in I/R control, Ipratropium bromide (1 x 10^{-7} M) is treatment groups perfused for 15 minutes isolated rat hearts. Results displayed as means + SEM, n=6.

3.5 Chapter Discussion

This study's findings support previous evidence suggested that Ip exacerbates myocardial injury via increases in infarct (Figure.3.4) and apoptosis (Figure.3.5) under stimulated I/R injury of myocardial. Since that *in vitro* models of stimulated I/R condition the myocardial injury was exacerbated by the administration of Ipratropium bromide, which occurred in this study as well, shown in the significant increase as seen in Figure.3.4 infarction in isolated perfused rat myocardial with the addtition of Ip (1×10^{-9} M – 1×10^{-7} M) and decreasing the viability in isolated left ventricular myocytes, this work further supports previously reported experimental findings that suggested that Ip promote exacerbation of reperfusion injury, however, the mechanism of its exacerbation of injury was not established (Harvey, Hussain and Maddock 2014).

The Langendorff results showed that haemodynamic parameters measured were decreased (LVDP and CF) with the exception of HR (Figure.3.1 - Figure.3.3), which was increased, with Ip (1×10^{-7} M) causing the most reduction followed by Ip (1×10^{-8} M) then Ip (1×10^{-9} M), in a concentration responsive manner. HR results showed increase when Ip (1×10^{-9} M – 1×10^{-7} M) were added, the highest concentration dependent manner. Findings showed a similar pattern to Harvey, Hussain and Maddock (2014) study with regards to the toxicity associated with the administration of Ip at the beginning and throughout reperfusion for 120 minutes with a noticeable decrease in LVDP and CF and increase in HR and the infarct size. Interestingly, Ip did not show to provide haemodynamic effect, despite the observed exacerbation of infraction development. These results also

support previously published literature that muscarinic antagonism in the myocardium can act with positive ionotropic and chronotropic effects, since the activity is mediated by the muscarinic receptors M2 subtype it was found that agonist treatments such as carbachol have negative effect on ionotropic in mice artery, also there was a link found between ionotropic and chronotropic and calcium influx as well as protein kinase C which have a positive ionotropic effect , since they effect may lead to contractility dysfunction as abnormal level of calcium influence contraction(Kitazawa et al. 2009, Sethi, Zakharyan and Muradyan 2019). It is postulated here that the gradual decrease in LVDP, which was ultimately significant from the control ($p<0.05$), identified in these studies is attributable to the exacerbation of damage caused by Ip following the insult of the I/R protocol to the experimental models used as highlighted in in sections 2.2.1.1 - 2.2.1.5 in chapter 2. In the infarct studies AAR% the injury in the groups treated by Ip, was exacerbation; showing that the injury by with the highest concentration being the most toxic and caused most injury with a significant difference compared with the control and the other concentrations Ip (1×10^{-9} M, 1×10^{-8} M, 1×10^{-7}) (Figure.3.4) ($p<0.05$, $p<0.01$, $p<0.001$) respectively. These studies were during for isolated heart with I/R stimulated conditons, and, again, support previously published literature that has demonstrated that Ip exacerbates RI in non-clinical models *in vitro* in a dose responsive manner (Harvey, Hussain and Maddock 2014). In the flow cytometry studies Ip (1×10^{-7} M) increased the level of total apoptosis significantly compared to the H/R control (Figures 3.5), and it decreased cell viability with a significant difference (Figures 3.7) ($p<0.05$) for both figures. In caspase-3 measurements Ip (1×10^{-7} M) was able to significantly

increase caspase-3 activity which suggest apoptosis (Figures 3.8) ($p<0.01$). The activity of caspase-3 was significantly more than the control as the results obtained from apoptosis. This suggest that the main cause of the injury is apoptosis rather than necrosis since necrotic cell death was not significantly differ than the untreated control (Figures 3.6) (Cassambai et al. (2019). Caspase-3 is an important key factor in both intrinsic and extrinsic apoptosis pathway, the high level of cleaved caspase-3 indicates that the myocytes are undergoing apoptosis (Wu et al. 2013).

The western blotting analysis for the isolated heart perfused with Ip (1×10^{-9} M – 1×10^{-7} M) at the onset and throughout reperfusion that lasted for 15 or 30 minutes for the measurements of Akt, Erk1/2, Drp1 and caspase-3, resulted in the expression of phospho-Akt, Erk1/2, Drp1 and caspase-3 as to be increased showed in Figures 3.9 - 3.12, A and B, for all concentration at both time points with an observed increase compared to untreated the control. Ip (1×10^{-7} M) was able to significantly increase the phosphorylation of Akt at 15 and 30 minutes post reperfusion ($p<0.05$) (Figures 3.9 A, B). With Erk1/2 and capase-3 there was no significant difference (Figures 3.10, 3.12 A, B). These findings agree with the finding of Harvey, Hussain and Maddock (2014) regarding the administration of Ip at the onset of reperfusion has shown that Akt and Erk1/2 phosphorylation levels increased in the deregulate Reperfusion Injury Salvage Kinase (RISK) pathway (Khan, 2015). Interestingly, these findings also agree with those of Gharanei et al. (2013), who also observed pathological increases in the levels of RISK pathway signalling proteins and this was associated with an increase in cell death his study investigating the mechanism of Doxorubicin. This could

potentially be due to a shared anti-muscarinic action by both Doxorubicin and Ip, although the exact mechanism is not yet fully understood (Gharanei et al. 2013). Increasing the phosphorylation of Akt excludes the possibility of ipratropium inducing Akt and Erk1/2 with down regulation at both time points of Langendorff experiments as shown in the results with relative increase in the phosphorylated Akt and Erk1/2 upon Ip administration treated group (Derek et al. 2004). The activation of Akt and Erk1/2 regulate apoptosis according to the published literature (Khan, 2015). The phosphorylation of Erk 1/2 was found to play a role in caspase-dependent apoptosis as well as Akt activation plays an even greater effect in caspase-independent apoptosis (Li et al. 2013). The activation of Bcl-2 family members (BAD and BAX) pro-apoptotic proteins as a result to Akt chronic phosphorylation in this case that leads to the opening of mPTP releasing cytochrome-c leading to intrinsic apoptosis (Liang et al. 2014). In general, the activation or increase in Akt and Erk1/2 levels are considered to be protective mechanisms against insults such as ischaemia/reperfusion injury inside the cell (Li et al. 2013). The active Akt and subsequently protein kinase C are considered as proteins with cardioprotective properties against ischaemic conditions via apoptosis and necrosis inhibition (Winnay et al. 2013). protect the heart against ischemia/reperfusion-induced injury by activating signal transduction pathways and sustaining mitochondrial functions reduced the ratio of myocardial infarct size to area at risk (Wang et al. 2011). cardioprotective effect by decreasing apoptosis of cardiomyocytes and inhibiting expression of inflammatory mediators after myocardial ischemia (Wang et al. 2011). PI3K/Akt activation is considered to maintain the inhibition of apoptosis and alerting the survival mechanism, by the

release of protection signal to the mitochondria from the surface of the cell (Winnay et al. 2013). In ischaemic/ Reperfusion preconditioning setting which release non- lethal cycle of I/R to gain protection from lethal sustained episode of IRI (Li et al. 2013, Hausenloy and Yellon 2013). The continuous expression of Akt after reperfusion was associated with negative effect, leading to cell death actions, including apoptosis, to the cell survival pathway during I/R conditions (O'Neill and Abel 2005, Nagoshi et al. 2005, Harvey, Hussain and Maddock 2014). A mutation occurrence in mammalian hearts resulting in Akt over expression can lead to the potential of injury in myocardium as a result of the constitutive activation of Akt (Harvey, Hussain and Maddock 2014). Injury observed with in the current study correlates with finding displayed in Harvey study (2014). It is therefore postulated that the constitutive over-expression of Akt via a still unknown mechanism is partially culpable for the observed increase in injury observed following Ip administration. Attribution to overstimulation of Akt signaling, the more Akt is phosphorylated the increase level of infraction and vis versa the decreased level of Akt phosphorylation resulted in reduction in infraction (Sussman et al. 2010). Ascertained Akt levels and its detrimental effect proposed Ip induce injury via the continuative over activation of Akt which is possible due to the overactivation of PI3K , the upstream regulate Akt and Erk1/2 (Sussman et al. 2010). The phosphorylation of Erk1/2 results were similar to Akt results with an observed increase at 15 minutes and 30 minutes of reperfusion for Ip treated group (1×10^{-9} M – 1×10^{-7} M) compared with I/R untreated group (Figures 3.10 A, B). These finding are similar to Harvey, Hussian and Maddock (2014) in terms of pattern. Despite the apparent pattern within Erk 1/2 results

there was no significant difference, as shown in the results section 3.3.1.1 (Figures 3.10), Ip (1 x 10^{-7} M) was able to increase the phosphorylation of Erk1/2 compared to untreated control, however, the statistical analysis did not present significant difference. Erk1/2 showed similar pattern to Akt both kinases have anti-apoptotic properties (Yin et al. 2013). This is thought to be due to not efficient time of reperfusion of 15 or 30 minutes, for Erk1/2 phosphorylation to increase significantly (Maddock, Mocanu and Yellon 2003). Erk1/2 phosphorylation provide similar action of Akt activation, both kinases have apoptotic inhibition properties maintaining cell survival (Yin et al. 2013). PI3K/Akt was one of the main kinases to inhibit cell death programme as well as evoking the proliferation of the cell providing mechanism of defense against apoptosis consequently reducing related injury (Yin et al. 2013). Erk1/2 is considered to provide cardio-protection against I/R insults with an importance towards RISK (Yin et al. 2013). Erk1/2 mechanism of action is based on the inhibition of the dephosphorylation of the Bcl-2 the latter is associated with (BAD) the death promoter, the later inhibited apoptosome development which restrict executioner caspases activation (Yin et al. 2013). Harvey study (2014) suggested the detrimental effect of Erk1/2 overexpression in the cellular survival programme which is supported by the current studies and, as such, whilst the results are supported, the nature of this over-activation is still not fully understood. Erk1/2 activation restrict caspase activation in normal condition, and it prevent the formation of apoptosome (Derek et al. 2004). However, in stress condition Erk1/2 overactivation can result in negative effect on the cell shown in Ip induced injury

with continuation of Erk1/2 activation (Sussman et al. 2010) further explained in relation to calcium overload in section 5.5.

In contrast to previous studies by Disatnik et al. (2013) and Duan et al. (2020) identification for the involvement of Drp1 in Ip induced myocardial injury were carried out in this study in order to indicate whether there was mitochondria element in Ip injury induction (Figures 3.11 A, B). The obtained Drp1 results indicated a role for the mitochondria and a potential, currently unknown, mechanism leading to Ip induced apoptosis following I/R injury (Disatnik et al. 2013, Duan et al. 2020). The main role of Drp1 is that it helps regulate vital processes within the cell such as apoptosis, necrosis and cell division (Hu, Huang and Li 2017). Drp1 is responsible for mitochondrial fission, and a result the phosphorylation of Drp1 causes mitochondria dysfunction (Ko et al. 2016). Dynamic large GTPase Drp1/Dnm1Dynamin related proteins with a very important role in mitochondria (Hu, Huang and Li 2017). The mitochondria balance fission and fusion and gene encoded GTPase fission relates to DNA replication fusion occurs when two adjacent mitochondria join whereas fission is when one mitochondrion separates into two (Liu, et al 2020). Dephosphorylation in Drp1 Serine ($_{637}$) inhibits fission and promote fusion, Drp1 Serine ($_{616}$) phosphorylation by B/cyclin dependent kinase 1 leading to apoptotic cell death via mitochondria fission (Roe, and Qi, 2018). By promoting mitochondrial fission, Drp1 activation leads to fragmentation of mitochondria and mPTP opening releasing pro-apoptotic protein cytochrome c resulting in apoptosis (Hu, Huang and Li 2017). Therefore, the results (Figures 3.11 A, B). from this current study indicate a role for the mitochondria in Ip mediated injury via a mechanism

involving B/cyclin dependent kinase 1 potentially contributing via the phsphorleation of Drp1 Serine ($_{616}$), or initiating, the observed increases in apoptosis seen follow Ip administration (Ko et al. 2016).

PCR results did not present a significant difference of Dnm1l expression between Ip treated group and the untreated control used (Figure 3.13). Despite the increase in expression in Ip treated group. This might be as a result of the period of reperfusion, as 15 minutes might not be adequate for the gene to be expressed because in Troncoso et al. (2014) study which measured the expression of Dnm1l after 6 hours of reperfusion. Not to mention the possibility that the n number of the samples might not be enough. As well and not having the chance to preform PCR reaction on the tissue samples that are collected after 30 minutes of reperfusion because the Roto-Gene, PCR machine, that were used for the detection of PCR reaction were given from the university to the university hospital due to COVID 19 pandemics.

Normoxic studies in the presence of the pharmacological agents were not conducted as they are not considered to be clinically relevant, because Ip was administered during normoxia in pervious study by Harvey, Hussain and Maddock (2014) and no injury was detected. The results showed that Ip presented no significant increase in infraction or apoptosis when compared to the normoxic control, previous preliminary studies demonstrated that Ip did not affect infarction or cellular viability in normoxic conditions, and this was established by Harvey et al. and other, unpublished work, from our laboratory (Harvey, Hussain and Maddock 2014). This study supports previous findings that Ip exacerbates myocardial injury via increase in infarct and apoptosis, but it is the first one to link

Drp1 phosphorylation with the induced injury. Therefore, the results from this experimental chapter helps to validate the experimental techniques that were employed in this project and also, for the first time, provide direct evidence to link that there may be specific mitochondrial involvement in the observed Ip mediated myocardial injury.

Chapter 4: Ipratropium Bromide Mediated Myocardial Injury Is Attenuated By the Mitochondrial Division Inhibitor Mdivi-1

The previous chapter (chapter 3) indicated that the exacerbation of Ip induced injury occurred during the administration of Ip at the onset of reperfusion in models of stimulated I/R conditions and the main caused for exacerbated injury were mainly apoptosis and via an increase in infarction (AAR%). However, whilst Akt and Erk1/2 phosphrlyation involved in a manner previously reported, it is still not evident that the changes in these protein levels are required for Ip induced myocardial injury. Evidence from previous studies have suggested the mitochondria may have a role in exasperating the injury (Harvey, Hussain and Maddock 2014, Intachai et al. 2018), but this has never been characterised. In addition to this, the work in the previous chapter demonstrated (Figure 3.11), for the first time, that Drp-1 action may be a reason in Ip-induced myocardial injury, which, for the first time provides more definitive evidence of mitochondrial involvement. Therefore, to further investigate mitochondria role of action, Mdivi-1 was used in the current study as Mdivi-1 is a well-reported mitochondrial involvement indicator (Ruiz, Alberdi and Matute 2018). Gharanei et al. (2013) study showed that Mdivi-1, which showed anti-cancer properties, was also cardio-protective against I/R against doxorubicin. The aim of the current study was to identify whether Mdivi-1 demonstrated the same protective properties as in previous studies such as Sharp et al. (2014) studies and Maneechote et al. (2018), importantly, to assess whether this had an influence on Ip mediated injury as this would imply that there is mitochondrial involvement in Ip mediated injury and, importantly, if there was the ability for Mdivi-1 to abrogate Ip induced injury

as this could provide new information to help with the development of potential adjunctive therapies in clinical cases of Ip mediated myocardial injury.

4.1 Langendorff Model Of Perfused Rat Heart Results

Ipratropium bromide (1 x 10^{-7} M) and Mdivi-1(1 x 10^{-7} M) ± Ipratropium bromide (1 x 10^{-7} M) were added at the start and during the period of reperfusion in order to measure haemodynamic parameters during reperfusion as well as the infarct size (which was calculated as Area At Risk% (AAR %)), for the Langendorff model studies, (explained in detail in section 2.2.1.1-2.2.1.5).

4.1.1 Haemodynamic Parameters (I/R And Ipratropium Bromide (1x10^{-7} M) And Mdivi-1(1x10^{-7} M) ± Ipratropium Bromide (1x10^{-7} M))

The haemodynamic parameters measured were: LVDP, HR and CF. The period of the measurement that readings were taking was for stabilisation period, ischaemia and after initiating reperfusion for 120 minutes the recordings were taken every 15 minutes. Following the end of the experiment, the heart was taken out and frozen at -20 °C prior to assessment for infarct/risk ratio and Area At Risk (AAR %) analysis.

4.1.1.1 The Left Ventricular Developed Pressure (LVDP)

LVDP was determined for I/R and Ip (1×10^{-7} M) and Mdivi-1 (1×10^{-7} M) ± Ip (1×10^{-7} M) (explained in detail in section 2.2.1.6.1 in chapter 2). The results showed that LVDP was enhanced with the co-administration of Mdivi-1 (1×10^{-7} M) and Ip (1×10^{-7} M). At 160 and 175 minutes Mdivi-1(1×10^{-7} M) significantly increased the LVDP compared to the Ip (1×10^{-7} M) treated group (66.2 ± 5.9%, 62.3 ± 7.1% vs. 47.5 ± 6.2%, 45.4 ± 6.7%) ($p<0.05$) (The significant difference between I/R control and Ip (1×10^{-7} M) in LVDP is mentioned in section 3.1.1.1). Left ventricular developed pressure measurements for I/R control and Ipratropium bromide (1×10^{-7} M) and Mdivi-1 (1×10^{-7} M) ± Ipratropium bromide (1×10^{-7} M) (Figure 4.1).

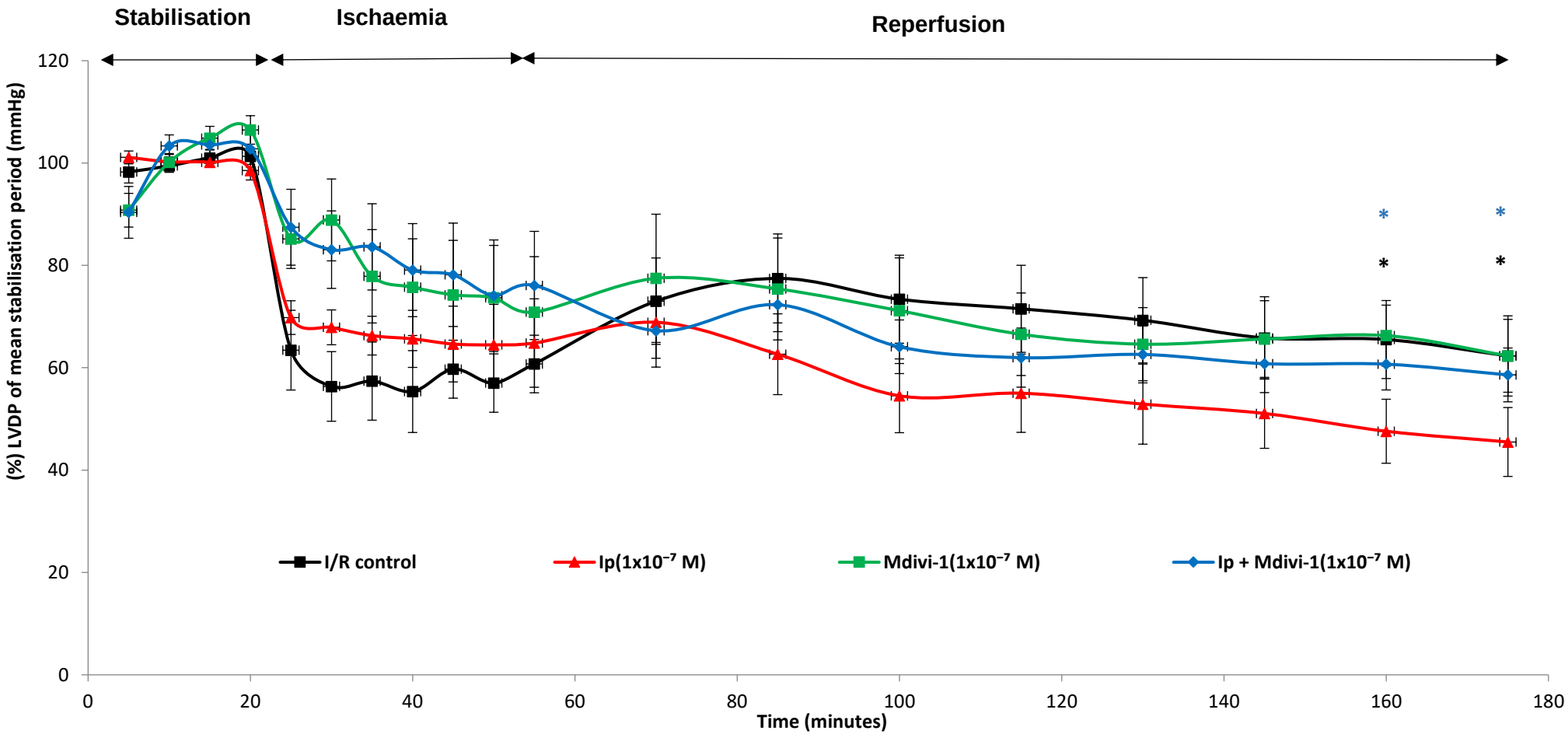

Figure 4. 1: Changes in left ventricular developed pressure % of (mmHg) in isolated perfused rat hearts group's I/R and Ipratropium bromide (1 x 10^{-7} M) and Mdivi-1(1 x 10^{-7} M) ± Ipratropium bromide (1 x 10^{-7} M), n=6. * p<0.05 vs. I/R control against Ipratropium bromide (1 x 10^{-7} M). * *p*<0.05 for Mdivi-1 (1 x 10^{-7} M) treated group against Ipratropium (1 x 10^{-7} M).

4.1.1.2 Heart Rate (HR)

HR was measured for I/R control, Ipratropium bromide (1 x 10^{-7} M) and Mdivi-1(1 x 10^{-7} M) ± Ipratropium bromide (1 x 10^{-7} M) (explained in detail in section 2.2.1.6.2 in chapter 2). The results show that hearts rate were significant for Mdivi-1 treated group vs. I/R control at 70 minutes (109.8 ± 6.1% vs. 91.4 ± 4.7%), 100 minutes (115.4 ± 7.2% vs. 97.7 ± 6.9%), 145 minutes (121.1 ± 6.6% vs. 103.8 ± 7%) 160 minutes (119.9 ± 6.2% vs. 99.7 ± 6.9%) of reperfusion ($p<0.05$) and 115 minutes (117.2 ± 5.3% vs. 97.2 ± 6.4%), 130 minutes (116.1 ± 5.2% vs. 98.3 ± 6.1%) 175 minutes (119.9 ± 11.4% vs. 97.3 ± 6.5%) ($p<0.01$). there was a significant difference between Ip vs. Ip +Mdivi-1 ($p<0.05$) and for Mdivi-1 against Ip+Mdivi-1 at 100 minutes (113.8 ± 6.2% vs. 96.2 ± 3.6%), 115 minutes (117.2 ± 5.3% vs. 99.2 ± 4.1%),130 minutes (116.1 ± 5.2% vs. 96.2 ± 3.4%), 145 minutes, (121.1 ± 6.6% vs. 98.7 ± 3.7%) 160 minutes (119.9 ± 6.2% vs. 96.8 ± 3.4%) and 175 minutes of reperfusion (119.9 ± 11.4% vs. 98.1 ± 2.8%) ($p<0.01$, 0.05) respectively (The significant difference between I/R control and Ip (1 x 10^{-7} M) in HR is mentioned in section 3.1.1.2). Heart rate for I/R control and Ipratropium bromide (1x10^{-7} M) and Mdivi-1(1x10^{-7} M) ± Ipratropium bromide (1x10^{-7} M) (Figure 4.2).

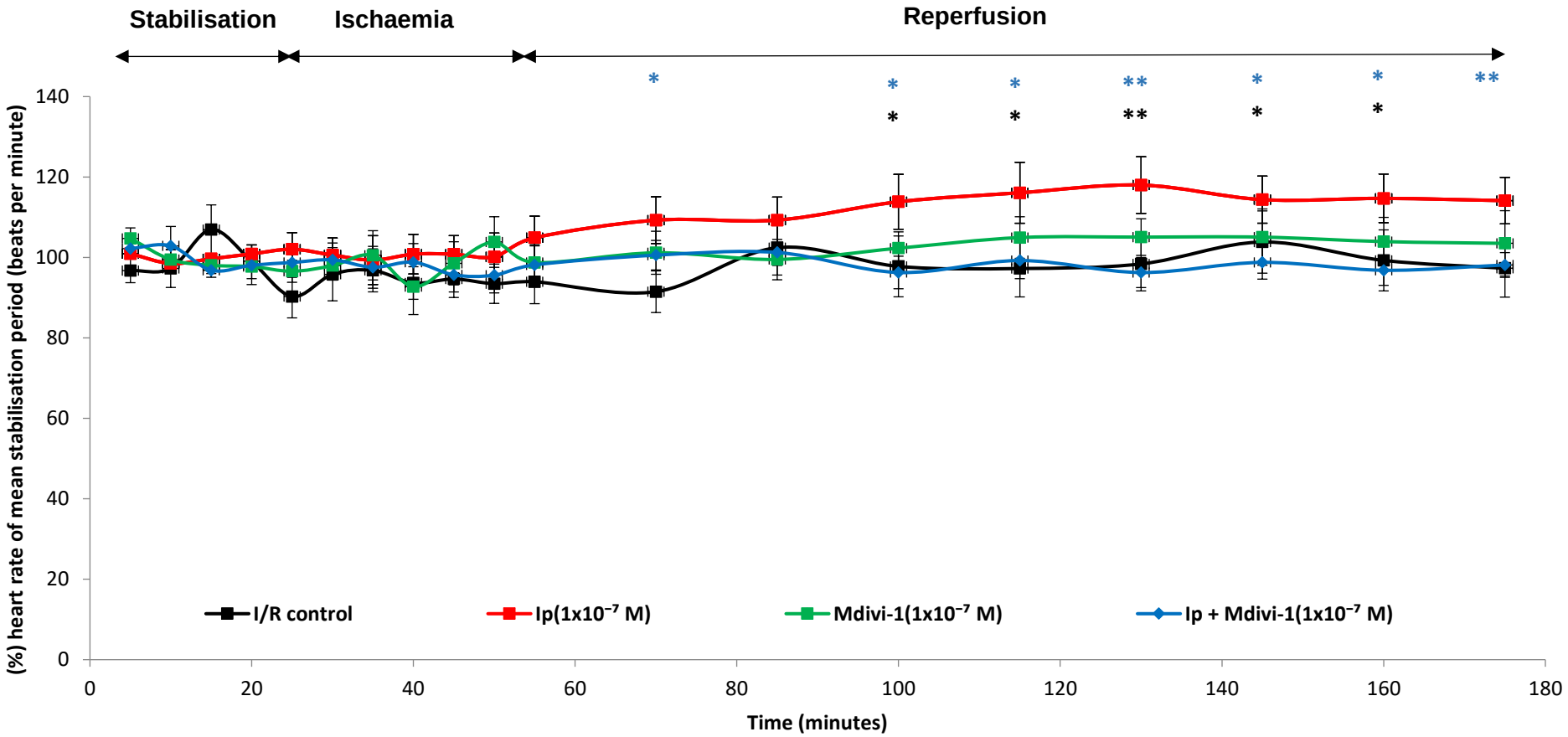

Figure 4. 2: Changes in heart rate (bpm) in isolated perfused rat hearts. All groups I/R control, Ipratropium bromide (1 x 10^{-7} M) and Mdivi-1(1 x 10^{-7} M) ± Ipratropium bromide (1 x 10^{-7} M), n=6. * p<0.05 for Mdivi-1 (1 x 10^{-7} M) treated group against I/R control. * p<0.05 for Ip + Mdivi-1(1 x 10^{-7} M) treated group against Ipratropium (1 x 10^{-7} M). ** p<0.01 Mdivi-1(1 x 10^{-7} M) treated group against I/R control. ** p<0.01 Ip + Mdivi-1(1 x 10^{-7} M) treated group against Ipratropium (1 x 10^{-7} M).

4.1.1.3 Coronary Flow (CF)

Coronary flow (CF) was measured (explained in detail in section 2.2.1.6.3 in chapter 2). The results for coronary flow showed no significant differences between the different experimental groups compared with the I/R control. Coronary flow results for I/R control and Ipratropium bromide (1 x 10^{-7} M) and Mdivi-1(1 x 10^{-7} M) ± Ipratropium bromide (1 x 10^{-7} M) (Figure 4.3).

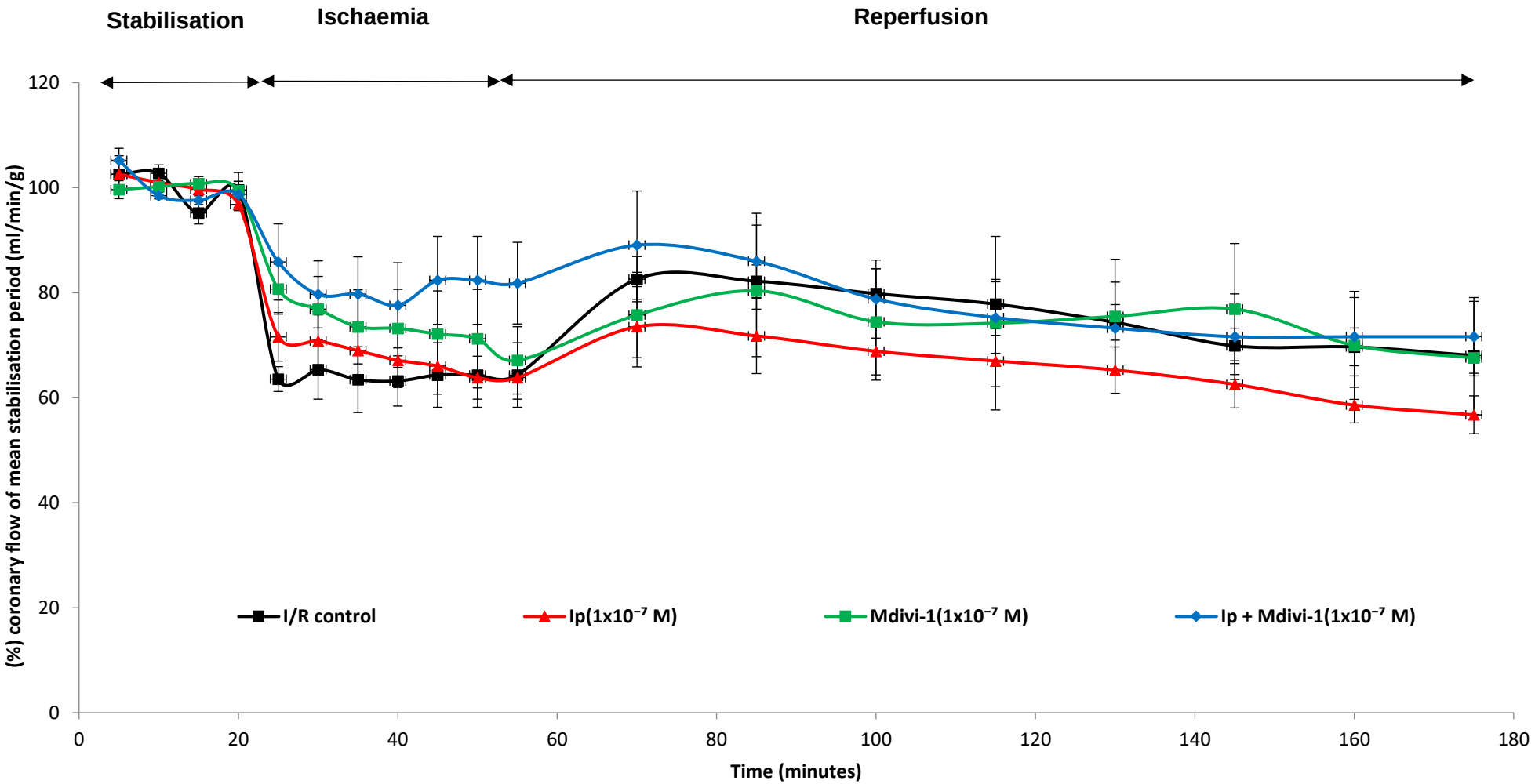

Figure 4. 3: Changes in coronary flow (ml.min-1) in isolated perfused rat hearts, n= 6. I/R control, Ipratropium bromide (1 x 10^{-7} M) and Mdivi-1(1 x 10^{-7} M) ± Ipratropium bromide (1 x 10^{-7} M), n=6.

4.1.2 The Infarct Risk Ratio Area At Risk (AAR %)

Ipratropium bromide (1 x 10^{-7} M) or Mdivi-1 (1 x 10^{-7} M) ± Ipratropium bromide (1 x 10^{-7} M) were added at the start and throughout reperfusion which lasted for 120 minutes, Evans blued and TTC protocol was followed for the measurement of AAR% (explained in detail in section 2.2.1.7). There was a significant difference between the Ip treated group and the I/R control (158.5 ± 6.2% vs. 100 ± 0) ($p < 0.001$). Mdivi-1 showed cardio-protection; importantly there was a significant reduction in infarction compared with the untreated control (65.5 ± 4.5% vs. 100 ± 0) ($p < 0.001$), There was also significant difference between Ip and both Mdivi-1 and Ip+ Mdivi-1 the co-administration of abrogates Ip mediated increases in infarction against Ip treated group (65.5 ± 4.5, 82.7 ± 2.9% vs. 158.5 ± 6.2%) ($p < 0.001$ for both groups). It is important to note, a reduction was also significant when Mdivi-1 with Ip (82.7 ± 2.9% vs. 100 ± 0) ($p < 0.01$), thus abrogating the IP mediated increase in myocardial injury. I/R control, Ipratropium bromide (1 x 10^{-7} M) or Mdivi-1 (1 x 10^{-7} M) ± Ipratropium bromide (1 x 10^{-7} M) treatment groups, the Mdivi-1 treatment group demonstrated protection against both Ip mediated injury and I/R injury (Figure 4.4).

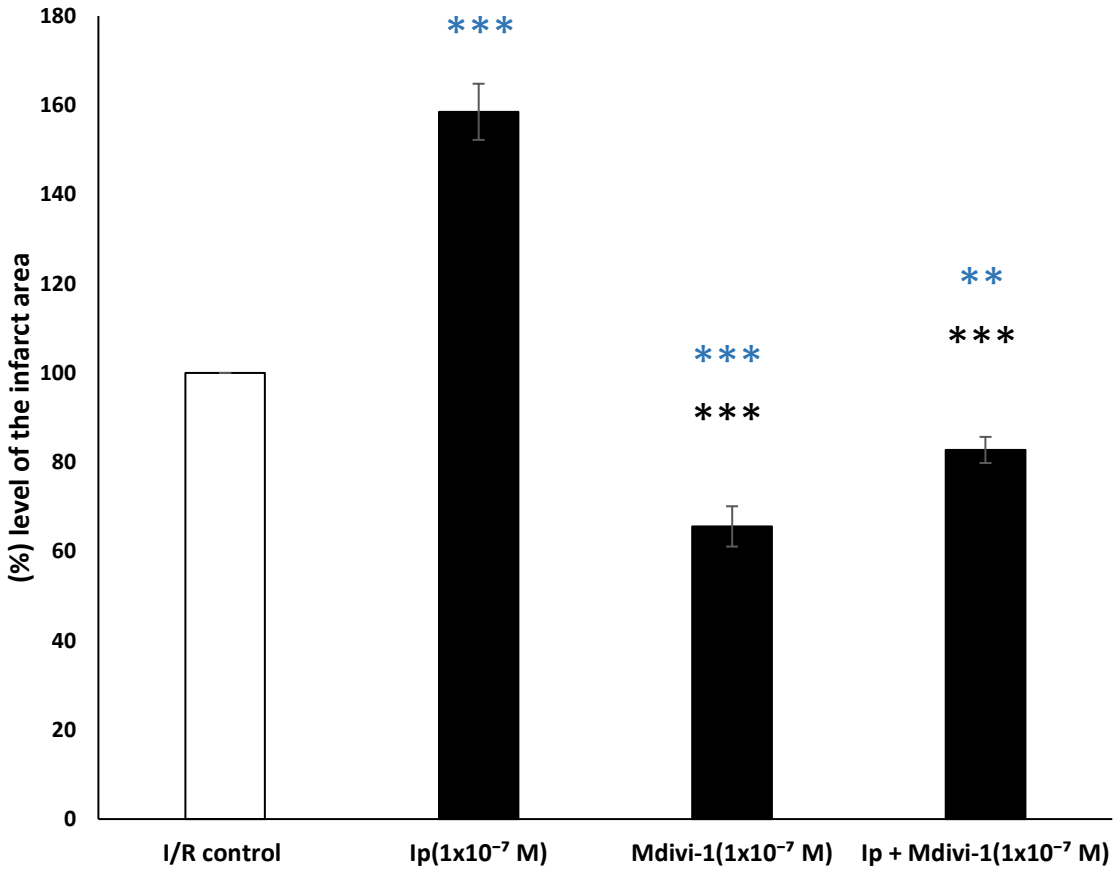

Figure 4. 4: Infarct development in I/R control, Ipratropium bromide (1 x 10^{-7} M) or Mdivi-1 (1 x 10^{-7} M) ± Ipratropium bromide (1 x 10^{-7} M) treatment groups perfused isolated rat hearts. Results displayed as means + SEM, n=6. *** p<0.001 against I/R control. ** p<0.01 against I/R control. *** p<0.001 against Ipratropium (1 x 10^{-7} M).

4.2 Flow Cytometry Results

For the flow cytometry studies, (explained in detailed in section 2.2.2.1 and 2.2.2.2). The drug treatments were added at the start and throughout reoxygenation to measure apoptosis necrosis, live cells and the activities of caspase-3 for the cardio myocytes that were treated with Ipratropium bromide (1

x 10^{-7} M) or Mdivi-1(1 x 10^{-7} M) ± Ipratropium bromide (1 x 10^{-7} M) in comparison with the H/R control.

4.2.1 Cell Death Assay

For the cell death assay cardiac myocyte isolation and Hypoxia/Reoxygenation protocols were carried out, described in sections 2.2.2.1, 2.2.2.2 and 2.2.2.4.1 and while the cells were alive Annexin V-FITC A and Propidium iodide were added to the cells incubated with the reagents, covered by in foil prior to analysis by flow cytometry. The cell death assay results obtained for cardiomyocytes that were simulated by inducing hypoxia/reoxygenation (H/R), showed an exacerbation in the injury for the myocardial via the administration of Ip in compression with the controls normoxic and H/R (Explained in detail in section 2.2.2.4.1).

4.2.2 Effects Of Mdivi-1 On Apoptosis

With regards to apoptosis, Ip was able to increase the level of apoptotic cells (total apoptosis) measured by the flow cytometry. There was an increase in total apoptosis induced by Ipratropium following the H/R protocol (table 4.1) which represents the normolised data values and the significant difference. The percentages of apoptosis are presented in (Figure 4.5). There was an observed increase which was significant in total apoptosis induced by Ipratropium during H/R, which was abrogated via the co-administration of Mdivi-1 with Ip. For the

necrosis assay, there was no significant difference. Overall Mdivi-1 increased myocyte viability with the co-administration of Ipratropium.

Samples groups	Means	SEM
H/R control	100	0%
Ipratropium bromide (1 x 10^{-7} M)	116.22	6.40%*
Mdivi-1(1 x 10^{-7} M)	80.36	5.77%* **
Mdivi-1 (1 x 10^{-7} M) ± Ipratropium bromide (1 x 10^{-7} M)	86.35	9.09%* *

Table 4. 1: Represents the values for apoptosis normalised to the control (H/R) (100%) following of the drug treatments administration at the start and troughout reoxygenation, results presented as means+ SEM. * p<0.05 against H/R control. ** p<0.01 against Ipratropium (1 x 10^{-7} M). * p<0.05 against Ipratropium (1 x 10^{-7} M).

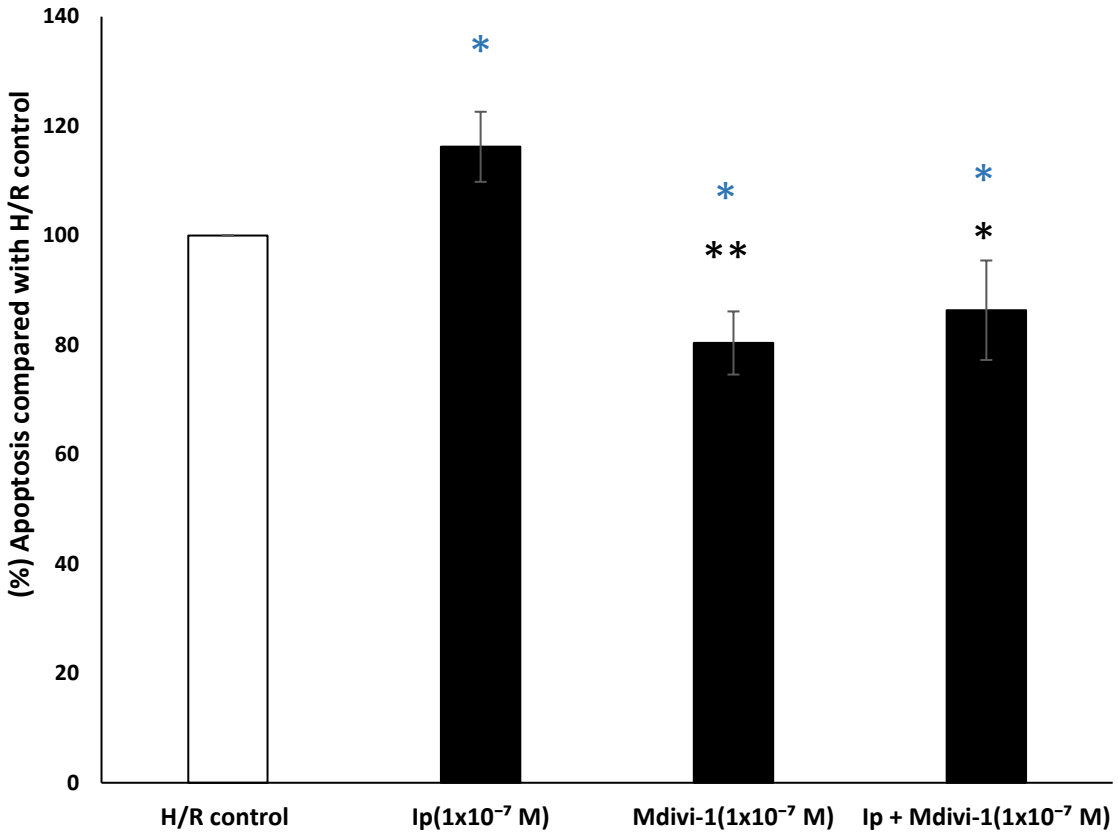

Figure 4. 5: Total apoptosis percentage results stained by Annexin V shown in flow cytometry for H/R control Ipratropium bromide (1 x1 0^{-7} M) or Mdivi-1(1 x 10^{-7} M) ± Ipratropium bromide (1 x 10^{-7} M). The data was analysed after changing it into arithmetic means by normalised to H/R control, ± SEM, the recorded number myocytes is 10,000, n = 6. * p<0.05 against H/R control. ** p<0.01 against Ipratropium (1 x 10^{-7} M). * p<0.05 against Ipratropium (1 x 10^{-7} M).

4.2.3 Effects Of Mdivi-1 On Necrosis

The percentages of necrotic cell deaths are presented in, (table 4.2) (Figure 4.6). No overall significant difference although there is a clear pattern that suggest that Mdivi-1 was able to decrease the percentage of necrotic cell death.

Samples groups	Means	SEM
H/R control	100	0%
Ipratropium bromide (1 x 10^{-7} M)	119.37	14.22%
Mdivi-1(1 x 10^{-7} M)	94.43	15.77%
Mdivi-1 (1 x 10^{-7} M) ± Ipratropium bromide (1 x 10^{-7} M)	98.64	16.33%

Table 4. 2 : Represent the values for necrosis normalised to the control (H/R) (100%) of the drug treatments at the start and throughout reoxygenation, results presented as means+ SEM. This table showed analysed values after changing it into arithmetic means by normalised to H/R control. The statistical analysis resulted in no significant difference despite the pattern presented in Figure.4.6.

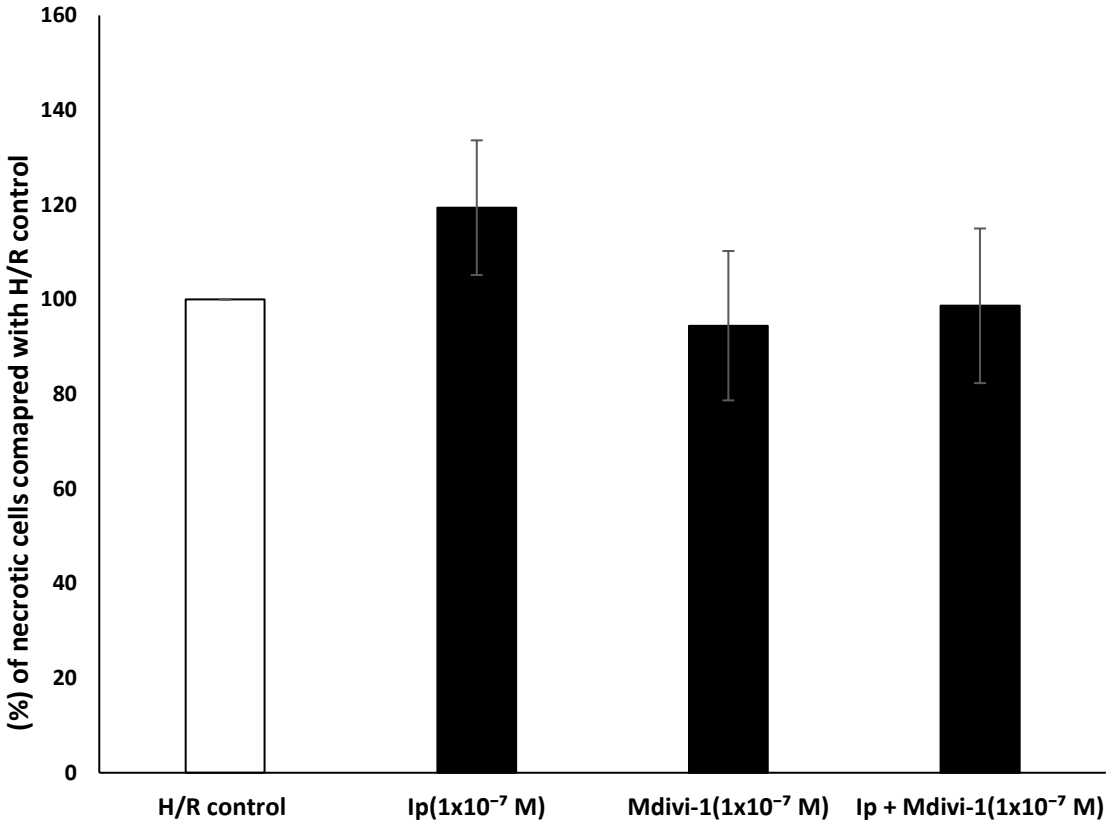

Figure 4. 6: Necrotic cells percentage results stained by Annexin V shown in flow cytometry for H/R control Ipratropium bromide (1 x 10^{-7} M) or Mdivi-1 (1 x 10^{-7} M) ± Ipratropium bromide (1 x 10^{-7} M). The data was analysed after changing it into arithmetic means by normalised to H/R control, ± SEM, the recorded number myocytes is 10,000, n = 6.

4.2.4 Effects Of Mdivi-1 On Cell Viability

Cell viability percentage for the drug treatment group is presented in (table 4.3) (Figure 4.7). There was a significant difference for Mdivi-1 treated group against the control as Ip treated group. Mdivi-1 was able to significantly increase cell viability. As well, it was able to abrogate the injury caused by Ip when co-administered (P<0.05).

Samples groups	Means	SEM
H/R control	100	0%
Ipratropium bromide (1 x 10^{-7} M)	80.42	9.4%*
Mdivi-1(1 x 10^{-7} M)	128.56	8.22%** *
Mdivi-1 (1 x 10^{-7} M) ± Ipratropium bromide (1 x 10^{-7} M)	118.74	10.59%*

Table 4. 3: Represent the values of the drug treatments for cell viability of the drug treatments at the start and troughout reoxygenation, results presented as means+ SEM. * p<0.05 against H/R control. ** p<0.01 against H/R control. * p<0.05 against Ipratropium (1 x 10^{-7} M).

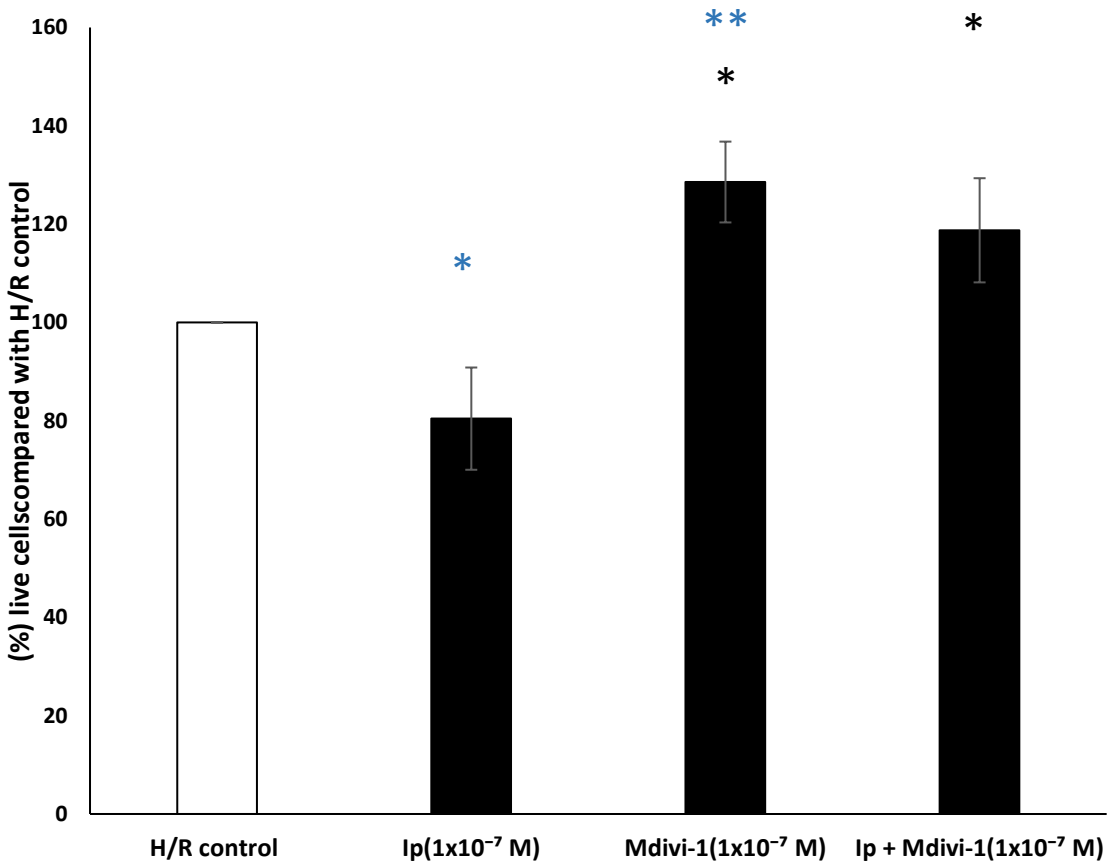

Figure 4. 7: Effect of Ipratropium bromide (1 x 10^{-7} M) or Mdivi-1(1 x 10^{-7} M) ± Ipratropium bromide (1 x 10^{-7} M) in cell viability level in comparison to H/R control the data was analysed after changing it into arithmetic means by normalised to H/R control, ± SEM, the recorded number myocytes is 10,000, n = 6. * p<0.05 against H/R control. ** p<0.01 against H/R control. * p<0.05 against Ipratropium (1 x 10^{-7} M).

4.2.5 The Level Of Caspase-3 Activity

The activity of caspase-3 percentage is presented in (Figure 4.8). There was significant difference between Ip and H/R control1 (116.8 ± 4% vs. 100 ± 0) ($p < 0.01$), as well as a reduction is significant when Mdivi-1 and the co administered treated group against the H/R control (43 ± 6.6, 51.8 ± 11.3% vs. 100 ± 0) ($p < 0.001$), There was also significant difference between Ip and both Mdivi-1 and Ip+ Mdivi-1 the co-administration of abrogates Ip mediated increases in infarction against Ip treated group (43 ± 6.6, 51.8 ± 11.3% vs. 116.8 ± 4%) ($p < 0.001$).

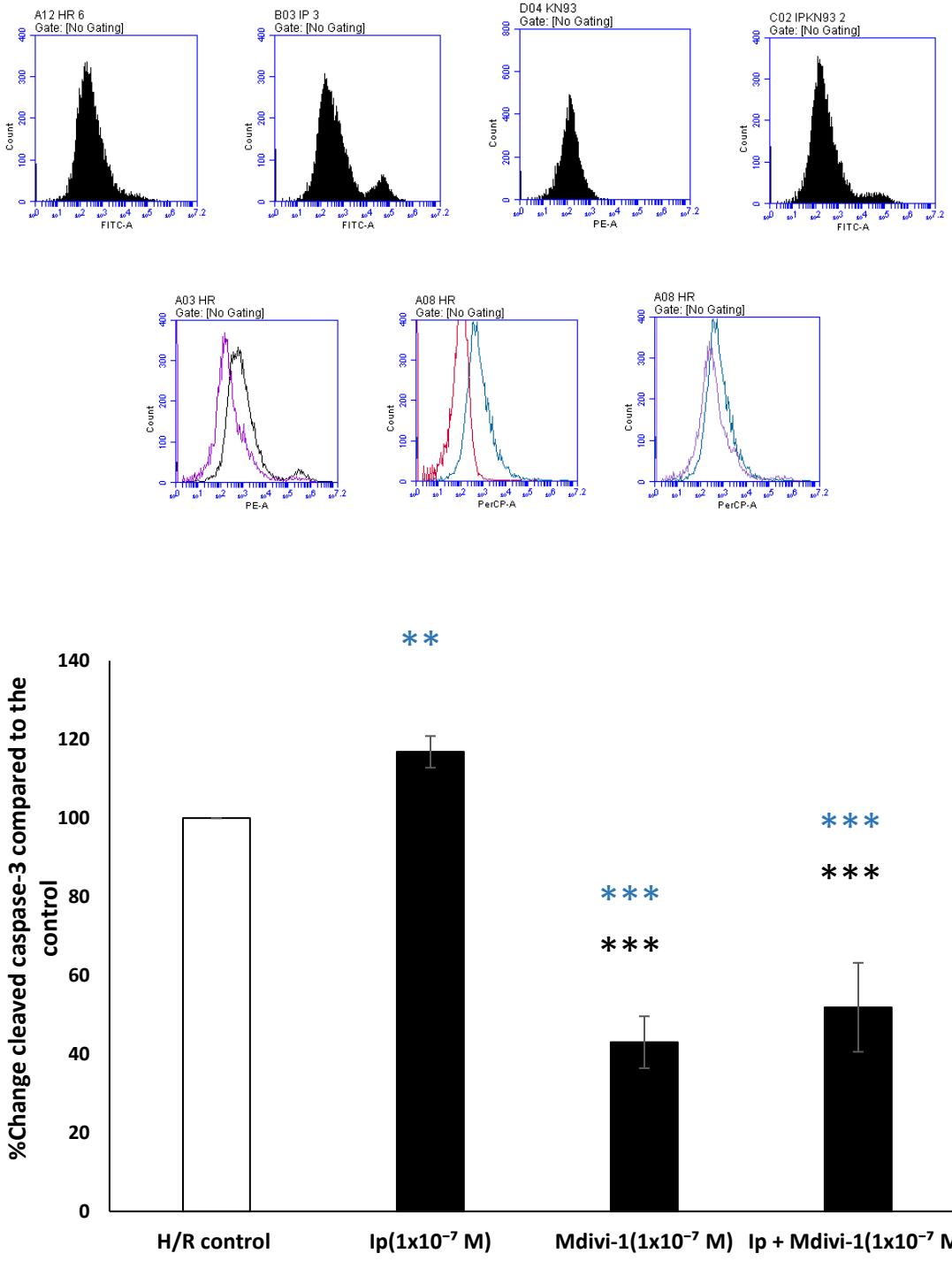

Figure 4. 8: Effect of Ipratropium bromide (1 x 10^{-7} M) or Mdivi-1 (1 x 10^{-7} M) ± Ipratropium bromide (1 x 10^{-7} M) in caspase-3 activity in comparison to H/R control the data was analysed after changing it into arithmetic means by normalised to H/R control, ± SEM, the recorded number myocytes is 10,000, n = 6. *** p<0.001 against H/R control. ** p<0.01 against H/R control. *** p<0.001 against Ipratropium (1 x 10^{-7} M).

4.3 Western Blot Results

For Western blotting studies the Langendorff protocol (section 2.2.1.1-2.2.1.4) was followed to sacrifice the rat, extracted the heart and mounting it on a modified Langendorff perfusion apparatus. After stabilisation ischaemia was induced then reperfusion for 15 or 30 minutes. I/R control and Ipratropium bromide (1×10^{-7} M) and Mdivi-1(1×10^{-7} M) ± Ipratropium bromide (1×10^{-7} M), during reperfusion. Homogenising the tissue for the preparation of Western blot analysis for Drp1, Akt, Erk1/2 and caspase-3. The tissues were collected (*in vitro*) (Explained in detailed in section 2.2.3.1- 2.2.3.7).

4.3.1 Western Blot Results For 15 And 30 Minutes Post Reperfusion Administration

The study was divided into two different time points order to see the effect of the drug treatment in the proteins of interest following reperfusion as both 15 minutes and 30 minutes time points are considered to be clinically significant. explained in detailed in section 2.2.3.8 and 2.2.3.9) (Figure 4.9 - Figure 4.12).

4.3.1.1 The Measurements Of (I/R Control And Ipratropium Bromide (1×10^{-7} M) And Mdivi-1 (1×10^{-7} M) ± Ipratropium Bromide (1×10^{-7} M).

RISK pathway proteins Akt (Protein Kinase B (PKB)) Erk1/2, Drp1 and caspase-3 were measured from the isolated left ventricular which was treated with the treatments group prior to extracting the proteins of interests, by running

electrophoresis and subsequent Western Blot, the samples were loaded to the gel and the primary antibody P-Akt, P-Erk 1/2, P- Drp1, cleaved caspase-3 were added (antibody buffer) to the membrane which was used after transferring the proteins from the loaded gel. The membrane was then incubated then washed prior to secondary antibody incubation, washed again before it was visualised using the ChemiDoc. The membrane then was stripped for the measurement of the total form of the proteins incubated overnight with the total antibodies Akt, Erk1/2, Drp 1, Active caspase-3 and GAPDH (housekeeping gene) for visualizing (Figures 4.9 - 4.12). The phosphorylation of the protein Akt, Erk 1/2, Drp1, cleaved to active caspase-3 resulted in activities in the isolated perfused hearts with Ip (1 x 10^{-7} M) or Mdivi-1(1 x 10^{-7} M) ± Ipratropium bromide (1 x10^{-7} M) in comparison with I/R untreated control. Ip (1 x 10^{-7} M) are mentioned in (section 3.3.1.1) (Figures 3.9). Importantly, the administration of Mdivi-1 demonstrates cardio-protection via a reduction in Dynamin related protein 1 (Drp-1), Akt, Erk1/2 and caspase-3 compared with I/R control in all studies at both time points. Mdivi-1compare to Ip (141 ± 15.4% vs. 51.7 ± 14.1%) p <0.01 (Figure 4.11). Co-administration of Mdivi-1 treatment significantly reduce Ip effect in increasing Drp1 levels compare to the untreated control at 15 minutes reperfusion compared to Ip (141 ± 15.4% vs. 56.8 ± 29.1%) p <0.01(Figure 4.11, A). In the 30 minutes reperfusion results there was a significant decrease in Drp 1 level in Ip+Mdivi-1 in comparison to Ip treated group (125.8 ± 23.1% vs. 27.8 ± 9.6%) p <0.01(Figure 4.11, B), moreover, significant decrease in the phosphorylation of Drp 1 in Ip+Mdivi-1 in comparison to I/R treated group (100 ± 0 vs. 27.8 ± 9.6%) p <0.001. In addition, Mdivi-1 treated group has shown significant difference against

Ip+Mdivi-1 (85.8 ± 24% vs. 27.8 ± 9.6%) p <0.05. Also in Erk 1/2 results in co-administration of Mdivi-1 treatment abrogated Ip at 15 minutes reperfusion but not significant (Figure 4.10, A). Akt level shows similar results at the same time point for Mdivi-1 against Ip (96.9 ± 24.2% vs. 208.4 ± 58.7%) p <0.05 (Figure 4.9, A, B). Mdivi-1administration in with Ip conjunction resulted in significant attenuation in protein levels compared with groups treated solely with Ip (122.2 ± 22.1% vs. 208.4 ± 58.7%) p <0.05. For caspase-3 group there was a significant decrease in the level of caspase-3 activity in the Mdivi-1 group compared to Ip treated group (70.2 ± 14.7% vs. 126.7 ± 10.6%) against Ip (p <0.01) at 15 minutes reperfusion (Figure 4.12, A). Moreover, the co-administration of Ip+Mdivi-1 significantly decreases caspase-3 level (75.3 ± 19.4% vs. 126.7 ± 10.6%) against Ip (p <0.05) at 15 minutes' reperfusion. Whereas after 30 minutes reperfusion the only significant difference was between Mdivi-1 and Ip treated group (70.9 ± 12.1% vs. 113.7 ± 16.7%) against Ip (p <0.05) (Figure 4.12, B). The results above presented in the figure below and the figures which were not mentioned there was no significant difference compared with the treatment group against the control nor against other treated group.

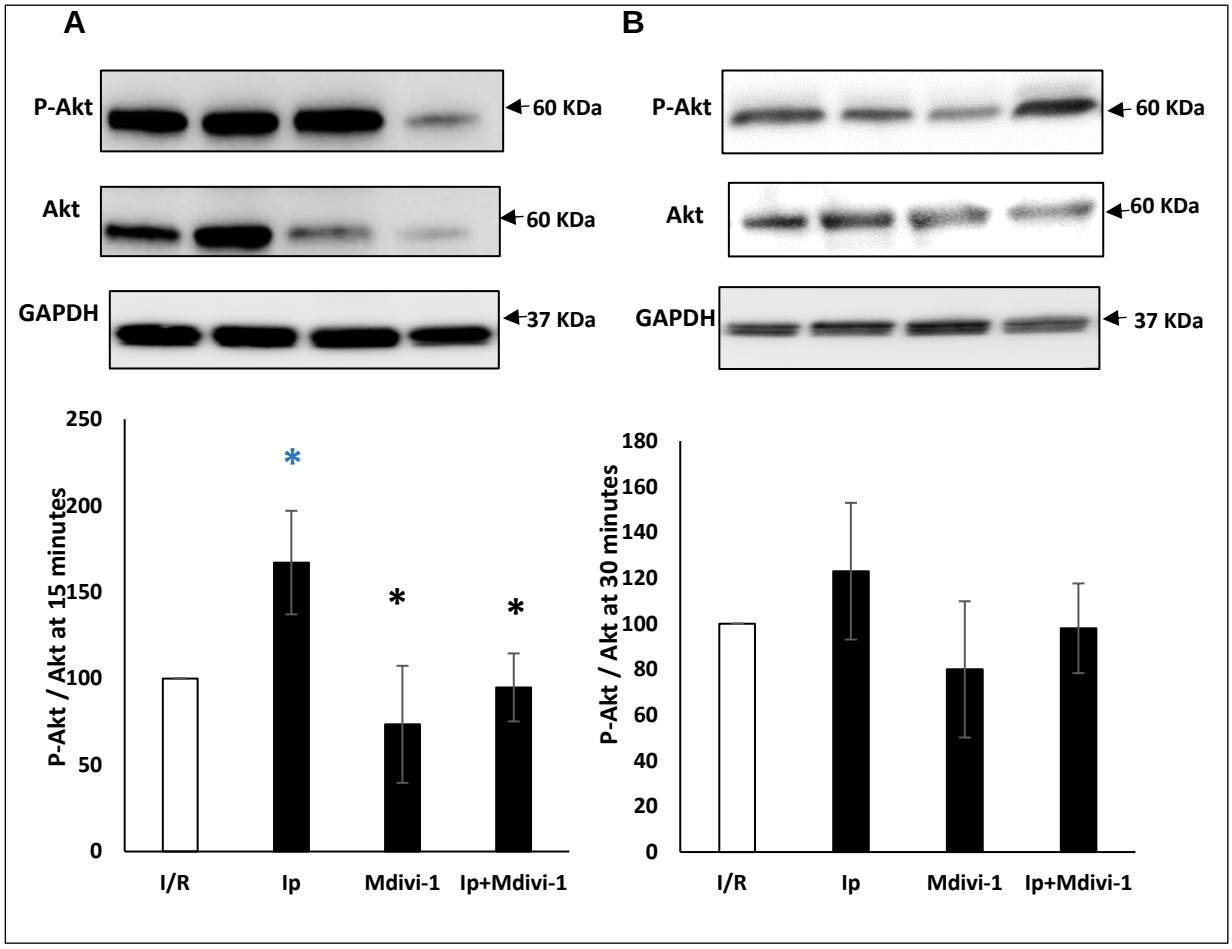

Figure 4. 9: The levels of phospho and Total Akt in I/R control, Ipratropium bromide (1 x 10^{-7} M) or Mdivi-1 (1 x 10^{-7} M) ± Ipratropium bromide (1 x 10^{-7} M). A is treatment groups perfused for 15 minutes isolated rat hearts. B is treatment groups perfused for 30 minutes isolated rat hearts. Results displayed as means + SEM, n=6. * $p<0.05$ vs. I/R control. * $p<0.05$ vs. Ipratropium bromide (1 x 10^{-7} M).

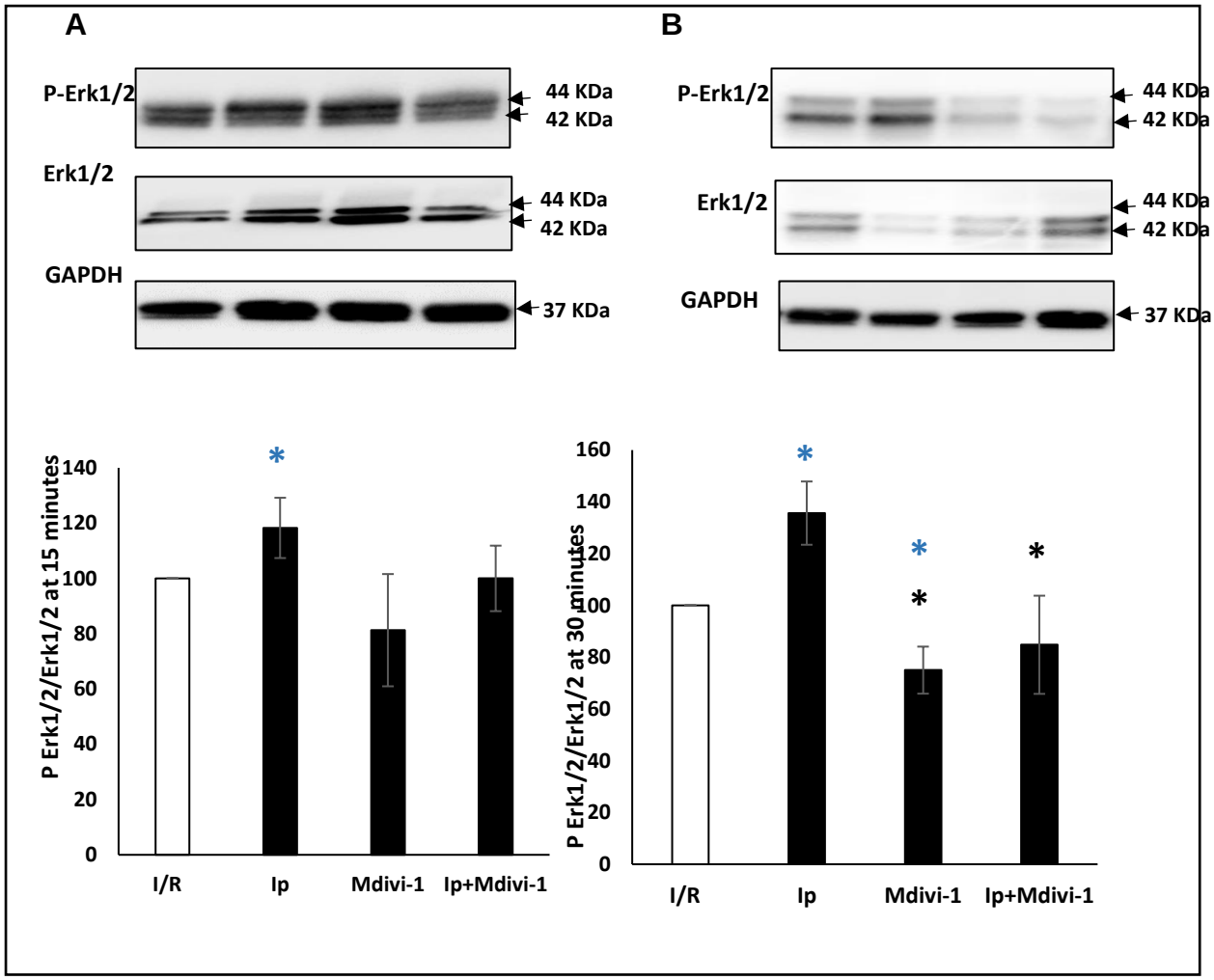

Figure 4. 10: The levels of phospho and Total Erk 1/2 in I/R control, Ipratropium bromide (1 x 10^{-7} M) or Mdivi-1(1 x 10^{-7} M) ± Ipratropium bromide (1 x 10^{-7} M). A is treatment groups perfused for 15 minutes isolated rat hearts. B is treatment groups perfused for 30 minutes isolated rat hearts. Results displayed as means + SEM, n=6. * $p<0.05$ vs. Ipratropium bromide (1 x 10^{-7} M).

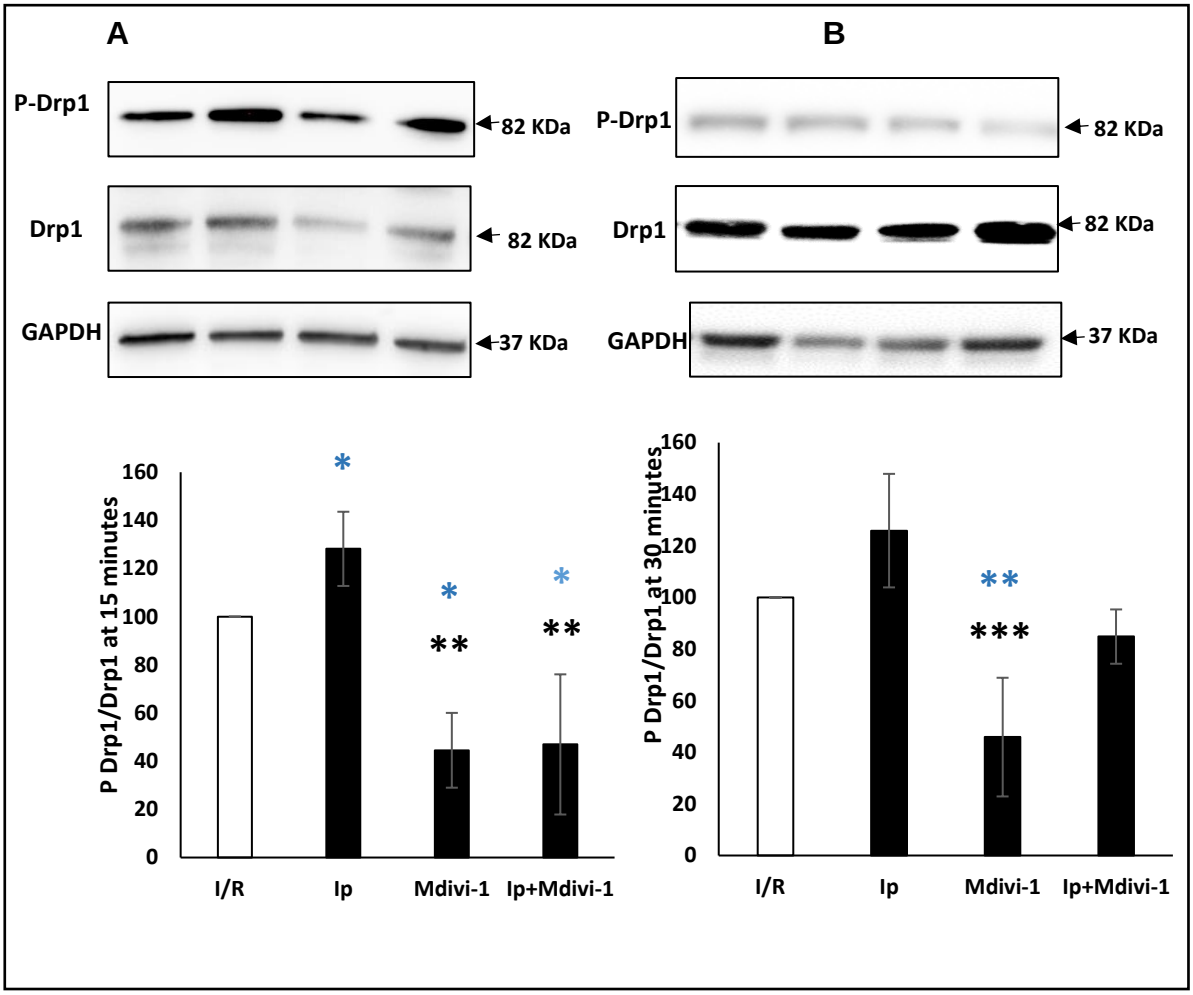

Figure 4. 11: The levels of phosphor and Total Drp1 in I/R control, Ipratropium bromide (1 x 10^{-7} M) or Mdivi-1(1x10^{-7} M) ± Ipratropium bromide (1 x 10^{-7} M). A is treatment groups perfused for 15 minutes isolated rat hearts. B is treatment groups perfused for 30 minutes isolated rat hearts. Results displayed as means + SEM, n=6. * p<0.05 vs. I/R control. * p<0.05 vs. Ipratropium bromide (1 x 10^{-7} M), * *p<0.01 vs. Ipratropium bromide (1 x 10^{-7} M).* * *p<0.001 vs. Ipratropium bromide (1 x 10^{-7} M).

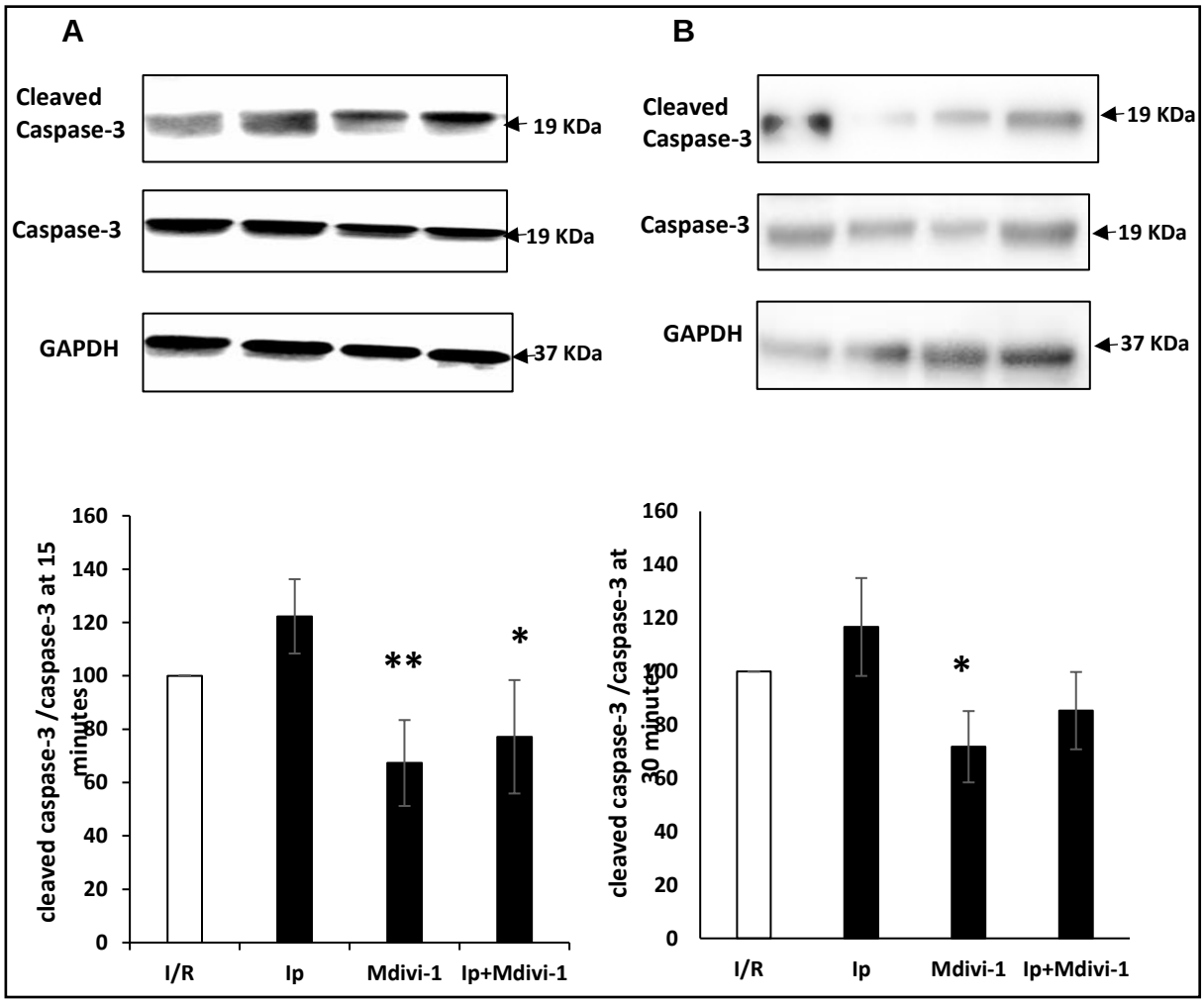

Figure 4. 12: The levels of cleaved and active caspase-3 in I/R control, Ipratropium bromide (1 x 10^{-7} M) or Mdivi-1(1 x 10^{-7} M) ± Ipratropium bromide (1 x 10^{-7} M). A is treatment groups perfused for 15 minutes isolated rat hearts. B is treatment groups perfused for 30 minutes isolated rat hearts. Results displayed as means + SEM, n=6. * p<0.05 vs. Ipratropium bromide (1 x 10^{-7} M), ** p<0.01 vs. Ipratropium bromide (1 x 10^{-7} M).

4.4 PCR Results

For PCR protocol the left ventricular tissue was obtained similar to the method utilised to obtain Western Blot tissue (explained in details in 2.2.11-2.2.14).

Tissue was at the same time points post reperfusion, however, tissue was submerged in RNAlater® and kept in the -80 °C freezer prior to the tissue being homogenised in TRIsure™ to extract RNA to synthesis cDNA in order to make PCR reaction and to measure the percentage change induced by the drug treatment against the control using the house keeping gene as the baseline. The gene of interest used was Dnm1l against GAPDH primers for I/R control and Ipratropium bromide (1 x 10^{-7} M) and Mdivi-1 (1 x 10^{-7} M) ± Ipratropium bromide (1 x 10^{-7} M). Overall there was no significant difference between the two groups (table 4.4) (Figure 4.13) (Explained in detail in section 2.2.4.1- 2.2.4.3).

Sample groups	Means	SEM
I/R control	100	0%
Ipratropium bromide (1 x 10^{-7} M)	1419	900.45%
Mdivi-1(1 x 10^{-7} M)	609.95	400.14%
Mdivi-1 (1 x 10^{-7} M) ± Ipratropium bromide (1 x 10^{-7} M)	224.79	150.92%

Table 4. 4 : Represent the values of the drug treatments for PCR.

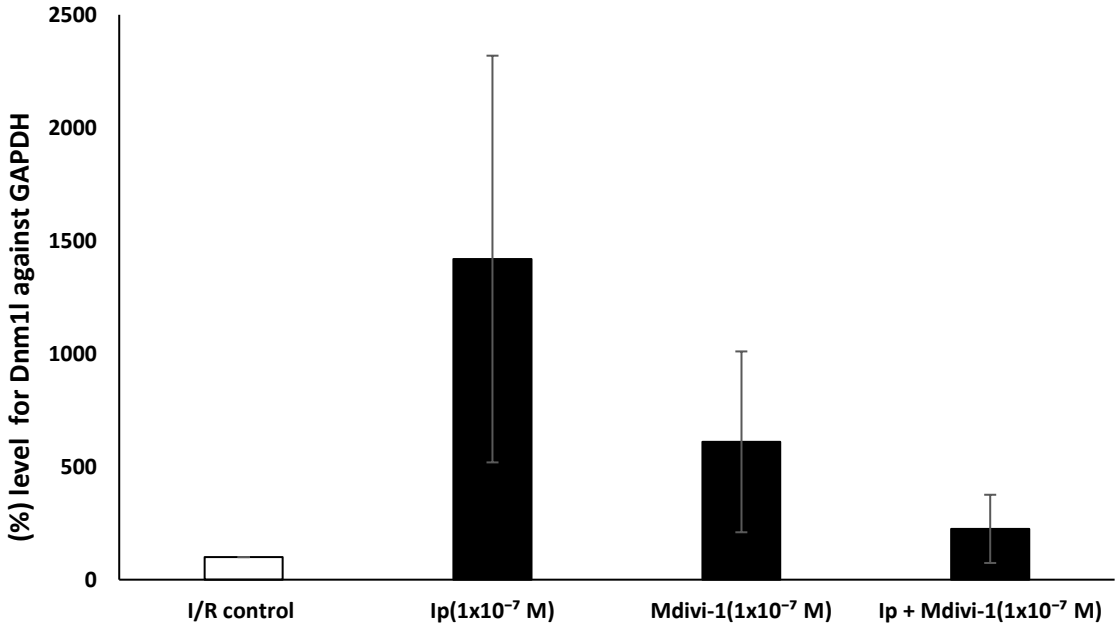

Figure 4. 13: The levels of fold change in Dnm1l in I/R control, Ipratropium bromide (1 x 10^{-7} M) or Mdivi-1(1 x 10^{-7} M) ± Ipratropium bromide (1 x 10^{-7} M) is treatment groups perfused for 15 minutes isolated rat hearts. Results displayed as means + SEM, n=6. The large error bars are generated form the data obtained, the data was inconclusive further explain in the limitation section and the statistical analysis resulted in no significant difference.

PCR data did not result in significant difference after the addition of drug treatments compared with the I/R control, due to the speculation that the 15 minutes of reperfusion might not be enough to express the genes with in the left ventricle tissue, as in Troncoso et al. (2014) study which measured the expression of Dnm1l after 6 hours of reperfusion, And there was no data collected for 30 minutes of reperfusion due to unavailability of PCR machines following the start of the COVID-19 global pandemic.

4.4 Chapter Discussion

The injury induced by Ipratropium bromide in non-clinical modles was reduced via the co-administration of Mdivi-1 under the Ischaemia/Reperfusion, as well as in Hypoxia/Re-oxygenation, stimulated conditions. This indicates that the signalling mechanism occurred during the stress condition (I/R) which caused the Ipratropium bromide toxicity, was to be prevented by Mdivi-1, indicating mitochondria involvement. As suggested by the results of the infarct size, as Mdivi-1 managed to reduce the increase in the infarction with a significant different when co-administered with Ipratropium bromide (Figure 4.4) in comparasion with untreated control. Not to mention the inhibition that was further identified by a reduction in caspase-3 activity and apoptosis in myocyte which was also significant compared with the Ip group alone (Figure 4.5 - 4.8), as well as increasing cell viability which was similar to Kim and Kang (2018) finding which is further explain in this chapter (Figure 4.7).

In the previous chapter (chapter 3) it was established that in *in vitro* models of stimulated I/R conditions the myocardial injury was exacerbated by the administration of Ip, shown in the significant increase in infarction in isolated perfused rat hearts, decreasing the viability in isolated left ventricular myocytes and increasing levels of apoptosis. As mentioned in Chapter Discussion 3.4 this was due to the antagonism effect of Ip on mAChRs. The results of study demonstrate for the first time Mdivi-1 has the ability to reduce the observed exacerbation of injury when co-administered with Ip in both I/R and the H/R stimulated conditions. Other study showed Mdivi-1 protection to cardiac

myocytes was done by Gharanei et al. (2013) against anti-cancer drug Doxorobisin in stimulated I/R, H/R conditions. The findings of Mdivi-1 study experiments (langendorff, western blot and flow cytometry) showed Mdivi-1 was able to reduce the injury induced by reperfusion when compared to the untreated I/R control and H/R control. This study found that, via the Langendorff studies, Mdivi-1 administration during reperfusion maintained the heart haemodynamics in comparison with that of the I/R control and the Ip treated groups alone (Figure 4.1 - 4.3), as shown in chapter 3. The haemodynamic parameters were closer to the nomoxic control. Despite the speculation that haemodynamic can be due to cardiac dysfunction due to reperfusion injury, Mdivi-1 was able to enhance the parameter and limit the injury occurring at the onset of reperfusion. The administration of Mdivi-1 (1×10^{-7} M) showed cardio-protection via a reduction in infarct size compared with the untreated control (Figure 4.4) ($p<0.001$). Importantly, when Ip (1×10^{-7} M) was co-administered with Mdivi-1 (1×10^{-7} M) this provided a reduction in infarct which was significant in AAR% compared to the untreated control (Figure 4.4) ($p<0.01$), thus reducing the Ip mediated increase in myocardial injury in this model, completely, these results suggest that Mdivi-1 is able to maintain mitochondria integrity, irrespective of a further myocardial insult, during reperfusion hence it prevented reperfusion injury as has been supported in a previous study by Veeranki and Tyagi (2017) in female mice. The infarct size was reduced upon the administration of Mdivi-1. The results also represent for the first time that the co-administration of Ip (1×10^{-7} M), the highest concentration used in this study with Mdivi-1 abrogates the injury induced by Ip giving the potential that the cellular pathway involves the mitochondria. For the

first time, this gives a specific target for further investigation of induced toxicity as well as provide the chance for therapeutic solution as shown in the results. Mdivi-1 was able to increase the level of LVDP and CF as well as decrease HR and the infarct size once co-administered with Ip, this indicates that cardiac function, as well as cardio myocyte salvage may be therapeutically possible suggested by Maneechote et al. (2021). The significances is that not only Mdivi-1 alone was able to provide salvation to the heart, it also managed to degrase the excerrbated injury induced by Ip signifacntly.

Mdivi-1 was also shown reduce the level of apoptosis in the flow cytometry studies by the measurement of apoptosis (Figure 4.5, table 4.1) which was decreased when co administered with Ip ($p<0.05$), necrosis (Figure 4.6, table 4.2) and live cells (Figure 4.7, table 4.3) Mdivi-1 alone increase cell viability ($p<0.001$) against H/R control. Caspase-3 activity (Figure 4.8). Since Mdivi-1 was able to significantly reduce the activity of the caspase-3 compared to the H/R control ($p<0.001$), it is due to maintaining mitochondrial integrity, since Mdivi-1 was design to inhibit Drp1 so mitochondria does not fragment the mitochinderia hence maintain its integrity and the pro-apoptotic proteins are not to be activated and mPTP will remain closed in the presence of Mdivi-1 (Wang and Youle 2009). Cytochrome c is not release and the caspases will remain inactive as shown in level of caspase activity which was significantly decreased upon the administration of Mdivi-1 ($p<0.001$) (Wang and Youle 2009). This suggest which means that the initiation for apoptosis pathway was intrinsic linking Drp1 and caspase-3. Mdivi-1 was also able to reduce the apoptosis and necrosis that were increased upon the administration of Ip as well as increase cell viability in

myocytes that underline H/R condition. Which suggest that mitochondria is involved in the pathway in which the toxicity occurs. This further supports that there is mitochondrial involvement in Ip mediated myocardial injury.

The study also found that Mdivi-1 has protective properties as shown in Western blot studies (Figure 4.9 - 4.12), it was able to decrease the phosphorylation of Drp1 (Figure 4.11 A) ($p<0.05$) (Figure 4.11 B) ($p<0.01$). Drp1 activation plays in important role in mitosis and apoptosis and programmed necrosis (Ko et al. 2016). The activity of Drp1 changed due to the treatment of Mdivi-1, Drp 1 phosphorylation resulted in mitochondrial fission stimulation (Kim et al. 2016). Western blot technique was used to assess the phosphorylation and expression level which was significant in Ip treated group. The results showed a reduction of Drp1 in the Ip + Mdivi-1 treated group indicating the possibility that the balance between activation and inhibition was impaired (Figure 4.11 A) ($p<0.05$) (Kim et al. 2016). The indication of the obtained data suggested that the mitochondrial division inhibitor was utilised to prevent the phosphorylation of Drp1 by blocking its activation site at Serine ($_{616}$), (Khan 2015). In previous literature mitochondria fission was able to promote cell death programmes and the mechanism is, thought to be, via opening of mPTP by BAX/BAK pro-apoptotic proteins activation (Kim et al. 2016). BAX/BAK-dependent cytochrome c activation was blocked by Mdivi-1 provide protection against infarct size (Kim et al. 2016). These findings indicate that Mdivi-1's protective properties to be by preventing mitochondrial fission which, subsequently, has a role in preventing Ip mediated myocardial injury (Rosdah et al. 2016). It is already known that Mdivi-1 inhibits complex I, which has a role in mitochondria receptor chain, this action prevents the

activation of GTPase of Drp1, no activation means that there is no localisation into the mitochondria (Gharanei et al. 2013). It also prevents caspase dependent cascade by stopping cytochrome c to escape into the cytoplasm via prevention of Drp1 activation of mitochondrial fission and fragmentation, which resulted in mPTP to remain close and cytochrome c is not released caspase-3 remain inactive hence no intrinsic apoptosis pathway (Ko et al. 2016). The Western blot studies were designed using Mdivi-1 to determine the involvement of the mitochondria, thus levels of Drp1, caspase-3, Akt and Erk1/2 were measured (Figure 4.9 - 4.12). Importantly, the administration of Mdivi-1 demonstrates cardio-protection via a reduction in Drp-1, Akt, Erk1/2 and caspase-3 compared with the untreated control, in all studies at 15 or 30 minutes post reperfusion since the increase in thes protiens level was found to correlate with injury in the heart tissue showed results similar to previous studies (Harvey, Hussain and Maddock 2014). Although a study by Rosdah et al. (2016) suggested that Mdivi-1 phosphorylates Akt as its cardio-protective mechanism, which means that the. The results from the current study presented Mdivi-1 to reduce Akt expression. Mdivi-1 administration in this chapter present a cardio protection via the reduction of Akt and Erk1/2 as explained in section 3.5 the overactivation of both kinases had a detrimental effect on the organ, hence the reduction of their expression provides cell survival. However, further research are needed to identify exactly what cellular pathways are taking place, May be by design a template with all the gene of interests and run a PCR for gene expression after an sufficient period of reperfusion. This is the first study to specifically relate a mitochondrial pathway to Ip induced myocardial injury by using Mdivi-1 as potential marker for

mitochondrial involvement. It is suggested that the abrogation of Akt and Erk1/2 are as a consequence of the action of Mdivi-1 on the mitochondria although the mechanism of which is not clear. This provides further evidence that the ipratropium-mediated myocardial injury mechanism has mitochondrial involvement.

Chapter 5: KN-93 (CaMKII inhibitor) Protects Against Ipratropium Bromide Exacerbation Of Injury In *In Vitro* Models Of Ischaemia/Reperfusion

The non-selective muscarinic receptor antagonist Ipratropium Bromide (Ip) mechanism of induced injury is not fully elucidated. However, previous studies have suggested that there is evidence for calcium involvement, as the injury exasperated by the administration of Ip at the onset of reperfusion was thought to be mediated via calcium overload, or involve the mPTP, as a consequence of calcium overload (Harvey, Hussain and Maddock 2014, Cassambai et al. 2019). As a result, KN-93 was used in this current study, along with co-administration with Ip in order to identify if calcium overload, or at least calcium signalling, had a role in mediating the injury caused by Ip. It has been well documented that KN-93 prevents calcium overload under I/R condition (Szobi et al. 2013, Wong et al. 2019). Thus, if calcium overload is involved it should be decreased via the administration of KN-93 and, potentially, this could enhance the observed Ip induced injury. Previous work, in chapter 4, has provided further information that Ip induced myocardial damage provided a mitochondrial component. It is documented the opening of mPTP and induction of myocyte death is, in part, due to calcium overload as previously described. The rationale behind this study was to try to ascertain whether the previously identified mitochondrial involvement was also associated with calcium signalling involvement in an effort to further gian an insite to the action of Ip elicits its damaging exacerbation effects.

5.1 Langendorff Model Of Perfused Rat Heart Results

Ipratropium bromide (1 x 10^{-7} M) and KN-93 (4 x 10^{-7} M) ± Ipratropium bromide (1 x 10^{-7} M) were added at the start and during the period of reperfusion. To measure haemodynamic parameters during reperfusion as well as the infarct size (which was calculated as Area At Risk% (AAR %)). (explained in detail in section 2.2.1.1 - 2.2.1.5).

5.1.1 Haemodynamic Parameters (I/R And Ipratropium Bromide (1x10^{-7} M) And KN-93 (4 x10^{-7} M) ± Ipratropium Bromide (1x10^{-7} M))

Haemodynamics measured were: LVDP, HR and CF. The period of the measurement that readings were taking for ischaemia and after initiating reperfusion for 120 minutes the recording were taken every 15 minutes. Following the end of the experiment, the heart was taken out and frozen at -20 °C prior to assessment for infarct/risk ratio and Area At Risk (AAR %) analysis.

5.1.1.1 The Left Ventricular Developed Pressure (LVDP)

LVDP was determined for I/R and Ipratropium bromide (1 x 10^{-7} M) and KN-93 (4 x 10^{-7} M) ± Ipratropium bromide (1 x 10^{-7} M) (explained in detail in section 2.2.1.6.1 in chapter 2). The results show that the left developed ventricular pressure (LVDP) was enhanced with the co-administration of KN-93 (4 x 10^{-7} M) and Ip (1 x 10^{-7} M) at 100, 130, 160 and 175 minutes of reperfusion (75.9 ± 4, 72.2 ± 4.2, 65.6 ± 2.9 and 66.2 ± 1.4% vs. 54.5 ± 6.5, 52.8 ± 7.1, 47.5 ± 6.2, 45.4 ± 6.7%) Ip (1 x 10^{-7} M) ($p<0.05$) KN-93 (4 x 10^{-7} M) significantly increased the

LVDP compare to Ip treated group at 175 minutes (64.8 ± 5.2% vs. 45.4 ± 6.7%) Ip (1 x 10^{-7} M) ($p<0.05$). The significant difference between I/R control and Ip (1 x 10^{-7} M) in LVDP is mentioned in section 3.1.1.1. Left ventricular developed pressure measurements for I/R control and Ipratropium bromide (1 x 10^{-7} M) and KN-93 (4 x 10^{-7} M) ± Ipratropium bromide (1 x 10^{-7} M) (Figure 5.1).

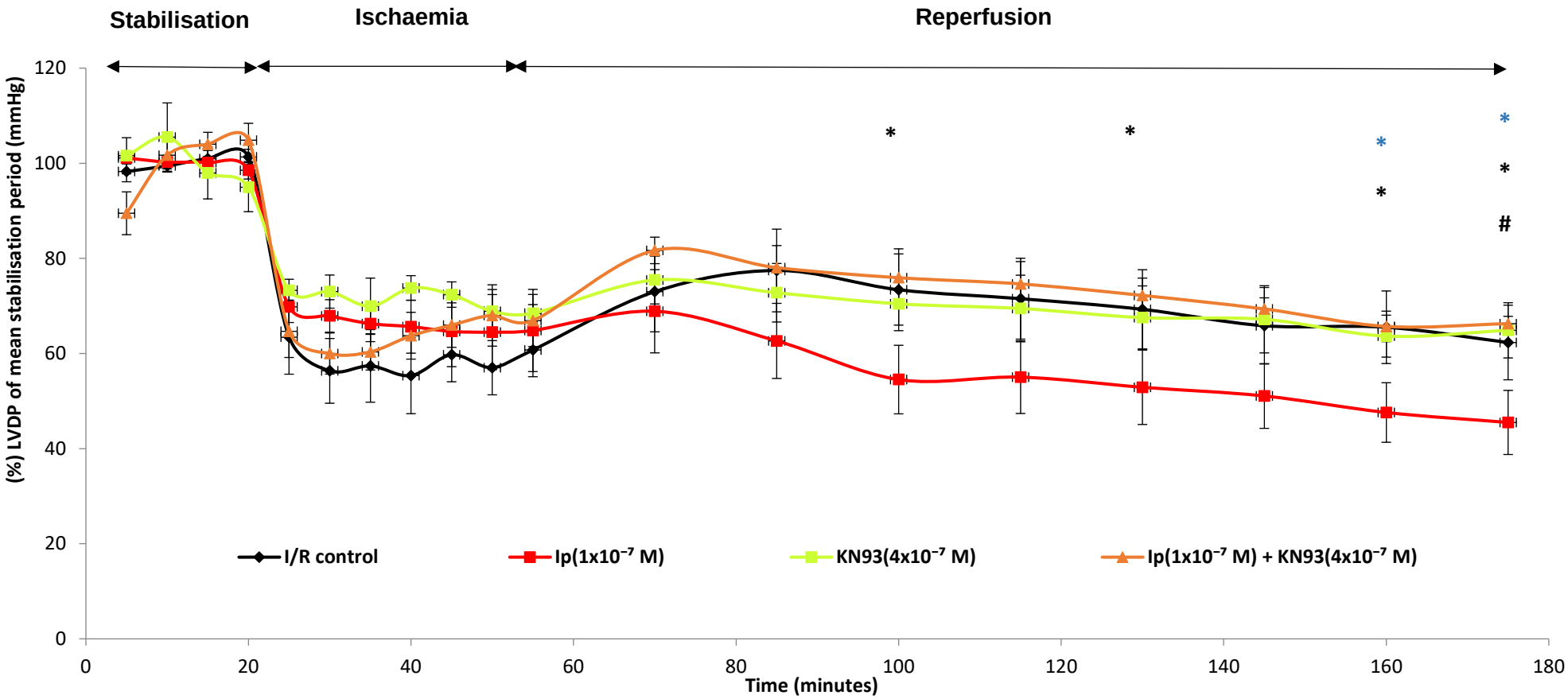

Figure 5. 1: Changes in left ventricular developed pressure % of (mmHg) in isolated perfused rat hearts group's I/R and Ipratropium bromide (1 x 10^{-7} M) and KN-93 (4 x 10^{-7} M) ± Ipratropium bromide (1 x 10^{-7} M). * p<0.05 for I/R control treated group against Ipratropium (1 x 10^{-7} M). * p<0.05 for KN-93 (4 x 10^{-7} M) treated group against Ipratropium (1 x 10^{-7} M). # p<0.05 for KN-93 (4 x10^{-7} M) + Ipratropium bromide (1 x 10^{-7} M) treated group against Ipratropium, n=6.

5.1.1.2 Heart Rate (HR)

The method by which HR was determined for I/R and Ipratropium bromide ($1x10^{-7}$ M) and KN-93 ($4 x10^{-7}$ M) ± Ipratropium bromide ($1x10^{-7}$ M) (explained in detail in section 2.2.1.6.2 in chapter 2). The results show that hearts rate (HR) at the Ipratropium bromide vs. Ip + KN-93 at 115, 160 and 175 minutes of reperfusion (100.5 ± 3.5, 96.2 ± 4, 95.6 ± 2.8% vs. 116 ± 6.9, 114.6 ± 5.5, 114.1 ± 5.2%) Ip ($1x10^{-7}$ M) ($p<0.05$). As well as at 130 minutes (99.3 ± 3.2% vs. 118 ± 6.4%) ($p<0.01$). For KN-93 ($4 x 10^{-7}$ M) against Ip 115,130, 145 minutes (97.5 ± 2.6, 95 ± 2.4, 91.3 ± 1.5% vs. 116 ± 6.9, 118 ± 6.4, 114.3 ± 5.3%) ($p<0.01$). And at 160 and 175 minutes (96.8 ± 2.4, 95.7 ± 2.1% vs. 114.6 ± 5.5, 114.1 ± 5.2%) ($p<0.05$). The significant difference between I/R control and Ip ($1 x 10^{-7}$ M) in HR is mentioned in section 3.1.1.2. Heart rate for I/R control and Ipratropium bromide ($1 x 10^{-7}$ M) and KN-93 ($4 x 10^{-7}$ M) ± Ipratropium bromide ($1 x 10^{-7}$ M) (Figure 5.2).

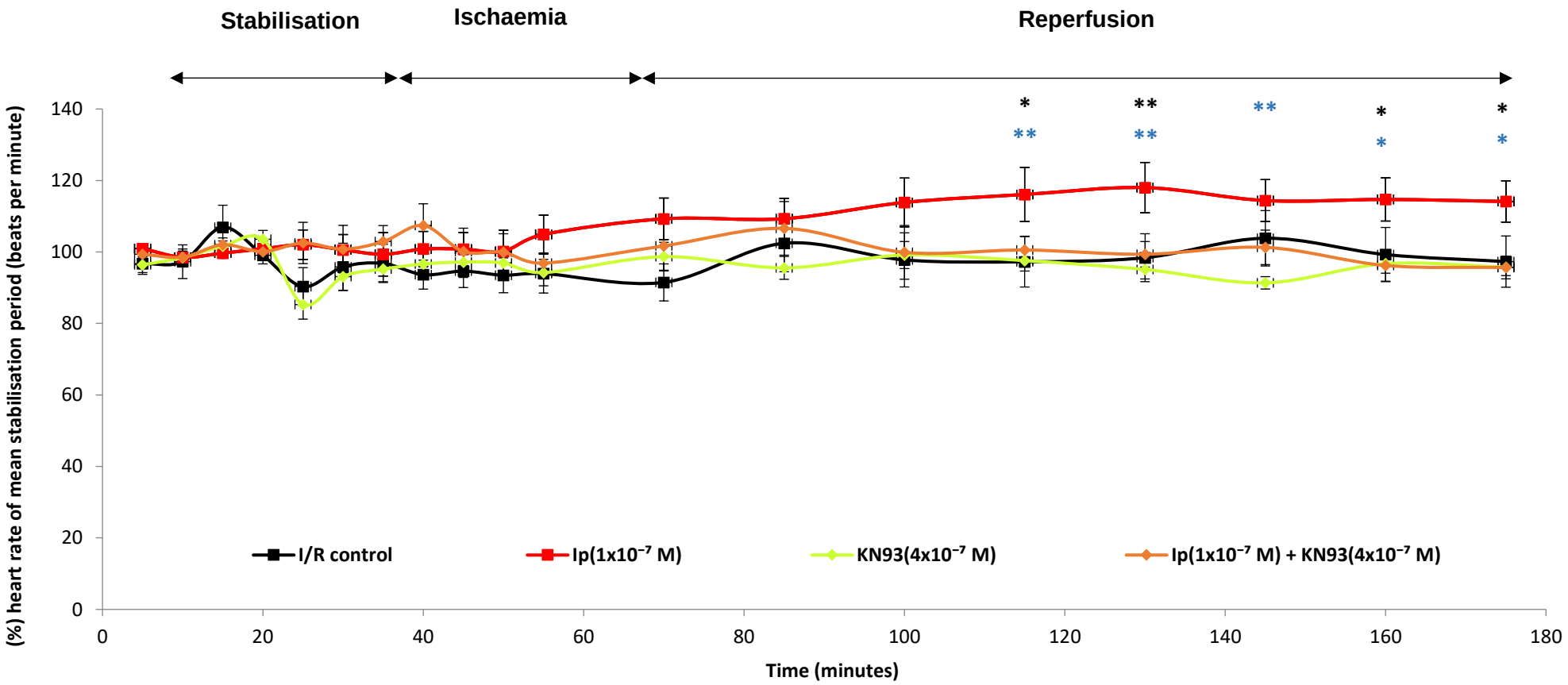

Figure 5. 2: Changes in heart rate (bpm) in isolated perfused rat hearts. All groups I/R control, Ipratropium bromide ($1x10^{-7}$ M) and KN-93($4 x10^{-7}$ M) ± Ipratropium bromide ($1 x 10^{-7}$ M). * $p<0.05$ for Ip + KN-93 ($4 x 10^{-7}$ M) treated group against Ipratropium ($1 x 10^{-7}$ M). ** $p<0.01$ Ip + KN-93 ($4 x1 0^{-7}$ M) treated group against Ipratropium ($1 x 10^{-7}$ M). * $p<0.05$ for KN-93 ($4 x 10^{-7}$ M) treated group against Ipratropium ($1 x 10^{-7}$ M). ** $p<0.01$ KN-93 ($4 x 10^{-7}$ M) treated group against Ipratropium ($1 x 10^{-7}$ M), n=6.

5.1.1.3 Coronary Flow (CF)

Coronary flow (CF) was for I/R and Ipratropium bromide (1 x 10^{-7} M) and KN-93 (4 x 10^{-7} M) ± Ipratropium bromide (1 x 10^{-7} M) explained in detail in section 2.2.1.6.3 in chapter 2). The results for coronary flow showed no significant difference between any group at any time point, compared to the control. Coronary flow results for I/R control and Ipratropium bromide (1 x 10^{-7} M) and KN-93 (4 x 10^{-7} M) ± Ipratropium bromide (1 x 10^{-7} M) are shown in (Figure 5.3).

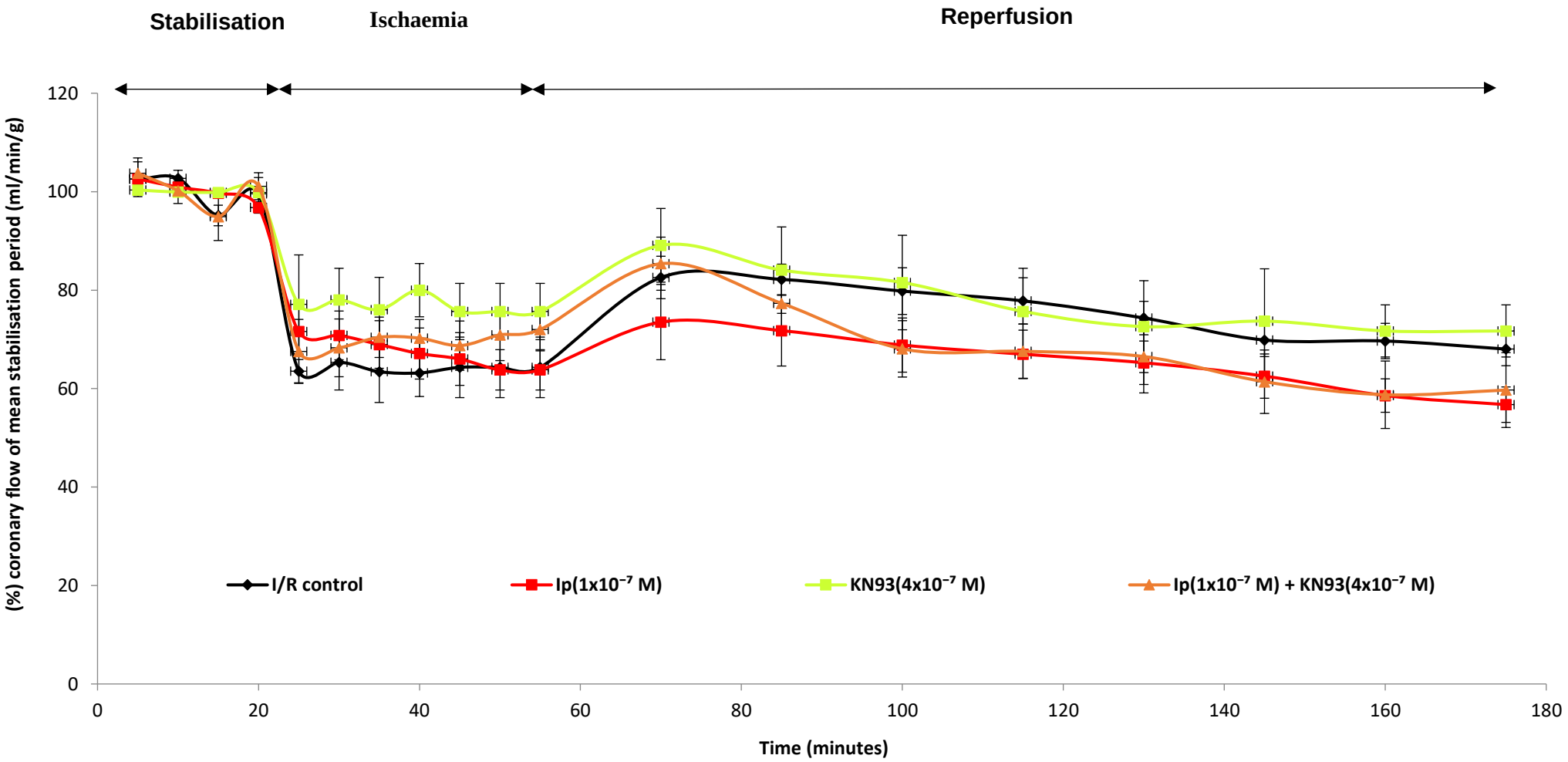

Figure 5. 3: Changes in coronary flow (ml.min-1) in isolated perfused rat hearts, n= 6. I/R control, Ipratropium bromide (1 x 10^{-7} M) and KN-93 (4 x 10^{-7} M) ± Ipratropium bromide (1 x 10^{-7} M), n=6.

5.1.2 The Infarct Risk Ratio Area At Risk (AAR %)

As explained in details in section 2.2.1.7, Ipratropium bromide ($1x10^{-7}$ M) and KN-93 ($4 x10^{-7}$ M) ± Ipratropium bromide ($1x10^{-7}$ M) were administered at the onset of reperfusion to preforming the TTC for Area At Risk ratio (AAR %) measurements. There was a significant difference between the Ip treated group and the I/R control (158.5 ± 6.2% vs. 100 ± 0) ($p < 0.001$). KN-93 shows cardio-protection importantly this demonstrated a significant reduction in infarction compared with the untreated control (74 ± 4.4% vs. 100 ± 0) ($p < 0.001$). There was also significant difference between Ip and both KN-93 and Ip+ KN-93 the co-administration of abrogates Ip mediated increases in infarction against Ip treated group (74 ± 4.4, 97.2 ± 2.2% vs. 158.5 ± 6.2%) ($p < 0.001$, $p<0.01$) respectively, thus abrogating the Ip mediated increase in myocardial injury. These obtained results present the comparison between the untreated I/R control, Ipratropium bromide ($1 x 10^{-7}$ M) or KN-93 ($4 x 10^{-7}$ M) ± Ipratropium bromide ($1 x 10^{-7}$ M) treatment groups (Figure 5.4).

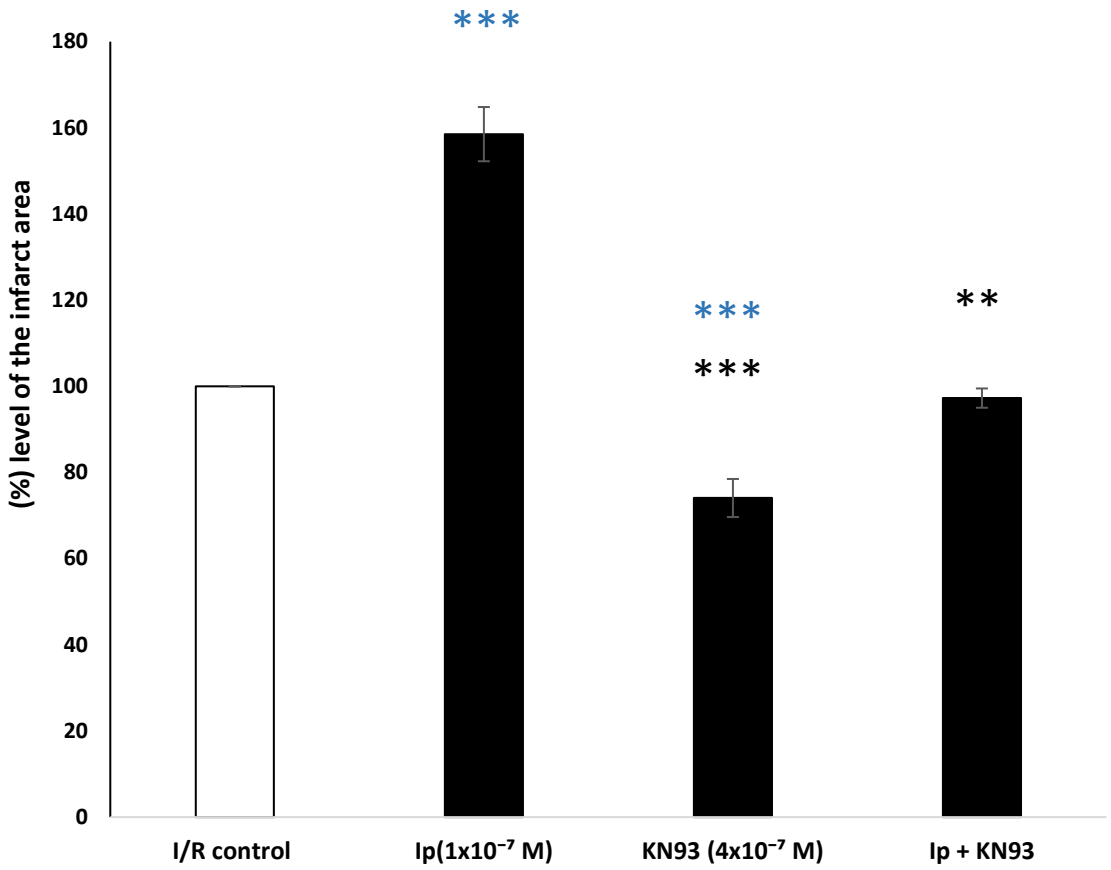

Figure 5. 4: Infarct development in I/R control, Ipratropium bromide ($1x10^{-7}$ M) or KN-93 ($4 x10^{-7}$ M) ± Ipratropium bromide ($1 x 10^{-7}$ M) treatment groups perfused isolated rat hearts. Results displayed as means + SEM, n=6. *** $p<0.001$ against I/R control. *** $p<0.001$ against Ipratropium ($1x10^{-7}$ M). ** $p<0.01$ against Ipratropium ($1x10^{-7}$ M).

5.2 Flow cytometry Data

In flow cytometry studies the protocol was followed to measure Apoptosis Necrosis, live cells and the activity of caspase-3 for the cardio myocytes that were treated with Ipratropium bromide (1 x 10^{-7} M) or KN-93 (4 x 10^{-7} M) ± Ipratropium bromide (1 x 10^{-7} M). In comparison with H/R control (Explained in detailed in section 2.2.2.1 and 2.2.2.2).

5.2.1 Cell Death Assay

For cell death assay cardiac myocytes isolation and Hypoxia/Reoxygenation protocols were carried out (section, described in section while the cells were alive Annexin V-FITC A and Propidium iodide were added to the cells incubated with the reagents, covered by in foil prior to analysis by flow cytometry. The cell death assay obtained results for cardiomyocytes that were simulated by inducing hypoxia/reoxygenation (H/R), has showed an exacerbation in the injury for the myocardial via the administration of Ip in compression with the controls normoxic and H/R (Explained in detailed in section 2.2.2.4.1).

5.2.2 Effects Of KN-93 On Apoptosis

For apoptosis results there was an increased in total apoptosis induced by Ip during H/R (table 5.1). The percentages of apoptosis are presented in (Figure 5.5). The increased in total apoptosis induced by Ipratropium during H/R was abrogated via the co administration of KN-93 with Ip both (1 x 10^{-7} M). In necrosis

there was no significant difference. Overall KN-93 increase myocyte viability with the co-administration of Ipratropium, although it was not significant.

Sample groups	Means	SEM
H/R control	100	0%
Ipratropium bromide (1 x 10^{-7} M)	116.22	6.4%*
KN-93 (1 x 10^{-7} M)	85.21	13.81%
KN-93 (1 x 10^{-7} M) ± Ipratropium bromide (1 x 10^{-7} M)	96.34	10.87%

Table 5. 1 : Represent the values of the drug treatments for apoptosis. The data was analysed after changing it into arithmetic means by normalised to H/R control, ± SEM, the recorded number myocytes is 10,000, n = 6. *p<0.05 against H/R control.

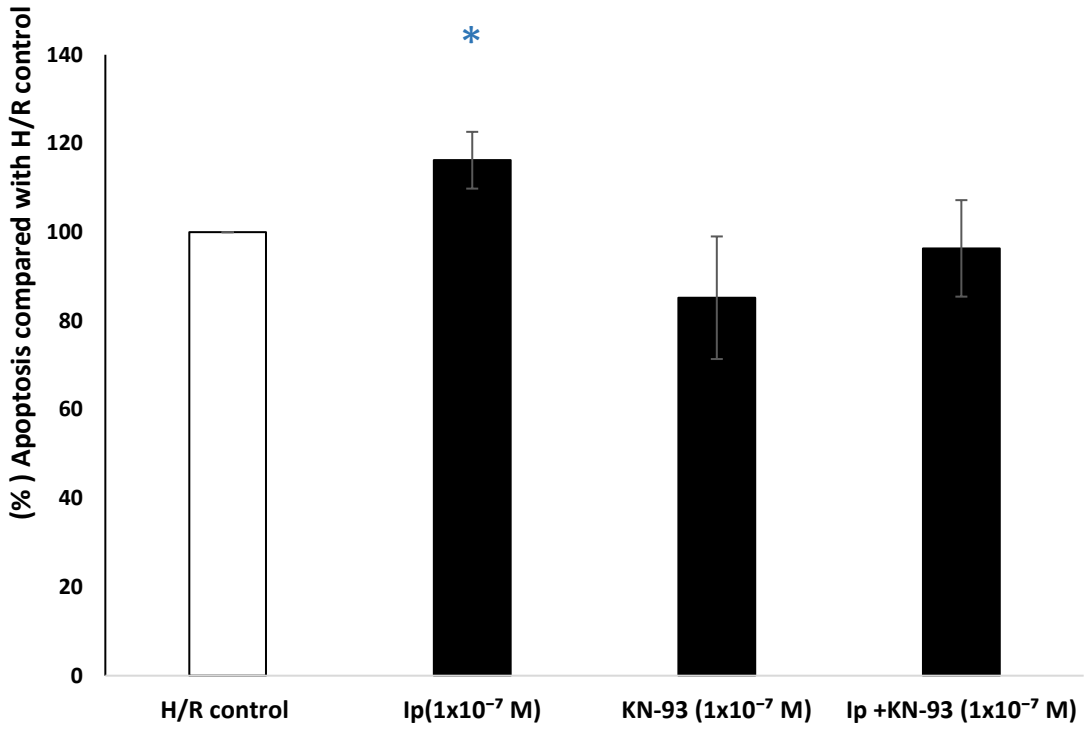

Figure 5. 5: Total apoptosis percentage results stained by Annexin V shown in flow cytometry for H/R control Ipratropium bromide ($1x10^{-7}$ M) or KN-93 ($1x10^{-7}$ M) ± Ipratropium bromide ($1x10^{-7}$ M). The data was analysed after changing it into arithmetic means by normalised to H/R control, ± SEM, the recorded number myocytes is 10,000, n = 6. *p<0.05 against H/R control.

5.2.3 Effects Of KN-93 On Necrosis

The percentages of necrotic cell death are presented in (table 5.2) (Figure 5.6). No significant difference was observed overall, despite the fact that, there is a pattern to suggest that Ip treated group had the most percentage of necrosis. Whereas KN-93 and Ip+ KN-93 treatment group necrotic cell deaths were less than the percentage of the control.

Sample groups	Means	SEM
H/R control	100	0%
Ipratropium bromide (1 x 10^{-7} M)	119.37	14.22%
KN-93 (1 x 10^{-7} M)	72.3	20.89%
KN-93 (1 x 10^{-7} M) ± Ipratropium bromide (1 x 10^{-7} M)	84.33	15.32%

Table 5. 2 : Represent the values of the drug treatments for necrosis. This table present the obtained results normalised to the H/R control and the statistical test showed no significant difference.

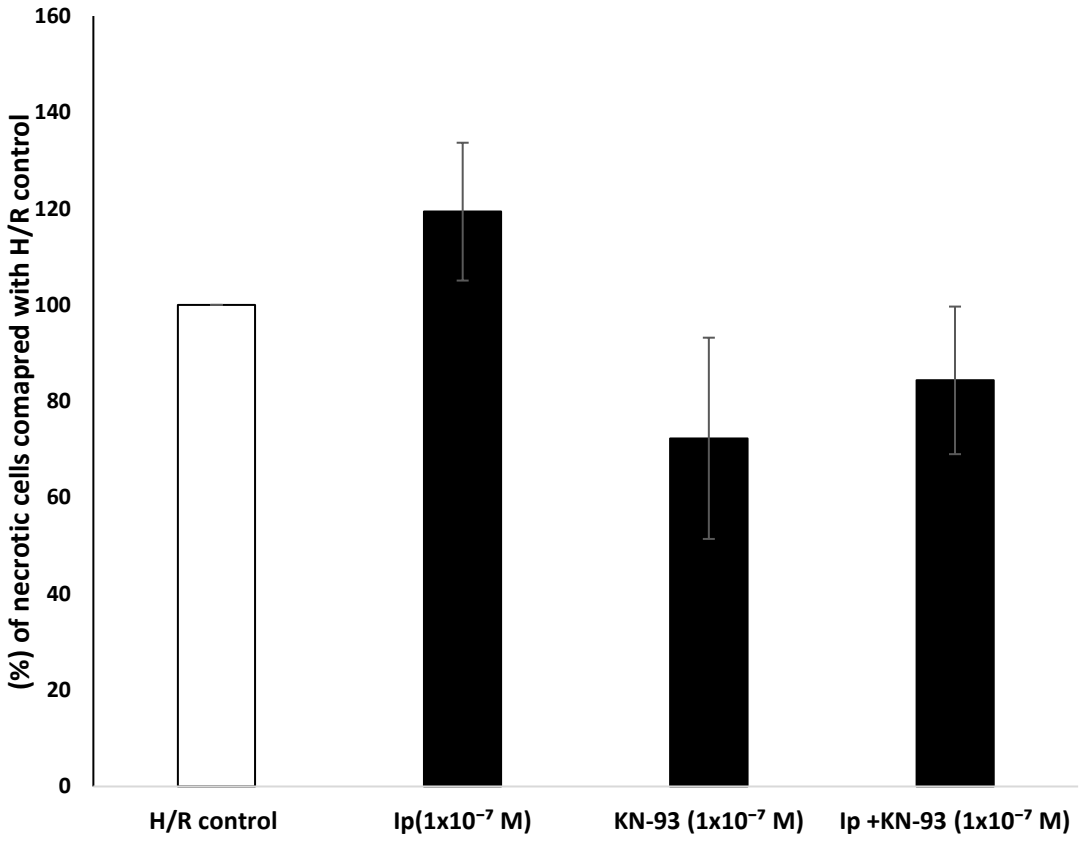

Figure 5. 6: Necrotic cells percentage results stained by Annexin V shown in flow cytometry for H/R control Ipratropium bromide (1x10^{-7} M) or KN-93 (1x10^{-7} M) ± Ipratropium bromide (1x10^{-7} M). The data was analysed after changing it into arithmetic means by normalised to H/R control, ± SEM, the recorded number myocytes is 10,000, n = 6.

5.2.4 Effects Of KN-93 On Cell Viability

The percentages of live cells are presented in (table 5.3) (Figure 5.7). Although there is no significant difference between KN-93 and the H/R control, there is a clear pattern that suggest that KN-93 increases cell viability, and when co-administered with Ip the percentage of live cells is approximately as the percentage of the control.

Sample groups	Means	SEM
H/R control	100	0%
Ipratropium bromide (1 x 10^{-7} M)	80.42	9.4%*
KN-93 (1 x 10^{-7} M)	109.93	15.74%
KN-93 (1 x 10^{-7} M) ± Ipratropium bromide (1 x 10^{-7} M)	103.22	13.76%

Table 5. 3 : Represent the values of the drug treatments for cell viability. The data was analysed after changing it into arithmetic means by normalised to H/R control, ± SEM, the recorded number myocytes is 10,000, n = 6. *p<0.05 against H/R control.

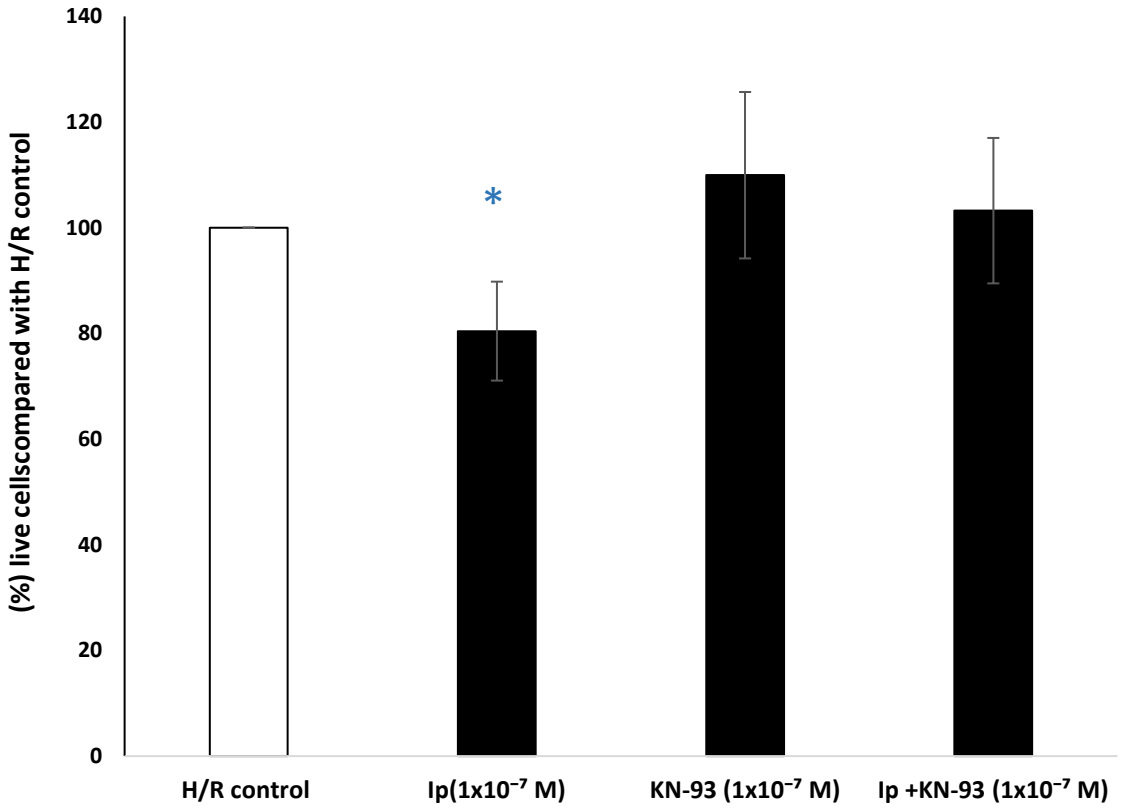

Figure 5. 7: Effect of Ipratropium bromide ($1x10^{-7}$ M) or KN-93 ($1x10^{-7}$ M) ± Ipratropium bromide ($1x10^{-7}$ M) in cell viability level in comparison to H/R control the data was analysed after changing it into arithmetic means by normalised to H/R control, ± SEM, the recorded number myocytes is 10,000, n = 6. *p<0.05 against H/R control.

5.2.5 The Level Of Caspase-3 Activity

The percentages of caspase-3 activity level is presented in (Figure 5.8). There was significant increase caused by Ip compared with H/R control1 (116.8 ± 4% vs. 100 ± 0) ($p < 0.01$), a significant reduction occurred when KN-93 was administered compared with the H/R control (57.7 ± 7, 59.9 ± 6.3% vs. 100 ± 0) ($p < 0.001$), There was also significant difference between Ip and both KN-93 and Ip+ KN-93 the co-administration reduces the activity of caspase-3 which means it abrogates Ip mediated injury caused by apoptosis (57.7 ± 7, 59.9 ± 6.3% vs. 116.8 ± 4%) ($p < 0.001$). The images graph generated from the flow cytometry software, once the samples had been processed, they presented as the above images. For the measurements of caspase-3 the figure shift to the right if there was caspase-3 activity such as the IP3 image. Whereas Mdivi1 data shift to the left which suggest that the caspase-3 was not active as much as in Ip treated group. When analysed in the software the images, three images, overlap to show the graph in comparison and in the H/R compared with Ip , the latter was sifted to the right due to the increased activity of caspase-3 in Ip treated group as seen in the Figure 5.8. However, in Mdivi-1 treated group when compared with H/R control the blot shift to the left which sugguest that caspase-3 was inhibited in the Mdivi-1 treated group.

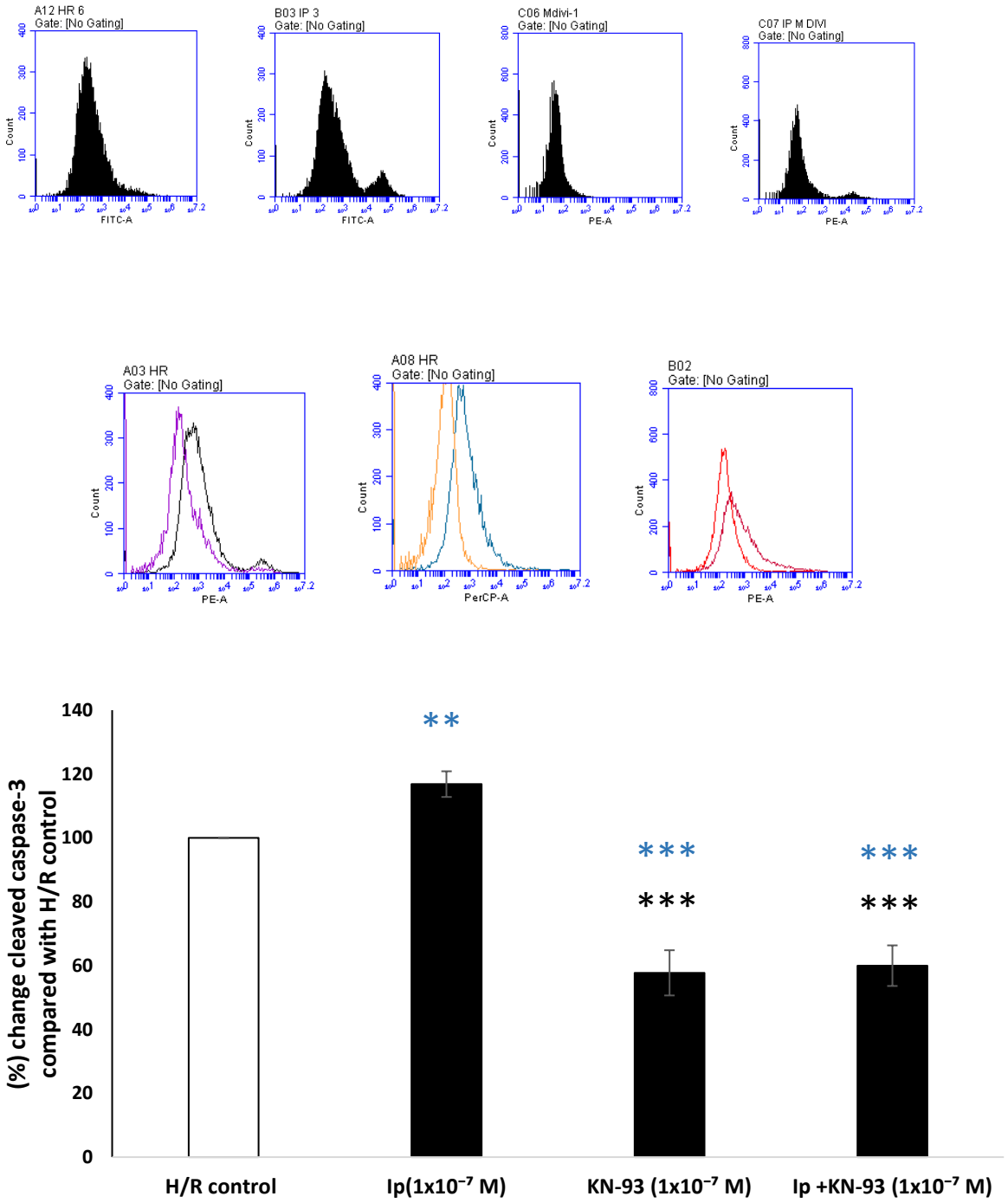

Figure 5. 8: Effect of Ipratropium bromide (1 x 10^{-7} M) or KN-93 (1x 10^{-7} M) ± Ipratropium bromide (1 x 10^{-7} M) in caspase-3 activity in comparison to H/R control the data was analysed after changing it into arithmetic means by normalised to H/R control, ± SEM, the recorded number myocytes is 10,000, n = 6. *** p<0.001 against H/R control. ** p<0.01 against H/R control. *** p<0.001 against Ipratropium (1 x 10^{-7} M).

5.3 Western Blot Results

For Western blotting studies the Langendorff protocol (section 2.2.1.1- 2.2.1.4) was followed the experimental group were I/R control and Ipratropium bromide ($1x10^{-7}$ M) and KN-93 ($4x10^{-7}$ M) ± Ipratropium bromide ($1x10^{-7}$ M), during reperfusion. The tissues were collected *in vitro* for the measurements of Drp1, Akt, Erk1/2 and caspase-3 (explained in detailed in section 2.2.3.1- 2.2.3.7).

5.3.1 Western Blot Results For The 15 And 30 Minutes Perfused Left Ventricular

The study was divided into two different time points (explained in detailed in section 2.2.3.8 - 2.2.3.9) (Figures 5.9 - 5.12). To see the effect of the drug treatment in the proteins of interest following reperfusion as both 15 minutes and 30 minutes time points are considered to be clinically significant (Hausensloy et al 2013).

5.3.1.1 The Measurements Of (I/R Control And Ipratropium Bromide ($1x10^{-7}$ M) And KN-93 ($4 x10^{-7}$ M) ± Ipratropium Bromide ($1x10^{-7}$ M)).

The percentage of the phosphorylation of Akt, Erk 1/2, Drp1 and cleaved caspae-3 to total/active activity in the isolated perfused hearts treated with Ipratropium bromide ($1 x10^{-7}$ M) or KN-93 ($4 x10^{-7}$ M) ± Ipratropium bromide ($1 x10^{-7}$ M) compared with I/R control. Ipratropium bromide ($1 x 10^{-7}$ M) data are mentioned in (section 3.3.1.1) (Figures 5.9 - 5.12).

The administration of KN-93 demonstrates cardio-protection via a reduction in Dynamin related protein 1 (Drp-1), Akt, Erk1/2 and caspase-3 compared with the untreated control in all studies at both time points. In Figure 5.9, A, co-administration of KN-93 treatment abrogated Ip induced decreases in Drp1 levels compared with the I/R and Ip at 15 minutes reperfusion groups (52.1 ± 21.3% vs.100 ± 0) $p < 0.05$ (52.1 ± 21.3% vs.128.1 ± 14%) $p < 0.01$ respectively and KN-93 reduce the level of Drp1 compared with Ip (79.9 ± 19.1% vs.128.1 ± 14%) $p < 0.05$. In the 30 minutes reperfusion results there was a significant decrease in Drp 1 level in Ip+KN-93 in comparison to Ip treated group (48.8 ± 15.2% vs. 125.8 ± 23.1%) $p < 0.01$, moreover, significant decrease in the phosphorylation of Drp 1 in KN-93 in comparison to Ip treated group (73.6 ± 20.1% vs. 125.8 ± 23.1%) $p < 0.5$ (Figure 5.9, B).

For caspase-3 group there was a significant decrease in the level of caspase-3 activity in the KN-93 group compared to the Ip treated group (78.9 ± 15.1% vs 122.2 ± 12.7%) $p < 0.05$. Co-administration of KN-93 treatment abrogated Ip induced decreases in caspase-3 levels compare the Ip at 15 minutes reperfusion (85.5 ± 12.6% vs 122.2 ± 12.7%) $p < 0.05$ (Figure 5.12, A). No significant difference for other treatment group against the control at 30 minutes reperfusions nor against the treated group (Figure 5.12, B).

Figure 5.10 overall no significant difference appeared in the level of Akt despite the pattern compared to the untreated control or the treated group at both time points, the same for and Figure 5.10 which represent the expression of Erk1/2.

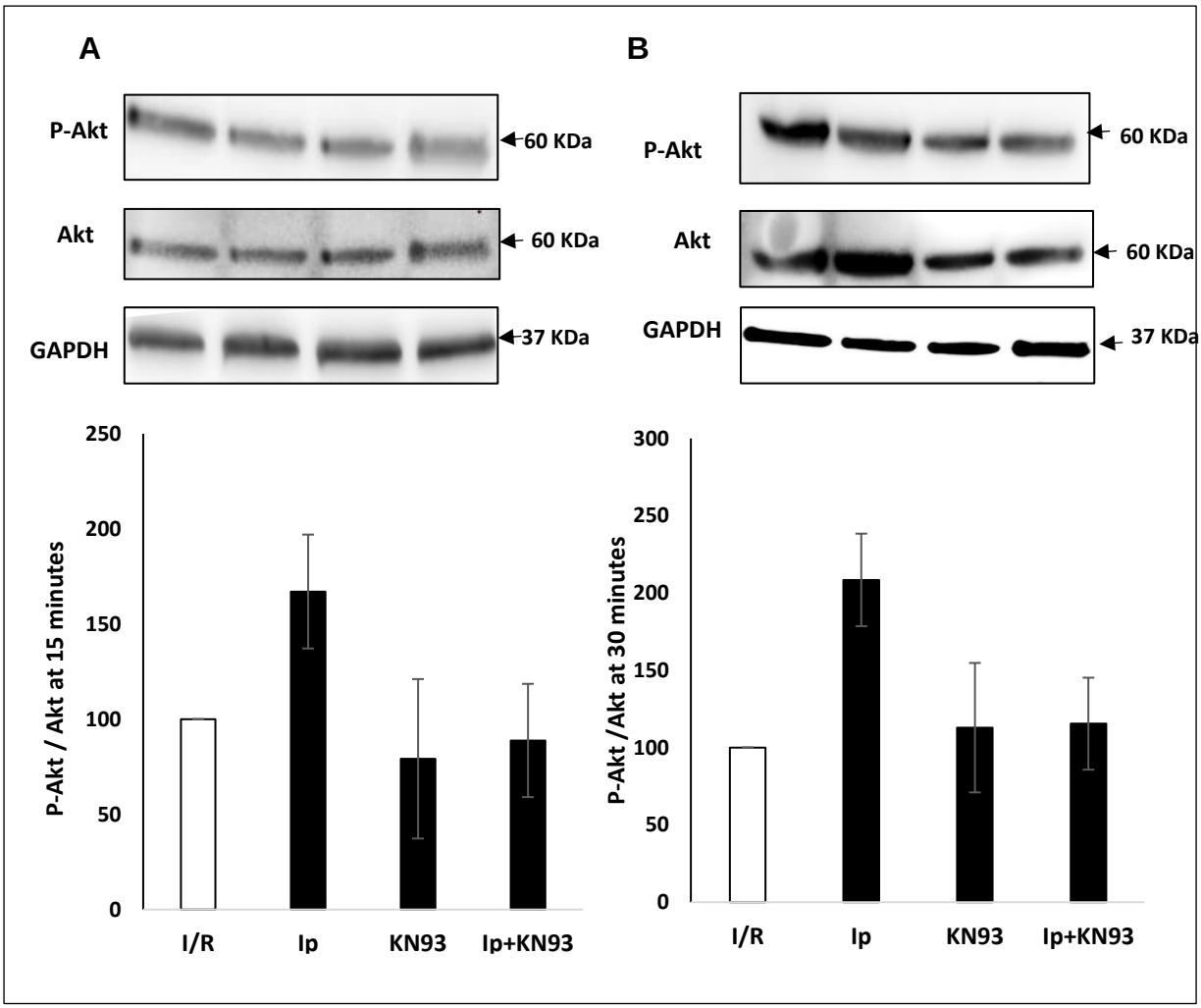

Figure 5. 9: The levels of phospho and Total Akt in I/R control, Ipratropium bromide (1 x 10^{-7} M) or KN-93 (4 x 10^{-7} M) ± Ipratropium bromide (1 x 10^{-7} M). A is treatment groups perfused for 15 minutes isolated rat hearts. B is treatment groups perfused for 30 minutes isolated rat hearts. Results displayed as means + SEM, n=6.

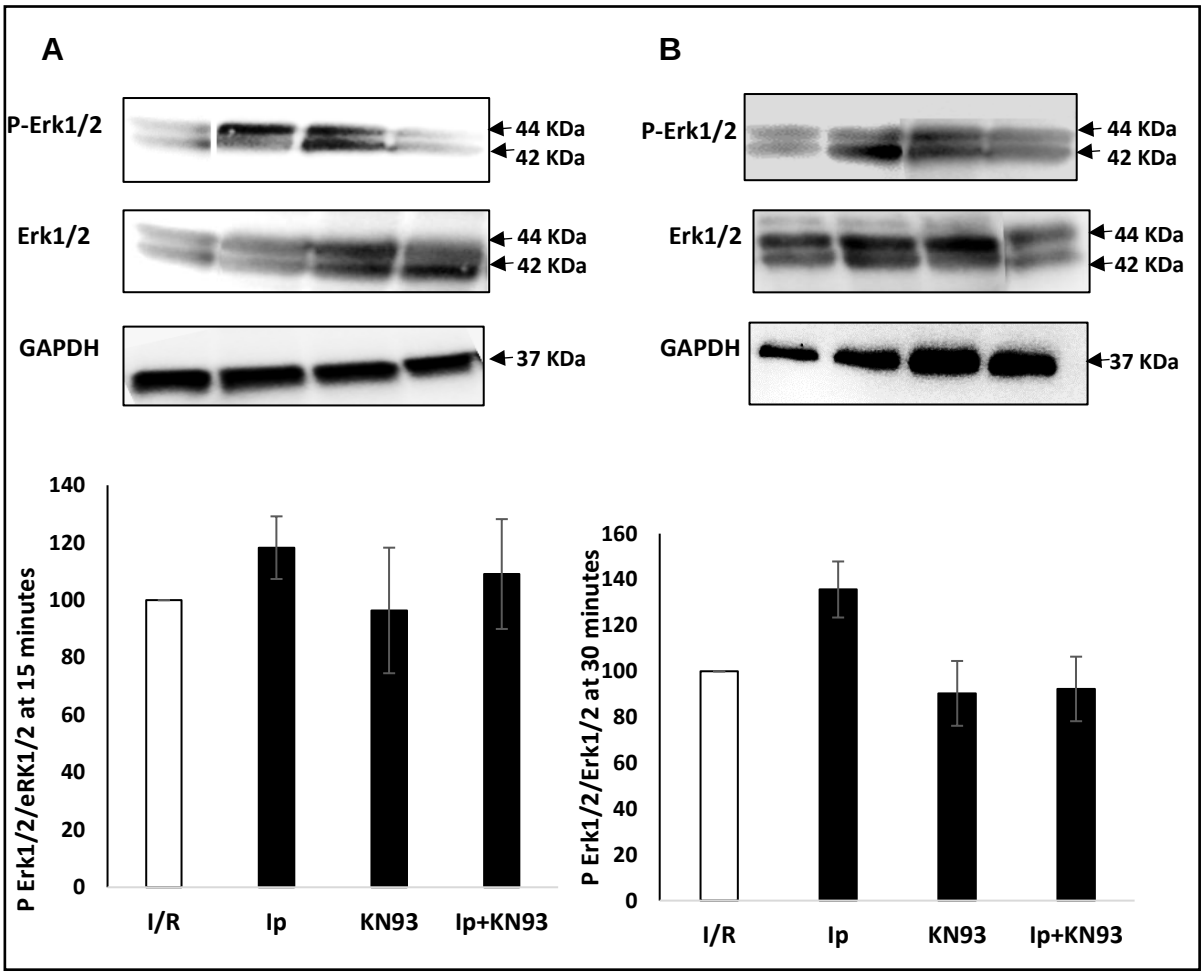

Figure 5. 10: The levels of phospho and Total Erk 1/2 in I/R control, Ipratropium bromide (1 x 10^{-7} M) or KN-93 (4 x 10^{-7} M) ± Ipratropium bromide (1 x 10^{-7} M). A is treatment groups perfused for 15 minutes isolated rat hearts. B is treatment groups perfused for 30 minutes isolated rat hearts. Results displayed as means + SEM, n=6. No significant difference was observed between any groups at either time point.

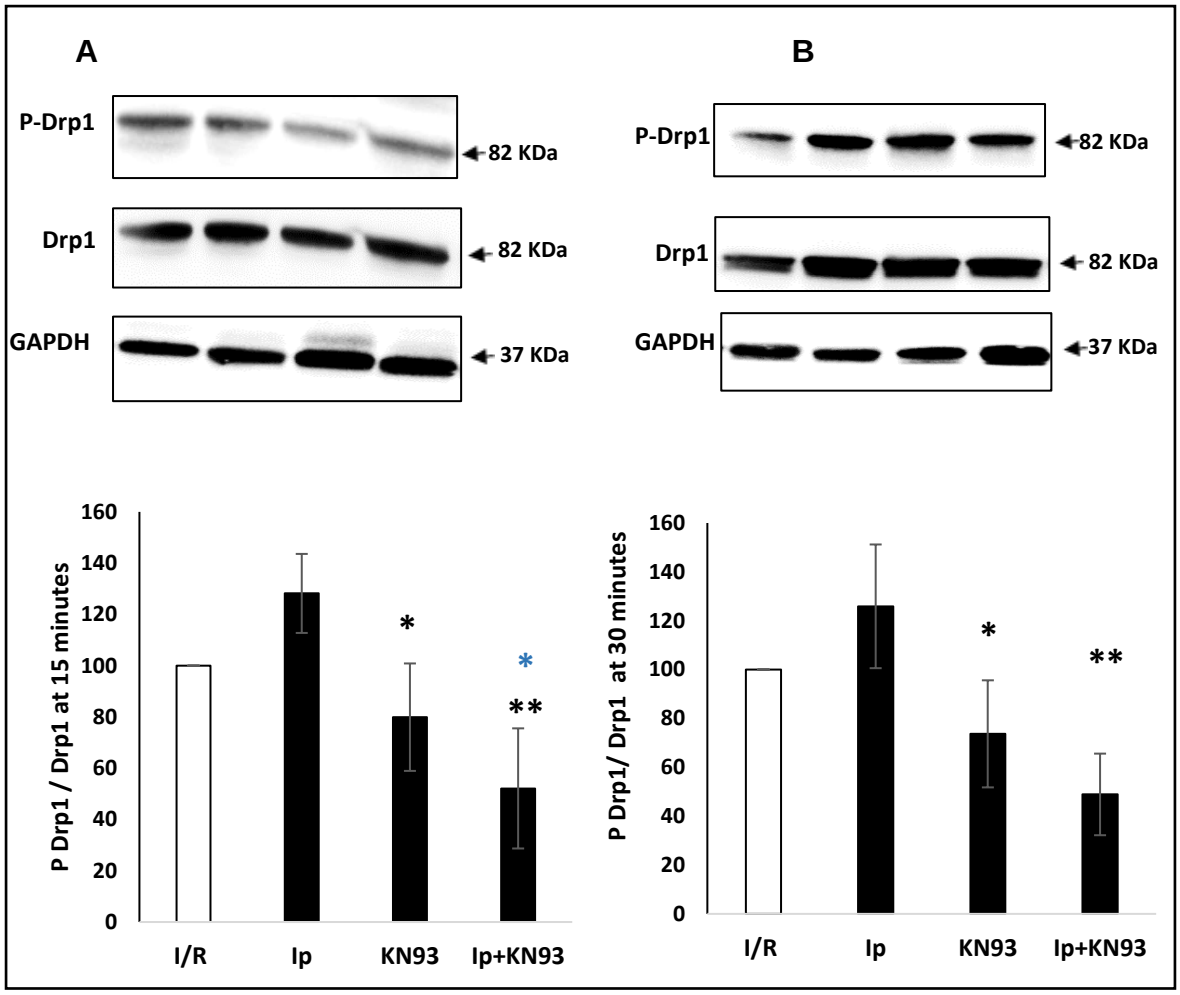

Figure 5. 11: The levels of phospho and Total Drp1 in I/R control, Ipratropium bromide (1 x 10^{-7} M) or KN-93 (4 x 10^{-7} M) ± Ipratropium bromide (1 x 10^{-7} M). A is treatment groups perfused for 15 minutes isolated rat hearts. B is treatment groups perfused for 30 minutes isolated rat hearts. Results displayed as means + SEM, n=6. * $p<0.05$ vs I/R control, * $p<0.05$ vs Ipratropium bromide (1 x 10^{-7} M), * *$p<0.01$ vs Ipratropium bromide (1 x 10^{-7} M).

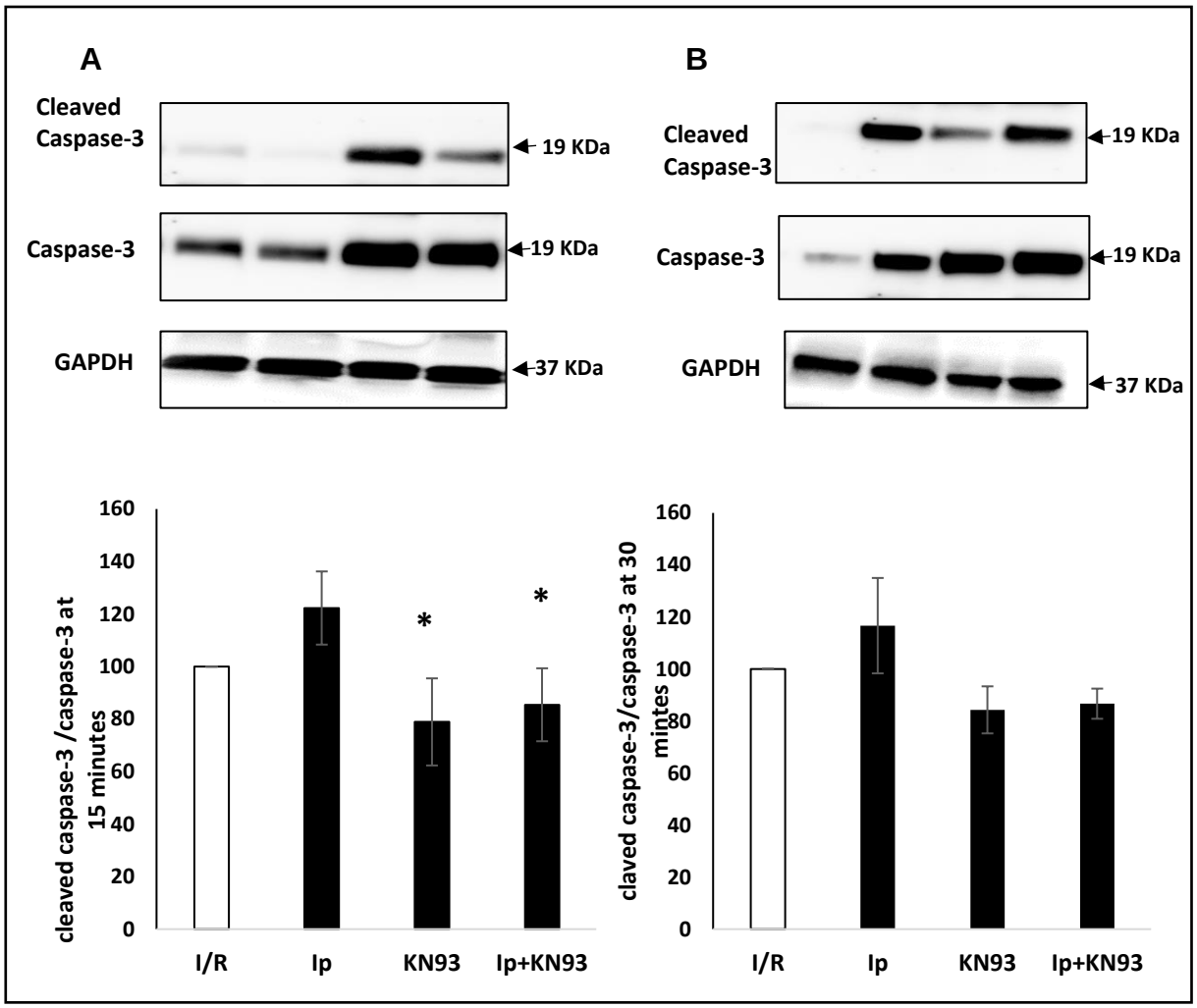

Figure 5. 12: The levels of cleaved and active capsae-3 in I/R control, Ipratropium bromide (1 x 10^{-7} M) or kn-93 (4 x 10^{-7} M) ± Ipratropium bromide (1 x 10^{-7} M). A is treatment groups perfused for 15 minutes isolated rat hearts. B is treatment groups perfused for 30 minutes isolated rat hearts. Results displayed as means + SEM, n=6. * $p<0.05$ vs Ipratropium bromide (1 x 10^{-7} M).

5.4 PCR Results

For PCR experiments, (explained in detail in 2.2.11- 2.2.14) the left ventricle was taken out at the same time points as western blot. The gene of interest used was Dnm1l against GAPDH primers for I/R control and Ipratropium bromide (1 x 10^{-7} M) and KN-93 (4 x 10^{-7} M) ± Ipratropium bromide (1 x 10^{-7} M). The data presented no significant difference between the control and Ip treated group (table 5.4) (Figure 5.13) (Explained in detail in section 2.2.4.1- 2.2.4.3).

Sample groups	Means	SEM
I/R control	100	0%
Ipratropium bromide (1 x 10^{-7} M)	1419	900.45
KN-93 (1 x 10^{-7} M)	770.51	200.3%
KN-93 (1 x 10^{-7} M) ± Ipratropium bromide (1 x 10^{-7} M)	168.84	100.67%

Table 5. 4 : Represents the values of the drug treatments for PCR reaction.

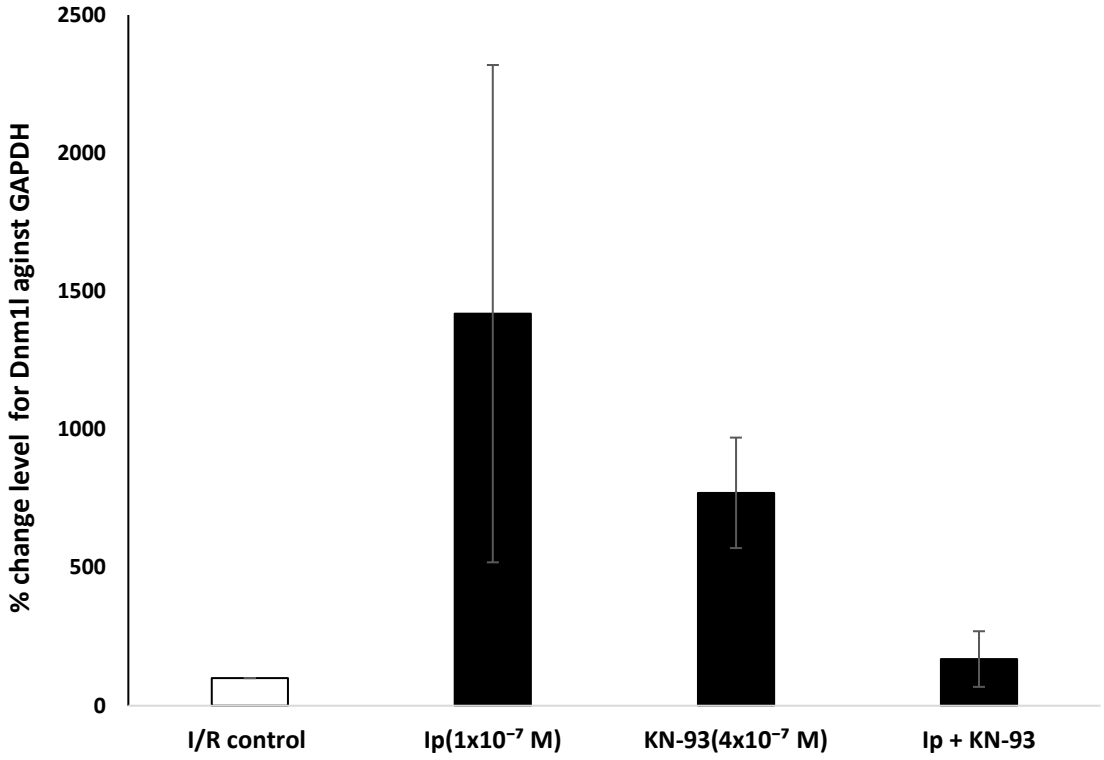

Figure 5. 13: The levels of fold change in Dnm1l in I/R control, Ipratropium bromide (1 x 10^{-7} M) or KN-93 (4 x 10^{-7} M) ± Ipratropium bromide (1 x 10^{-7} M) is treatment groups perfused for 15 minutes isolated rat hearts. Results displayed as means + SEM, n=6. The large error bars are generated form the data obtained, the data was inconclusive further explain in the limitation section and the statistical analysis resulted in no significant difference.

5.5 Chapter Discussion

The study aim was to further elucidate the signalling mechanisms which lead to Ip mediated myocardial injury. By identifying whether there is calcium overload involvement in Ipratropium induced toxicity in myocardial ischaemia/reperfusion. Co-administration KN-93 with Ip was utilised to ascertain the involvement of CaMK Kinase (CaMKII signalling) in Ip induced injury which was similar to the results demonstrated in chapter 4.5 with the clinically relevant concentration. The potential involvement of calcium overload was investigated a possible reason of Ip exacerbation of myocardial injury, since the calcium signalling was regulated was the activation of CaMKII, KN-93 was used as an indicator for Ca^{2+} signalling as KN93 inhibitor CaMKII activity which reduce Ca^{2+} overload (Xu et al. 2016).

The key finding of this chapter is that the injury induced by Ipratropium bromide was attenuated via the co-administration of KN-93 in the Ischaemia/Reperfusion as well as in Hypoxia/Re-oxygenation stimulated conditions. This indicates Ca^{2+} involvement via the inhibition of CaMKII, which in normal condition maintain Ca^{2+} level, however, during stress conditions CaMKII can increase Ca^{2+} level in the cell leading to overload (Huang, Qin and Lu 2014). Since Ip induce injury was reduced by KN93 this suggest the induce injury is due to Ca^{2+} overload by the results of the infarct size (Figure 5.4) ($p<0.001$), as KN-93 protective properties managed to reduce the increase in the infarction with a significant difference when co administered with Ipratropium bromide. Not to mention the inhibition that was identified in caspase-3 activity in myocytes was also significant (Figure 5.8) ($p<0.001$). This study demonstrates for the first time KN-93's ability to reduce the

exacerbation in myocardial injury when combined with Ip (at the highest concentration) Ip (1 x 10^{-7} M) in the I/R and the H/R stimulated condition. The administration of KN-93 (4 x 10^{-7} M) showed cardio-protection via a reduction in infarct size compared with the untreated control. When Ip (1 x 10^{-7} M) was added with KN-93 (4 x 10^{-7} M) the infarction percentage was significantly reduced compare with the untreated control I/R, thus abrogating the Ip mediated increase in myocardial injury in this model. Also the administration of KN-93 (1 x 10^{-7} M) for isolated cardiac myocytes resulted in reduction caspase-3 activity against untreated control. When Ip (1 x 10^{-7} M) was administered in the presene of KN-93 (1 x 10^{-7} M) the caspase-3 activity was significantly reduced compare with the untreated control H/R. This supports the previous evidence by Cassambai et al. (2019) which indicated involvement of calcium overload, however these mechanisms need to be identified, which is why the results from this study may prove to be invaluable in identifying the cellular mechanisms. This study found that, in Langendorff data, KN-93 administration at the start and throughout reperfusion managed maintain the heart haemodynamics compared with that the untreated control. The haemodynamic parameters were closer to the levels observed results in the normoxic control, KN-93 was able to increase the level of LVDP and CF as well as decrease HR and the infarct size once co administered with Ip (Figure 5.1 - Figure 5.3). This demonstrates that KN-93 can actually abrogate I/R induced injury, even in the absence of Ip. The results obtained from measuring both the haemodynamic parameters and the infarct risk ratio for Ip (AAR%). KN-93 abrogation of the injury induced by Ip.

The phosphorylation of Erk1/2 signalling pathway was analysed for the tissue treated with KN-93 + Ip demonstrated down-regulation of Erk1/2, as was the case for the KN-93 treated group whereas Erk1/2 activation expression was increased in the Ip treated group by 20 % after extra 15 minutes reperfusion (Figure 5.10 A, B). Erk 1/2 can be activated by depolarization and influx the increase in level leads to activation of CaMKII and erk1/2 via PI3K (53) (Cassambai et al. 2019). The indication provided by the study is that the administration at the onset and throughout reperfusion of CaMKII inhibitor (KN-93) is capable of eliciting protection from the injury Ip induced when co-administered with Ip. Akt, Erk1/2 and caspase-3 activation, (Figure 5.09 - 5.12), was reduced by KN-93 compared to the treated group with Ip alone at both time points (15 and 30 minutes post-reperfusion). Akt and Erk1/2 western results in the study link CaMKII inhibitor KN-93 in the ischaemic/reperfusion models, via the reduction in both kinase's phosphorylation. Ip obtained results however, showed increase in Akt, Erk1/2 and caspase-3 (Fujiki, Inamura, and Matsuoka, 2013). A study by Fujiki, Inamura, and Matsuoka, (2013) conducted mange to linked Akt kinase protein C and KN-93 CaMKII inhibitor, in his study KN93 was able to reduce Akt phosphorylation linking it to CaMKII and Ca^{2+} signalling (Fujiki, Inamura, and Matsuoka, 2013). Calcium signalling was connected to Erk1/2 due to the action provided by KN-93 by blocking Erk1/2 activation, consequently CaMKII associated with the phosphorylation of Erk1/2 by inducing cAMP/PKA which causes the activation of ERK 1/2 (Banerjee et al. 2014, Huang, Qin and Lu 2014). This action leads to mediating caspase-3 dependent apoptosis (Banerjee et al. 2014, Huang, Qin and Lu 2014). KN-93 causes a decrease in the activity of caspase-3 this might be

related the pathway of intrinsic apoptosis (Figure 5.08), These results are similar to Mdivi-1 data in chapter 4 section 4.5 regarding decreasing both Drp1 and caspase-3 suggesting intrinsic apoptosis (Cassambai et al. 2019). The lack in the published literature in regard to KN-93 and linking it to caspase-3 means that this conclusion cannot, currently, be definitively drawn since not much published literature written in this regard. CaMKII was found to phosphorylate Drp1 directly by bind to its activation site at Serine ($_{616}$), the latter translocates to the mitochondria if it was activated by Ca^{2+} or via its phosphorylation (Xu et al. 2016). This action was suggested to promote mPTP opening which leads to initiation of intrinsic apoptosis as the end results (Xu et al. 2016). The same study has found that, the process of intrinsic apoptosis was inhibited by KN-93, as it was also found to inhibit the phosphorylation of Drp1 via its inhibitory action in CaMKII (Xu et al. 2016). This study found that KN-93 has protective properties as shown in western blot studies, it decreased the phosphorylation of Drp1 compared to untreated control. Importantly, the administration of KN-93 demonstrates cardio-protection via a reduction in Drp-1, Akt, Erk1/2 and caspase-3 compared to I/R in all studies at both time points against Ip treated group.

KN-93 was also able to reduce the level of apoptosis in the flow cytometry studies by the measurement of apoptosis (Figure 5.5, table 5.1), necrosis (Figure 5.6, table 5.2). Caspase-3 is an important key factor in both intrinsic and extrinsic apoptosis pathway, the high level of cleaved caspase-3 indicates that the myocytes are undergoing apoptosis (Elmore 2007). Since KN-93 was able to significantly reduce the activity of the caspase-3 in comparison with H/R control, this may be due to maintaining mitochondrial integrity which suggest that the

initiation for apoptosis pathway was intrinsic (Elmore 2007). KN-93 was also able to reduce the apoptosis and necrosis that were increased upon the administration of Ipratropium bromide. KN-93 increased myocyte viability when co-administrated with of Ipratropium in H/R condition (Cassambai et al. 2019). There have been studies conducted for KN-93 to CaMKII that result in both decrease calcium ions level as well as reduction in apoptosis as a result increase in the cell viability with the group treated with KN-93 (Szobi et al. 2013, Cassambai et al. 2019). Similarly, to the obtained results in regards to the increase in cell viability with no significant difference (Figure 5.7, table 5.3) might be related to the potency of KN-93 capability of inhibiting CaMKII, or the level of concentrations used. However, due to limited studies, the most appropriate concentration of KN93 was used following dose response studies to try to identify the most therapeutic concentration. CaMKII activation is an important factor to mediate cell death programme apoptosis, therefore, CaMKII inhibitor administration little protect via effect on acid-induced endplate chondrocyte apoptosis, which is CaMKII independent manner, leading to CaMKII inhibitor preventing intrinsic apoptosis in a manner that is independent on CaMKII (Yuan et al. 2013). Overall, the conjunction between Ip and KN-93 had provided a reduction in the death of myocyte, the main finding of the results presented, in this chapter, suggest that the reduction occurring was mainly apoptosis rather than necrosis, although it was not significant. Szobi et al. (2013) has conducted a study in which CaMKII inhibitor data was normalised to I/R showed an increased the Bcl-2/BAX ratio and there was reduction in the level of caspase-3 concluding the possibility due to the reduction intrinsic apoptosis, cell loss was reduced as a consequence. (Szobi et

al. 2013). Regarding PCR results (Figure 5.13, table 5.4), the data presented showed an overall insignificant difference when KN-93 was administered at the onset of reperfusion for 15 minutes in the results obtained compared to the control and the treated group. Although there is a pattern seen in the presented figure, KN-93 was not able to significantly decrease the expression of Dnm1l as hypothesised. It is thought to be the period of reperfusion is not adequate to present a clear image of the expression of the gene Dnm1l. Not to mention the tool in which the PCR reaction was measured was given to the university Hospital of Coventry and Warwickshire as well as more data such as longer period of reperfusion, currently unavailable given the current global COVID pandemic.

CamKII inhibitor KN-93 presence and absence in the experiment indicate the association of calcium overload involvement utilizing Langendorff model, western blotting and flow cytometry to achieve data to help identify the involvement. The results yielded for the proteins of interest in a reduction in comparison to the untreated control, concluding the obtained results has presented indicating clearly for the possible effect of the induced myocardial injury induced by Ip is through an alteration in calcium signalling for apoptotic extrinsic pathway.

Chapter 6 General Discussion

6.1 Summary Of The Findings

Previous work in our laboratory has demonstrated in *in vitro* non-clinical models the myocardial injury mediated by I/R is exacerbated by the non-selective muscarinic receptor antagonist Ipratropium Bromide (Ip). This is due to the fact that patients with COPD are administered Ip as a treatment and there is a relationship that COPD patients are likely to develop IHD (Søyseth et al. 2007). In a non-clinical *ex vivo* model of stimulated conditions of I/R it was found that Ip was able to cause damage at the cellular level, by decreasing the percentage of viable cardiac myocytes and it increased the level of infarction (Harvey, Hussain and Maddock 2014). The nomoxic condition Ip administration appeared not to cause damage nor exacerbation of myocardial injury which was established by Harvey, Hussain and Maddock (2014). This means that Ip exacerbation on injury (Cassambai et al. 2019). These finding help determine the next stage in which this study comes in and the reason behind it. The mechanism of induced injury is not fully elucidated but appears to have mitochondrial involvement, the concentration of the drug treatments was chosen due to clinical relevancy. Hence mitochondria involvement was investigated to elucidate the signalling mechanisms, which lead to Ip exacerbation of RI in myocardial, in I/R stimulated conditions via the measurement of Drp1 (Abdallah et al. 2011). Drp1 was used to determine Mitochonderia fission the latter leads to apoptosis cell death (Ishikita et al. 2016). As well as investigating the potential involvement of calcium cellular overload as one of the reasons Ip exacerbated myocardial injury in

Ischaemia/Reperfusion hearts and Hypoxia/Reoxygenation cardiac myocytes using KN-93 CaMKII inhibitor to determine Ca^{2+} signalling (Xu et al. 2016). The Involvement of both respective pathways was to be identified via co-administration of Mdivi-1 and KN-93 with Ip.

Interstingly, Langendorff studies have shown that the muscarinic antagonist, Ipratropium bromide, has been shown to increase myocardial injury in *in vitro* non-clinical models of Ischaemia/Reperfusion. The results obtained in the isolated perfused hearts under stimulated I/R condition suggest that the presences of Ip at the onset of reperfusion causes damage to the hearts (Gharanei et al. 2013). From a clinical and physiological perspective this is important as for patients receiving Ip, irrespective of cardiovascular disease, there will be levels of the Ip present thorough the systemic circulation after inhalindthe drug (Irvin-Sellers and White, 2015). The measurements of haemodynamics and infarction showed that Ip at the highest concentration of (1×10^{-7} M) is capable of causing significant damage compared to the I/R control, in the *in vitro* models assessed (Figure 3.1 - 3.3) in chapter 3. The infraction size was significant compared to haemodynamics it is thought to be due to the the dysfunction of myocar competitive action of Ip to bind to mAChRs against the endogenous Ach as Ach reduce the conduction reate from the SA node resulting in negative chronotropy which was canceled by Ip (Wang et al. 2004). This action may be the result of Ca^{2+} overload, since muscarinic antagonists may cause MI which leads to deregulation of calcium regulation and signaling, and Ca^{2+} influx cardiac dysfunction necrosis reduces ATP formation, impairment severity (Harvey, Hussain and Maddock 2014, Cassambai et al. 2019).

Muscarinic acetylcholine receptor antagonists are used to treat many pathophysiological conditions such as respiratory system diseases by binding to mAChR receptors and preventing acetylcholine signaling transportation to the synaptic cleft to generate the signal for muscle contraction, which results in smooth muscular relaxation (Wang et al. 2004). However, since mAChR antagonists postulated to have the potential to increase both morbidity and mortality of patients with respiratory diseases such as COPD asthma underlying CVEs, which lead to the concern of the safety of the agents used which what this study proven, the co-administration of agents which are protective can provide the potential of patient survival (Singh, et al, 2009, Harvey, Hussain and Maddock 2014). Ip stimulates apoptosis during RI via calcium accumulation within the cell as well as mitochondria disfunction mainly by the opening of mPTP, previous studies suggested the protective properties of cyclosporine-A (CsA) (mPTP blocker) for myocardial Ischaemia reperfusion injury when administered with individual mAChR antagonists that set for myocardial Ischaemia reperfusion injury (Khan 2015). By preventing the release of free radical leading to cytochrome c, BcL-2 protein BAX/BAK mitochondrial fragmentation leading to cell death (Harvey 2015). This is similar to Mdivi-1 action which provided protection that is closest to the nomoxic control in the study giving the speculation that it can be utilized to prevent Ip exacerbation of injury thought more research are needed since Mdivi-1 is a synthesized agent.

6.1.1 Mdivi-1 Mechanism Of Protection

The pathway for Ip induces injury in the myocardial following stimulated conditions of ischaemia and reperfusion was further characterised, studies for Mdivi-1 and KN93, in the presence and absence of Ip, were conducted due to their protective properties under circumstances which were clinically relevant.

Mdivi-1 has a protective property by maintaining mitochondrial integrity, thus the inhibition of apoptosis and necrosis via preventing the release of cytochrome c (Gharanei et al. 2013). Mdivi-1 is the indicator used to determine mitochondrial involvement in induced damage by Ip due to inhibition of mitochondrial fragmentation, as Gharanei et al. (2013)'s study found that Mdivi-1 was able to reduce the level of ROS and they found that Mdivi-1 was able to reduce the cytosolic calcium overload thus maintaining the potential of mitochondrial membrane when co-administered with Doxorubincin, this is relavent to the study since Doxorubincin was found to have anticholinergic properties thought to be similar to Ip sugguesting that the exacerbation of the injury was due to anticholinergic properties (Gharanei et al. 2013). mPTP opening is thought to occur during the start of reperfusion which causes further injury of infarction and it leads to loss of myocytes (Abdallah et al. 2011). These conditions, exacerbated by Ip, were attenuated via the administration of Mdivi-1 with results which were demonstrated to be protective in our experimental models by abrogating the infarction that occurred due to I/R untreated control alone. It decreases the Drp1 level linked to maintaining mitochondria integrity thus preventing mitochondrial division (Bordt et al. 2017). Drp1 regulates vital processes in the cell such as programed cell death (apoptosis), necrosis and cell division (mitosis) (Kim et al.

2016). Mdivi-1 off target inhibits complex 1 of mitochondria respiratory chain this prevent GTPase activating of Drp1 via blocking self-assembly Drp1 which means no activation nor localisation from cytosol to mitochondrial surface preventing the activation of the caspase cascade via releasing of cytochrome c seen in the intrinsic apoptosis pathway (Bordt et al. 2017).

The detrimental effects of the mPTP has been a target for treatment since it first appeared to be in various pathological conditions such as neurodegenerative disease or ischaemia injury in brain and heart (Feldmann et al. 2000). mPTP opening occurs as anti-apoptotic proteins Bcl-2, Bcl-X are deactivated or blocked which means pro-apoptotic proteins BAK and BAX are activated leading to opening a channel in the mitochondrial membrane, mPTP, (Halestrap, Clarke and Javadov 2004) releasing cytochrome c which binds to APAF-1 which cleaved caspase-9 (the initiator caspase) which activates the executioner caspases such as caspase-3 to start the breakdown of the cell leading to apoptotic cell death (Pellegrini and Strasser 2013).

In this study Mdivi-1 was found to be protective due to the inhibition of Drp1 and prevention of its mechanism of action, so it may restrict the opening of mPTP. Since Drp1 activation triggers mitochondrial fragmentation resulted in mitochondrial depolarization leading to the activation of pro –apoptotic protein BAX which open mPTP (Filichia et al. 2016). Hence inhibiting Drp1 will have the opposite effect and prevent the opening of mPTP, however, this action appeared not to be direct indicating that there might be activation or inhibition processes involved in mPTP opening as a result of Drp1 activation (Ishikita et al. 2016, Kim et al. 2016). Ip potentially causes Drp1 phosphorylation to increase and this

action leads to mitochondrial fission, this supports the previous studies that the toxicity induced involves the mitochondria. However, despite this thesis, the mechanism of Ip phosphorylating/activating Drp1 is still not fully characterised.

6.1.2 KN-93 Mechanism Of Protection

According to the findings of this study, KN-93 showed cardio-protective abilities via the reduction of infarction size seen in Figure 5.4 in chapter 5 and caspase-3 activity (Figure 5.8) with significant difference compared with the controls. The injury induced by Ip was attenuated via the co-administration of KN-93 in the Ischaemia/Reperfusion groups as well as in Hypoxia/Re-oxygenation stimulated conditions. KN-93 was chosen as an indicator for Ca^{2+} involvement, it was found that high levels of Ca^{2+} initiated opening of the mPTP (Navaneetha Krishnan, Rosales and Lee 2020). Since calcium overload is one of the determining events in the mPTP opening process (Halestrap 2006), apoptosis occurred due to mPTP opening as a result of high concentrations of Ca^{2+} signaling as well high levels of cytoplasmic Ca^{2+} signaling leading to apoptosis via Ca^{2+} /calmodulin-dependent calcineurin which deactivates Bcl-2 (Chen et al. 2005). During ischaemic conditions the level of Ca^{2+} accumulates and, in acidic conditions, the mPTP remains closed with high levels of ADP and ATP, with the change in the pH increasing at the onset of reperfusion therefore these more alkaline conditions lead to the mPTP opening resulting in mitochondrial swelling (Kim et al. 2016). This is followed by the outer mitochondrial membrane rupture promoting cell

death with apoptosis cell death program or necrosis (Tani and Neely 1989, Yu et al. 2020).

Ip increased the injury in all I/R or H/R models and the injury occurred during and throughout reperfusion via apoptosis as it was established from the results conducted in this study. Ca^{2+} overload simulates intrinsic apoptosis by collapse of the mitochondrial membrane and, specially, low affinity of calcium channels localisation in the outer membrane of mitochondria (White and Reynolds 1995, Palty et al. 2010). Therefore, the action of KN-93 decreases the injury via the inhibition of Ca^{2+} overload via inhibiting CaMKII activities (Chen et al. 2005). In addition, it was found that CaMKII has the ability to phosphorylate Drp1 (Xu et al. 2016).

6.1.3 CaMKII And Drp1 Link

One of the key factors of triggering/initiating intrinsic apoptosis is the phosphorylation of Drp1, leading to cardiomyocyte death in I/R injury (Roe and Qi 2018). Mdivi-1 provides protective mechanisms to cells via inhibiting the phosphorylation and maintaining mitochondria integrity during the stressed conditions.

It was found that CaMKII phosphorylates Drp1 initiatiating mitochondrial fission that results in releasing cytochrome c which triggered intrinsic apoptosis, as observed in this study (Figure 6.1) (Xu et al. 2016). Mitochondria fission also can influence calcium flux within the cells (Steffen and Koehler 2018). Phosphorylated Drp1 translocates to the mitochondria leading to couple GTPase activation to the

surface mitochondria inner membrane space opening voltage dependent anion channel (VDAC) which is a calcium binding site and activates matrix (Ko et al. 2016). Ip was able to activate CaMKII resulting in Ca^{2+} overload and Ip was also able to phosphorylate Drp1 which promoted mitochondrial fission and both actions resulted in the release of cytochrome c and intrinsic apoptosis. Since KN-93 inhibits the activity of CaMKII leading to inhibition of calcium overload as well as preventing the activation of Drp1 and Mdivi-1 inhibits the phosphorylation of Drp1 preventing the mitochondria fission thus stopping apoptosis. This Implies the involvement of calcium overload and mitochondria involvement together in the induced injury in myocardium due to ipratropium administration and, more importantly, the reduction was mainly by inhibiting apoptosis. This is in accordance with previous findings that the majority of injury involves apoptosis, rather than necrosis (Harvey, Hussain and Maddock 2014).

Figure 6.1 illustrate the link between CaMKii and Drp1 in inducing intrinsic apoptosis which is prevented by KN-93 and Mdivi-1

Figure 6. 1: Represent the pathway in which CaMKII activates Drp1 at Serine ($_{616}$) activation site which promote mitochondria fission resulting in mPTP opening releasing cytochrome c and initiating apoptosis (Xu et al. 2016).

6.1.4 Proposed Signalling Pathway

The signalling pathway results showed that the survival pathway of Akt and Erk1/2 levels were increased following the administration of Ip and they were both decreased as a consequence of the co-administration of Mdivi-1 and KN-93.

Although activation of Akt and Erk1/2 is considered to be a protective mechanism against cellular assaults such as ischaemia (Noh et al. 2018). It was found by O'Neill and Abel (2005) and Nagoshi et al. (2005) that the continuation of activation can lead to detrimental effects and potential cellular death (O'Neill and Abel 2005, Nagoshi et al. 2005).

However, Akt and Erk1/2 activation cannot be the determiner to the exacerbation of the injury as it has been previously shown that inhibition of both does not equate to a reduction in cellular death (Harvey, Hussain and Maddock 2014, KKah 2015). It might mean that the cell is trying to overcome the toxicity by keeping on a continuation of activation of the survival pathway. Because other study was made that suggest Akt and Erk1/2 are not the cause of injury (Harvey, Hussain and Maddock 2014). It might be clinically relevant at the human receptor level, as the dosage are made to mimic the drug dosage and concentration effective on human heart (Khan 2015). However, hormonal level takes a place *in vivo* model which was not used or take place in full body system which has an effect entire organism suffering from the diseased states described.

The Erk1/2 delayed activation mechanism which was suggested was due to the idea that the mechanism of action for 15 minutes after reperfusion is not enough for Erk1/2 to be activated. Whereas 30 minutes demonstrated a pattern. The involvement of the Akt and Erk12 are a consequence of Ip administration but not injury related or cause. Again, this is where, although this thesis has demonstrated and provided further information to elucidate the mechanism of Ip mediated injury, there are still many unanswered questions.

6.2 Limitations

The aim of this study was to identify whether mitochondria is involved in Ip causing injury and that KN-93 and Mdivi-1 were able to abrogate the injury that occurs during reperfusion. The study has been successful as it has been to identify that Mdivi-1 and KN93 protect against Ip exacerbated injury in simulation conditions. However, due to time limitation, further studies are to identify and further elucidate the exact mechanism of the caused injury, more experimental methods were needed such as COPD model, systematically the interaction between the drug treatment and the organ in the presence of the disease. One of the primary limitations is not have carried out any experiments *in vivo* models with COPD which was not conducted more experiments needed future, could be done in human tissue from patients with the respective illness as this will provide a clearer picture of the pathway involved without the possibility of differences of the model used. also not been able to do the cardiac work-loop, which is a mimic technique for an intrinsic *in vivo* measurements of heart muscle function in terms of its characteristics and movements as well, for cardiac contractility with reliable measures for the prediction and understanding the change in complex conditions, contractility can be measured *in vitro* via the use of a whole heart or individual cardiac myocytes. (Fletcher et al. 2020).

One primary weakness for this thesis is that the PCR data are inconclusive, according to the data conducted, Dnm1l expression did not show significant difference despite the pattern with the mechanism of action, not to mention 15 minutes after reperfusion might not be enough for the expression. Therefore, we

have to draw the conclusion that it is not involved. We recognised that the data is not complete because PCR machine Q gene were given to the University Hospital of Coventry and Warwickshire during uncertain times. These data are inconclusive due to the COVID-19 pandemic and further exploration will be carried out in the future.

COPD is the third cause of death worldwide as mentioned before (Morgan, Zakeri and Quint 2018). Therefore, more research is needed regarding the disease but given the co-morbidities, this is a broad topic, muscarinic antagonist to fully characterized in disease models especially when considering MI in COPD patients, and healthy individual. Not to mention the limitation of the models used in this study, despite the best effort to ensure they were of clinical relevance. Studies *in vivo* are necessary to see the effect of the rest of the body to the heart during the stimulated condition as the administration of the Ip, Mdivi-1 and KN-93. Monitoring patients with COPD and are suffering from IHD.

6.3 Conclusion

The results of the studies, for the first time, support and fully indicate mitochondria and Ca^{2+} involvement in Ip induced toxicity via Drp1 activation as well as calcium overload in stimulated conditions of I/R and H/R, Moreover, this pathway is related since Ca^{2+} overload is the reason for Drp1 activity, and the intrinsic apoptosis was the main reason for myocytes loss. This gives us clear and strong new evidence for the mechanism of Ip mediated myocardial injury.

In the future this study would help regarding new target drug identification in for new respiratory diseases other than targeting just β-adrenergic and mAChR receptor absence of target action to have therapy junction for COPD patients who are suffering from IHD without causing excercerbation of patients who are to develop an ischaemic event since the injury is exacerbated during reperfusion. The current study suggests in the future the possibility of developing a new beneficial treatment, which avoid the pathways that caused Ip to induce injury such as calcium overload and mitochondria fission. Or the adjunction of therapy to protect against mitochondrial fission e.g. cyclosporine.

Whilst this thesis has provided evidence to help elucidate the pathway in which Ip mechanism of action elicits the damage occurred after I/R, clinically in those suffering from COPD and underlying IHD, it is still of paramount importance that Ip is prescribed with caution to any patient with COPD and that their cardiovascular function and stability is assessed prior to prescription.

References

Abdallah, Y., Kasseckert, S. A., Iraqi, W., Said, M., Shahzad, T., Erdogan, A., Neuhof, C., Gündüz, D., Schlüter, K.D., Tillmanns, H., Piper, H. M., Reusch, H. P., and Ladilov, Y. (2011) 'Interplay between Ca^{2+} cycling and mitochondrial permeability transition pores promotes reperfusion-induced injury of cardiac myocytes'. *Journal of cellular and molecular medicine* [online], 15(11), 2478-2485. available from <https://onlinelibrary.wiley.com/doi/full/10.1111/j.1582-4934.2010.01249.x> [14 November 2019]

Abotaleb, M., Samuel, S. M., Varghese, E., Varghese, S., Kubatka, P., Liskova, A., & Büsselberg, D. (2019) 'Flavonoids in cancer and apoptosis'. *Cancers* [online], 11(1), 28. available from <https://www.mdpi.com/2072-6694/11/1/28/htm> [12 May 2021]

Agarwal, B., Stowe, D.F., Dash, R.K., Bosnjak, Z.J. and Camara, A.K (2014) 'Mitochondrial targets for volatile anesthetics against cardiac ischaemia-reperfusion injury'. *Frontiers in physiology* [online], 5,341. available from <http://journal.frontiersin.org/article/10.3389/fphys.2014.00341/full> [23 April 2017]

Akyea, R. K., Leonardi-Bee, J., Asselbergs, F. W., Patel, R. S., Durrington, P., Wierzbicki, A. S., Ibiwoye, O., Kai, J., Qureshi, N. and Weng, S. F. (2020) 'Predicting major adverse cardiovascular events for secondary prevention: protocol for a systematic review and meta-analysis of risk prediction models'. *BMJ open,* 10(7) [online], e034564. available from <https://bmjopen.bmj.com/content/10/7/e034564.abstract> [05 April 2017]

Al-Rajaibi, H. M. (2008) *The Role of Caspase Inhibitors in Protecting the Myocardium from Ischaemia Reperfusion Injury* [online] Doctoral dissertation. Coventry University. available from <file:///C:/Users/my/Downloads/th_2015-113-3_23430.pdf> [22 July 2017]

Alqahtani, J. S., Oyelade, T., Aldhahir, A. M., Alghamdi, S. M., Almehmadi, M., Alqahtani, A. S., S. Quaderi. S. Manadal. And Hurst, J. R. (2020) 'Prevalence, severity and mortality associated with COPD and smoking in patients with COVID-19: a rapid systematic review and meta-analysis'. *PloS one*, 15(5) [online], e0233147**.** available from <https://journals.plos.org/plosone/article?id=10.1371/journal.pone.0233147> [19 April 2021]

Apel, K. and Hirt, H. (2004) 'Reactive oxygen species: metabolism, oxidative stress, and signal transduction'*. Annu. Rev. Plant Biol* [online], 55,373-399.

available from <http://www.annualreviews.org/doi/abs/10.1146/annurev.arplant.55.031903.141701> [11 April 2017]

Banerjee, C., Khatri, P., Raman, R., Bhatia, H., Datta, M. and Mazumder, S. (2014) 'Role of Calmodulin-Calmodulin Kinase II, cAMP/protein Kinase A and ERK 1/2 on Aeromonas hydrophila-induced Apoptosis of head kidney Macrophages'. *PLoS Pathogens* [online], 10(4), p. e1004018. doi: 10.1371/journal.ppat.1004018. available from <https://journals.plos.org/plospathogens/article?id=10.1371/journal.ppat.1004018> [20 March 2020]

Barnes, P.J. and Stockley, R.A. (2005) 'COPD: current therapeutic interventions and future approaches. European Respiratory Journal [online], 25(6), pp.1084-1106. available from< https://erj.ersjournals.com/content/25/6/1084.short > [Accessed 13 January 2022]

Barreiro, E., Fermoselle, C., Mateu-Jimenez, M., Sánchez-Font, A., Pijuan, L., Gea, J. and Curull, V. (2013) 'Oxidative stress and inflammation in the normal airways and blood of patients with lung cancer and COPD'. *Free radical biology & medicine* [online], 65, 859–71. available from <http://www.ncbi.nlm.nih.gov/pubmed/23954470> [12 July 2017]

Bartlett, J. M., & Stirling, D. (2003) ‘A short history of the polymerase chain reaction’. In *PCR protocols* [online], (pp. 3-6). Humana Press. available from <https://link.springer.com/protocol/10.1385/1-59259-384-4:3> [20 May 2021]

Bass, J. J., Wilkinson, D. J., Rankin, D., Phillips, B. E., Szewczyk, N. J., Smith, K., and Atherton, P. J. (2017) ‘An overview of technical considerations for Western blotting applications to physiological research’. *Scandinavian journal of medicine & science in sports* [online], *27*(1), 4-25. available from<https://onlinelibrary.wiley.com/doi/full/10.1111/sms.12702> [27 May 2021]

Bell, R. M., Mocanu, M. M., & Yellon, D. M. (2011) ‘Retrograde heart perfusion: The Langendorff technique of isolated heart perfusion’. *Journal of molecular and cellular cardiology* [online], *50*(6), 940-950. available from <https://www.sciencedirect.com/science/article/abs/pii/S0022282811000952> [20 May 2021]

Belloc, F., Belaud-Rotureau, M. A., Lavignolle, V., Bascans, E., Braz-Pereira, E., Durrieu, F., & Lacombe, F. (2000) ‘Flow cytometry detection of caspase 3 activation in preapoptotic leukemic cells’. *Cytometry: The Journal of the International Society for Analytical Cytology* [online], *40*(2), 151-160. available from <https://onlinelibrary.wiley.com/doi/full/10.1002/%28SICI%291097-

0320%2820000601%2940%3A2%3C151%3A%3AAID-CYTO9%3E3.0.CO%3B2-9> [27 May 2021]

Berridge, M. J. (1995) ‘Calcium signalling and cell proliferation’. *Bioessays* [online], 17(6), 491-500. available from <https://onlinelibrary.wiley.com/doi/abs/10.1002/bies.950170605 > [15 May 2017]

Bhatt, S.P. and Dransfield, M.T. (2013) 'Chronic obstructive pulmonary disease and cardiovascular disease'. Translational Research [online], 162(4), pp.237-251.available from<https://www.sciencedirect.com/science/article/abs/pii/S1931524413001412> [Accessed 10 January 2022]

Bissinger, R., Bhuyan, A. A. M., Qadri, S. M., & Lang, F. (2019) ‘Oxidative stress, eryptosis and anemia: a pivotal mechanistic nexus in systemic diseases’. *The FEBS journal* [online], *286*(5), 826-854. available from <https://febs.onlinelibrary.wiley.com/doi/full/10.1111/febs.14606 > [03 June 2021]

Bootman, M. D., Collins, T. J., Peppiatt, C. M., Prothero, L. S., MacKenzie, L., De Smet, P., Travers, M., Tovey, S. C., Seo, J. T., Berridge, M. J., Ciccolini, F. and

Lipp, P. (2001) ‘Calcium signalling—an overview’. *In Seminars in cell & developmental biology* [online], (Vol. 12, No. 1, pp. 3-10). Academic Press. available from <https://www.sciencedirect.com/science/article/abs/pii/S1084952100902118> [16 June 2017]

Bordt, E. A., Clerc, P., Roelofs, B. A., Saladino, A. J., Tretter, L., Adam-Vizi, V., Cherok, E., Khali, l A., Yadava, N., Ge, S. X., Francis, T. C., Kennedy, N. W., Picton, L. K., Kumar, T., Uppuluri, S., Miller, A. M, Itoh, K., Karbowski, M., Sesaki, H., Hill, RB. and Polster, B. M. (2017) ‘The putative Drp1 inhibitor mdivi-1 is a reversible mitochondrial complex I inhibitor that modulates reactive oxygen species’. *Developmental cell* [online], 40(6), 583-594.e6. available from <https://www.sciencedirect.com/science/article/pii/S1534580717301168> [23 November 2018]

Boulet, C., Doerig, C. D., and Carvalho, T. G. (2018) ‘Manipulating eryptosis of human red blood cells: a novel antimalarial strategy?’. *Frontiers in cellular and infection microbiology* [online], *8*, 419. available from <https://www.frontiersin.org/articles/10.3389/fcimb.2018.00419/full> [25 May 2021]

Brand, M. D., Orr, A. L., Perevoshchikova, I. V., and Quinlan, C. L. (2013) 'The role of mitochondrial function and cellular bioenergetics in ageing and disease'. *British Journal of Dermatology* [online], *169*, 1-8. available from <https://onlinelibrary.wiley.com/doi/abs/10.1111/bjd.12208> [21 May 2017]

Brentnall, M., Rodriguez-Menocal, L., De Guevara, R., Cepero, E. and Boise, L.H. (2013) 'Caspase-9, caspase-3 and caspase-7 have distinct roles during intrinsic apoptosis'. *BMC Cell Biology* [online], 14(1), p. 32. doi: 10.1186/1471-2121-14-32. available from <https://link.springer.com/article/10.1186/1471-2121-14-32> [25 June 2017]

Brookes, P.S., Yoon, Y., Robotham, J.L., Anders, M.W. and Sheu, S.S. (2004) 'Calcium, ATP, and ROS: a mitochondrial love-hate triangle'. *American Journal of Physiology-Cell Physiology* [online], *287*(4), pp.C817-C833. available from <http://ajpcell.physiology.org/content/287/4/C817.short> [15 July 2017]

Bullard, A. J., Govewalla, P., and Yellon, D. M. (2005) 'Erythropoietin protects the myocardium against reperfusion injury in vitro and in vivo'. *Basic research in cardiology* [online], *100*(5), 397-403. available from <https://link.springer.com/content/pdf/10.1007/s00395-005-0537-4.pdf> [15 June 2017]

Cai, L. L., Xu, H. T., Wang, Q. L., Zhang, Y. Q., Chen, W., Zheng, D. Y., Liu, F., Yuan, H.D., Li, Y. H. and Fu, H. L. (2020) ‘EP4 activation ameliorates liver ischaemia/reperfusion injury via ERK1/2-GSK3β-dependent MPTP inhibition’. *International journal of molecular medicine* [online], *45*(6), 1825-1837. available from <https://www.spandidos-publications.com/10.3892/ijmm.2020.4544> [20 May 2021]

Carden, D. L., and Granger, D. N. (2000) ‘Pathophysiology of ischaemia–reperfusion injury’. *The Journal of pathology* [online], *190*(3), 255-266. available from <https://onlinelibrary.wiley.com/doi/full/10.1002/%28SICI%291096-9896%28200002%29190%3A3%3C255%3A%3AAID-PATH526%3E3.0.CO%3B2-6> [01 June 2021]

Cassambai, S., Mee, C.J., Renshaw, D. and Hussain, A. (2019) ' Tiotropium bromide, a long-acting muscarinic receptor antagonist triggers intracellular calcium signalling in the heart'. Toxicology and applied pharmacology [online], 384, p.114778. available from< https://www.sciencedirect.com/science/article/abs/pii/S0041008X19303862> [Accessed 12 October 2021]

Centers for Disease Control and Prevention (CDC. (2012) ‘Chronic obstructive pulmonary disease among adults--United States, 2011’. *MMWR. Morbidity and*

mortality weekly report [online], 61(46), 938-943. available from <https://pubmed.ncbi.nlm.nih.gov/23169314/> [14 June 2017]

Chen, X., Zhang, X., Kubo, H., Harris, D. M., Mills, G. D., Moyer, J., Berretta, R., Potts, S. T., Marsh, J. D. and Houser, S. R. (2005) 'Ca^{2+} Influx–Induced Sarcoplasmic Reticulum Ca^{2+} Overload Causes Mitochondrial-Dependent Apoptosis in Ventricular Myocytes'. *Circulation research* [online], 97(10), 1009-1017. available from <https://www.ahajournals.org/doi/full/10.1161/01.RES.0000189270.72915.D1> [25 September 2018]

Chinnaswamy, S., Zameer, F., and Muthuchelian, K. (2020) 'Molecular and biological mechanisms of apoptosis and its detection techniques'. *Journal of Oncological Sciences* [online], 6(1), 49-64. available from <http://www.journalofoncology.org/uploads/pdf/450680498503149.pdf> [20 May 2021]

Creativebiomart.net. (2022) Western blot protocol - Creative BioMart. [online] available from<https://www.creativebiomart.net/resource/principle-protocol-Western-blot-protocol-351.htm. available from< https://www.creativebiomart.net/resource/principle-protocol-western-blot-protocol-351.htm> [Accessed 13 January 2022]

Demchenko, A. P. (2013) ‘Beyond annexin V: fluorescence response of cellular membranes to apoptosis’. *Cytotechnology* [online], 65(2), 157-172. available from <https://link.springer.com/article/10.1007%2Fs10616-012-9481-y> [27 May 2021]

Deng, Y., Li, S., Chen, Z., Wang, W., Geng, B. and Cai, J. (2021) ‘Mdivi-1, a mitochondrial fission inhibitor, reduces angiotensin-II-induced hypertension by mediating VSMC phenotypic switch’. Biomedicine & Pharmacotherapy [online],140, p.111689. available from< https://www.sciencedirect.com/science/article/pii/S0753332221004716> [Accessed 14 January 2022]

Deshmukh, K. and Khanna, A. (2021) ‘Implications of Managing Chronic Obstructive Pulmonary Disease in Cardiovascular Diseases’. *Tuberculosis and respiratory diseases* [online], *84*(1), 35–45. available from <https://doi.org/10.4046/trd.2020.0088> [12 May 2021]

Dhalla, N.S., Elmoselhi, A.B., Hata, T. and Makino, N. (2000) ‘Status of myocardial antioxidants in ischaemia–reperfusion injury’. *Review* [online], 47(3), pp. 446–456. doi: 10.1016/S0008-6363(00)00078-X. available from <http://cardiovascres.oxfordjournals.org/content/47/3/446> [7 August 2017]

Disatnik, M.H., Ferreira, J.C., Campos, J.C., Gomes, K.S., Dourado, P.M., Qi, X. and Mochly-Rosen, D. (2013) 'Acute inhibition of excessive mitochondrial fission after myocardial infarction prevents long-term cardiac dysfunction'. Journal of the American Heart Association [online], 2(5), p.e000461. available from<https://www.ahajournals.org/doi/full/10.1161/JAHA.113.000461> [Accessed 17 September 2021]

Doenst, T., Nguyen, T. D. and Abel, E. D. (2013) 'Cardiac metabolism in heart failure: implications beyond ATP production'. *Circulation research* [online], *113*(6), 709-724. available from <https://www.ahajournals.org/doi/full/10.1161/CIRCRESAHA.113.300376> [05 May 2019]

Douglas, D. L. and Baines, C. P. (2014) 'PARP1-mediated necrosis is dependent on parallel JNK and Ca2+/calpain pathways. *Journal of cell science* [online], 127(19), 4134-4145. available from <https://journals.biologists.com/jcs/article/127/19/4134/54550/PARP1-mediated-necrosis-is-dependent-on-parallel> [17 June 2019]

Duan, C., Kuang, L., Xiang, X., Zhang, J., Zhu, Y., Wu, Y., Yan, Q., Liu, L. and Li, T. (2020) 'Drp1 regulates mitochondrial dysfunction and dysregulated metabolism in ischemic injury via Clec16a-, BAX-, and GSH-pathways'. Cell death & disease [online], 11(4), pp.1-19. available

from<https://www.nature.com/articles/s41419-020-2461-9> [Accessed 22 January 2022]

Elnatan, D. and Agard, D. A. (2018) ‘Calcium binding to a remote site can replace magnesium as cofactor for mitochondrial Hsp90 (TRAP1) ATPase activity’. *The Journal of biological chemistry* [online], 293(35), 13717–13724. available from< https://www.ncbi.nlm.nih.gov/pmc/articles/PMC6120219/> [25 May 2021]

Erickson, J.R. (2013) ‘Diabetic hyperglycaemia activates CaMKII and arrhythmias by o-linked glycosylation’. *Nature* [online], 502(7471), pp. 372–376. doi: 10.1038/nature12537. available from <http://www.nature.com/nature/journal/v502/n7471/abs/nature12537.html> [20 July 2017]

Feldmann, G., Haouzi, D., Moreau, A., Durand-Schneider, A.M., Bringuier, A., Berson, A., Mansouri, A., Fau, D. and Pessayre, D., (2000) ‘Opening of the mitochondrial permeability transition pore causes matrix expansion and outer membrane rupture in Fas-mediated hepatic apoptosis in mice’. *Hepatology* [online], 31(3), 674-683. available from <http://onlinelibrary.wiley.com/doi/10.1002/hep.510310318/full> [27 April 2017]

Filichia, E., Hoffer, B., Qi, X. and Luo, Y., (2016) ‘Inhibition of Drp1 mitochondrial translocation provides neural protection in dopaminergic system in a Parkinson’s disease model induced by MPTP’. *Scientific reports*, 6(1), pp.1-13. available from <https://doi.org/10.1038/srep32656 Inhibition of Drp1 mitochondrial translocation provides neural protection in dopaminergic system in a Parkinson’s disease model induced by MPTP | Scientific Reports (nature.com)> [15 December 2021]

Finegold, J.A., Asaria, P. and Francis, D.P. (2013) ‘Mortality from ischaemic heart disease by country, region, and age: statistics from World Health Organisation and United Nations’. *International journal of cardiology* [online], 168(2), pp.934-945. available from<http://www.internationaljournalofcardiology.com/article/S0167-5273 (12)01421-0/abstract> [15 March 2017]

Fletcher, S., Maddock, H., James, R.S., Wallis, R. and Gharanei, M., (2020) ‘The cardiac work-loop technique: An in vitro model for identifying and profiling drug-induced changes in inotropy using rat papillary muscles’. *Scientific reports*, 10(1), pp.1-13. available from<https://doi.org/10.1038/s41598-020-58935-2> [15 December 2021]

Forey, B. A., Thornton, A. J. and Lee, P. N. (2011) ‘Systematic review with meta-analysis of the epidemiological evidence relating smoking to COPD, chronic bronchitis and emphysema’. *BMC pulmonary medicine* [online], 11(1), 1-61.

available from <https://bmcpulmmed.biomedcentral.com/articles/10.1186/1471-2466-11-36> [24 February 2021]

Frasch, M. G., Herry, C. L., Niu, Y., and Giussani, D. A. (2020) 'First evidence that intrinsic fetal heart rate variability exists and is affected by hypoxic pregnancy'. *The Journal of physiology* [online], *598*(2), 249-263. available from <https://physoc.onlinelibrary.wiley.com/doi/full/10.1113/JP278773> [20 May 2021]

Fujiki, K., Inamura, H. and Matsuoka, M. (2013) 'Phosphorylation of FOXO3a by PI3K/Akt pathway in HK-2 renal proximal tubular epithelial cells exposed to cadmium'. *Archives of Toxicology* [online], 87(12), pp. 2119–2127. doi: 10.1007/s00204-013-1077-6. available from <https://link.springer.com/article/10.1007%2Fs00204-013-1077-6> [14 December 2018]

Genelink.com. (2017*). Gene Link - Genetic Tools and Reagents - Introduction.* [Online] available from < http://www.genelink.com/newsite/products/GTRomniarray.asp> [6 April 2018].

Gershon, A.S., Khan, S., Klein-Geltink, J., Wilton, D., To, T., Crighton, E.J., Pigeau, L., MacQuarrie, J., Allard, Y., Russell, S.J. and Henry, D.A. (2014)

‘Asthma and chronic obstructive pulmonary disease (COPD) prevalence and health services use in Ontario Métis: A population-based cohort study’. *PLoS ONE* [online], 9(4), p. e95899. available from http://journals.plos.org/plosone/article?id=10.1371/journal.pone.0095899 [28 February 2018]

Gharanei, M., Hussain, A., Janneh, O., and Maddock, H. (2013) ‘Attenuation of doxorubicin-induced cardiotoxicity by mdivi-1: a mitochondrial division/mitophagy inhibitor’. *PloS one* [online], 8(10), e77713. available from <https://journals.plos.org/plosone/article?id=10.1371/journal.pone.0077713> [17 July 2019]

Gibbons, J. (2014) ‘Western blot: Protein transfer overview’. *North American journal of medical sciences* [online], *6*(3), 158–159. available from <https://www.ncbi.nlm.nih.gov/pmc/articles/PMC3978941/> [27 May 2021]

Giulietti, A., Overbergh, L., Valckx, D., Decallonne, B., Bouillon, R., and Mathieu, C. (2001) ‘An overview of real-time quantitative PCR: applications to quantify cytokine gene expression’. *Methods* [online], *25*(4), 386-401. available from <https://www.sciencedirect.com/science/article/abs/pii/S1046202301912617> [20 May 2021]

Griffo, R., Spanevello, A., Temporelli, P. L., Faggiano, P., Carone, M., Magni, G., Ambrosino, N. and Tavazzi, L. (2017) 'Frequent coexistence of chronic heart failure and chronic obstructive pulmonary disease in respiratory and cardiac outpatients: Evidence from SUSPIRIUM, a multicentre Italian survey'. *European journal of preventive cardiology* [online], *24*(6), 567-576. available from <https://academic.oup.com/eurjpc/article/24/6/567/5926789?login=true> [15 December 2019]

Guo, C., Zeng, X., Song, J., Zhang, M., Wang, H., Xu, X., Du, F. and Chen, B. (2012) 'A soluble receptor for advanced Glycation end-products inhibits Hypoxia/Reoxygenation-Induced Apoptosis in rat Cardiomyocytes via the Mitochondrial pathway'. *International Journal of Molecular Sciences* [online], 13(9), pp. 11923–11940. doi: 10.3390/ijms130911923. available from <https://www.mdpi.com/1422-0067/13/9/11923> [24 May 2020]

Halestrap, A.P. and Richardson, A.P. (2015) 'The mitochondrial permeability transition: a current perspective on its identity and role in ischaemia/reperfusion injury'. *Journal of molecular and cellular cardiology* [online], *78*, pp.129-141. available from <http://www.jmmc-online.com/article/S0022-2828(14)00265-X/pdf> [15 July 2017]

Halestrap, A.P. and Pasdois, P. (2009) ‘the role of the mitochondrial permeability transition pore in heart disease’. *Biochimica et Biophysica Acta (BBA)-Bioenergetics* [online], 1787(11), 1402-1415. available from <http://www.sciencedirect.com/science/article/pii/S0005272809000073> [19 April 2017]

Halestrap, A. P. (2006) ‘Calcium, mitochondria and reperfusion injury: a pore way to die’. *Biochemical Society Transactions* [online], 34(2), 232-237. available from <https://portlandpress.com/biochemsoctrans/article-abstract/34/2/232/63714/Calcium-mitochondria-and-reperfusion-injury-a-pore> [28 July 2017]

Halestrap, A. P., Clarke, S. J. and Javadov, S. A. (2004) ‘Mitochondrial permeability transition pore opening during myocardial reperfusion—a target for cardioprotection’. *Cardiovascular research* [online], *61*(3), 372-385. available from <https://academic.oup.com/cardiovascres/article/61/3/372/401383?login=true> [24 May 2018]

Harvey, K.L., Hussain, A. and Maddock, H.L. (2014) ‘Ipratropium bromide-mediated myocardial injury in in vitro models of myocardial ischaemia/reperfusion’. *Toxicological Sciences* [online], 138(2), 457-467. available from <https://toxsci.oxfordjournals.org/content/138/2/457.full> [12 April 2017]

Hausenloy, D.J. and Yellon, D.M. (2013) ‘Myocardial ischaemia-reperfusion injury: A neglected therapeutic target’. *The Journal of Clinical Investigation* [online], 123(1), pp. 100–92. doi: 10.1172/JCI62874. available from <http://www.jci.org/articles/view/62874?utm_campaign=impact_2013_january&utm_content=short_url&utm_medium=pdf&utm_source=impact> [21 December 2019]

Hausenloy, D. J. and Yellon, D. M. (2007) 'Reperfusion injury salvage kinase signalling: Taking a RISK for cardio protection'. *Heart Failure Reviews* [online], 12 (3-4), 217–234. available from <http://link.springer.com/article/10.1007/s10741-007-9026-1> [12 April 2017]

Hausenloy, D.J., Maddock, H.L., Baxter, G.F. and Yellon, D.M. (2002) ‘Inhibiting mitochondrial permeability transition pore opening: a new paradigm for myocardial preconditioning?’. *Cardiovascular research* [online], 55(3),534-543. available from <https://cardiovascres.oxfordjournals.org/content/55/3/534> [12 April 2017]

Hayes, M. J., Rescher, U., Gerke, V., and Moss, S. E. (2004) ‘Annexin–actin interactions’. *Traffic* [online], *5*(8), 571-576. available from

<https://onlinelibrary.wiley.com/doi/full/10.1111/j.1600-0854.2004.00210.x> [27 May 2021]

He, Z., Chen, Y., Chen, P., Wu, G. and Cai, S. (2010) 'Local inflammation occurs before systemic inflammation in patients with COPD'. *Respirology* [online], *15*(3), 478-484. available from https://onlinelibrary.wiley.com/doi/full/10.1111/j.1440-1843.2010.01709.x?casa_token=x9hxhxkk1qkAAAAA%3Az1G_JmCkbpneZG5wZ1zuXIiBsAPbHd_6jzc5PUzxV9Tlzw-0Vd8YysY8sQBKx2X_QjutpSgZ1ROm3xo [20 May 2020]

Hegde, U., Filie, A., Little, R. F., Janik, J. E., Grant, N., Steinberg, S. M., Dunleavy, K., Jaffe, E. S., Abati, A., Stetler-Stevenson, M. and Wilson, W. H. (2005) 'High incidence of occult leptomeningeal disease detected by flow cytometry in newly diagnosed aggressive B-cell lymphomas at risk for central nervous system involvement: the role of flow cytometry versus cytology'. *Blood* [online],*105*(2), 496-502. available from <https://ashpublications.org/blood/article/105/2/496/20072> [20 May 2021]

Hegyi, B., Chen-Izu, Y., Jian, Z., Shimkunas, R., Izu, L.T. and Banyasz, T. (2015) 'KN-93 inhibits I Kr in mammalian cardiomyocytes'. *Journal of molecular and cellular cardiology* [online], *89*, pp.173-176. available from

<http://www.sciencedirect.com/science/article/pii/S0022282815300833> [20 July 2017]

Helle, S. C., Kanfer, G., Kolar, K., Lang, A., Michel, A. H., and Kornmann, B. (2013) 'Organization and function of membrane contact sites'. *Biochimica et Biophysica Acta (BBA)-Molecular Cell Research* [online], *1833*(11), 2526-2541. available from <https://www.sciencedirect.com/science/article/pii/S0167488913000438> [25 May 2021]

Hnasko, T. S., and Hnasko, R. M. (2015) 'The western blot'. In *ELISA* [online], (pp. 87-96). Humana Press, New York, NY. available from <https://link.springer.com/protocol/10.1007/978-1-4939-2742-5_9> [20 May 2021]

Hou, W., Zhang, Q., Yan, Z., Chen, R., Zeh Iii, H.J., Kang, R., Lotze, M.T. and Tang, D. (2013) 'Strange attractors: DAMPs and autophagy link tumor cell death and immunity'. *Cell death & disease* [online], *4*(12), pp.e966-e966. available from <https://www.nature.com/articles/cddis2013493> [25 May 2021]

Hong, S. H., and Choi, Y. H. (2012) 'Bufalin induces apoptosis through activation of both the intrinsic and extrinsic pathways in human bladder cancer

cells'. *Oncology reports* [online], *27*(1), 114-120. available from <https://www.spandidos-publications.com/10.3892/or.2011.1451> [27 May 2021]

Hu, C., Huang, Y. and Li, L. (2017) 'Drp1-dependent mitochondrial fission plays critical roles in physiological and pathological progresses in mammals'. *International journal of molecular sciences* [online], *18*(1), 144. available from <https://www.mdpi.com/1422-0067/18/1/144> [09 March 2021]

Hu, W. P., Lhamo, T., Zhang, F. Y., Hang, J. Q., Zuo, Y. H., Hua, J. L., Li, S. Q., and Zhang, J. (2020) 'Predictors of acute cardiovascular events following acute exacerbation period for patients with COPD: a nested case–control study'. *BMC cardiovascular disorders* [online], 20(1), 1-10. available from <https://link.springer.com/article/10.1186/s12872-020-01803-8> [20 April 2021]

Huang, X., Qin, J. and Lu, S., (2014) 'Magnesium isoglycyrrhizinate protects hepatic L02 cells from ischaemia/reperfusion induced injury'. *Int J Clin Exp Pathol* [online], *7*(8), p.4755 available from <https://www.ncbi.nlm.nih.gov/pmc/articles/PMC4152036/> [14 November 2018]

Humeau, J., Bravo-San Pedro, J.M., Vitale, I., Nuñez, L., Villalobos, C., Kroemer, G. and Senovilla, L. (2018) 'Calcium signaling and cell cycle: progression or death'. Cell calcium[online], 70, pp.3-15. available

from<https://www.sciencedirect.com/science/article/abs/pii/S0143416017300611> [Accessed 02 February 2022]

Ichim, G. and Tait, S. W. (2016) ‘A fate worse than death: apoptosis as an oncogenic process’. *Nature Reviews Cancer* [online], 16(8), 539. available from <https://www.nature.com/articles/nrc.2016.58> [15 May 2019]

Ip, Y.T. and Davis, R.J. (1998) ‘Signal transduction by the c-Jun N-terminal kinase (JNK)—from inflammation to development’. Current opinion in cell biology [online], 10(2), pp.205-219. available from<https://www.sciencedirect.com/science/article/abs/pii/S0955067498801439> [Accessed 30 January 2022]

Intachai, K., C Chattipakorn, S., Chattipakorn, N. and Shinlapawittayatorn, K. (2018) 'Revisiting the cardioprotective effects of acetylcholine receptor activation against myocardial ischemia/reperfusion injury'. International journal of molecular sciences [online], 19(9), p.2466. available from<https://www.mdpi.com/1422-0067/19/9/2466> [Accessed 10 December 2021]

Irvin-Sellers, M.J. and White, J. (2015) ‘Tiotropium versus ipratropium bromide for chronic obstructive pulmonary disease’. *Cochrane Database of Systematic Reviews* [online], doi: 10.1002/14651858.cd009552.pub3. available from

<https://www.cochranelibrary.com/cdsr/doi/10.1002/14651858.CD009552.pub2/full> [22 March 2017]

Ishikita, A., Matoba, T., Ikeda, G., Koga, J. I., Mao, Y., Nakano, K.,Takeuchi, O., Sadoshima, J. and Egashira, K. (2016) 'Nanoparticle-mediated delivery of mitochondrial division inhibitor 1 to the myocardium protects the heart from ischaemia-reperfusion injury through inhibition of mitochondria outer membrane permeabilization: a new therapeutic modality for acute myocardial infarction'. *Journal of the American Heart Association* [online], *5*(7), e003872. available from <https://www.ahajournals.org/doi/full/10.1161/JAHA.116.003872> [10 May 2018]

Jiang, M., Li, J., Peng, Q., Liu, Y., Liu, W., Luo, C., Peng, J., Li, J., Yung, K. K. L. and Mo, Z. (2014) 'Neuroprotective effects of bilobalide on cerebral ischaemia and reperfusion injury are associated with inhibition of pro-inflammatory mediator production and down-regulation of JNK1/2 and p38 MAPK activation'. *Journal of neuroinflammation* [online], 11(1), 167. available from <https://jneuroinflammation.biomedcentral.com/articles/10.1186/s12974-014-0167-6> [11 May 2017]

Jin, C. and Reed, J.C. (2002) 'Yeast and apoptosis'. *Nature Reviews Molecular Cell Biology* [online], 3(6), 453-459. available from <http://www.nature.com/nrm/journal/v3/n6/abs/nrm832.html> [29 April 2017]

Kalogeris, T., Baines, C. P., Krenz, M. and Korthuis, R. J. (2012) ‘Cell biology of ischaemia/reperfusion injury’. *International review of cell and molecular biology* [online], *298*, 229-317. available from <https://www.sciencedirect.com/science/article/pii/B9780123943095000067> [21 August 2019]

Keung, W., Boheler, K.R. and Li, R.A. (2014) ‘Developmental cues for the maturation of metabolic, electrophysiological and calcium handling properties of human pluripotent stem cell-derived cardiomyocytes’. *Stem Cell Research & Therapy* [online], 5(1), p. 17. doi: 10.1186/scrt406. available from <https://link.springer.com/article/10.1186/scrt406> [22 June 2017]

Khan, J. (2015) *Investigation into the effects of specific muscarinic acetylcholine receptor antagonists on the myocardium in pre-clinical conditions of ischaemia reperfusion injury and oxidative stress model*. (Doctoral dissertation, Coventry University). available from <http://ethos.bl.uk/OrderDetails.do?uin=uk.bl.ethos.681419> [23 August 2017]

Kiefer, E., Heller, W. and Ernst, D. (2000) 'A simple and efficient protocol for isolation of functional RNA from plant tissues rich in secondary metabolites'. Plant Molecular Biology Reporter [online], 18(1), pp.33-39. available

from<https://link.springer.com/article/10.1007/BF02825291> [Accessed 09 January 2022]

Kim, H., Lee, J. Y., Park, K. J., Kim, W. H. and Roh, G. S. (2016) ‘A mitochondrial division inhibitor, Mdivi-1, inhibits mitochondrial fragmentation and attenuates kainic acid-induced hippocampal cell death’. *BMC neuroscience* [online], 17(1), 1-10. available from <https://link.springer.com/article/10.1186/s12868-016-0270-y> [22 February 2020]

Kim, B. (2017) ‘Western blot techniques. In *Molecular Profiling* [online], (pp. 133-139). Humana Press, New York, NY. available from <https://link.springer.com/protocol/10.1007/978-1-4939-6990-6_9> [20 May 2021]

Kim, Ji-Eun, and Tae-Cheon Kang (2018) 'Differential roles of mitochondrial translocation of active caspase-3 and HMGB1 in neuronal death induced by status epilepticus'. Frontiers in cellular neuroscience [online], 12: 301. available from<https://www.frontiersin.org/articles/10.3389/fncel.2018.00301/full> [Accessed 13 January 2022]

Kitazawa, T., Asakawa, K., Nakamura, T., Teraoka, H., Unno, T., Komori, S.I., Yamada, M. and Wess, J. (2009) 'M3 muscarinic receptors mediate positive

inotropic responses in mouse atria: a study with muscarinic receptor knockout mice'. Journal of Pharmacology and Experimental Therapeutics [online], 330(2), pp.487-493. available from<https://jpet.aspetjournals.org/content/330/2/487.short?casa_token=pz4igP4p-2cAAAAA:EPmeVgiNZsx9VH12t_jEhNCfqcQq2DrXbMxJQ0_CqhsrI9ZCxXOQnkVKlwN7HnjTTHOlBe_FHRwf> [Accessed 10 October 2021]

Ko, A. R., Hyun, H. W., Min, S. J. and Kim, J. E. (2016) ‘The Differential DRP1 Phosphorylation and Mitochondrial Dynamics in the Regional Specific Astroglial Death Induced by Status Epilepticus’. *Frontiers in cellular neuroscience* [online], *10*, 124. https://doi.org/10.3389/fncel.2016.00124 PMID: 27242436; PMCID: PMC4870264. available from <https://www.frontiersin.org/articles/10.3389/fncel.2016.00124/full> [20 May 2021]

Koch, M. B., Davidsen, M., Andersen, L. V., Juel, K. and Jensen, G. B. (2015) ‘Increasing prevalence despite decreasing incidence of ischaemic heart disease and myocardial infarction’. A national register based perspective in Denmark, 1980–2009. *European journal of preventive cardiology* [online], 22(2), 189-195. available from <https://journals.sagepub.com/doi/abs/10.1177/2047487313509495> [11 June 2019]

Kohajda, Z., Loewe, A., Tóth, N., Varró, A. and Nagy, N. (2020) ‘The Cardiac Pacemaker Story—Fundamental Role of the Na+/Ca2+ Exchanger in Spontaneous Automaticity’. *Frontiers in pharmacology* [online], *11*. available from <https://www.ncbi.nlm.nih.gov/pmc/articles/PMC7199655/> [11 June 2021]

La Marca, J. E. and Richardson, H. E. (2020) ‘Two-faced: roles of JNK signalling during tumourigenesis in the Drosophila model’. *Frontiers in cell and developmental biology* [online], *8*, 42. available from <https://www.frontiersin.org/articles/10.3389/fcell.2020.00042/full> [20 May 2021]

Lan, X., Zhang, X., Zhou, G. P., Wu, C. X., Li, C. and Xu, X. H. (2017) ‘Electroacupuncture reduces apoptotic index and inhibits p38 mitogen-activated protein kinase signaling pathway in the hippocampus of rats with cerebral ischaemia/reperfusion injury’. *Neural regeneration research* [online], *12*(3), 409–416. available from <https://www.ncbi.nlm.nih.gov/pmc/articles/PMC5399718/> [20 May 2021]

Lab test online (2021) *flow cytometry* [online] available from <https://labtestsonline.org/flow-cytometry> [20 May 2021]

Li, Q., Huai, L., Zhang, C., Wang, C., Jia, Y., Chen, Y., Yu, P., Wang, H., Rao, Q., Wang, M. and Wang, J. (2013) 'Icaritin induces AML cell apoptosis via the MAPK/ERK and PI3K/AKT signal pathways'. *International Journal of Hematology* [online], 97(5), pp. 617–623. doi: 10.1007/s12185-013-1317-9. available from <https://link.springer.com/article/10.1007/s12185-013-1317-9> [28 January 2021]

Li, W., Sun, K., Hu, F., Chen, L., Zhang, X., Wang, F. and Yan, B. (2021) 'Protective effects of natural compounds against oxidative stress in ischemic diseases and cancers via activating the Nrf2 signaling pathway: A mini review'. *Journal of Biochemical and Molecular Toxicology* [online], *35*(3), e22658. available from <https://onlinelibrary.wiley.com/doi/full/10.1002/jbt.22658> [18 May 2021]

Li, X., Wei, R., Wang, M., Ma, L., Zhang, Z., Chen, L., Guo, Q., Guo, S., Zhu, S., Zhang, S. and Min, L. (2020) 'MGP Promotes Colon Cancer Proliferation by Activating the NF-κB Pathway through Upregulation of the Calcium Signaling Pathway'. *Molecular Therapy-Oncolytics* [online], *17*, 371-383. available from < https://www.sciencedirect.com/science/article/pii/S2372770520300553> [03 June 2021]

Li, X., Luo, R., Jiang, R., Meng, X., Wu, X., Zhang, S. and Hua, W. (2013) 'The role of the Hsp90/Akt pathway in myocardial calpain-induced caspase-3

activation and apoptosis during sepsis'. *BMC Cardiovascular Disorders* [online], 13(1). doi: 10.1186/1471-2261-13-8. available from <http://bmccardiovascdisord.biomedcentral.com/articles/10.1186/1471-2261-13-8> [11 June 2018]

Liang, K., Ye, Y., Wang, Y., Zhang, J. and Li, C. (2014) 'Formononetin mediates neuroprotection against cerebral ischaemia/reperfusion in rats via downregulation of the Bax/Bcl-2 ratio and upregulation PI3K/Akt signaling pathway'. *Journal of the Neurological Sciences* [online], 344(s 1–2), pp. 100–104. doi: 10.1016/j.jns.2014.06.033. available from <https://www.sciencedirect.com/science/article/abs/pii/S0022510X14004031> [12 June 2021]

Lippe, G., Coluccino, G., Zancani, M., Baratta, W. and Crusiz, P. (2019) 'Mitochondrial F-ATP synthase and its transition into an energy-dissipating molecular machine'. *Oxidative medicine and cellular longevity* [online], *2019.* available from <https://www.hindawi.com/journals/omcl/2019/8743257/> [29 July 2020]

Liu, M. M., Shen, Y. F., Chen, C., Lai, X. Y., Zhang, M. Y. and Yu, R (2016) 'Protective effect of glucagon-like peptide-1 analogue on cardiomyocytes injury induced by hypoxia/reoxygenation'. *Zhonghua nei ke za zhi* [online], 55(4), pp.

311–316. doi: 10.3760/cma.j.issn.0578-1426.2016.04.013. available from <http://europepmc.org/abstract/med/27030622> [20 July 2019]

Liu, Y. J., McIntyre, R. L., Janssens, G. E. and Houtkooper, R. H. (2020) ‘Mitochondrial fission and fusion: A dynamic role in aging and potential target for age-related disease’. *Mechanisms of ageing and development* [online], 186, 111212. available from <https://doi.org/10.1016/j.mad.2020.111212> [14 May 2021]

Lu, Y. Y., Chen, T. S., Qu, J. L., Pan, W. L., Sun, L. and Wei, X. B. (2009) ‘Dihydroartemisinin (DHA) induces caspase-3-dependent apoptosis in human lung adenocarcinoma ASTC-a-1 cells’. *Journal of biomedical science* [online], 16(1), 1-15. available from <https://jbiomedsci.biomedcentral.com/articles/10.1186/1423-0127-16-16> [27 May 2021]

Luna-Ortiz, P., Torres, J. C., Pastelin, G. and Martínez-Rosas, M. (2011) ‘Myocardial postconditioning: anaesthetic considerations’. *Arch Cardiol Mex* [online], 81(1), 33-46. available from <https://www.researchgate.net/profile/Martin-Martinez-5/publication/262718405_Posacondicionamiento_miocardico_consideraciones_

anestesicas/links/56ec19b908aed740cbb61193/Posacondicionamiento-miocardico-consideraciones-anestesicas.pdf> [25 May 2021]

Luo, C., Yang, Q., Liu, Y., Zhou, S., Jiang, J., Reiter, R.J., Bhattacharya, P., Cui, Y., Yang, H., Ma, H. and Yao, J. (2019) 'The multiple protective roles and molecular mechanisms of melatonin and its precursor N-acetylserotonin in targeting brain injury and liver damage and in maintaining bone health'. *Free Radical Biology and Medicine* [online], 130, pp.215-233. available from <https://www.sciencedirect.com/science/article/abs/pii/S0891584918309481> [20 March 2020]

lwyd, O. (2016) *The involvement of CaMKII in myocardial ischaemia-reperfusion injury* [online] Doctoral dissertation. Cardiff University. available from< http://orca.cf.ac.uk/43619/> [7 August 2017]

Maddock, H.L., Mocanu, M.M. and Yellon, D.M. (2002) 'Adenosine A 3 Receptor Activation Protects the Myocardium from Reperfusion/reoxygenation Injury.' *American Journal of Physiology - Heart and Circulatory Physiology* [online], 283 (4), H1307–H1313. available from <http://ajpheart.physiology.org/content/283/4/H1307.short> [29 April 2017]

Mäkelä, M.J., Backer, V., Hedegaard, M. and Larsson, K. (2016) ‘Adherence to inhaled therapies, health outcomes and costs in patients with asthma and COPD’. *Respiratory Medicine* [online], 107(10),. 1481–1490. available from< https://www.sciencedirect.com/science/article/pii/S0954611113001340> [16 July 2017]

Managò, A. (2016) *Mitochondrial potassium homeostasis and its relevance in pathophysiological contexts* [online] Doctoral dissertation. Università degli Studi di Padova. available from <http://paduaresearch.cab.unipd.it/9403/1/manago_antonella_tesi.pdf> [25 May 2021]

Maneechote, C., Palee, S., Kerdphoo, S., Jaiwongkam, T., Chattipakorn, S.C. and Chattipakorn, N. (2018) ‘Differential temporal inhibition of mitochondrial fission by Mdivi-1 exerts effective cardioprotection in cardiac ischemia/reperfusion injury’. Clinical Science [online], 132(15), pp.1669-1683. available from< https://portlandpress.com/clinsci/article-abstract/132/15/1669/71795/Differential-temporal-inhibition-of-mitochondrial> [Accessed 13 November 2021]

Maneechote, C., Palee, S., Kerdphoo, S., Jaiwongkam, T., Chattipakorn, S.C. and Chattipakorn, N. (2021) 'Modulating mitochondrial dynamics attenuates cardiac ischemia-reperfusion injury in prediabetic rats'. Acta Pharmacologica

Sinica [online], pp.1-13. available from<https://www.nature.com/articles/s41401-021-00626-3> [Accessed 13 January 2022]

Mannella C. A. (2020) ‘Consequences of Folding the Mitochondrial Inner Membrane’. *Frontiers in physiology* [online], *11*, 536. available from <https://doi.org/10.3389/fphys.2020.00536> [22 March 2021]

Mao, J., Lv, Z. and Zhuang, Y. (2014) ‘MicroRNA-23a is involved in tumor necrosis factor-α induced apoptosis in mesenchymal stem cells and myocardial infarction’. *Experimental and molecular pathology* [online], 97(1), 23-30. available from <http://www.sciencedirect.com/science/article/pii/S0014480013001391> [18 April 2018]

McKinnon K. M. (2018) ‘Flow Cytometry: An Overview’. *Current protocols in immunology* [online], 120(1), 5-1. available from <https://doi.org/10.1002/cpim.40> [23 April 2021]

Michele, T.M., Pinheiro, S. and Iyasu, S. (2010) ‘The safety of tiotropium—the FDA's conclusions. *New England Journal of Medicine* [online], 363(12), 1097-1099. available from <http://www.nejm.org/doi/full/10.1056/NEJMp1008502> [22 March 2020]

Miller, M. A. and Zachary, J. F. (2017) ‘Mechanisms and Morphology of Cellular Injury, Adaptation, and Death’. *Pathologic Basis of Veterinary Disease* [online], 2–43. e19. available from <https://doi.org/10.1016/B978-0-323-35775-3.00001-1> [10 March 2018]

Morgan, A. D., Zakeri, R. and Quint, J. K. (2018) ‘Defining the relationship between COPD and CVD: what are the implications for clinical practice?’. *Therapeutic advances in respiratory disease* [online], *12*, 1753465817750524. available from <https://journals.sagepub.com/doi/full/10.1177/1753465817750524> [19 April 2021]

Murata, M., Akao, M., O’Rourke, B. and Marbán, E. (2001) ‘Mitochondrial ATP-sensitive potassium channels attenuate matrix Ca^{2+} overload during simulated ischaemia and reperfusion: possible mechanism of cardio protection’. *Circulation research* [online], 89(10), 891-898. available from <https://www.ahajournals.org/doi/full/10.1161/hh2201.100205> [17 March 2017]

Nagoshi, T., Matsui, T., Aoyama, T., Leri, A., Anversa, P., Li, L., Ogawa, W., Monte, F. D., Gwathmey, J. K., Grazette, L., Hemmings, B., Kass, D. A., Champion, H. C. and Rosenzweig, A. (2005) ‘PI3K rescues the detrimental

effects of chronic Akt activation in the heart during ischaemia/reperfusion injury'. *The Journal of clinical investigation* [online], 115(8), 2128-2138. available from <https://www.jci.org/articles/view/23073> [02 February 2017]

NavaneethaKrishnan, S., Rosales, J. L. and Lee, K. Y. (2020) 'mPTP opening caused by Cdk5 loss is due to increased mitochondrial Ca^{2+} uptake'. *Oncogene* [online], 39(13), 2797-2806. available from <https://www.nature.com/articles/s41388-020-1188-5> [11 June 2021]

Noh, Y., Cheon, S., Kim, I. H., Kim, I., Lee, S. A., Kim, D. H. and Jeong, Y. (2018) 'The protective effects of ethanolic extract of Clematis terniflora against corticosterone-induced neuronal damage via the AKT and ERK1/2 pathway'. *BMB reports* [online], 51(8), 400. available from <https://www.ncbi.nlm.nih.gov/pmc/articles/PMC6130826/> [05 August 2019]

Oates, J.A., Wood, A.J.J. and Gross, N.J. (1988) 'Ipratropium Bromide'. *New England Journal of Medicine* [online], 319(8), pp. 486–494. doi: 10.1056/nejm198808253190806. available from <http://www.nejm.org/doi/pdf/10.1056/NEJM198808253190806> [22 July 2018]

Oddone, N., Boury, F., Garcion, E., Grabrucker, A.M., Martinez, M.C., Da Ros, F., Janaszewska, A., Forni, F., Vandelli, M.A., Tosi, G. and Ruozi, B. (2020) 'Synthesis, characterization, and in vitro studies of an reactive oxygen species

(ROS)-responsive methoxy polyethylene glycol-thioketal-melphalan prodrug for glioblastoma treatment'. *Frontiers in Pharmacology* [online], *11*, p.574. available from <https://www.frontiersin.org/articles/10.3389/fphar.2020.00574/full?report=reader> [17 May 2021]

Ogale, S., Lee, T., Au, D., Boudreau, D. and Sullivan, S. (2009) 'Cardiovascular events associated with ipratropium bromide in COPD'. *Chest* [online], 137(1), pp. 13–9. available from <http://www.ncbi.nlm.nih.gov/pubmed/19363211> [15 April 2021]

O'Neill, B. T. and Abel, E. D. (2005) 'Akt1 in the cardiovascular system: friend or foe?'. *The Journal of clinical investigation* [online], 115(8), 2059-2064. available from <https://www.jci.org/articles/view/25900> [12 March 2017]

Ong, S. B., Hall, A. R., Dongworth, R. K., Kalkhoran, S., Pyakurel, A., Scorrano, L. and Hausenloy, D. J. (2015) 'Akt protects the heart against ischaemia-reperfusion injury by modulating mitochondrial morphology'. *Thrombosis and haemostasis* [online], 113(3).513-521. available from <https://d1wqtxts1xzle7.cloudfront.net/35677401/th_2014-112-20140925_23430_3.pdf?1416617074=&response-content-disposition=inline%3B+filename%3DAkt_protects_the_heart_against_ischaemia.pdf&Expires=1623607601&Signature=aqZ5Zq98Cd4L-

Axg7whBxrIkOYc50FknmTeL2Y95LEyV~mE~TWnOOL62dWyOkPRSbVrIwS7
3T52IMpT~Gk~L9gtbJQPuH1zS6EvFYvGeD3JVEl5S7PpsxWAPbkKki89Xzqjsf
0HlsGtrAEObHWfFvuLsIfQog74Gk8WgiMXCvM7jtRmSTJ1VppDZYFTxRTnvh
Q9xXyx2kkZjhH2KuP4GKrK2Z0gVjcZ7VThOMU3KDyi5K0z5kCPBzrvf2HMD8
MlnBSHQgd1XH-
2NcKyUxob5HUS2Q6IsUQopH6saBPdYd2BDJ21Li64vVuxVB88p~IRJe9QR7w
omXpRIket5objUEA__&Key-Pair-Id=APKAJLOHF5GGSLRBV4ZA> [16 April
2017]

Onishi, K. (2017) 'Total management of chronic obstructive pulmonary disease (COPD) as an independent risk factor for cardiovascular disease'. *Journal of cardiology* [online], 70(2), 128-134. available from < https://www.sciencedirect.com/science/article/pii/S0914508717300552> [15 November 2019]

Ottolia, M., Torres, N., Bridge, J. H., Philipson, K. D. and Goldhaber, J. I. (2013) 'Na/Ca exchange and contraction of the heart'. *Journal of molecular and cellular cardiology* [online], 61, 28–33. available from <https://doi.org/10.1016/j.yjmcc.2013.06.001> [17 November 2019]

Pacher, P. and Hajnóczky, G. (2001) 'Propagation of the apoptotic signal by mitochondrial waves . *The EMBO journal* [online], *20*(15), 4107-4121. available

from <https://www.embopress.org/doi/full/10.1093/emboj/20.15.4107> [21 November 2018]

Patanè, S. (2015) ‘Regulator of G-protein signaling 2 (RGS2) in cardiology and oncology’. *International journal of cardiology* [online], *179*, pp.63-65. available from <http://www.internationaljournalofcardiology.com/article/S0167-5273(14)020257/pdf> [07 April 2018]

Patton, W. F. (2002) ‘Detection technologies in proteome analysis’. *Journal of Chromatography* [online], *B*, *771*(1-2), 3-31. available from <https://www.sciencedirect.com/science/article/abs/pii/S1570023202000430> [27 May 2021]

Pellegrini, M. and Strasser, A. (2013) ‘Caspases, Bcl-2 family proteins and other components of the death machinery: their role in the regulation of the immune response’. *In Madame Curie Bioscience Database* [online], Landes Bioscience. available from <https://www.sciencedirect.com/science/article/pii/S0914508717300552> [13 May 2019]

Pfeffer, C. M. and Singh, A. T. (2018) ‘Apoptosis: a target for anticancer therapy’. *International journal of molecular sciences* [online], 19(2), 448. available from <https://www.mdpi.com/1422-0067/19/2/448/htm> [12 May 2021]

Powell, S. R. and Wapnir, R. A. (1994) ‘Adventitious redox-active metals in Krebs-Henseleit buffer can contribute to Langendorff heart experimental results’. *Journal of molecular and cellular cardiology* [online], 26(6), 769-778. available from <https://www.sciencedirect.com/science/article/abs/pii/S0022282884710911> [23 April 2021]

Pray, L. (2008) ‘The Biotechnology Revolution: PCR and the Use of Reverse Transcriptase to Clone Expressed Genes’. *Nature Education* [online], 1(1):94. available from <https://www.nature.com/scitable/topicpage/the-biotechnology-revolution-pcr-and-the-use-553/> [20 May 2021]

Qian, J., Xu, Z., Meng, C., Liu, J., Hsu, P.L., Li, Y., Zhu, W., Yang, Y., Morris-Natschke, S.L., Lee, K.H. and Zhang, Y. (2020) 'Design and synthesis of benzylidenecyclohexenones as TrxR inhibitors displaying high anticancer activity and inducing ROS, apoptosis, and autophagy'. European Journal of Medicinal Chemistry [online], 204, p.112610. available from<https://www.sciencedirect.com/science/article/abs/pii/S0223523420305821> [Accessed 13 Octoper 2021]

Qu, F., Xu, W., Deng, Z., Xie, Y., Tang, J., Chen, Z., Luo, W., Xiong, D., Zhao, D., Fang, J., Zhou, Z. and Liu, Z. (2020) ‘Fish c-Jun N-Terminal Kinase (JNK) Pathway Is Involved in Bacterial MDP-Induced Intestinal Inflammation’. *Frontiers*

in immunology [online], 11, 459. available from <https://www.frontiersin.org/articles/10.3389/fimmu.2020.00459/full?report=reader> [20 April 2021]

Rabe, K. F., Hurst, J. R. and Suissa, S. (2018) 'Cardiovascular disease and COPD: dangerous liaisons?'. *European Respiratory Review* [online], 27(149). available from <https://err.ersjournals.com/content/27/149/180057.short> [20 November 2020]

Rattmann, Y.D., Anselm, E., Kim, J.H., Dal-Ros, S., Auger, C., Miguel, O.G., Santos, A.R., Chataigneau, T. and Schini-Kerth, V.B. (2012) 'Natural product extract of Dicksonia sellowiana induces endothelium-dependent relaxations by a redox-sensitive Src-and Akt-dependent activation of eNOS in porcine coronary arteries'. *Journal of vascular research* [online], 49(4), pp.284-298 available from <http://www.karger.com/Article/FullText/336647> [16 June 2017]

Rieseberg, M., Kasper, C., Reardon, K. F. and Scheper, T. (2001) 'Flow cytometry in biotechnology'. *Applied microbiology and biotechnology* [online], 56(3), 350-360. available from <https://link.springer.com/article/10.1007/s002530100673> [20 May 2021]

Roe, A. J. and Qi, X. (2018) 'Drp1 phosphorylation by MAPK1 causes mitochondrial dysfunction in cell culture model of Huntington's disease'. *Biochemical and biophysical research communications* [online], 496(2), pp.706–

711. available from <https://www.sciencedirect.com/science/article/pii/S0006291X18301293> [27 December 2019]

Rosdah, A. A., K Holien, J., Delbridge, L. M., Dusting, G. J. and Lim, S. Y. (2016) 'Mitochondrial fission - a drug target for cytoprotection or cytodestruction?'. *Pharmacology research & perspectives* [online], *4*(3), e00235. available from <https://doi.org/10.1002/prp2.235> [11 December 2018]

Roskoski Jr. R. (2012) 'ERK1/2 MAP kinases: structure, function, and regulation'. *Pharmacological research* [online], 66(2), 105-143. available from <https://www.sciencedirect.com/science/article/abs/pii/S1043661812000977> [03 June 2018]

Roversi, S., Roversi, P., Spadafora, G., Rossi, R. and Fabbri, L. M. (2014) 'coronary artery disease concomitant with chronic obstructive pulmonary disease'. *European journal of clinical investigation* [online], 44(1), 93-102. available from <https://onlinelibrary.wiley.com/doi/full/10.1111/eci.12181> [28 December 2019]

Ruiz, A., Alberdi, E. and Matute, C. (2018) 'Mitochondrial Division Inhibitor 1 (mdivi-1) Protects Neurons against Excitotoxicity through the Modulation of

Mitochondrial Function and Intracellular Ca^{2+} Signaling'. *Frontiers in molecular neuroscience* [online], *11*, 3. available from <https://doi.org/10.3389/fnmol.2018.00003> [09 October 2019]

Rysavy, N. M., Shimoda, L. M., Dixon, A. M., Speck, M., Stokes, A. J., Turner, H. and Umemoto, E. Y. (2014) 'Beyond apoptosis: the mechanism and function of phosphatidylserine asymmetry in the membrane of activating mast cells'. *Bioarchitecture* [online], 4(4-5), 127–137. available from <https://doi.org/10.1080/19490992.2014.995516> [28 December 2019]

Saha, S. and Brightling, C. E. (2006) 'Eosinophilic airway inflammation in COPD'. *International journal of chronic obstructive pulmonary disease* [online], *1*(1), 39. available from <https://www.ncbi.nlm.nih.gov/pmc/articles/PMC2706606/> [22 December 2017]

Santulli, G., Xie, W., Reiken, S. R. and Marks, A. R. (2015) 'Mitochondrial calcium overload is a key determinant in heart failure'. *Proceedings of the National Academy of Sciences* [online], 112(36), pp. 11389–11394. doi: 10.1073/pnas.1513047112. available from <http://www.pnas.org/content/112/36/11389.short> [15 July 2018]

Seidlmayer, L. K., Juettner, V. V., Kettlewell, S., Pavlov, E. V., Blatter, L. A. and Dedkova, E. N. (2015) ‘Distinct mPTP activation mechanisms in ischaemia-reperfusion: contributions of Ca^{2+}, ROS, pH, and inorganic polyphosphate’. *Cardiovascular research* [online], *106*(2), 237–248. available from <https://doi.org/10.1093/cvr/cvv097> [23 December 2017]

Schamberger, A.C., Mise, N., Meiners, S. and Eickelberg, O. (2014) ‘Epigenetic mechanisms in COPD: Implications for pathogenesis and drug discovery’. *Expert Opinion on Drug Discovery* [online], 9(6), pp. 609–628. doi: 10.1517/17460441.2014.913020. available from <https://www.tandfonline.com/doi/abs/10.1517/17460441.2014.913020> [25 May 2020]

Shah, M., Yellon, D. M. and Davidson, S. M. (2020) ‘The role of extracellular DNA and histones in ischaemia-reperfusion injury of the myocardium’ *Cardiovascular drugs and therapy* [online], 34(1), 123-131. available from <https://link.springer.com/article/10.1007/s10557-020-06946-6 > [20 April 2021]

Shaik, N., Alhourani, E., Bosc, A., Liu, G., Towhid, S., Lupescu, A. and Lang, F. (2012) ‘Stimulation of suicidal erythrocyte death by ipratropium bromide’. *Cellular Physiology and Biochemistry* [online], 30(6), 1517-1525. available from <http://www.karger.com/Article/Abstract/343339> [08 January 2018]

Shang, X., Zhang, Y., Xu, J., Li, M., Wang, X. and Yu, R. (2020) ‘SRV2 promotes mitochondrial fission and Mst1-Drp1 signaling in LPS-induced septic cardiomyopathy’. *Aging* [online], *12*(2), 1417–1432. available from <https://www.ncbi.nlm.nih.gov/pmc/articles/PMC7053598/> [25 May 2021]

Sharp, W.W., Fang, Y.H., Han, M., Zhang, H.J., Hong, Z., Banathy, A., Morrow, E., Ryan, J.J. and Archer, S.L. (2014) ‘Dynamin-related protein 1 (Drp1) - mediated diastolic dysfunction in myocardial ischemia-reperfusion injury: therapeutic benefits of Drp1 inhibition to reduce mitochondrial fission’. The FASEB Journal [online], 28(1), pp.316-326. available from< https://faseb.onlinelibrary.wiley.com/doi/full/10.1096/fj.12-226225> [Accessed 08 January 2022]

Simon, H. U., Haj-Yehia, A. and Levi-Schaffer, F. (2000) ‘Role of reactive oxygen species (ROS) in apoptosis induction’. *Apoptosis* [online], 5(5), 415-418. available from <https://link.springer.com/article/10.1023/A:1009616228304> [29 December 2019]

Singanayagam, A., Glanville, N., Walton, R.P., Aniscenko, J., Pearson, R. M., Pinkerton, J. W., Horvat, J. C., Hansbro, P. M., Bartlett, N. W. and Johnston, S. L. (2015) ‘A short-term mouse model that reproduces the immunopathological features of rhinovirus-induced exacerbation of COPD’. *Clin. Sci* [online], 129(3),

pp. 245–258. doi: 10.1042/cs20140654. available from <https://portlandpress.com/clinsci/article/129/3/245/71277> [19 December 2019]

Singh, S., Loke, Y. K. and Furberg, C. D. (2008) 'Inhaled anticholinergics and risk of major adverse cardiovascular events in patients with chronic obstructive pulmonary disease: a systematic review and meta-analysis'. *Jama* [online], 300 (12), 1439-1450. available from <http://jama.jamanetwork.com/article.aspx?articleid=1028648> [30 March 2018]

Siouta, N., van Beek, K., Preston, N., Hasselaar, J., Hughes, S., Payne, S., Garralda, E., Centeno, C., van der Eerden, M., Groot, M., Hodiamont, F., Radbruch, L., Busa, C., Csikos, A. and Menten, J. (2016) 'Towards integration of palliative care in patients with chronic heart failure and chronic obstructive pulmonary disease: A systematic literature review of European guidelines and pathways'. *BMC Palliative Care* [online], 15(1) -07-12. available at <http://bmcpalliatcare.biomedcentral.com/articles/10.1186/s12904-016-0089-4> [09 January 2019]

Skrzypiec-Spring, M., Grotthus, B., Szelag, A., & Schulz, R. (2007) 'Isolated heart perfusion according to Langendorff---still viable in the new millennium'. *Journal of pharmacological and toxicological methods* [online], 55(2), 113–126. available from <https://doi.org/10.1016/j.vascn.2006.05.006> [23 April 2021]

Søyseth, V., Brekke, P. H., Smith, P. and Omland, T. (2007) ‘Statin use is associated with reduced mortality in COPD’. *European Respiratory Journal* [online], 29(2), 279-283. available from <https://erj.ersjournals.com/content/29/2/279.short> [06 January 2018]

Srinivas, U. S., Tan, B. W., Vellayappan, B. A. and Jeyasekharan, A. D. (2019) ‘ROS and the DNA damage response in cancer’. *Redox biology* [online], *25*, p.101084. available from <https://www.sciencedirect.com/science/article/pii/S2213231718309017> [17 May 2021]

Steffen, J. and Koehler, C. M. (2018) ‘ER-mitochondria contacts: Actin dynamics at the ER control mitochondrial fission via calcium release’. *The Journal of cell biology* [online], *217*(1), 15–17. available from https://doi.org/10.1083/jcb.201711075 [28 December 2019]

Sterea, A. M. and El Hiani, Y. (2020) ‘The role of mitochondrial calcium signaling in the pathophysiology of cancer cells’. *Calcium Signaling* [online], 747-770. available from <https://link.springer.com/chapter/10.1007/978-3-030-12457-1_30> [28 January 2021]

Suchal, K., Malik, S., Gamad, N., Malhotra, R. K., Goyal, S. N., Chaudhary, U., Bhatia, J., Ojha, s. and Arya, D. S. (2016) 'Kaempferol attenuates myocardial ischemic injury via inhibition of MAPK signaling pathway in experimental model of myocardial ischaemia-reperfusion injury'. *Oxidative medicine and cellular longevity* [online], available from <https://www.hindawi.com/journals/omcl/2016/7580731/abs/> [21 October 2019]

Syntichaki, P. and Tavernarakis, N. (2003) 'The biochemistry of neuronal necrosis: rogue biology?'. *Nature Reviews Neuroscience* [online], 4(8), 672-684. available from <http://www.nature.com/nrn/journal/v4/n8/abs/nrn1174.html> [08 April 2019]

Szobi, A., Rajtik, T., Carnicka, S., Ravingerova, T. and Adameova, A. (2013) 'Mitigation of postischemic cardiac contractile dysfunction by CaMKII inhibition: Effects on programmed necrotic and apoptotic cell death'. *Molecular and Cellular Biochemistry* [online], 388(1-2), pp. 269–276. doi: 10.1007/s11010-013-1918-x. available from <https://link.springer.com/article/10.1007/s11010-013-1918-x> [30 July 2018]

Tani, M. and Neely, J. R. (1989) 'Role of intracellular Na^+ in Ca^{2+} overload and depressed recovery of ventricular function of reperfused ischemic rat hearts. Possible involvement of H^+-Na^+ and Na^+-Ca^{2+} exchange'. *Circulation research*

[online], 65(4), 1045-1056. available from <https://pubmed.ncbi.nlm.nih.gov/2551525/> [01 October 2019]

Tanimura, S. and Takeda, K. (2017) ‘ERK signalling as a regulator of cell motility’. *The Journal of Biochemistry* [online], 162(3), 145-154. available from <https://academic.oup.com/jb/article/162/3/145/3954057?login=true> [12 May 2021]

Tarasov, A. I., Griffiths, E. J. and Rutter, G. A. (2012) ‘Regulation of ATP production by mitochondrial Ca^{2+}’. *Cell calcium* [online], 52(1), 28-35. available from <https://www.sciencedirect.com/science/article/pii/S0143416012000541> [14 May 2017]

Troncoso, R., Paredes, F., Parra, V., Gatica, D., Vásquez-Trincado, C., Quiroga, C., Bravo-Sagua, R., López-Crisosto, C., Rodriguez, A.E., Oyarzún, A.P. and Kroemer, G. (2014) 'Dexamethasone-induced autophagy mediates muscle atrophy through mitochondrial clearance'. Cell Cycle [online], 13(14), pp.2281-2295. available from <https://www.tandfonline.com/doi/full/10.4161/cc.29272> [Accessed 20 January 2022]

Ullrich, V. and Apell, H. J. (2021) ‘Electromagnetic Fields and Calcium Signaling by the Voltage Dependent Anion Channel’. *Open Journal of Veterinary Medicine* [online], 11, 57-86. available from <https://doi.org/10.4236/ojvm.2021.111004> [08 April 2021]

Veeranki, S. and Tyagi, S. C. (2017) ‘Mdivi-1 induced acute changes in the angiogenic profile after ischaemia-reperfusion injury in female mice’. *Physiological reports* [online], 5(11), e13298. available from <https://doi.org/10.14814/phy2.13298> [12 July 2019]

Vermes, I., Haanen, C., Steffens-Nakken, H. and Reutellingsperger, C. (1995) ‘A novel assay for apoptosis flow cytometric detection of phosphatidylserine expression on early apoptotic cells using fluorescein labelled Annexin V’. *Journal of Immunological Methods* [online], 184(1), 39–51. available from <https://www.sciencedirect.com/science/article/abs/pii/002217599500072I> [15 October 2018]

Wang, C. and Youle, R. J. (2009) ‘The role of mitochondria in apoptosis*’. *Annual review of genetics* [online], *43*, 95–118. available from <https://doi.org/10.1146/annurev-genet-102108-134850> [08 April 2019]

Wang, K., Liu, F., Liu, C. Y., An, T., Zhang, J., Zhou, L. Y., Wang, M., Dong Y. H., Li, N., Gao, J. N., Zhao, Y. F. and Li, P. F. (2016) 'The long noncoding RNA NRF regulates programmed necrosis and myocardial injury during ischaemia and reperfusion by targeting miR-873'. *Cell Death & Differentiation* [online], 23(8), 1394-1405. available from <https://www.nature.com/articles/cdd201628> [01 June 2021]

Wang, W., Zhang, H., Gao, H., Kubo, H., Berretta, R. M., Chen, X. and Houser, S.R. (2010) 'B1-Adrenergic receptor activation induces mouse cardiac myocyte death through both l-type calcium channel-dependent and -independent pathways'. *Article* [online], 299(2), pp. 322–331. doi: 10.1152/ajpheart.00392.2010. available from <https://journals.physiology.org/doi/full/10.1152/ajpheart.00392.2010> [09 April 2020]

Watanabe, M. and Okada, T. (2018) 'Langendorff perfusion method as an ex vivo model to evaluate heart function in rats'. *In Experimental Models of Cardiovascular Diseases* [online], (pp. 107-116). Humana Press, New York, NY. available from <https://link.springer.com/protocol/10.1007/978-1-4939-8597-5_8> [08 June 2021]

Wells, P. G., McCallum, G. P., Chen, C. S., Henderson, J. T., Lee, C. J., Perstin, J., Preston, T.J., Wiley, M.J. and Wong, A. W. (2009) 'Oxidative stress in developmental origins of disease: teratogenesis, neurodevelopmental deficits,

and cancer'. *Toxicological sciences* [online], 108(1), 4-18. available from <https://academic.oup.com/toxsci/article/108/1/4/1673173?login=true> [25 May 2021]

White, R. J. and Reynolds, I. J. (1995) 'Mitochondria and Na^+/Ca^{2+} exchange buffer glutamate-induced calcium loads in cultured cortical neurons'. *Journal of Neuroscience* [online], 15(2), 1318-1328. available from <https://www.jneurosci.org/content/15/2/1318.short> [16 February 2019]

Winnay, J., Li, Q., Rask-Madsen, C., Mima, A., Mizutani, K., Park, K., Maeda, Y., D'Aquino, K., White, M.F. and Feener, E.P. (2013) 'Serine Phosphorylation sites on IRS2 activated by angiotensin II and protein Kinase C to induce selective insulin resistance in endothelial cells', *Molecular and Cellular Biology* [online], 33(16), pp. 3227–3241. doi: 10.1128/MCB.00506-13. available from <https://www.ncbi.nlm.nih.gov/pmc/articles/PMC3753901/> [18 May 2017]

Wong, M.H., Samal, A.B., Lee, M., Vlach, J., Novikov, N., Niedziela-Majka, A., Feng, J.Y., Koltun, D.O., Brendza, K.M., Kwon, H.J. and Schultz, B.E. (2019) 'The KN-93 molecule inhibits calcium/calmodulin-dependent protein kinase II (CaMKII) activity by binding to Ca2+/CaM'. Journal of molecular biology [online], 431(7), pp.1440-1459. available from<https://www.sciencedirect.com/science/article/abs/pii/S0022283618311045 > [Accessed 23 September 2021]

Wu, M. Y., Yiang, G. T., Liao, W. T., Tsai, A. P. Y., Cheng, Y. L., Cheng, P. W., Li, C. Y. and Li, C. J. (2018) 'Current mechanistic concepts in ischaemia and reperfusion injury'. *Cellular Physiology and Biochemistry* [online], *46*(4), 1650-1667. available from <https://www.karger.com/Article/Abstract/489241> [15 November 2019]

Xu, S., Wang, P., Zhang, H., Gong, G., Cortes, N. G., Zhu, W., Yoon, Y., Tian, R. and Wang, W. (2016) 'CaMKII induces permeability transition through Drp1 phosphorylation during chronic β-AR stimulation'. *Nature communications* [online], 7(1), 1-13. available from <https://www.nature.com/articles/ncomms13189?origin=ppub> [13 May 2019]

Xu, W. W., Zhang, Y. Y., Su, J., Liu, A. F., Wang, K., Li, C., Liu, Y. E., Zhang, Y. Q., Lv, J. and Jiang, W. J. (2018) 'Ischaemia reperfusion injury after gradual versus rapid flow restoration for middle cerebral artery occlusion rats '. *Scientific reports* [online], 8(1), pp.1-9. available from <https://www.nature.com/articles/s41598-018-20095-9> [14 March 2019]

Yang, B., Chen, Y. and Shi, J. (2019) 'Reactive oxygen species (ROS)-based nanomedicine'. *Chemical reviews* [online], *119*(8), pp.4881-4985. available from <https://pubs.acs.org/doi/full/10.1021/acs.chemrev.8b00626> [22 March 2020]

Yang, Z., Kirton, H. M., MacDougall, D. A., Boyle, J. P., Deuchars, J., Frater, B., Ponnambalam, S., Hardy, M. E., White, E., Calaghan, S. C., Peers, C. and Steele, D. S. (2015) 'The Golgi apparatus is a functionally distinct Ca^{2+} store regulated by the PKA and Epac branches of the β1-adrenergic signaling pathway'. *Science signaling* [online], 8(398), ra101. available from <https://doi.org/10.1126/scisignal.aaa7677> [18 April 2017]

Yang, Y., Li, Y., Wang, J., Hong, L., Qiao, S., Wang, C. and An, J. (2021) 'Cholinergic receptors play a role in the cardioprotective effects of anesthetic preconditioning: Roles of nitric oxide and the CaMKKβ/AMPK pathway'. Experimental and Therapeutic Medicine [online], 21(2), pp.1-1. available from<https://www.spandidos-publications.com/10.3892/etm.2020.9569> [Accessed 14 January 2022]

Yin, Y., Guan, Y., Duan, J., Wei, G., Zhu, Y., Quan, W., Guo, C., Zhou, D., Wang, Y., Xi, M. and Wen, A. (2013) 'Cardioprotective effect of Danshensu against myocardial ischaemia/reperfusion injury and inhibits apoptosis of H9c2 cardiomyocytes Akt and ERK1/2 phosphorylation'. *European Journal of Pharmacology* [online], 699(s 1–3), pp. 219–226. doi: 10.1016/j.ejphar.2012.11.005. available from <https://www.sciencedirect.com/science/article/abs/pii/S0014299912009363> [25 March 2017]

Yu, J., Zhong, B., Xiao, Q., Du, L., Hou, Y., Sun, H. S., Lu, J. J. and Chen, X. (2020) ‘Induction of programmed necrosis: A novel anti-cancer strategy for natural compounds ‘. *Pharmacology & Therapeutics* [online], 107593. available from <https://www.sciencedirect.com/science/article/abs/pii/S0163725820301212> [19 April 2021]

Yu, W., Gao, D., Jin, W., Liu, S. and Qi, S. (2018) ‘Propofol prevents oxidative stress by decreasing the ischemic accumulation of succinate in focal cerebral ischaemia–reperfusion injury’. *Neurochemical research* [online], *43*(2), 420-429. available from <https://link.springer.com/article/10.1007/s11064-017-2437-z> [17 May 2019]

Yuan, F. L., Wang, H. R., Zhao, M. D., Yuan, W., Cao, L., Duan, P. G., Jiang, Y. Q., Li, X. L. and Dong, J. (2014) ‘Ovarian cancer G protein-coupled receptor 1 is involved in acid-induced Apoptosis of Endplate Chondrocytes in Intervertebral discs’. *Journal of Bone and Mineral Research* [online], 29(1), pp. 67–77. doi: 10.1002/jbmr.2030. available from <https://asbmr.onlinelibrary.wiley.com/doi/full/10.1002/jbmr.2030> [22 March 2018]

Yue, P., Zhang, Y., Du, Z. M., Xiao, J., Pan, Z., Wang, N., Yu, H., Ma, W., Qin, H., Wang, W. and Lin, D. (2006) ‘Ischaemia impairs the association between

connexin 43 and M3 subtype of acetylcholine muscarinic receptor (M3-mAChR) in ventricular myocytes'. *Cellular Physiology and Biochemistry* [online], 17(3-4), 129-136. available from <http://www.karger.com/Article/Abstract/92074> [28 January 2020]

Zaja, I., Bai, X., Liu, Y., Kikuchi, C., Dosenovic, S., Yan, Y., Canfield, S. G. and Bosnjak, Z. J. (2014) 'Cdk1, PKCδ and calcineurin-mediated Drp1 pathway contributes to mitochondrial fission-induced cardiomyocyte death'. *Biochemical and biophysical research communications* [online], *453*(4), 710-721. available from <https://www.sciencedirect.com/science/article/abs/pii/S0006291X14018087> [18 May 2021]

Zhao, R., Jiang, S., Zhang, L. and Yu, Z. (2019) 'Mitochondrial electron transport chain, ROS generation and uncoupling (Review)'. *International Journal of Molecular Medicine* [online], 44, 3-15. available from <https://doi.org/10.3892/ijmm.2019.4188> [28 April 2020]

Zhao, Z. Q., Corvera, J. S., Halkos, M. E., Kerendi, F., Wang, N. P., Guyton, R. A. and Vinten-Johansen, J. (2003) 'Inhibition of myocardial injury by ischemic postconditioning during reperfusion: comparison with ischemic preconditioning'. *American Journal of Physiology-Heart and Circulatory Physiology* [online],

285(2), H579-H588. available from <http://ajpheart.physiology.org/content/285/2/H579.short> [17 April 2020]

Zhou, L., Zhang, Q., Zhang, P., Sun, L., Peng, C., Yuan, Z. and Cheng, J. (2017) 'C-Abl-mediated Drp1 phosphorylation promotes oxidative stress-induced mitochondrial fragmentation and neuronal cell death'. *Cell death & disease* [online], *8*(10), e3117-e3117. available from <https://doi.org/10.1038/cddis.2017.524> [10 June 2018]

Zorov, D. B., Juhaszova, M. and Sollott, S. J. (2014) 'Mitochondrial reactive oxygen species (ROS) and ROS-induced ROS release'. *Physiological reviews* [online], 94(3), 909–950. available from <https://doi.org/10.1152/physrev.00026.2013> [08 July 2019]

Zweier, J. L., Flaherty, J. T. and Weisfeldt, M. L. (1987) 'Direct measurement of free radical generation following reperfusion of ischemic myocardium'. *Proceedings of the National Academy of Sciences* [online], 84(5), 1404-1407. available from <http://www.pnas.org/content/84/5/1404.short> [12 April 2018]